AN INVESTIGATION OF SOME DYNAMIC ASPECTS AND ADAPTIVE CONTROL OF METAL TURNING

by

© Chi-Hung Heman HUI, B. Eng.

A Thesis submitted to the Faculty of Graduate Studies and Research in partial fulfilment of the requirements for the degree of Master of Engineering

Department of Mechanical Engineering
McGill University
Montreal, Canada.

November 1982

ABSTRACT

This study is concerned with the dynamic behavior and adaptive control of the turning of eccentric workpieces. The practical application is rough turning of forgings or castings which may have considerable variations in initial shape and size.

A simple but detailed analysis on the dynamics of rotating eccentric workpiece is first presented.

A micro-processor based adaptive control system retrofitted to a numerical control lathe is then described and investigated. Adaptive control implies that some of the main cutting variables (e.g. cutting force) are measured in real time and the appropriate controlled parameters (e.g. feedrate) are modified in an on-line basis. A mathematical model of the adaptive control system is developed for the study of the performance of various adaptive control algorithms. Particularly, a non-linear peak-value memory algorithm especially suitable for eccentric workpieces is investigated along with standard proportional-plus-integral control.

RESUME

La dynamique et le contrôle adaptable du tournage de pièces montées eccentriquement sont le sujet de la présente étude. Les résultats s'appliquent au dégrossissement de pièces de forge ou de coulée dont les dimensions diffèrent souvent largement de celles du morceau fini.

Une analyse de la dynamique d'une telle pièce conduit à une équation matricielle du mouvement et des forces impliquées.

Un système de tour à contrôle numérique adaptable par micro-processeur constitue la source de données expérimentales. Contrôle adaptable signifie que certaines variables du processus de tournage (e.g. force radiale) sont mesurées et les paramètres de contrôle appropriés (e.g. vitesse d'avance) sont modifiés selon les valeurs obtenues.

Un modèle mathématique du système de contrôle adaptable a été développé afin d'étudier le rendement des divers algorithmes de contrôle possibles. En particulier, un algorithme non-linéaire à rappel de valeur de pointe, spécialement adapté aux pièces eccentriques est étudié en conjonction avec le contrôle proportionnel-plus-intégral standard.

ACKNOWLEDGEMENTS

The author wishes to express his sincere gratitude and thankfulness to his research supervisor, Prof. Roy Hoffman, for his attentive guidance and continuous encouragement throughout the course of this work.

Sincere thanks are due to Prof. Arun Misra and Mr. Steve Chan who gave numerous constructive suggestions in solving the mathematical problems encountered in this work.

Special thanks are also directed to Miss Jane Law for the preparation of the figures and Mr. Oscar Sy for the tedious work of proof-reading the manuscript. The author wishes to thank Mr. George Robenheimer as well for the writing of the French abstract.

The help offered by all the technical staffs in Datac and Machine Tool Laboratories is also acknowledged.

TABLE OF CONTENTS

LIST OF FIGURES

LIST OF TABLES

NOMENCLATURE

SYMBOL	DESCRIPTION
A	Cross-sectional area of workpiece
$A_n(t)$	Generalized coordinate of the horizontal variable y
$B_n(t)$	Generalized coordinate of the vertical variable z
b	Desired depth-of-cut
c	Structual damping factor
C	Neutral centre of a rotating beam
C'	Instantaneous centre of a rotating beam with deflection
C(t)	Continuous signal
C(n)	Sampled continuous signal
C^*_n	Logical output of C(n) from PVM
d	Eccentricity of workpiece
E	Young's modulus
F	Decaying factor of PVM per revolution
F'	Effective decaying factor of PVM per sample
Fnom	Nominal force
G_C	Transfer function of the chip formation
G_F	Transfer function of the force formation
G_I	Transfer function of the integrator
G_M	Transfer function of the control algorithm
G_N	Transfer function of the NC servo

SYMBOL	DESCRIPTION
I	Moment of inertia of workpiece
IPM	Inches per minute
K_d	Specific energy of workpiece
K_f	Transfer function of the force transducer
K_g	NC servo gain
Kint	Integral controller gain
Kpro	Proportional controller gain
ℓ	total length of workpiece
m	unit mass of workpiece
O	Origin of coordinate system
P	Resultant cutting force
P_1	Main cutting force
P_2	Feed force
P_3	Lateral force
R	Radius of workpiece
RPM	Revolution per minute
s	Feedrate of the cutting tool
t	Independent variable of time
T	Kinetic energy
T_1, T_2	Time constants of the NC lathe
T_c	Sampling period
T_r	Revolution period
V	Potential energy
Vnom	Nominal voltage

SYMBOL	DESCRIPTION
X	Axis of rotation of workpiece
Y	Horizontal axis of coordinate system
y	Horizontal distance between C' and C
y'	Horizontal distance between any point on the cross-section of beam from C'
Z	Vertical axis of coordinate system
z	Vertical distance between C' and C
z'	Horizontal distance between any point on the cross-section of beam from C'
ω	Angular velocity of workpiece
ρ	Density of workpiece
$\phi_n(x)$	Admissible function of a clamped-free beam
$\phi_k(x)$	Comparison function of a clamped-free beam
δ_{kn}	Kronecker delta
λ	Eigenvalues of a rotating beam
λ_R	Real part of an eigenvalue
λ_I	Imaginary part of an eigenvalue
ω_n	Natural frequency of a rotating beam
$\delta(x-x_0)$	Dirac delta function
Δy	Horizontal projection of eccentricity on Y-axis
Δz	Vertical projection of eccentricity on Z-axis

TABLE OF EQUIVALENT UNITS

BRITISH UNITS		SI UNITS	
0.001	in	0.0254	mm
0.002	in	0.0508	mm
0.00345	in	0.08763	mm
0.03	in	0.76	mm
0.06	in	1.524	mm
0.09	in	2.286	mm
3.0	in	76.2	mm
8.0	in	203.2	mm
12.0	in	304.8	mm
18.0	in	457.2	mm
19.0	in	482.6	mm
0.015	in/rev	0.381	mm/rev
0.1	in/rev	2.54	mm/rev
100.0	in/rev	2540.0	mm/rev
0.3	hp	0.2238	kW
1.0	lbf	4.45	N
10.0	lbf	44.5	N
80.0	lbf	356.0	N
550.0	lbf.ft	742.5	J
118800.0	psi	8185.32	kPa
69.0	RPM	7.226	rad/sec
180.0	RPM	18.849	rad/sec
1800.0	RPM	188.495	rad/sec

CHAPTER 1

INTRODUCTION

1.1 GENERAL ASPECTS OF NUMERICAL CONTROL MACHINING AND ADAPTIVE CONTROL SYSTEMS

Present day metal-working manufacturing systems can be divided into two main categories; namely, mass production and batch production. Mass production accounts for only 25% of the total metal work in North America. Its automatic production lines such as those applied in automotive industry are efficient but give relatively little flexibility in design changes and manufacturing procedures. The remaining 75% is produced via batch production and 50% of it is made in batches sizes of less than fifty [1]. Therefore, there will be a significant impact on the national economy if the efficiency of batch production can be increased.

The main drawbacks of present batch production systems are long lead time, low response to design changes, high manufacturing cost, poor control in processing and machining time, long tooling time, and low tolerances. Hence, the three most critical factors in batch production are flexibility, adaptability, and efficiency.

The implementation of numerical control (NC) machines has

improved the above deficiencies considerably in some respects. However, there are at least two important factors which limit the full utilization of NC machines. The first one is the dynamic behaviour of the whole system during the machining process, whereas the second factor is the effort required in programming of the parts.

Every physical system experiences vibration to a certain degree while it is operating. In a turning operation, the dynamic behavior is a self-excited vibration between the tool and workpiece. During a steady operation, if an external disturbance intervenes, the tool may move relative to the workpiece. This relative motion produces a force between the tool and workpiece. This force in turn may produce an oscillation between them. If the dynamic system is unstable, the oscillation will build up to a large magnitude which is very undesirable. External disturbances come in many forms such as variation in depth-of-cut, non-homogeneity of workpiece, backlash in feed mechanisms, and interaction of machine components.

The other limiting factor is that, since an NC machine follows exactly the programmed instructions, it is basically an open loop system. Because it has no capability of detecting and adjusting itself according to the cutting conditions, for safety reasons, a programmer may tend to be conservative in programming. As a result, inefficiency takes place. On the

other hand, if the programmer lacks practical experience, he may program the parts with improper commands which may cause serious damage to the machine structure.

In view of these two problems, there is considerable interest in the so-called adaptive control of NC machine tools. Generally speaking, in the metal cutting field, an adaptive control system is a system which, in real time, monitors some significant variables of the cutting operation and adjusts the controllable parameters to modify the cutting conditions in some desirable fashion. The process variables which may be monitored are the cutting force, cutting torque, or cutting power, whereas the commanded correcting variables may be the feedrate, cutting speed, or depth-of-cut.

Adaptive control systems, depending on their philosophy of operation, can be divided into two broad categories; namely, Adaptive Control Constraint (ACC) and Adaptive Control Optimization (ACO) systems. In ACC system, the cutting parameters are controlled in such a way that the cutting process variables are maintained within certain constraints or limits. In ACO system, the output parameters are controlled in order to optimize some performance criteria related to variables such as manufacturing time, cost, tool life and etc. In general, an ACO system is more complex than an ACC system mainly because the optimization criterion is usually relatively complex, especially when several controlled parameters are

taken into account. In fact, the practical value of ACO systems is questionable and currently most practical adaptive control schemes are of the ACC type. This thesis will also limit itself to the investigation of ACC system.

1.2 REVIEW AND EVALUATION OF THE LITERATURE

1.2.1 Dynamic Behavior of Turning

Extensive research on the dynamic behavior of turning has been carried out for years. Many theories have been developed independently. Attention is paid to two of them, one by Tobias and Fishwick [2] and the other by Tlusty and Polacek [3]. Tlusty and Polacek considered the problem as a forced vibration between the machine structure and workpiece, whereas Tobias and Fishwick considered it as a problem of dynamic stability. The essential difference between these approaches lies in the different initial assumptions and not in their theoretical approaches.

Most researchers follow the above investigators' concept of an incremental cutting force. Typically, their works end up with developing, comparing, or refining the machinability and stability charts for various machines [4,5,6,7].

Bhat and Sankar [8] used the classical method of analysis, that is, they modelled the turning process by considering the workpiece as a Bernouli-Euler beam in contact with a travelling tool. An equation of motion was derived by

them. Instead of solving the exact solution, they concentrated on predicting the deflection of the beam at the moving tool location. Their main result was a graph showing the relationship between the normalized mean displacement of workpiece and tool location. Although their work was not on the eccentric turning, it gives this work a guideline of how to approach the analysis of such a dynamic process.

It would appear that very little research has been done on the dynamics of eccentric turning. Doi and Kato [9] did an experiment set up in such a way that a fixed tool cut a chip with sinusoidal variation in thickness. Although because of the complexity involved, one may assume a fixed tool position in one's analysis, their work is not directly applicable because their objective was to find the phase lags between the maximun depth-of-cut and force. Fine [10] investigated off-centre turning as well, but his prime concern was the resulting surface finish rather than the dynamic behavior. Hence knowledge, both analytical and experimental, on the turning of an eccentrically mounted workpiece with a continuously fed tool is not extensive.

1.2.2 Digital Adaptive Control Systems

Studies on the adaptive control of metal cutting have generally been undertaken in three main areas. The first one is to investigate the general features of ACC and ACO systems

applied to machine tools such as lathes, milling, grinding, and drilling machines. The emphasis has been particularly on the micro-computer adaptive control system, for examples Weck, Stute, and Lee's works [11,12,13]. Special attention is paid to Weck's studies because his paper describes in detail the general features of a micro-computer adaptive control system implemented on an NC lathe. The experimental set-up employed in this project is very similar to that described in his paper. Unfortunately, Weck did not compare the performance of any control algorithms.

The second area undertaken is to develop mathematical models and control algorithms for different applications such as optimization of process or time, and control of time lag and multi-variables system [14,15,16,17]. Although one of the objectives of this work is to evaluate the performance of control algorithms, these available references are so mathematically and theoretically orientated that they are often good only for their own specific problems for which they are developed. Their practical value is very limited for this research.

The third area that has been undertaken on adaptive control of metal cutting, is examining the performance of different control algorithms for various cutting conditions such as eccentric cutting [18,19]. A valuable reference is Weck and Schafer's work in which they outlined the general features

of proportional, integral, and proportional-plus-integral controllers with a special section on the peak-value memory used in eccentric turning [20]. However, their work did not compare the performance of the peak-value memory working along with other common controllers. So one of the objectives of this research is to examine this neglected aspect.

1.3 OBJECTIVES OF THE THESIS

From a practical point of view, this research is related to the problem of rough turning of a workpiece from a forging or casting. Because castings and forgings often have varying amounts of excessive material and a poor degree of roundness when they are initially turned on a lathe, the depth-of-cut may vary with time. In some cases when there is little excessive stock the tool may not even contact the workpiece during the first few passes. If the raw workpiece is out-of-round then the depth-of-cut will vary periodically at the same frequency as the spindle speed; i.e., revolution per minute (RPM).

There are two main objectives in this thesis. The first one is to get an insight into the dynamic behavior of an eccentrically mounted workpiece on a lathe as it is being cut by a travelling tool. To model such a phenomenon, a perfectly round workpiece is eccentrically mounted on the chuck of a lathe. The dynamic behavior is then investigated. The analysis is performed using the classical method that is by considering

the workpiece as a Bernouli-Euler beam and using the variational principle to derive the equations of motion. Expressions for the natural frequencies of such a system are found because they are the prime concern in a dynamic system.

The second objective is to examine and compare the merits of different adaptive control algorithms applied to different turning conditions for an NC lathe. The experiment is focused particularly on the practical desirability of a particular peak-value memory scheme working along with conventional proportional or proportional-plus-integral control. The control algorithms are investigated by observing the transient behavior, overshooting, settling time, and steady-state errors when cutting both normal round and eccentric workpieces.

1.4) OUTLINE OF THE THESIS

The dynamic analysis of a rotating eccentrically mounted beam on a lathe is presented in Chapter 2. Two equations of motion describing the free vibration of the beam are determined first, then expressions for the natural frequencies are found. Following a section on the determination of the cutting forces, the forced vibration (i.e., the real turning operation) of the beam is analyzed and discussed.

In Chapter 3, the experimental micro-computer adaptive control system is described. The functions and features of each component are explained in detail. Following the description of

the hardware, a section on the software aspects of the control system is presented. Particularly, the function of peak-value memory is introduced and explained. The chapter is concluded finally with a flow-chart of the micro-computer program used in the experiment.

The derivation of a mathematical model for the experimental closed-loop adaptive control system is presented in Chapter 4. The mathematical model is then used for analyzing the stability for selected cutting conditions. Nyquist plot and digital simulation are employed in the prediction of stability. The chapter is concluded with a brief discussion and comment on the method of modelling and the accuracy of stability analysis.

Chapter 5 is a discussion of the experimental results. It comments in detail on the performance of experimental controllers for both eccentric and non-eccentric turning.

In chapter 6, conclusions and recommendations for future research work are presented.

CHAPTER 2

ANALYSIS OF THE DYNAMIC BEHAVIOUR OF AN ECCENTRIC TURNING OPERATION

The purpose of this analysis is to obtain an insight into the dynamic behavior of eccentric turning. There are three main sections in this chapter. The first one, Section 2.1, is an analysis of the free vibration of an eccentrically rotating beam. It is followed by Section 2.2 showing the determination of cutting forces. The third section, Section 2.3, considers the vibration of the rotating beam, taking into account the impressed forces from the cutting tool. The chapter is finally concluded with a discussion on the analysis.

2.1 VIBRATION OF AN ECCENTRICALLY MOUNTED WORKPIECE

2.1.1 Coordinate System

Fig. 2.1 shows the coordinate system used in the analysis.

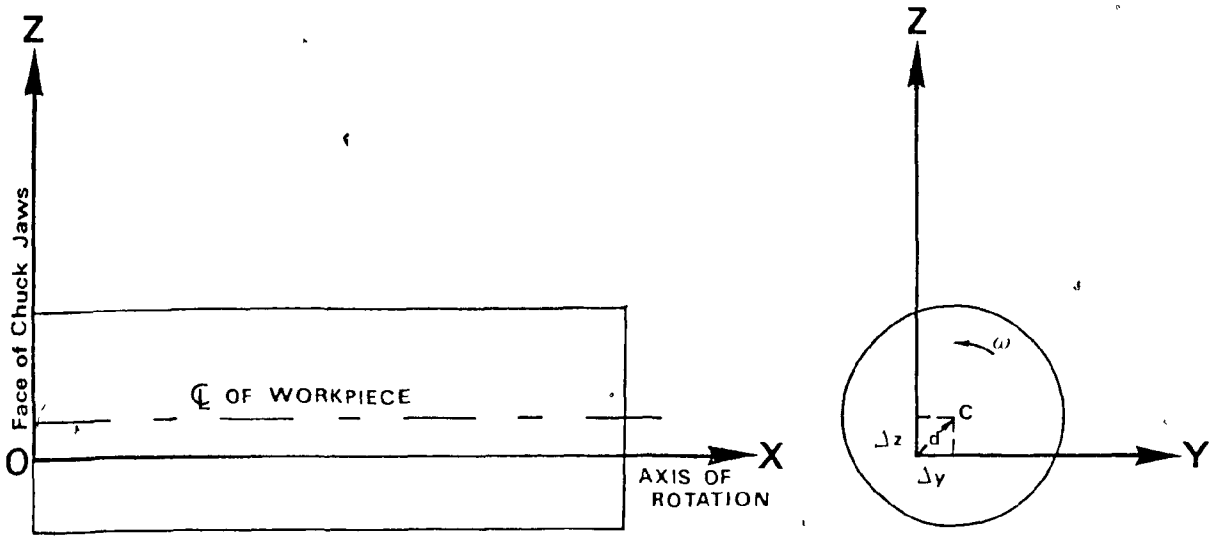

FIG 2.1a SIDE VIEW

FIG 2.1.b END VIEW

FIG 2.1 COORDINATE SYSTEM

The origin of the coordinate system is located at the chuck jaw face at the centre of rotation. The X-axis is the axis of rotation. The Z-axis is in the vertical direction and the Y-axis is the horizontal axis. The workpiece is assumed to be a perfect cylinder with its center-line parallel to the lathe axis of rotation but offset a distance Δy and Δz in the horizontal and vertical directions as shown in Fig. 2.1.b . The angular velocity is designated as ω which is counterclockwise from the end view. In terms of the angular velocity, ω, amount of eccentricity, d, and time, Δy and Δz can be expressed as: $\Delta y = d*\cos(\omega t)$; $\Delta z = d*\sin(\omega t)$. Note particularly that X, Y, Z are reference axes and are fixed in space.

2.1.2 Free Vibration (i.e., No Contact with the Cutting Tool)

To derive the equations of motion, Hamilton's Principle is used:

$$\delta \int_{t_1}^{t_2} (T-V)\,dt = 0 \qquad (2.1.1)$$

where T is the kinetic energy and V is the potential energy. To find the expression for T in Eq.(2.1.1), one must consider the dynamic deflections of the beam as it is vibrating.

Fig. 2.2 shows a cross-sectional view of the workpiece with the workpiece deflected. The instantaneous centre C' has deflected a horizontal distance y and a vertical distance z from the neutral position C. The horizontal and vertical distances from any point A to the centre C' on the cross-section are denoted as y' and z' in the figure.

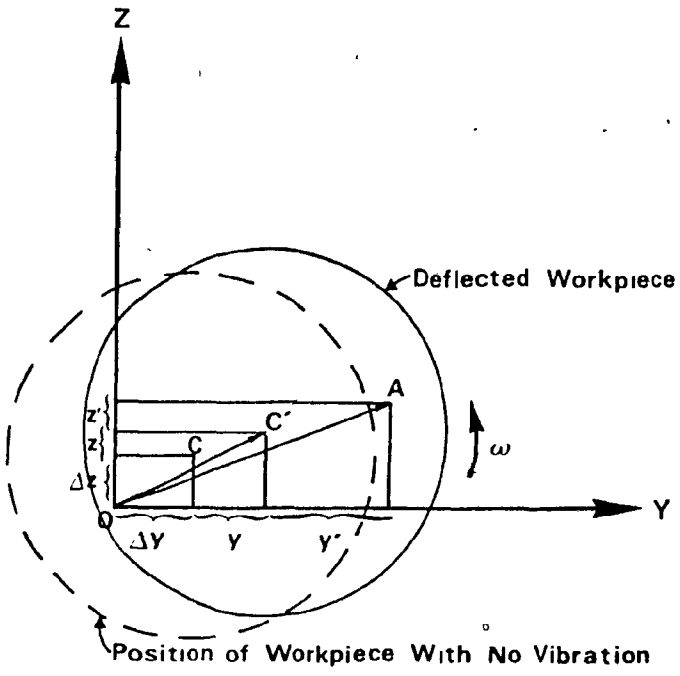

FIG 2-2 END-VIEW OF THE BEAM WITH VIBRATION

The velocity of any point (A) on the workpiece with respect to the origin can be written as:

$$V_{A/O} = V_{A/C'} + V_{C'/O} \tag{2.1.2}$$

As shown in Appendix A, Eq.(2.1.2) can be rewritten in terms of the variables denoted in Fig. 2.2 as:

$$V_{A/O} = (\dot{y} - \omega(\Delta z+z) - \omega z')\vec{j} + (\dot{z}+\omega(\Delta y+y) + \omega y')\vec{k} \tag{2.1.3}$$

Squaring Eq.(2.1.3), the expression for kinetic energy (T), neglecting the effects of precession, becomes:

$$\begin{aligned} T &= \frac{1}{2}\int_0^{\ell} V_{A/O}^2 dm \\ &= \frac{1}{2}\int_0^{\ell} [\dot{y}^2+\omega^2(\Delta z+z)^2 + \omega^2(y'^2+z'^2) - 2\omega(\Delta z+z)\dot{y} \\ &\quad + \dot{z}^2 + \omega^2(\Delta y+y)^2 + 2\omega(\Delta y+y)\dot{z}]dm \\ &= \frac{\rho A}{2}\int_0^{\ell} [\dot{y}^2+\omega^2(\Delta z+z)^2 - 2\omega(\Delta z+z)\dot{y} + \dot{z}^2 + \omega^2(\Delta y+y)^2 \\ &\quad + 2\omega(\Delta y+y)\dot{z}]dx + \frac{1}{2}\omega^2 I_{xx} \end{aligned} \tag{2.1.4}$$

By neglecting the static potential, only the bending moment accounts for the potential energy (V) of the beam [21] which can be expressed as:

$$V = \int_0^{\ell} \frac{1}{2}EI\left(\frac{\partial^2 y}{\partial x^2}\right)^2 dx + \int_0^{\ell} \frac{1}{2}EI\left(\frac{\partial^2 z}{\partial x^2}\right)^2 dx \tag{2.1.5}$$

Taking the variation of T (δT) and V (δV) for Eqs.(2.1.4) and (2.1.5) separately, one gets:

$$\delta T = \frac{\rho A}{2}\int_0^{\ell} [2\dot{y}\delta\dot{y} + 2\omega^2\Delta z\delta z + 2\omega^2\delta z - 2\omega\Delta z\delta\dot{y} - 2\omega z\delta\dot{y} - 2\omega\dot{y}\delta z + 2\dot{z}\delta\dot{z} + 2\omega^2\Delta y\delta y + 2\omega^2 y\delta y + 2\omega\Delta y\delta\dot{z} + 2\omega\delta\dot{z} + 2\omega\dot{z}\delta y]\, dx \qquad (2.1.6)$$

$$\delta V = \int_0^{\ell} EI\frac{\partial^2 y}{\partial x^2}\delta\left(\frac{\partial^2 y}{\partial x^2}\right)dx + \int_0^{\ell} EI\frac{\partial^2 z}{\partial x^2}\delta\left(\frac{\partial^2 z}{\partial x^2}\right)dx \qquad (2.1.7)$$

Applying Hamilton's Principle: $\delta\int_{t_1}^{t_2}(T-V)\, dt = 0$, one gets the following relationship (refer to Appendix B for intermediate steps):

$$\delta\int_{t_i}^{t_2}(T-V)dt = \int_{t_1}^{t_2}\Big\{\int_0^{\ell}\rho A[-\frac{\partial^2 y}{\partial x^2}\delta y + \omega^2 d\sin\omega t\,\delta z + \omega^2 z\delta z + \omega^2 d\cos\omega t\,\delta y + \omega\dot{z}\delta y - \omega\dot{y}\delta z - \frac{\partial^2 z}{\partial t^2}\delta z + \omega^2 d\cos\omega t\,\delta y + \omega^2 y\delta y + \omega^2 d\sin\omega t\,\delta z - w\dot{y}\delta z + w\dot{z}\delta y - \frac{EI}{\rho A}\frac{\partial^4 z}{\partial x^4}\delta z - \frac{EI}{\rho A}\frac{\partial^4 y}{\partial x^4}\delta y]dx - \frac{EI}{\rho A}\frac{\partial^2 z}{\partial x^2}\delta\left(\frac{\partial z}{\partial x}\right)\Big|_0^{\ell} + \frac{EI}{\rho A}\frac{\partial^3 z}{\partial x^3}\delta z\Big|_0^{\ell} - \frac{EI}{\rho A}\frac{\partial^2 y}{\partial x^2}\delta\left(\frac{\partial y}{\partial x}\right)\Big|_0^{\ell} + \frac{EI}{\rho A}\frac{\partial^3 y}{\partial x^3}\delta y\Big|_0^{\ell}\Big\}dt \qquad (2.1.8)$$

Factoring Eq.(2.1.8) for δy, and δz and, since they are

arbitary, so by setting the coefficients of δy and δz to be zero, equations of motion are obtained:

$$\left.\begin{aligned} \frac{\partial^2 z}{\partial t^2} + \frac{EI}{\rho A}\frac{\partial^4 z}{\partial x^4} - \omega^2 z + 2\omega\dot{y} - 2\omega^2 d \sin \omega t = o \\ \frac{\partial^2 y}{\partial t^2} + \frac{EI}{\rho A}\frac{\partial^4 y}{\partial x^4} - \omega^2 y - 2\omega\dot{z} - 2\omega^2 d \cos \omega t = o \end{aligned}\right\} \qquad (2.1.9)$$

The four terms: $\frac{EI}{\rho A}\frac{\partial^2 z}{\partial x^2}$; $\frac{EI}{\rho A}\frac{\partial^3 z}{\partial x^3}$; $\frac{EI}{\rho A}\frac{\partial^2 y}{\partial x^2}$; $\frac{EI}{\rho A}\frac{\partial^3 y}{\partial x^3}$ are determined by the boundary conditions which are those of a clamped-free beam in our case.

To solve Eq.(2.1.9), infinite series solutions are assumed of the forms $z(x,t) = \sum_{n=1}^{\infty} \phi_n(x) A_n(t)$ and $y(x,t) = \sum_{n=1}^{\infty} \phi_n(x) B_n(t)$ in which the $\phi_n(x)$ are clamped-free beam modes.

Substituting the assumed solutions, and applying the Galerkin method of multiplying another comparison function (ϕ_k) into Eq.(2.1.9) gives:

$$\left.\begin{aligned} \sum_{n=1}^{\infty}\int_0^{\ell} \phi_k\phi_n \ddot{A}_n dx + \frac{EI}{\rho A}\sum_{n=1}^{\infty}\int_0^{\ell} \phi_k\phi_n^{(4)} A_n dx - \omega^2 \sum_{n=1}^{\infty}\int_0^{\ell} \phi_k\phi_n A_n dx \\ + 2\omega \sum_{n=1}^{\infty}\int_0^{\ell} \phi_k\phi_n \dot{B}_n dx = 2\omega^2 d \sin \omega t \int_0^{\ell} \phi_k dx \\ \sum_{n=1}^{\infty}\int_0^{\ell} \phi_k\phi_n \ddot{B}_n dx + \frac{EI}{\rho A}\sum_{n=1}^{\infty}\int_0^{\ell} \phi_k\phi_n^{(4)} B_n dx - \omega^2 \sum_{n=1}^{\infty}\int_0^{\ell} \phi_k\phi_n B_n dx \\ - 2\omega \sum_{n=1}^{\infty}\int_0^{\ell} \phi_k\phi_n \dot{A}_n dx = 2\omega^2 d \cos \omega t \int_0^{\ell} \phi_k dx \end{aligned}\right\} \qquad (2.1.10)$$

Because the various comparison functions are orthogonal to each other, the above expressions can be simplified by using the Kronecker delta; i.e., δ_{kn} which is defined to be equal to 1 if and only if k=n, and is equal to zero otherwise. Also it can be shown that:

$$\text{(i)} \int_0^{\ell} \phi_k \phi_n \, dx = \ell \, \delta_{kn} \qquad \text{and} \qquad \text{(ii)} \int_0^{\ell} \phi_k \phi_n^{(4)} \, dx = \beta_n^4 \, \ell \, \delta_{kn}.$$

Denoting $\int_0^{\ell} \phi_k \, dx = h_k$, Eq.(2.1.10), hence, becomes:

$$\left.\begin{aligned} \sum_{n=1}^{\infty} \ell \ddot{A}_k \delta_{kn} + \frac{EI}{\rho A} \sum_{n=1}^{\infty} \ell A_k \beta_n^4 \delta_{kn} - \omega^2 \sum_{n=1}^{\infty} \ell A_k \delta_{kn} + 2\omega \sum_{n=1}^{\infty} \ell \dot{B}_k \delta_{kn} \\ = 2\omega^2 d \sin \omega t \, h_k \\ \sum_{n=1}^{\infty} \ell \ddot{B}_k \delta_{kn} + \frac{EI}{\rho A} \sum_{n=1}^{\infty} \ell B_k \beta_n^4 \delta_{kn} - \omega^2 \sum_{n=1}^{\infty} \ell B_k \delta_{kn} - 2\omega \sum_{n=1}^{\infty} \ell \dot{A}_k \delta_{kn} \\ = 2\omega^2 d \cos \omega t \, h_k \end{aligned}\right\} \quad (2.1.11)$$

Eq.(2.1.11) can be further simplified as:

$$\left.\begin{aligned} \ell \ddot{A}_k + 0\dot{A}_k + \ell\left(\frac{EI}{\rho A} \beta_k^4 - \omega^2\right) A_k + 0\ddot{B}_k + 2\omega \ell \dot{B}_k + 0B_k \\ = (2\omega^2 d \sin \omega t) \, h_k \\ \ell \ddot{B}_k + 0\dot{B}_k + \ell\left(\frac{EI}{\rho A} \beta_k^4 - \omega^2\right) B_k + 0\ddot{A}_k - 2\omega \ell \dot{A}_k + 0A_k \\ = (2\omega^2 d \cos \omega t) \, h_k \end{aligned}\right\} \quad (2.1.12)$$

Letting $f_k(t) = (2\omega^2 d \sin \omega t) h_k$, $g_k(t) = (2\omega^2 d \cos \omega t) h_k$, and $K_k = (\frac{EI}{\rho A} \beta_k^4 - \omega^2) \ell$, Eq.(2.1.12) can be written in a matrix form as:

$$\begin{bmatrix} \ell & 0 \\ 0 & \ell \end{bmatrix} \begin{Bmatrix} \ddot{A}_k \\ \ddot{B}_k \end{Bmatrix} + \begin{bmatrix} 0 & 2\omega\ell \\ -2\omega\ell & 0 \end{bmatrix} \begin{Bmatrix} \dot{A}_k \\ \dot{B}_k \end{Bmatrix} + \begin{bmatrix} K_k & 0 \\ 0 & K_k \end{bmatrix} \begin{Bmatrix} A_k \\ B_k \end{Bmatrix} = \begin{Bmatrix} f_k(t) \\ g_k(t) \end{Bmatrix} \quad (2.1.13)$$

By the reduced order method, it can be shown (see Appendix C) that the natural frequencies of Eq.(2.1.13) are:

$$\omega_n^2 = \alpha = \left[\frac{1}{\ell^2} \left(-(K_k + 2\omega^2) \pm 2\omega \sqrt{\omega^2 + K_k} \right) \right]^{1/2} \quad (2.1.14)$$

Therefore, if the rotational frequency ω of $f_k(t)$ or $g_k(t)$ equals to one of the natural frequencies governed by Eq.(2.1.14), resonance will take place. In order to know the exact rotational frequencies at which resonance takes place, a graph of α versus ω should have been plotted. When the intersection points of the graph between the curves of Eq.(2.1.14) and $\alpha = \omega$ are projected on the ω axis, they give the resonant rotational frequencies. Since the main concern of this work is to understand the actual turning process rather than free vibration of the beam, this graph is therefore of limited use.

2.2 DETERMINATION OF THE CUTTING FORCES IN TURNING

The purpose of this section is to develop analytical expressions for the cutting forces which can be added to the previously developed equations of motion. Orthogonal rather than oblique cutting is assumed in the analysis because of its simple nature in that the force components can be decomposed independently. Fig. 2.3 shows the three force components in orthogonal cutting.

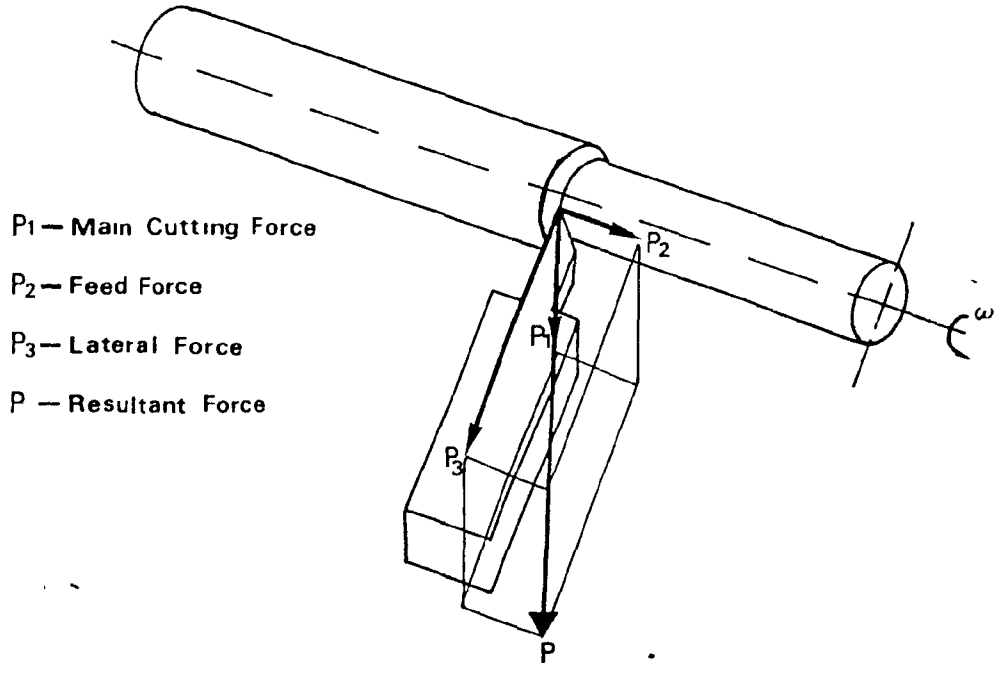

FIG 2·3 FORCE COMPONENTS IN ORTHOGONAL TURNING

Merchant [22] has analyzed the cutting forces. He derived two equations to predict P_1 and P_2 based on his thin shear model. These expressions are rather complicated equations relating the tool rake angle, un-deformed chip thickness, shear stress angle, and friction angle. Due to their complexity, they have very little practical value for our forced vibration analysis. A simple relationship between the force, depth-of-cut, and feedrate is more desirable.

Koenigsberger and Kaczmarek [23,24] both have showed that the feed force (P_2) is always the smallest among the three components. Therefore, as a first-order of approximation, the effects of P_2 are neglected in our forced vibration analysis. Through experimentation, they both concluded that the radial force (P_3) can be approximated to be from 0.3 to 0.6, depending on the material of workpiece, of the main cutting force (P_1) [23,24].

Koenigsberger further collected and plotted the empirical results of the main cutting force (P_1), depth-of-cut (a), and feedrate (s) for a variety of materials on a log-log graph paper as shown in Fig. 2.4 . This plots the main cutting force (P_1) as a function of the product of depth-of-cut and feedrate (a.s).

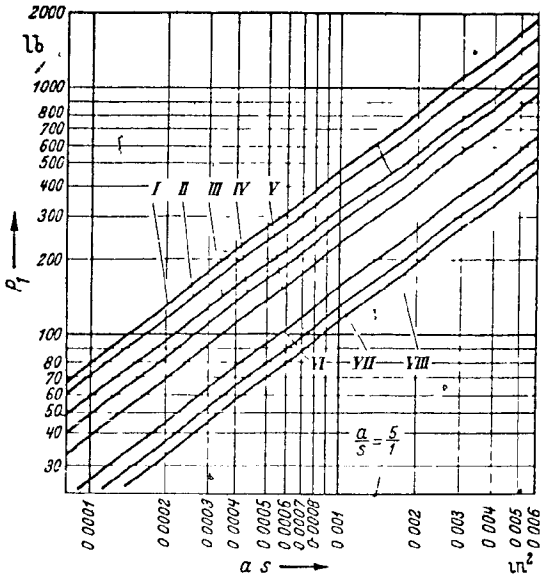

I Alloy steel up to 115 tons/in²
II Alloy steel up to 64 tons/in²
III Carbon steel up to 38 tons/in²
IV Cast steel and carbon steel up to 32 tons/in².
V Cast iron 200–250 Brinell.
VI Cast iron up to 200 Brinell
VII Brass 80–120 Brinell
VIII Aluminium alloy

FIG 2·4 EMPIRICAL RELATIONSHIPS BETWEEN P_1 AND (a·s) FOR TURNING OF DIFFERENT MATERIALS FOUND BY F. Koenigsberger

For example, line VIII is the result for aluminum. By taking two points on the graph, A_1 (P_1=300, a.s=0.0035), and A_2 (P_1=80, a.s=0.0006) the relationship of the cutting force, feedrate, and depth-of-cut is found. The intermediate procedures are shown in Appendix D. The final result is:

$$P_1 = 20786*(a.s)^{0.75} \quad \text{lbf} \quad (2.2.1)$$

If one assumes $P_3 = 0.6*P_1$, according to Koenigsberger and Kaczmarek, P_3 becomes:

$$P_3 = 12471*(a.s)^{0.75} \quad \text{lbf} \quad (2.2.2)$$

Since the workpiece is eccentrically mounted, the depth-of-cut (a) becomes a time-varying function. In Appendix E it is shown that the depth-of-cut has the form $a = d*(\cos(\omega t)-1)+b+y$ where d is the amount of eccentricity, b is the desired depth-of-cut, and y is the workpiece lateral displacement due to vibraton. Substituting the expression into Eqs.(2.2.1) and (2.2.2), the expressions for the cutting forces in an eccentric turning operation of aluminum parts are:

$$P_1 = 20786*s^{0.75}*(d(\cos\ \omega t-1)+b+y)^{0.75} \quad \text{lbf} \quad (2.2.3)$$

$$P_3 = 12471*s^{0.75}*(d(\cos\ \omega t-1)+b+y)^{0.75} \quad \text{lbf} \quad (2.2.4)$$

Notice that the variable 'y' is raised to the power of 0.75 in above equations. This factor will complicate the equations of motion to the extent that they cannot be solved by any analytical way. The reason is that this factor destroys the unity power of the variable y in different terms in the equations of motion. As a result, another expression with the depth-of-cut raised to the power of unity is preferable.

Kaczmarek [24] reported the following empirical co-relation for cutting of carbon steel using a carbide tool:

$$P_1 = 191*a*s^{0.75} \quad \text{kg} \quad (2.2.5)$$

The units for the main cutting force in Eq.(2.2.5) is kg whereas those for depth-of-cut and feedrate are mm and mm/rev

respectively. It is noticed that for a fixed depth-of-cut, Eq.(2.2.1) can be expressed as Eq.(2.2.5) multiplied by a fraction. The procedures for obtaining this fraction are shown in Appendix F in which three constants corresponding to values of 0.03", 0.06", and 0.09" are evaluated. The three fractions are 0.413, 0.347, and 0.314 respectively. In the experiments an intermediate depth-of-cut of 0.06" is selected. Hence, the main cutting force for an aluminum workpiece can be expressed as: $(191)(0.347)a*s^{0.75}$ kg or $P_1 = 66.277*a*s^{0.75}$ kg. To convert the unit of this equaton to Newtons (N), it is further multiplied by the factor 9.81. Thus,

$$P_1 = 650.18*a*s^{0.75} \quad \text{N} \qquad (2.2.6)$$

Again assuming $P_3 = 0.6*P_1$, this yields:

$$P_3 = 390.11*a*s^{0.75} \quad \text{N} \qquad (2.2.7)$$

Substituting the expression for depth-of-cut from Appendix E, the final forms for P_1 and P_3 are:

$$P_1 = 650.18*(d(\cos \omega t-1)+b+y)*s^{0.75} \quad \text{N} \qquad (2.2.8)$$

$$P_3 = 390.11*(d(\cos \omega t-1)+b+y)*s^{0.75} \quad \text{N} \qquad (2.2.9)$$

Note that in these equations the displacement y occurs with a power of unity.

2.3 FORCED VIBRATION ANALYSIS

Eq.(2.1.9) is the equation of motion for a free beam. To analyze the forced vibration, the external forcing terms are put on the right hand side of the equation. In turning, the external forces acting on the beam come from the tool. Taking into consideration the directions of forces and sign of the coordinate system as defined in Section 2.1.1, the equations of motion for forced vibration are:

$$\left.\begin{aligned} &\frac{\partial^2 z}{\partial t^2} + \frac{EI}{\rho A}\frac{\partial^4 z}{\partial x^4} - \omega^2 z + 2\omega\dot{y} - 2\omega^2 d \sin \omega t \\ &\qquad = \frac{650.18}{\rho A} S^{0.75}(d(\cos \omega t - 1) + b + y)\delta(x - x_o) \\ &\frac{\partial^2 y}{\partial t^2} + \frac{EI}{\rho A}\frac{\partial^4 y}{\partial x^4} - \omega^2 y - 2\omega\dot{z} - 2\omega^2 d \cos \omega t \\ &\qquad = \frac{390.11}{\rho A} S^{0.75}(d(\cos \omega t - 1) + b + y)\delta(x - x_o) \end{aligned}\right\} \quad (2.3.1)$$

Re-arranging Eq.(2.3.1) yields:

$$\left.\begin{aligned} &\frac{\partial^2 z}{\partial t^2} + \frac{EI}{\rho A}\frac{\partial^4 z}{\partial x^4} - \omega^2 z + 2\omega\dot{y} = 2\omega^2 d \sin \omega t \\ &\qquad + \frac{650.18}{\rho A} S^{0.75}(d(\cos \omega t - 1) + b + y)\delta(x - x_o) \\ &\frac{\partial^2 y}{\partial t^2} + \frac{EI}{\rho A}\frac{\partial^4 y}{\partial x^4} - \omega^2 y - 2\omega\dot{z} = 2\omega^2 d \cos \omega t \\ &\qquad + \frac{390.11}{\rho A} S^{0.75}(d(\cos \omega t - 1) + b + y)\delta(x - x_o) \end{aligned}\right\} \quad (2.3.2)$$

Since the cutting force is a point force, in above equations, Eqs.(2.3.1) and (2.3.2), the forcing terms are multiplied by the Dirac delta function, $\delta(x-x_0)$, which has the property that $\int_{-\infty}^{\infty} f(x)\,\delta(x-x_0) = f(x_0)$. Furthermore, to keep the dimensions consistent on both sides of the equation, the forcing terms are divided by the density and cross-sectional area of the workpiece as well.

Re-arranging the variable terms of the above equation, one obtains:

$$\left.\begin{aligned}
&\frac{\partial^2 z}{\partial t^2} + \frac{EI}{\rho A}\frac{\partial^4 z}{\partial x^4} - \omega^2 z + 2\omega\dot{y} - \left(\frac{650.18}{\rho A}\, S^{0.75}\right) y\,\delta(x-x_o) \\
&\quad = 2\omega^2 d \sin\omega t + \frac{650.18}{\rho A}\, S^{0.75}\,(d(\cos\omega t - 1)+b)\,\delta(x-x_o) \\
&\frac{\partial^2 y}{\partial t^2} + \frac{EI}{\rho A}\frac{\partial^4 y}{\partial x^4} - \omega^2 y - 2\omega\dot{z} - \left(\frac{390.11}{\rho A}\, S^{0.75}\right) y\,\delta(x-x_o) \\
&\quad = 2\omega^2 d \cos\omega t + \frac{390.11}{\rho A}\, S^{0.75}\,(d(\cos\omega t - 1)+b)\,\delta(x-x_o)
\end{aligned}\right\} \quad (2.3.3)$$

To solve Eq.(2.3.3), it is again assumed that the solutions can be expressed as infinite series of the forms $z(x,t) = \sum_{n=1}^{\infty} \phi_n(x) A_n(t)$ and $y(x,t) = \sum_{n=1}^{\infty} \phi_n(x) B_n(t)$, where $\phi_n(x)$ is an admissible function of a clamped-free beam.

Substituting the solutions and multiplying Eq.(2.3.3) by another comparison function, ϕ_k, it becomes:

$$
\left.
\begin{aligned}
&\sum_{n=1}^{\infty}\int_0^{\ell}\phi_k\phi_n\ddot{A}_n dx + \frac{EI}{\rho A}\sum_{n=1}^{\infty}\int_0^{\ell}\phi_k\phi_n^{(4)}A_n dx - \omega^2\sum_{n=1}^{\infty}\int_0^{\ell}\phi_k\phi_n A_n dx \\
&+ 2\omega\sum_{n=1}^{\infty}\int_0^{\ell}\phi_k\phi_n\dot{B}_n dx - \left(\frac{650.18}{\rho A}\right)S^{0.75}\sum_{n=1}^{\infty}\int_0^{\ell}\phi_k\phi_n B_n\delta(x-x_o)dx \\
&= \int_0^{\ell}\left\{2\omega^2 d\sin\omega t + \frac{650.18}{\rho A}S^{0.75}[d(\cos\omega t-1)+b]\delta(x-x_o)\right\}\phi_k dx \\
&\sum_{n=1}^{\infty}\int_0^{\ell}\phi_k\phi_n\ddot{B}_n dx + \frac{EI}{\rho A}\sum_{n=1}^{\infty}\int_0^{\ell}\phi_k\phi_n^{(4)}B_n dx - \omega^2\sum_{n=1}^{\infty}\int_0^{\ell}\phi_k\phi_n B_n dx \\
&- 2\omega\sum_{n=1}^{\infty}\int_0^{\ell}\phi_k\phi_n\dot{A}_n dx - \left(\frac{390.11}{\rho A}\right)S^{0.75}\sum_{n=1}^{\infty}\int_0^{\ell}\phi_k\phi_n\delta(x-x_o)dx \\
&= \int_0^{\ell}\left\{2\omega^2 d\cos\omega t + \frac{390.11}{\rho A}S^{0.75}[d(\cos\omega t-1)+b]\delta(x-x_o)\right\}\phi_k dx
\end{aligned}
\right\} \quad (2.3.4)
$$

Let $\langle fz\rangle = 2\omega^2 d\sin\omega t + 650.18 * s^{0.75}(d(\cos\omega t-1)+b)\delta(x-x_o)$

$\langle Fy\rangle = 2\omega^2 d\cos\omega t + 390.11 * s^{0.75}(d(\cos\omega t-1)+b)\delta(x-x_o)$

By integration, Eq.(2.3.4) becomes:

$$
\left.
\begin{aligned}
&\ell\sum_{n=1}^{\infty}\delta_{kn}\ddot{A}_n + \frac{EI}{\rho A}\beta_n^4\ell\sum_{n=1}^{\infty}\delta_{kn}A_n - \omega^2\ell\sum_{n=1}^{\infty}\delta_{kn}A_n + 2\omega\ell\sum_{n=1}^{\infty}\delta_{kn}\dot{B}_n \\
&- \left(\frac{650.18}{\rho A}S^{0.75}\right)\sum_{n=1}^{\infty}\int_0^{\ell}\phi_k\phi_n\delta(x-x_o)B_n dx = \langle F_z\rangle\int_0^{\ell}\phi_k dx \\
&\ell\sum_{n=1}^{\infty}\delta_{kn}\ddot{B}_n + \frac{EI}{\rho A}\beta_n^4\ell\sum_{n=1}^{\infty}\delta_{kn}B_n - \omega^2\ell\sum_{n=1}^{\infty}\delta_{kn}B_n - 2\omega\ell\sum_{n=1}^{\infty}\delta_{kn}\dot{A}_n \\
&- \left(\frac{390.11}{\rho A}S^{0.75}\right)\sum_{n=1}^{\infty}\int_0^{\ell}\phi_k\phi_n\delta(x-x_o)B_n dx = \langle F_y\rangle\int_0^{\ell}\phi_k dx
\end{aligned}
\right\} \quad (2.3.5)
$$

Denoting $S_1 = \frac{650.18}{\rho A} * s^{0.75}$ and $S_2 = \frac{390.11}{\rho A} * s^{0.75}$, Eq.(2.3.5) can be further simplified as:

$$\left.\begin{aligned} &\ell \sum_{n=1}^{\infty} \delta_{kn} \ddot{A}_n + \frac{EI}{\rho A} \beta_n^4 \ell \sum_{n=1}^{\infty} \delta_{kn} A_n - \omega^2 \ell \sum_{n=1}^{\infty} \delta_{kn} A_n + 2\omega \ell \sum_{n=1}^{\infty} \delta_{kn} \dot{B}_n \\ &\quad - S_1 \sum_{n=1}^{\infty} \phi_k(x_o) \phi_n(x_o) B_n = \langle F_z \rangle \int_0^{\ell} \phi_k dx \\ &\ell \sum_{n=1}^{\infty} \delta_{kn} \ddot{B}_n + \frac{EI}{\rho A} \beta_n^4 \ell \sum_{n=1}^{\infty} \delta_{kn} B_n - \omega^2 \ell \sum_{n=1}^{\infty} \delta_{kn} B_n - 2\omega \ell \sum_{n=1}^{\infty} \delta_{kn} \dot{A}_n \\ &\quad - S_2 \sum_{n=1}^{\infty} \phi_k(x_o) \phi_n(x_o) B_n = \langle F_y \rangle \int_0^{\ell} \phi_k dx \end{aligned}\right\} \quad (2.3.6)$$

Eq.(2.3.6) is the most compact and general equation of motion describing the eccentric turning process. In the equation, the functions $\phi_n(x_0)$ and $\phi_k(x_0)$ depend on the position of the tool. Hence, for further evaluation of the equation, one has to specify x_0, the location of tool, and the number of terms to be used in the infinite series.

For example, let x_0 be ℓ, the total length of the beam, which corresponds to the start-up motion. It is shown in Appendix G that $\phi_n(x=\ell) = 2*(-1)^{n+1}$. Therefore, for $x=x_0=\ell$, Eq.(2.3.6) can be written as:

$$
\left.
\begin{aligned}
&\ell \sum_{n=1}^{\infty} \delta_{kn} \dot{A}_n + \frac{EI}{\rho A} \beta_n^4 \ell \sum_{n=1}^{\infty} \delta_{kn} A_n - \omega^2 \ell \sum_{n=1}^{\infty} \delta_{kn} A_n + 2\omega\ell \sum_{n=1}^{\infty} \delta_{kn} \dot{B}_n \\
&\qquad - 4S_1 \sum_{n=1}^{\infty} (-1)^{n+k+2} B_n = \langle F_z \rangle \int_0^{\ell} \phi_k \, dx \\
&\ell \sum_{n=1}^{\infty} \delta_{kn} \ddot{B}_n + \frac{EI}{\rho A} \beta_n^4 \ell \sum_{n=1}^{\infty} \delta_{kn} B_n - \omega^2 \ell \sum_{n=1}^{\infty} \delta_{kn} B_n - 2\omega\ell \sum_{n=1}^{\infty} \delta_{kn} \dot{A}_n \\
&\qquad - 4S_2 \sum_{n=1}^{\infty} (-1)^{n+k+2} B_n = \langle F_y \rangle \int_0^{\ell} \phi_k \, dx
\end{aligned}
\right\} \qquad (2.3.7)
$$

which can be further expanded to a matrix form as follows:

$$
\left.
\begin{aligned}
&\ell \begin{bmatrix} 1 & & \\ & \ddots & \\ & & 1 \end{bmatrix} \begin{Bmatrix} \dot{A}_1 \\ \vdots \\ \dot{A}_n \end{Bmatrix} + \ell \begin{bmatrix} \frac{EI}{\rho A}\beta_1^4 & & \\ & \ddots & \\ & & \frac{EI}{\rho A}\beta_n^4 \end{bmatrix} \begin{Bmatrix} A_1 \\ \vdots \\ A_n \end{Bmatrix} - \ell \begin{bmatrix} \omega^2 & & \\ & \ddots & \\ & & \omega^2 \end{bmatrix} \begin{Bmatrix} A_1 \\ \vdots \\ A_n \end{Bmatrix} \\
&+ 2\omega\ell \begin{bmatrix} 1 & & \\ & \ddots & \\ & & 1 \end{bmatrix} \begin{Bmatrix} \dot{B}_1 \\ \vdots \\ \dot{B}_n \end{Bmatrix} - 4S_1 \begin{bmatrix} 1 & -1 & 1 & \cdots \\ -1 & 1 & -1 & \cdots \\ 1 & -1 & 1 & \cdots \\ \cdot & \cdot & \cdot & \cdots \end{bmatrix} \begin{Bmatrix} B_1 \\ \vdots \\ B_n \end{Bmatrix} = \begin{Bmatrix} \langle F_z \rangle \int \phi_1 dx \\ \vdots \\ \langle F_z \rangle \int \phi_n dx \end{Bmatrix} \\
&\begin{bmatrix} 1 & & \\ & \ddots & \\ & & 1 \end{bmatrix} \begin{Bmatrix} \ddot{B}_1 \\ \vdots \\ \ddot{B}_n \end{Bmatrix} + \ell \begin{bmatrix} \frac{EI}{\rho A}\beta_1^4 & & \\ & \ddots & \\ & & \frac{EI}{\rho A}\beta_n^4 \end{bmatrix} \begin{Bmatrix} B_1 \\ \vdots \\ B_n \end{Bmatrix} - \ell \begin{bmatrix} \omega^2 & & \\ & \ddots & \\ & & \omega^2 \end{bmatrix} \begin{Bmatrix} B_1 \\ \vdots \\ B_n \end{Bmatrix} \\
&- 2\omega\ell \begin{bmatrix} 1 & & \\ & \ddots & \\ & & 1 \end{bmatrix} \begin{Bmatrix} \dot{A}_1 \\ \vdots \\ \dot{A}_n \end{Bmatrix} - 4S_2 \begin{bmatrix} 1 & -1 & 1 & \cdots \\ -1 & 1 & -1 & \cdots \\ 1 & -1 & 1 & \cdots \\ \cdot & \cdot & \cdot & \cdots \end{bmatrix} \begin{Bmatrix} B_1 \\ \vdots \\ B_n \end{Bmatrix} = \begin{Bmatrix} \langle F_y \rangle \int \phi_1 dx \\ \vdots \\ \langle F_y \rangle \int \phi_n dx \end{Bmatrix}
\end{aligned}
\right\} \qquad (2.3.8)
$$

Eq.(2.3.8) can be assembled to become:

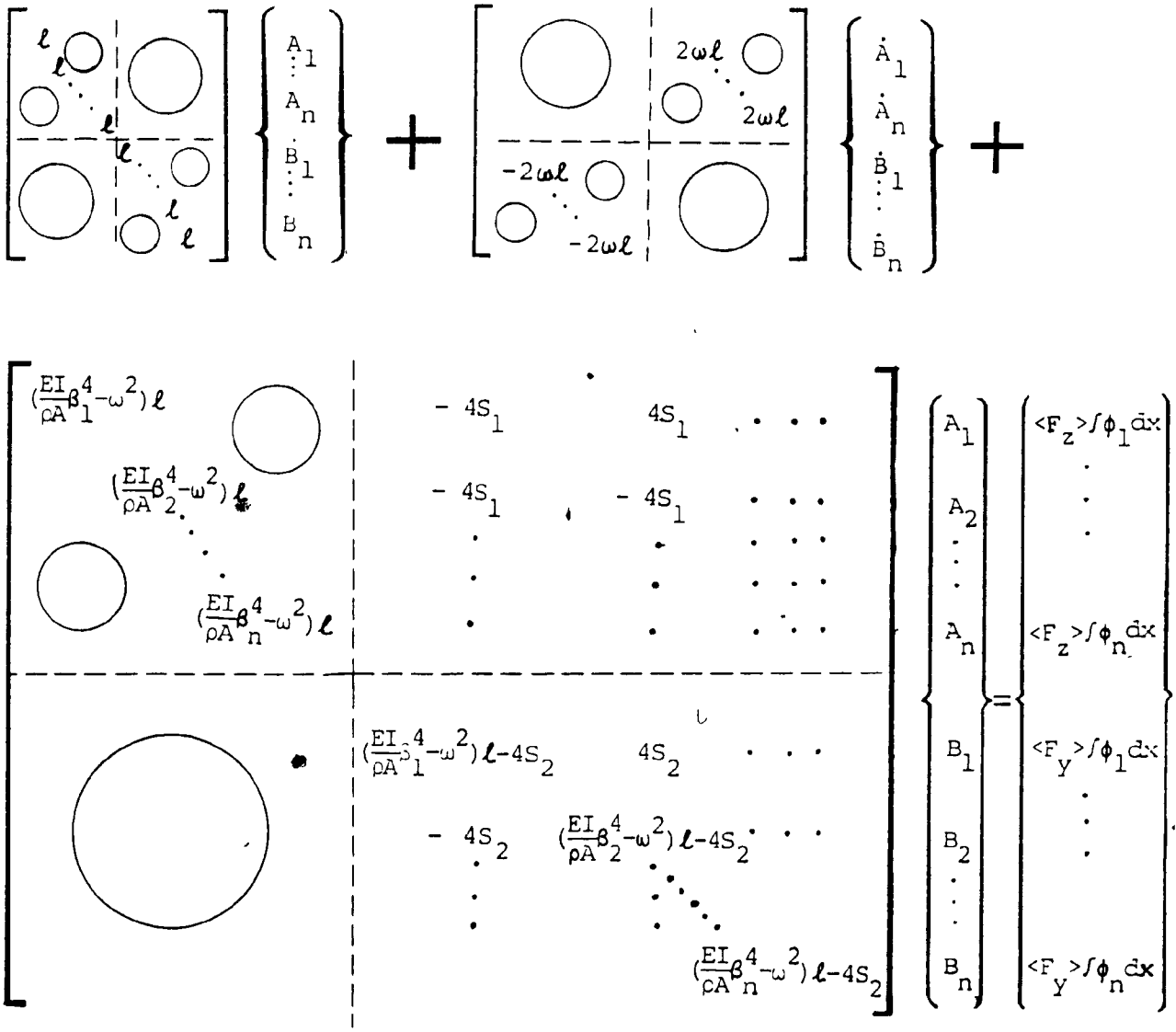

The above equation has both homogeneous and particular solutions of the general form: $[A]\{\ddot{q}\}+[B]\{\dot{q}\}+[C]\{q\} = \{Q\}$

where $\{q\} = \begin{Bmatrix} A_1 \\ \vdots \\ A_n \\ B_1 \\ \vdots \\ B_n \end{Bmatrix}$ $\{Q\} = \begin{Bmatrix} \langle F_z \rangle \int \phi_1 dx \\ \vdots \\ \langle F_z \rangle \int \phi_n dx \\ \langle F_y \rangle \int \phi_1 dx \\ \vdots \\ \langle F_y \rangle \int \phi_n dx \end{Bmatrix}$

Two terms of the infinite series (i.e., k=1,2 and n=1,2) are used to demonstrate how to evaluate the equation. The above matrix equation becomes:

$$\begin{bmatrix} \ell & 0 & 0 & 0 \\ 0 & \ell & 0 & 0 \\ 0 & 0 & \ell & 0 \\ 0 & 0 & 0 & \ell \end{bmatrix} \begin{Bmatrix} \ddot{A}_1 \\ \ddot{A}_2 \\ \ddot{B}_1 \\ \ddot{B}_2 \end{Bmatrix} + \begin{bmatrix} 0 & 0 & 2\omega\ell & 0 \\ 0 & 0 & 0 & 2\omega\ell \\ -2\omega\ell & 0 & 0 & 0 \\ 0 & -2\omega\ell & 0 & 0 \end{bmatrix} \begin{Bmatrix} \dot{A}_1 \\ \dot{A}_2 \\ \dot{B}_1 \\ \dot{B}_2 \end{Bmatrix} +$$

$$\begin{bmatrix} (\frac{EI}{\rho A}\beta_1^4 - \omega^2)\ell & 0 & -4S_1 & 4S_1 \\ 0 & (\frac{EI}{\rho A}\beta_1^4 - \omega^2)\ell & 4S_1 & -4S_1 \\ 0 & 0 & (\frac{EI}{\rho A}\beta_1^4 - \omega^2)\ell - 4S_2 & 4S_2 \\ 0 & 0 & 4S_2 & (\frac{EI}{\rho A}\beta_2^4 - \omega^2)\ell - 4S_2 \end{bmatrix} \begin{Bmatrix} A_1 \\ A_2 \\ B_1 \\ B_2 \end{Bmatrix} = \begin{Bmatrix} \langle F_z \rangle \int \phi_1 dx \\ \langle F_z \rangle \int \phi_2 dx \\ \langle F_y \rangle \int \phi_1 dx \\ \langle F_y \rangle \int \phi_2 dx \end{Bmatrix} \quad (2.3.9)$$

Exact solutions for Eq.(2.3.9) are still difficult to find. However, since the eigenvalues are of particular interest in a dynamic system, instead of evaluating the total solution for Eq.(2.3.9), only the eigenvalues are determined.

Moreover, a close look at Eq.(2.3.9) indicates that once the physical dimensions of the workpiece is selected, the eigenvalues will become a function of the angular velocity and feedrate. Appendix H shows the change of eigenvalues with respect to three different angular velocities and four different feedrates.

A computer program is employed in the computation. Specifically, the IMSL subroutine, EIGZF, is used to save programming effort. In the program, the length and diameter of the workpiece are set to be 8" and 3" respectively, which are equal to the physical dimensions of the experimental specimen. All properties of aluminum are obtained from the reference by Shigley [25]. From the appendix, the results are further collected in the following table for reference.

SPINDLE SPEED(RPM)	FEEDRATE(IPR)	EIGENVALUES
69	0.000	$\pm 0.247*10^{-8} \pm 0.830*10^{4}$ i $\pm 0.272*10^{-6} \pm 0.520*10^{5}$ i
	0.005	$\pm 0.373*10^{-4} \pm 0.830*10^{4}$ i $\pm 0.111*10^{-4} \pm 0.520*10^{5}$ i
	0.015	$\pm 0.883*10^{-5} \pm 0.830*10^{4}$ i $\pm 0.146*10^{-3} \pm 0.520*10^{5}$ i
	0.030	$\pm 0.143*10^{-3} \pm 0.830*10^{4}$ i $\pm 0.212*10^{-4} \pm 0.520*10^{5}$ i
180	0.000	$\pm 0.329*10^{-8} \pm 0.832*10^{4}$ i $\pm 0.339*10^{-6} \pm 0.520*10^{5}$ i
	0.005	$\pm 0.373*10^{-4} \pm 0.832*10^{4}$ i $\pm 0.911*10^{-4} \pm 0.520*10^{5}$ i
	0.015	$\pm 0.849*10^{-4} \pm 0.832*10^{4}$ i $\pm 0.309*10^{-3} \pm 0.520*10^{5}$ i
	0.030	$\pm 0.143*10^{-3} \pm 0.832*10^{4}$ i $\pm 0.491*10^{-3} \pm 0.520*10^{5}$ i
1800	0.000	$\pm 0.311*10^{-8} \pm 0.848*10^{4}$ i $\pm 0.289*10^{-6} \pm 0.522*10^{5}$ i
	0.005	$\pm 0.373*10^{-4} \pm 0.848*10^{4}$ i $\pm 0.117*10^{-4} \pm 0.522*10^{5}$ i
	0.015	$\pm 0.849*10^{-4} \pm 0.848*10^{4}$ i $\pm 0.149*10^{-4} \pm 0.522*10^{5}$ i
	0.030	$\pm 0.143*10^{-3} \pm 0.848*10^{4}$ i $\pm 0.164*10^{-4} \pm 0.522*10^{5}$ i

TABLE 2-1. COLLECTIVE RESULTS FROM APPENDIX H

2.4 RESULTS AND DISCUSSIONS

In Section 2.1.2, the equation of the free vibration of the beam (i.e., Eq.(2.1.9)) has a form resembling to that developed by Bhat and Sankar [8]. This similarity suggests that the derivation of the equations of motion for the eccentric turning is correct.

However, the difference between them is two-fold. In this work, both the lateral and vertical motions of the workpiece are considered. This is why Eq.(2.1.9) actually consists of two equations describing the motions in the horizontal and vertical directions respectively. In Bhat and Sankar's work, only the vertical deflection is considered. On the other hand, there are coupling terms with opposite signs in Eq.(2.1.9). These coupling terms come from the eccentricity imposed on the problem.

Attention is next drawn to the Dirac delta function, $\delta(x-x_0)$, in Eq.(2.3.1). Although the equation is claimed to be the equation of motion for eccentric turning, it is only an approximation of the problem since the delta function is a stationary function valid only for the tool at one particular location. In reality, a constant velocity function, such as $\delta(x-st)$, where s represents the feedrate, should be used. However, such a function will complicate the equation of motion to the extent that further analytical analysis of the equation will be extremely difficult. To compensate for such deficiency,

the delta function without a constant velocity is used in the analysis, which seems reasonable as long as the feedrate is confined to a low value.

Another approximation in Eq.(2.3.1) is the moment of inertia, I, which is assumed to be a constant. Strictly speaking, it should vary with time as chips are continuously being formed during the process. Again the analysis would be exceedingly difficult and is not attempted in this work. Furthermore, since the only scope of the analysis is to have a conspectus about the dynamics of eccentric turning, such an assumption is good enough for this purpose.

The first observation with respect to the results from Appendix H and Tabele 2.1 is that for each specific feedrate, the eight corresponding eigenvalues are actually two complex conjugates pairs. The complex conjugate pairs have almost the same corresponding imaginary values for all feedrates. Obviously, the difference comes from the changes in feedrate. In spite of the significant change of feedrate, the difference is small for the imaginary values. Therefore, the analysis shows that the feedrate has little effect on the natural frequencies of an eccentric turning process. However, the real parts of the eigenvalues are larger for a higher feedrate. This implies that a higher degree of instability is obtained for a higher feedrate, which is physically true. If the feedrate is zero, which corresponds to a non-cutting situation,

the real part of the eigenvalue is so small (in the order of 10^{-8}) that it is believed to come from the round-off error in the computation.

The second observation with respect to the appendix is the existence of both the imaginary and the real parts for all the eigenvalues. Since the solution is assumed to be in the form of $e^{\lambda t}$, a positive real part of the eigenvalue implies that the system solution will build up to a large amplitude. Hence, from a mathematical point of view, the analysis shows the eccentric turning is an unstable process.

The final observation of the appendix reveals that all the real parts of the eigenvalues are relatively much smaller than their corresponding imaginary parts. Actually, the real parts are usually 10^{8} times smaller than the imaginary parts. Thus the degree of instability is actually very small and as noted from above, it may be due only to computational round-off error.

It is important to note that the analysis has neglected the inherent structural damping. Should it have been taken into consideration, a solution of the form $e^{(\lambda_R+\lambda_I-c)t}$, where λ_R, λ_I are the real and imaginary parts of λ and c is the structural damping factor, would have been assumed. Since the structural damping is neglected, it seems safe to assume that the actual process will be stable for low feedrates.

Table 2.1 indicates that the natural frequency changes

noticeably with the change of angular velocity. Hence, the analysis shows that the RPM has a greater effect on the natural frequency of the system than the feedrate.

To sum up the above discussion, it is concluded that for a low feedrate, the experimental eccentric turning operation is a stable process regardless of the presence of a small positive real part in the eigenvalue.

Of course, the analysis performed and consequently the results obtained are still quite crude due to the numerous assumptions and approximations that have been made to obtain a manageable model. Also, only a small number of feedrates and angular velocity have been used in the calculations and therefore the results of this analysis should be used with caution.

CHAPTER 3

THE EXPERIMENTAL MICRO-COMPUTER ADAPTIVE CONTROL SYSTEM

This chapter is divided into three main sections. The first section describes the basic structure of a micro-computer adaptive control (AC) system while the last two outline the hardware and software of the experimental set-up employed in this project.

3.1 BASIC STRUCTURE OF A MICRO-COMPUTER ADAPTIVE CONTROL (AC) SYSTEM

The basic function of an AC system is to maintain a prescribed relationship between the output and the reference input by comparing them and using their difference as a means of control. When an AC unit is used in a machining process, its main purpose is to maintain the cutting conditions within certain desired limits in order to satisfy some criteria such as safety, reduction of time or cost, tool life and etc.

Since micro-computer technology has developed very rapidly in recent years, micro-computers are a logical tool to use to construct an AC system. When a micro-computer adaptive control is retrofitted to an NC machine tool, the resulting system can be separated into two basic parts, as shown in

Fig. 3.1 . One part consists of the NC servo and the physical process. The other part is the micro-computer control unit.

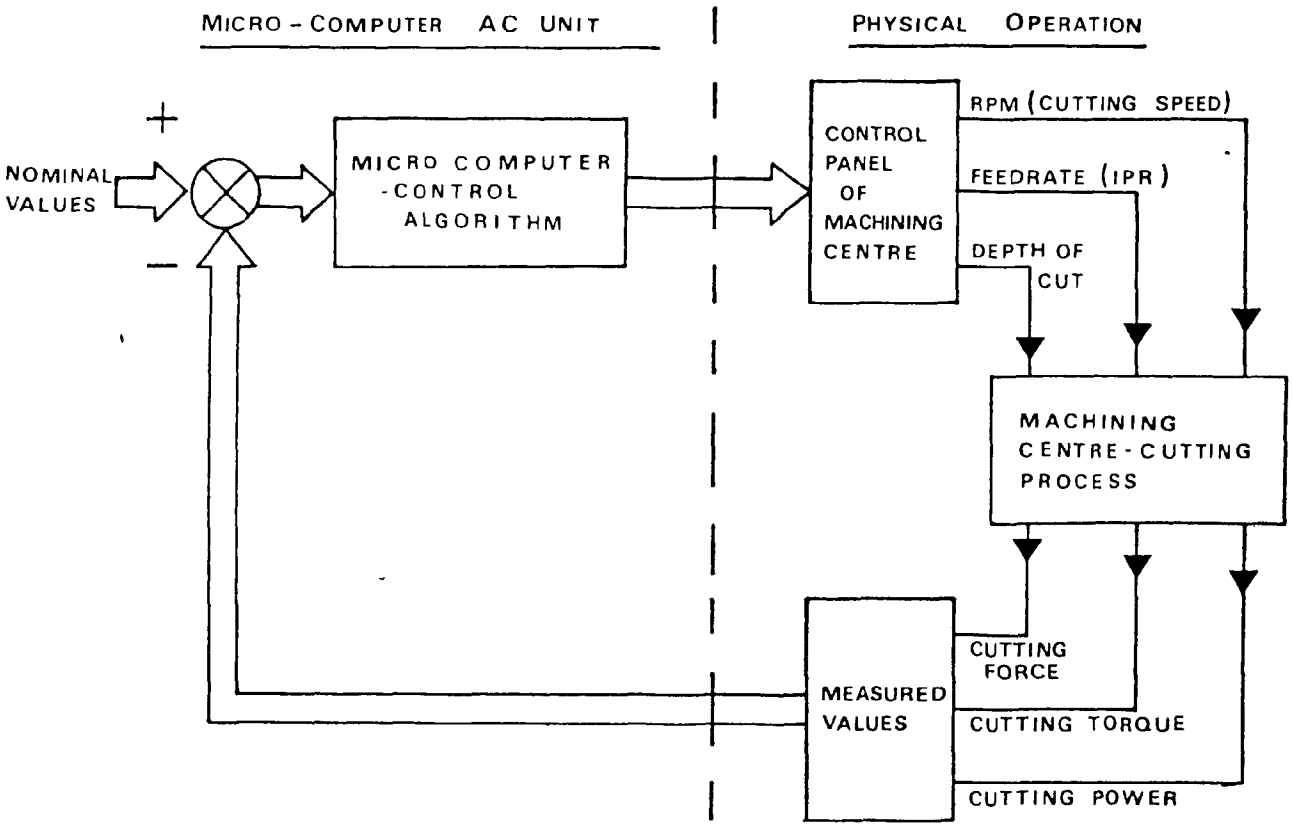

FIG 3.1 GENERAL FEATURES OF A DIGITAL ADAPTIVE SYSTEM

The basic function of the micro-computer unit is to monitor key process variables such as cutting force, cutting torque, or cutting power, and to adjust the available controllable parameters such as cutting speed, feedrate, or depth-of-cut. Its basic components consists of an amplifier, an

analog-to-digital (A/D) converter, a micro-processor, and a digital-to-analog (D/A) converter.

3.2 THE HARDWARE STRUCTURE OF THE EXPERIMENTAL AC SYSTEM

This section describes the features and functions of each hardware component in the experimental AC system. The existing AC system was designed and built by Leung [26].

3.2.1 The NC Lathe Employed in the Project

The NC machine employed in this project is a LeBlond Tape Turn Regal Lathe with General Electric (GE) 550L control unit. It is capable of contour turning of parts. It has a 19" swing over the bed and carriage wings and 12" swing over the cross slide.

The NC lathe is equipped with a 10 horsepower motor and has twelve spindle speed selections from 45 to 1800 RPM. The spindle speed must be set manually but can be indicated by tape. When spindle speed is being changed, there is a short period of idle time when the gears are switched from one to another. Its feedrate ranges from 0.1 to 100 IPR and typical accuracy is ± 0.001" on diameter and ± 0.002" on length.

The program can be entered through one inch wide, eight channel punched tape, or by direct programming through the control panel. The tape reader accepts both EIA and ASCII tapes. Manual control through power differential resolvers is

also available.

The control panel has been modified slightly by the addition of a simple switch to allow the feedrate override function to be controlled either by the standard potentiometer or by means of an external voltage source. The permissible external voltage range is 0.0 to +5.0 volts corresponding linearly to an actual feedrate in the range 0 to 100 % of the programmed feedrate. Currently this is the only feature provided by the NC control to change the cutting conditions during normal real-time operation. Fig. 3.2 is a view of the lathe without the AC unit.

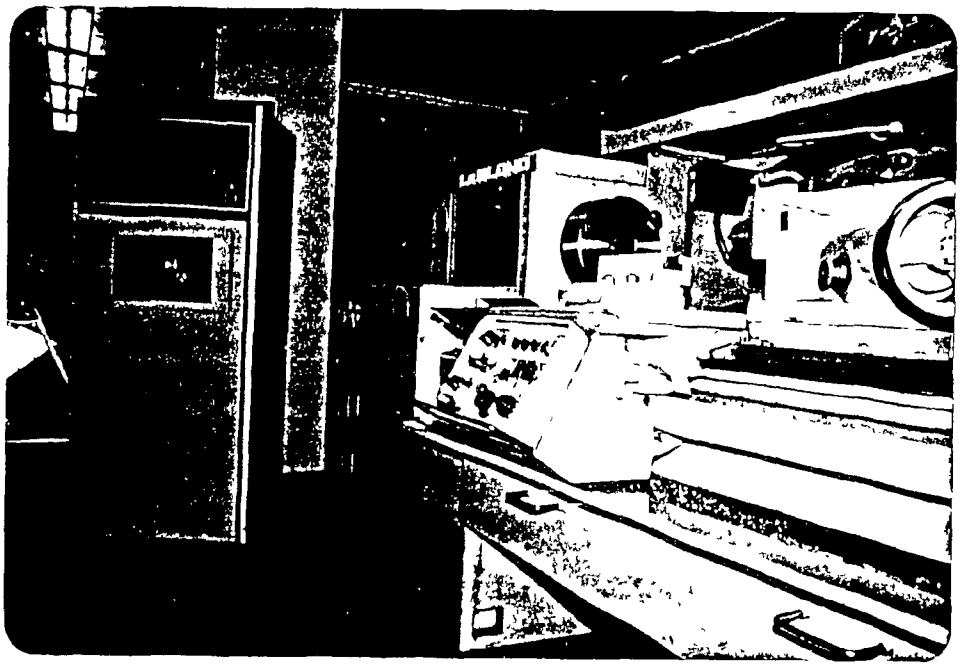

FIG 3·2 A PICTURE OF THE LEBLOND LATHE

3.2.2 The General Features and Functions of the Components of the Micro-computer AC System

In this project, direct measurement of the main cutting force is used as the process-determining value. The cutting force rather than the cutting torque is used because it is easy to implement. The principle reason for not choosing cutting power as the variable to be monitored is that, though it is very easy to measure, it has a fairly slow dynamic response to changing cutting conditions due to the rotary inertia of the lathe.

A schematic diagram of the experimental set-up is shown in Fig. 3.3 . Observation of the figure shows that it has a similar structure to that shown in Fig. 3.1 .

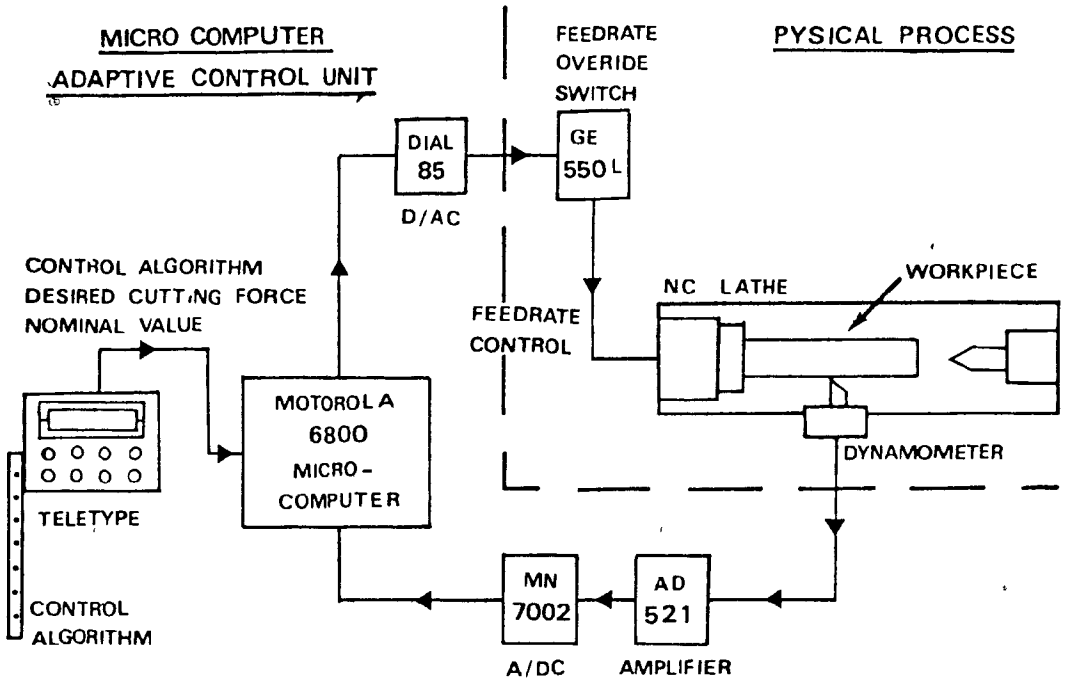

FIG 3.3 SCHEMATIC DIAGRAM OF THE EXPERIMENTAL SET UP

Fig. 3.4 is a picture of the actual hardware used. In this picture, the oscilloscope is used to record the transient behaviour of the cutting force and the computer controlled feedrate override signal.

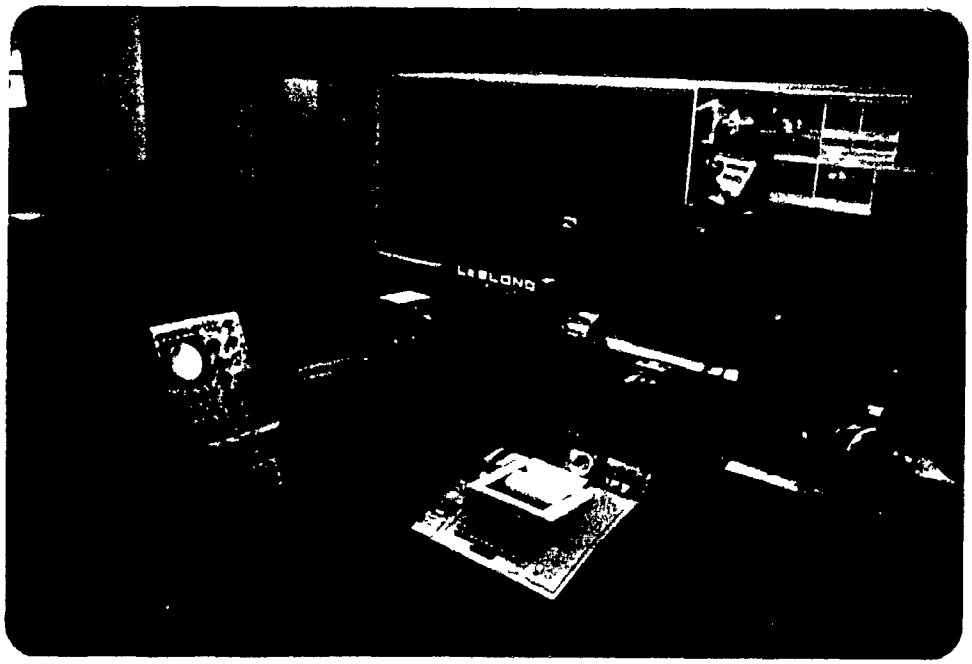

FIG 3.4 A PICTURE OF THE ENTIRE EXPERIMENTAL SET UP

The experimental micro-computer AC unit consists of six components; namely, the dynamometer, the amplifier, the A/D converter, the micro-computer, the D/A converter, and the teletype. The function of the dynamometer is to convert a force signal to a voltage. The voltage output is linearly proportional to the force. The employed dynamometer uses multiple strain gauges and is capable of measuring three

orthogonal forces independently at the same time. It is mounted on the tool holder of the NC lathe. It is built by COOK, SMITH, & ASSOCIATES CORPORATION.

The continubus signal from the dynamometer is amplified by the amplifier. The amplifier used in this project is Model AD521 from ANALOG DEVICES. Its maximum output voltage is restricted to 10 volts and it can be operated at gains from 0.1 to 1000 with the addition of two external resistors. For this experiment, the configuration of the amplifier is set to be a gain of 1000. For high accuracy, the amplifier has gain and offset trims to adjust the gain and eliminate the input offset voltage.

The conversion from an analog to digital signal is carried out by a MN7002 integrated circuit (IC) chip from MICRO NETWORKS CORPORATION. It can be operated by either 16-channels single-ended or 8-channels true differential. For this experiment, the differential input configuration is selected to give a better noise immunity. The analog voltage range is +10 volts and the digital output is 12 bits. The MN7002 data acquisition system is very flexible. It can be operated from the internal 1MHz clock, or a user supplied clock signal. In the set-up, an external clock triggering device is used.

The computing and decision making device in the experimental AC system is a MOTOROLLA 6800 micro-computer. It is an 8-bits processor supported by a crystal clock oscillator,

data bus buffer, read only memory (ROM), and random access memory (RAM). It is equipped with peripheral address lines and a bi-directional 8-bits data bus through which the computer communicates with the outside. The memory of the computer can also be increased by inserting additional memory boards. On the memory board MPA2 two TM2516JDL ultraviolet light erasable programmable read only memories (EPROM) chips are added to store the floating point arithmetic package developed by Zsombor-Murray [27] (McGill University).

The conversion of the digital signal from the computer to an analog signal is carried out by a D/A C 85 series IC chip from MICRO NETWORKS CORPORATION. It is this signal which is applied to the NC lathe to adjust the controlled parameter; i.e., feedrate, in the AC system. The chip is a 12-bits D/A converter and provides different output ranges by connecting the pins in different configurations. The selected output range is -5.0 to +5.0 volts in this experiment. The converter guarantees ±1/2 LSB (least significant bit) linearity on the full operating temperature. External offset and gain adjustment are provided as well to adjust for positive full scale voltage.

The micro-computer program or any command to the computer is input through a teletype. The teletype is actually a serial peripheral device and the computer is a parallel one. The data to be transmitted between them is carried out by an asynchronous communications interface adapter (ACIA) which is a

serial to parallel converter.

Further detail functions and circuitry of each device are described by Leung [26].

Fig. 3.5 is a general view of the micro-computer AC system with the covers removed from the various components.

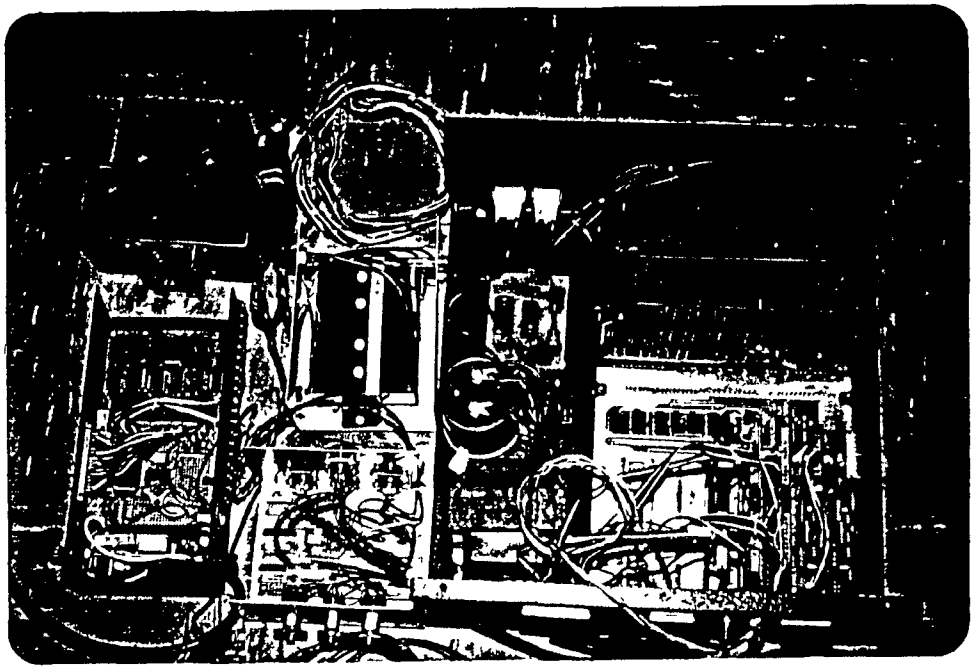

FIG 3·5 A PICTURE OF THE HARDWARE COMPONENTS

3.3 THE SOFTWARE STRUCTURE OF THE CONTROL ALGORITHM

Since one of the aims of this work is to develop an efficient and flexible control algorithm, this section outlines the peculiarities of the micro-computer control algorithm employed in this project. It consists of four sub-sections. The first one points out the distinctive features in the program and the second one describes in detail the function of

"peak-value memory". The third one illustrates the way of manipulating data in order to accomplish the proportional (P) and integral (I) actions. In the last section, the flow-chart of the micro-computer program is presented.

3.3.1 General Features of the Control Algorithm

The control algorithm is written in Assembler language. However, the mathematical computation is carried out by means of the floating point package developed by Zsombor-Murray [27]. The use of floating point operations permits one to change the values of the control algorithm parameters freely without worrying about the manipulation of the bits inside the computer. It also simplifies the programming procedures and effort to a great extent. The package is stored in 2K bytes of EPROM in the computer unit. The main drawback of using floating point operations, however, is that it slows down the execution rate of the control algorithm considerably.

The program is designed to allow the user both to select the mode of control and to specify the parameter values with ease. It is set up in such a way that the computer will request and obtain information sequentially through the teletype. For debugging and testing purposes, the measured cutting force input value can be printed optionally. However, because the teletype is very slow (i.e., 110 band), this feature cannot be used in real-time operation.

3.3.2 Functions and Features of the Peak-Value Memory

As stated in the introduction, one of the underlying assumptions behind this research was that adaptive control systems are particularly useful during rough turning of forgings or castings. In this context, very frequently the actual depth-of-cut, and therefore the cutting force, may vary periodically with the spindle rotation. In the design of the control algorithm, particular attention was directed toward this situation.

The problem obviously is: if one designs a highly responsive feedrate adaptive control action based on cutting force, it is conceivable that for an out-of-round workpiece (in cases where the spindle is turning relatively slowly) the adaptive control action might increase the feedrate substantially during that portion of the spindle rotation period when the depth-of-cut (and therefore the cutting force) is small; consequently during the next portion when the depth-of-cut is larger, the tool may have moved far enough such that the actual chip thickness may also be large resulting in a very large cutting force. Furthermore, even when the spindle is turning rapidly so that the adaptive feedrate changes do not have enough time to occur substantially during a fraction of a spindle revolution, it is likely that the feedrate would be determined essentially by the average cutting force, and that the peak cutting force could be too large.

To cope with this problem, a feature termed "peak-value memory" (PVM) has been designed. The aim of the PVM is to make the control action be based on the peak value of the cutting force measured during a revolution period.

Conceptually, the most straightforward and accurate way of implementing such a feature in the control algorithm (assuming that the algorithm knew how many measurements occurred in one revolution) would be to keep a running record of the measurements for one spindle revolution and to select always the largest value. This method, however, was not used because it was felt it would be too time-consuming computationally.

The method implemented is an approximaton to the above exact method and is essentially a non-linear low-pass filter which responds instantaneously to an increasing signal but very slowly to a decreasing signal. The low-pass filtering action to a decreasing signal is achieved by decaying the current value by some factor (F) somewhat less than one. The aim is to have the response to a negative step decay by a factor of about 0.8 during one spindle revolution.

The flow-chart of the PVM feature is shown in the following figure in which C(t) represents a continuous signal which, after sampled, becomes C(n). C_n^* in this figure represents the logical output from the function of PVM.

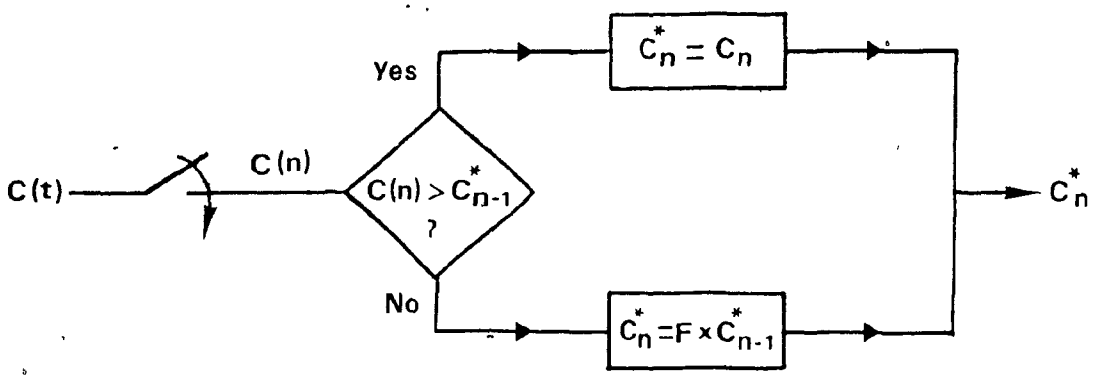

FIG 3 6 SCHEMATIC DIAGRAM OF THE PEAK VALUE MEMORY

Therefore, the overall effect of the PVM action is to modify the apparent rate at which the cutting force decreases when the actual measured force decreases rapidly. Consequently, in eccentric cutting when the actual cutting force is varying in a cyclic manner, the PVM output responds exactly to the peak value of the periodic cutting force, but generates an apparent cutting force which is an approximate exponential decay of the peak value between peaks. The ultimate effect in turning an eccentric workpiece will be to prevent the feedrate from increasing rapidly in response to a rapidly decreasing cutting force.

Schematically, for a pure sinusoidal signal, the PVM will generate a modified signal with less difference between the extreme values as shown in Fig. 3.7 .

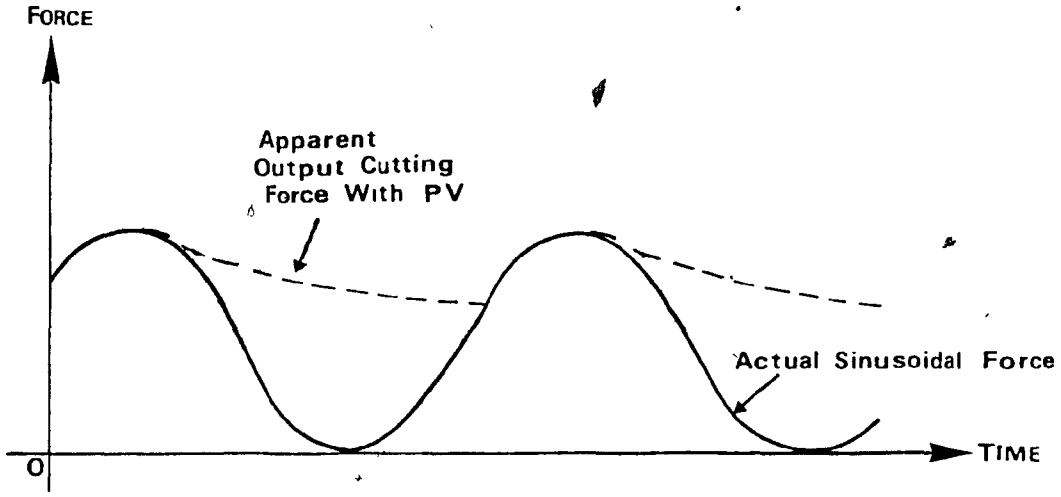

FIG 3.7 FIGURE SHOWING A SINUSOIDAL SIGNAL RESULTED FROM THE FUNCTION OF PV MEMORY

It is obvious that the amount of difference between the modified extreme values in Fig. 3.7 depends on the rate of decay. Since the micro-computer AC system digitizes a signal, the desired rate of decay per revolution, F, has to be modified to work on a periodic basis. The rate of decay per sample, F', becomes a function of the rate of decay per revolution, F, sampling period, T_c, and spindle revolution period, T_r. Their relationship is:

$$F' = F^{1/(T_r/T_c)} \qquad (3.3.1)$$

In order to be programmed in Assembler language, Eq.(3.3.1) has to be modified to an expression with simple

mathematical operations. The first two terms of the corresponding series expansion is used to approximate the equation. The approximation is:

$$F' = 1-(1-F)/T_r/T_c \qquad (3.3.2)$$

Since the time for one revolution is equal to 60/RPM, Eq.(3.3.2) can be written as:

$$F' = 1-(1-F)/(60/RPM)/T_c \qquad (3.3.3)$$

Eq.(3.3.3) is the relationship used in the micro-computer program (see Appendix I) to provide to the computer the periodic decaying instruction.

3.3.3 Modelling of the Proportional (P) and Integral (I) Action

Though the comparison and manipulation of the data are accomplished by the PVM in the program, the actual controlling action is implemented by a proportional-plus-integral (PI) controller. To understand and interpret the resultant output signals, one has to model the P and I action in the control algorithm. The model is in the following mathematical form:

$$Vout = Vnom + Kint \int ERROR + Kpro*ERROR \qquad (3.3.4)$$

where Vout = output voltage of micro-computer

Vnom = nominal voltage of micro-computer

Kint = integral gain

Kpro = proportional gain .

Depending on whether or not PVM is used, ERROR in the above equation has two different forms. It is equal to the difference between the nominal force and the data when there is no peak-value memory action. On the other hand, it becomes the difference between the nominal force and the PVM modified output when peak-value memory action is desired.

Because of the discrete nature of a micro-computer system, the integration cannot be performed in a continuous mode. Hence, it is carried out as a summation of the error signal. Therefore, the actual PI control action is:

$$Vout = Vnom + Kint*INT + Kpro*ERROR \qquad (3.3.5)$$

where INT = $\sum$ of the error signals.

In the program, the integral action is further modified. If Vout exceeds 5.0 volts or is less than 0.0 volt, instead of further accumulation to the errors, the integral action is suspended and the old INT value is used until $0.0 < Vout < 5.0$. This feature is commonly implemented in analog PI controllers and is used to prevent the occurrence of reset windup.

3.3.4 Flow-Chart of the Control Algorithm

A complete flow-chart of the micro-computer control algorithm is presented in Fig. 3.8 to illustrate some of the points described in previous sections, and to help understanding the listings of the micro-computer program. The listings of the M-6800 Assembler language program is collected in Appendix I.

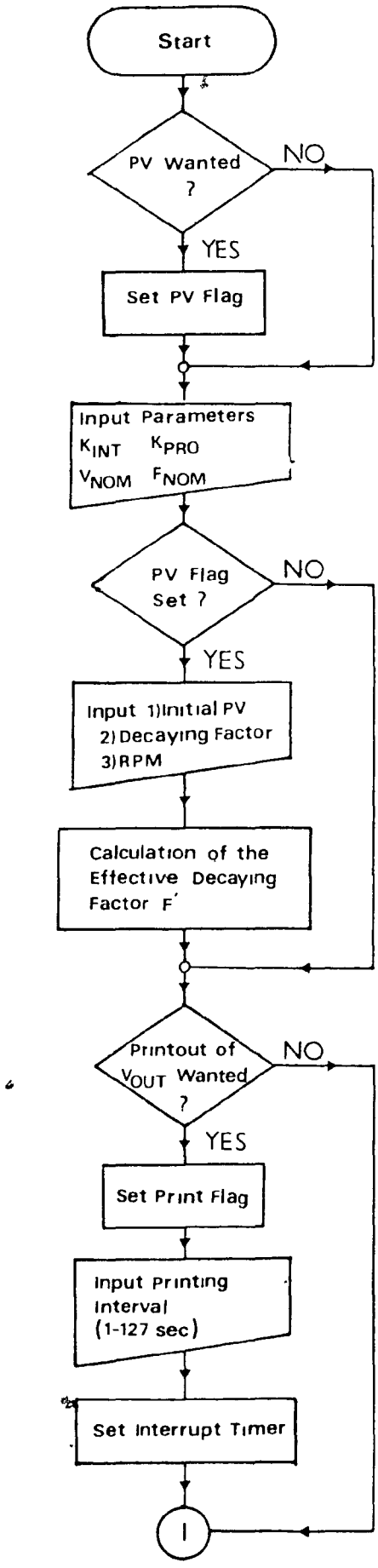
Start
PV Wanted ?
NO
YES
Set PV Flag
Input Parameters
K_{INT} K_{PRO}
V_{NOM} F_{NOM}
PV Flag Set ?
NO
YES
Input 1)Initial PV
2) Decaying Factor
3)RPM
Calculation of the Effective Decaying Factor F'
Printout of V_{OUT} Wanted ?
NO
YES
Set Print Flag
Input Printing Interval (1-127 sec)
Set Interrupt Timer
1

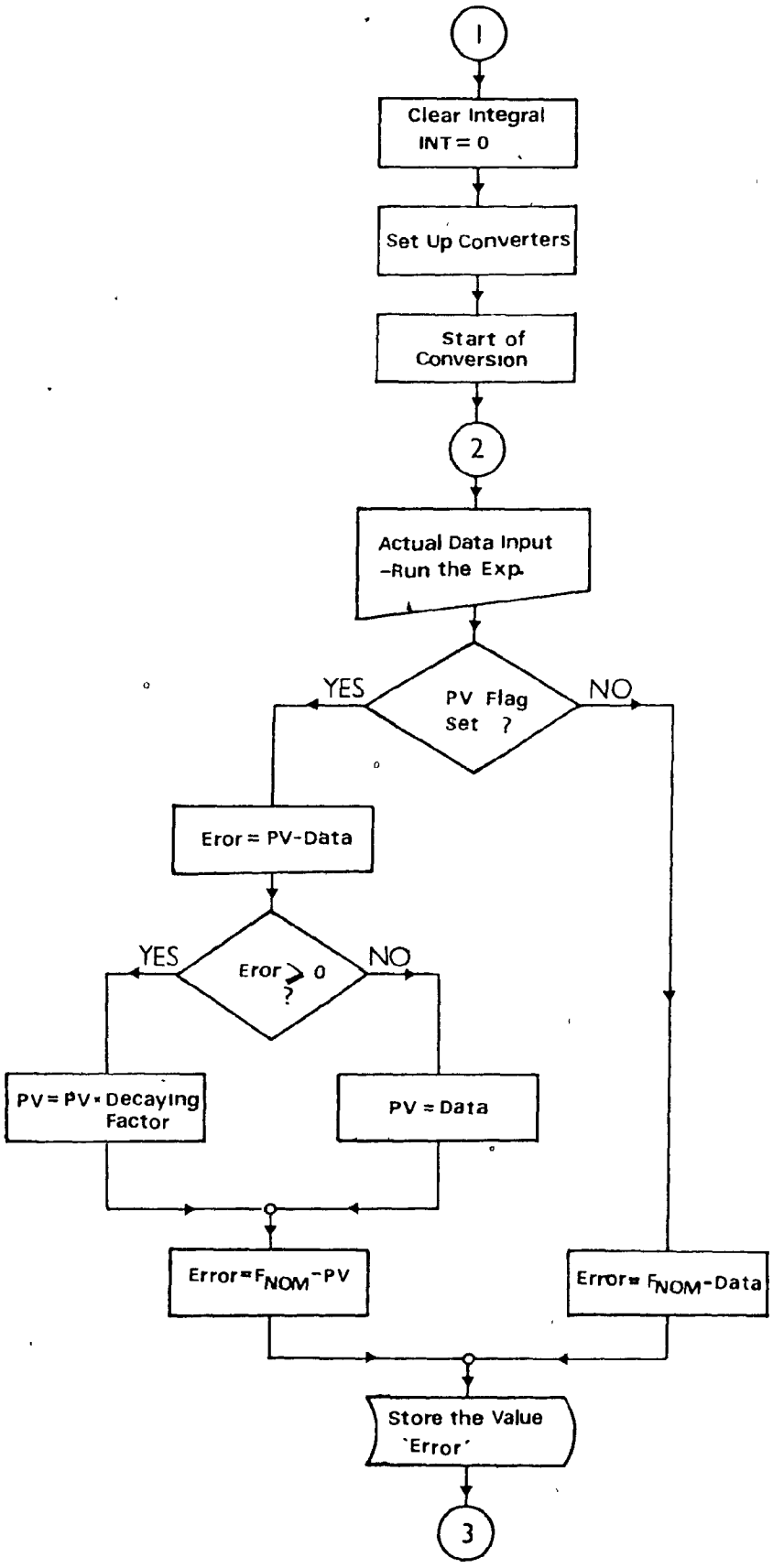
1
Clear Integral
INT = 0
Set Up Converters
Start of
Conversion
2
Actual Data Input
-Run the Exp.
YES
PV Flag
Set ?
NO
Eror = PV-Data
YES
Eror > 0
?
NO
PV = PV * Decaying
Factor
PV = Data
Error = F_NOM - PV
Error = F_NOM - Data
Store the Value
'Error'
3

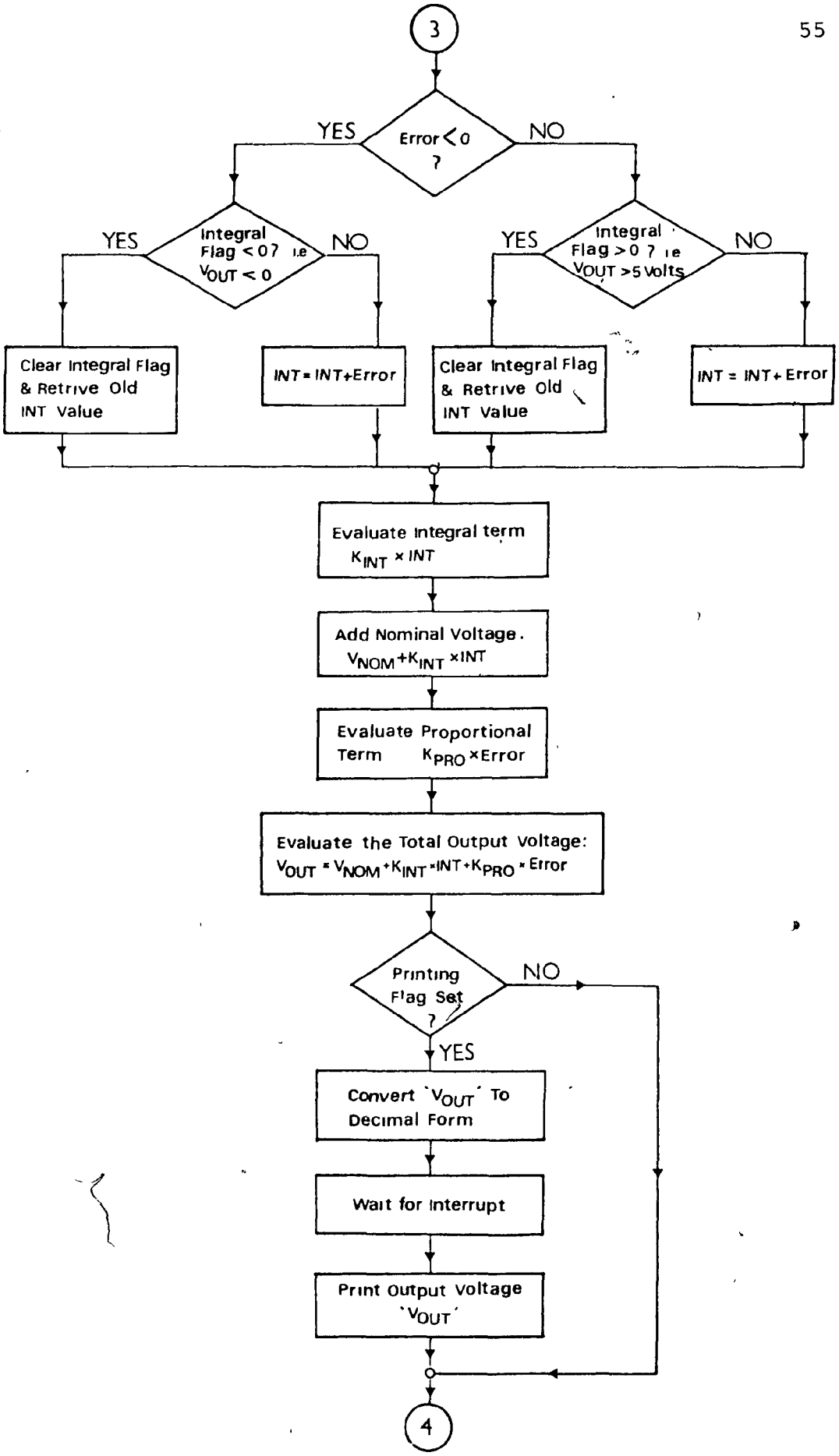
3
Error < 0 ?
YES
NO
Integral Flag < 0 ? i.e V_{OUT} < 0
YES
NO
Integral Flag > 0 ? i.e V_{OUT} > 5 Volts
YES
NO
Clear Integral Flag & Retrive Old INT Value
INT = INT + Error
Clear Integral Flag & Retrive Old INT Value
INT = INT + Error
Evaluate Integral term $K_{INT} \times INT$
Add Nominal Voltage. $V_{NOM} + K_{INT} \times INT$
Evaluate Proportional Term $K_{PRO} \times Error$
Evaluate the Total Output Voltage: $V_{OUT} = V_{NOM} + K_{INT} \times INT + K_{PRO} \times Error$
Printing Flag Set ?
NO
YES
Convert 'V_{OUT}' To Decimal Form
Wait for Interrupt
Print Output Voltage 'V_{OUT}'
4

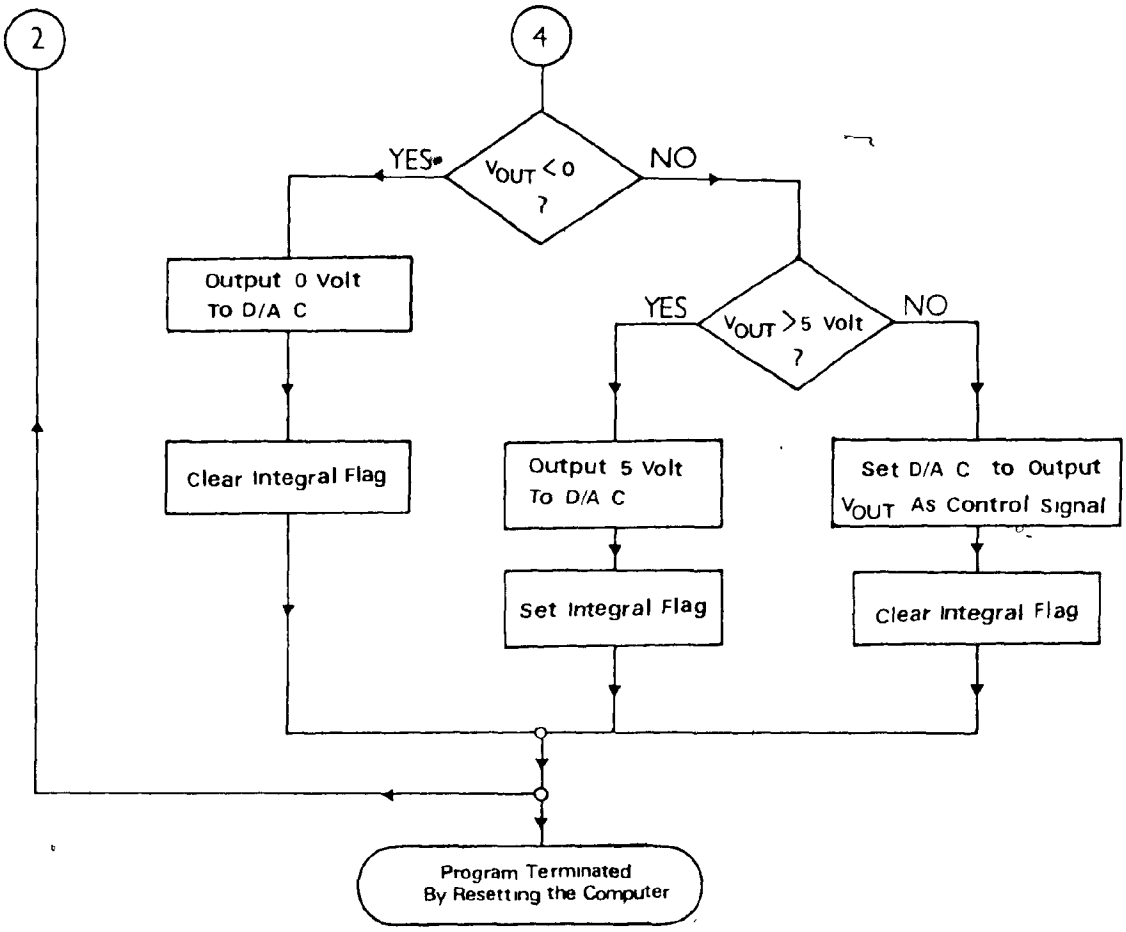

FIG 3·8 FLOW CHART OF THE CONTROL ALGORITHM

CHAPTER 4

MATHEMATICAL MODELLING OF THE EXPERIMENTAL AC SYSTEM

In this chapter, a mathematical model is derived for the experimental closed-loop system described in previous chapter. This mathematical model is used to analyze and predict both the dynamic behavior and the stability limits of the AC system. Also it is used to perform a simulation of the adaptive system.

This chapter has two main sections. The first section, Section 4.1, shows in detail the derivation of the closed-loop system model. In Sectin 4.2 the stability of the closed-loop system is analyzed. Finally, the chapter is concluded with a brief discussion and comment on both the modelling and stability analysis.

4.1 MODELLING OF THE CLOSED-LOOP AC SYSTEM

Since a micro-computer AC system can be divided into two main parts, the modelling of the overall closed-loop system can be accomplished by separate modelling of these two parts and then combining them together. Hence, this section has two sub-sections. The first one is the modelling of the NC servo and the turning process. The second one presents a model of the micro-computer unit and the overall combined system.

4.1.1 Determination and Evaluation of the Open-Loop Transfer Function (TF) of the NC servo and the Turning process

Although a conventional NC machine tool usually has closed-loop position servos, the operation is open-loop in the sense that the cutting path and feedrate are pre-programmed and will be executed regardless of what cutting action is taking place. The aim in this section is to review the transfer function relating commanded feedrate (at the NC control unit feedrate override) to the main cutting force generated at the cutting tool. Physically the situation considered is that of turning a cylinder with a constant depth-of-cut while varying the feedrate override command. The dynamics of the machine tool compliance is assumed to be negligible. Schematically, the problem is shown in Fig. 4.1 .

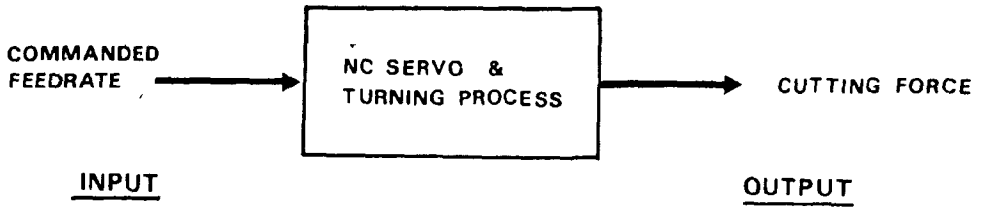

FIG 4.1 SCHEMATIC DIAGRAM OF THE OPEN LOOP TF OF TURNING

Modelling of the turning operation is based on an elementary understanding of the physical process. Physically one can easily visualize that the commanded feedrate, through the NC servo is firstly converted to an actual tool velocity

and position as a function of time, which in turn determines the chip thickness. Multiplication of the chip thickness and the depth-of-cut gives rise to the cutting force on the assumption that the cutting force is proportional to the chip cross-sectional area. Hence, the process can be broken down into four steps as shown in Fig. 4.2 .

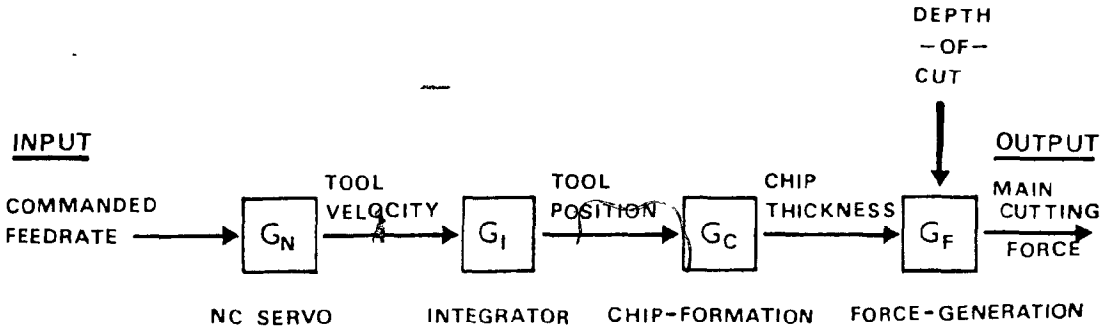

FIG 4·2 SCHEMATIC BLOCK DIAGRAM OF THE TURNING OPERATION

The mathematical expression for the transfer functions of each separate block in Fig. 4.2 will now be discussed.

Leung [26] showed that, to a good accuracy, the NC servo can be approximated as a second-order system. Leung did actual experimental tests on the NC servo using a frequency analyzer and obtained the following form for the NC servo : $G_N = \frac{K_g}{(1+T_1 s)(1+T_2 s)}$, where K_g is the servo gain, and T_1, T_2 are the time constants of the machine.

Integration of tool velocity yields the tool position. Hence, G_I is an integrator with a transfer function of 1/s.

The un-deformed chip thickness for orthogonal cutting is determined by the difference in tool positions during one workpiece revolution. Therefore, G_C consists of a unity term minus a time delay function with a time delay equal to one workpiece revolution (T_r); $G_C = 1-e^{T_r}$.

Multiplication of the instantaneous chip thickness by the depth-of-cut yields the un-deformed chip cross-sectional area. As mentioned in Chapter 2, the exact expression relating the cutting force to the chip cross-sectional area is quite complicated. For simplicity, it is assumed that the cutting force is linearly related to the un-deformed chip cross-sectional area by a factor known as the specific cutting energy of the workpiece material (K_d); i.e., the energy required to remove a unit volume of metal. Obviously, the factor is a function of the workpiece material.

Gathering the above expressions into Fig. 4.2 yields Fig. 4.3 . Note that the depth-of-cut, a, in general will vary with time and appears in the model as a gain term.

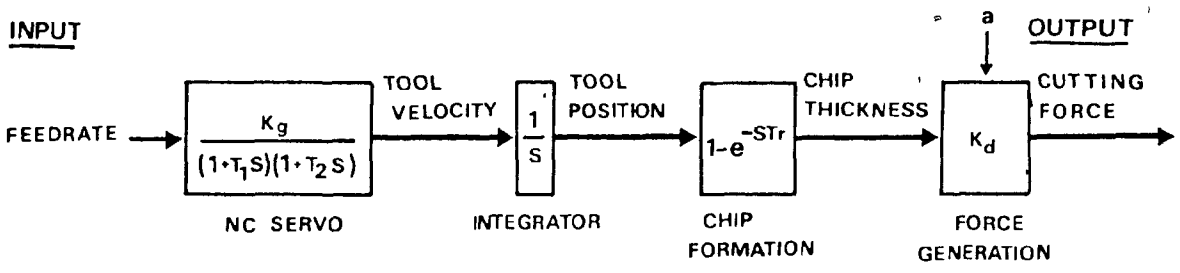

FIG 4·3 OPEN LOOP TF OF THE NC TURNING PROCESS

4.1.2 Determination and Evaluation of the Closed-Loop Transfer Function (TF) of the Micro-Computer AC System

Once the system is augmented to be adaptive, the overall system becomes closed-loop because the function of the adaptive control is to adjust the commanded feedrate based on real-time measurements of the cutting force. The aim of this section is to develop expressions for the adaptive control system components and then to combine these with the previous model to get the overall closed-loop model.

Since the computer digitizes the input force, does some calculations, and gives a step-wise constant output signal, there exists a time delay and a zero-order hold (ZOH) function. The time lag comes from the computation time, T_c, between the input and output by the computer. The ZOH is the mathematical expression for holding the generated output constant for a sampling period (T_c) of time. Their corresponding expressions are e^{-sT_c} and $\frac{1-e^{-sT_c}}{s}$. Moreover, the computer calculates the output according to a control algorithm, G_M. It is the flexibility available by using different control algorithms that makes the software system advantageous.

The transfer function of the dynamometer and amplifier lumped together were modelled as a first-order time system orginally, but experiments showed that the time constant for a rigidly mounted dynamometer is extremely small [26]. Thus, this transfer function can be modelled as a pure proportional

gain with a value of K_f.

Hence the transfer function of the adaptive unit is as shown in Fig. 4.4.

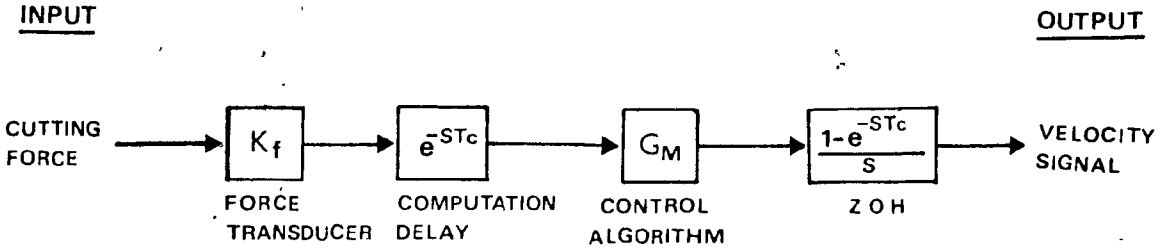

FIG 4.4 OPEN LOOP TF OF THE MICRO COMPUTER ADAPTIVE UNIT

Combining Figs. 4.3 and 4.4, the overall closed-loop experimental AC system is as shown in Fig. 4.5 .

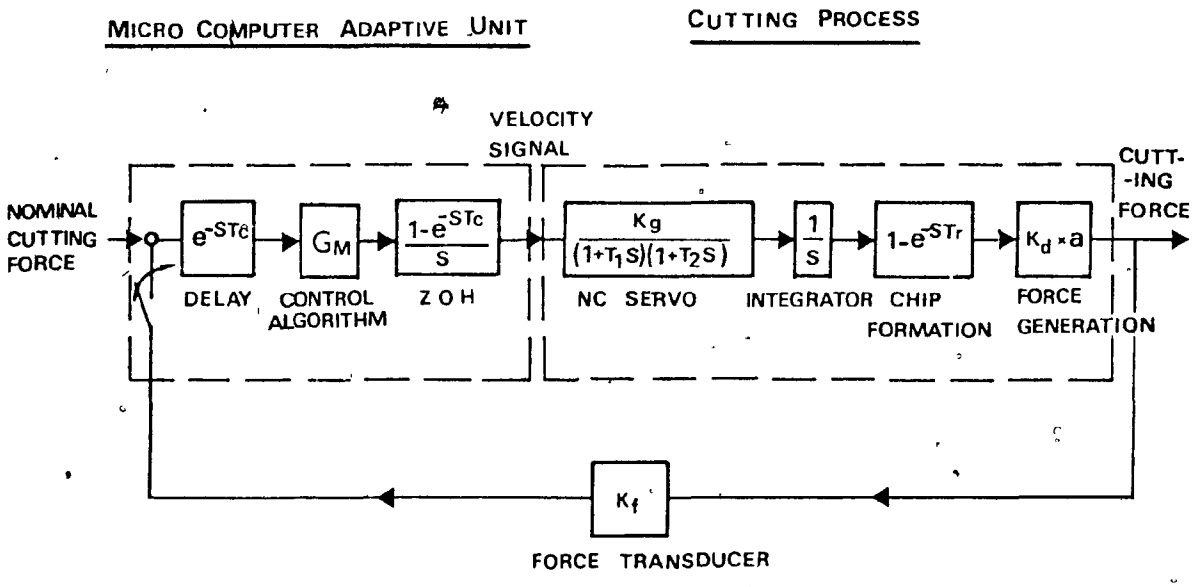

FIG 4.5 CLOSED LOOP TF OF THE MICRO-COMPUTER AC SYSTEM

It should be noted that once the system is set up for a particular cutting condition (i.e., fixing the RPM and IPR) all the constants in the transfer functions are fixed accordingly, except for the depth-of-cut. The reason is that, although it can be set to a desired value, the actual depth-of-cut depends on some other uncontrollable variables such as the degree of roundness of workpiece and the displacement of workpiece due to dynamic vibration. Hence, one of the prime objectives of the AC system is to compensate for the effects of varying depth-of-cut by controlling the commanded feedrate override signal by selection of a suitable control algorithm, G_M.

4.2 STABILITY ANALYSIS OF THE EXPERIMENTAL AC SYSTEM

For a feedback control systems, one of the main concerns of the control designer is to ensure that the system is stable. There are numerous ways to predict the stability. Choice of the methods depends on the nature and complexity of each individual problem. Complexity of a system arises in many ways. Two common ones are non-linearities and time-varying functions such as the peak-value memory and variable depth-of-cut in the adaptive system under consideration.

The closed-loop model derived in previous section will be used in the following stability analysis. Nyquist plot and computer simulation are particularly selected for demonstration. The Nyquist plot is used to analyze that part of

experiment with non-eccentric cutting condition and simple PI controller. The computer simulation is used for analyzing the eccentric turning with an additional function of peak-value memory in the control algorithm.

In all of the stability analysis, all of the physical units and conversion factors have been evaluated and collected in Appendix J.

4.2.1 Stability Analysis on the Non-Eccentric Turning with a PI Controller

Because the system is micro-computer based, it is a discrete-time sampling system. Strictly speaking, the analysis should be carried out in discrete-time domain by performing the Z-transform on the transfer functions. The characteristic equation found from these transfer functions will end up with a rather high order polynomial expression. The exact degree of the polynomial depends on the ratio of the computer sampling time and the workpiece rotation period. Leung [26] did an actual stability analysis of the closed-loop system as in Fig. 4.5 in the discrete-time domain. One of his final conclusions is that the system can adequately be modelled as a continuous one. Based on his conclusion, the adaptive system as in Fig. 4.5 is regarded as a continuous system and the stability analysis on the non-ecentric cutting is carried out by the Nyquist plot. The following analysis focuses on the case

where PI controller action is used. Also, the ZOH transfer function is removed from the closed-loop system in the analysis because the ZOH is meaningful only for a discrete-time system. Hence, the closed-loop system becomes:

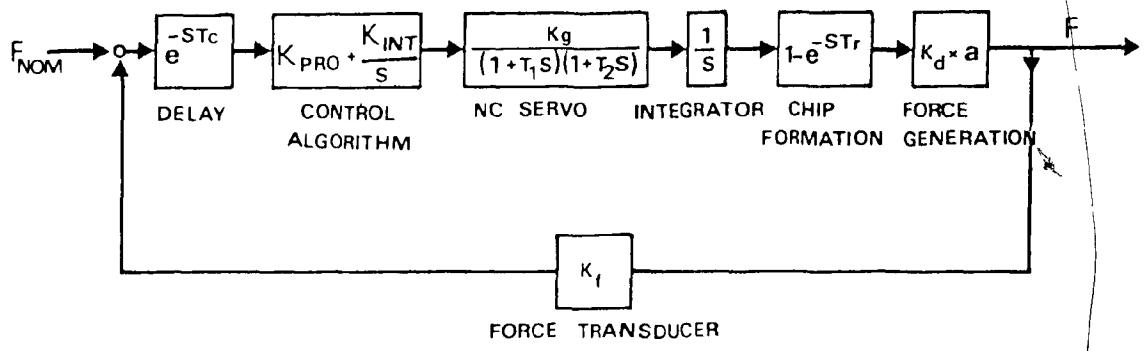

FIG 4 6 THE CLOSED LOOP TF OF THE AC SYSTEM IN CONTINUOUS MODE

By substituting the values of constants and gains and further approximating $\frac{Kg}{(1+T_1 s)(1+T_2 s)}$ to be K_g (refer to Appendix J), Fig. 4.6 becomes:

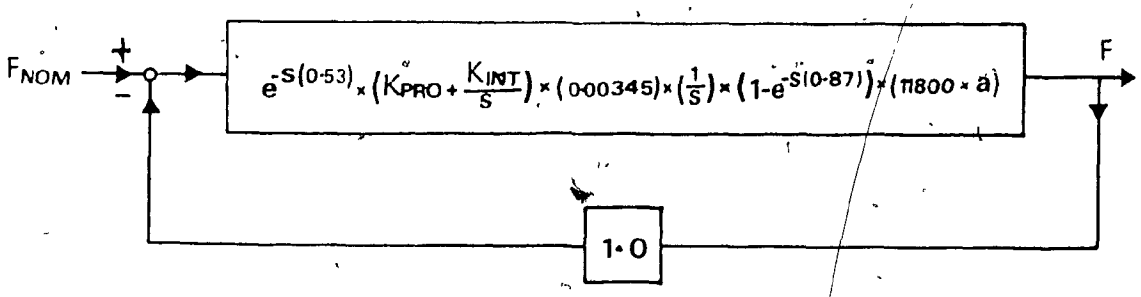

FIG 4·7 THE APPROXIMATED CLOSED LOOP TF OF THE AC SYSTEM WITH CORRESPONDING VALUES OF CONSTANTS & GAINS

In the above figure, all of the parameters are fixed by the equipment and workpiece material except for the depth-of-cut and the proportional and integral controller gains; i.e., Kpro and Kint. Therefore, in effect, the stability of the system for a given depth-of-cut is governed by the controller gains. The following analysis is concerned with determining the limiting values of Kpro and Kint for the system to be stable.

Fig. 4.7 has the same structure as a general closed-loop system:

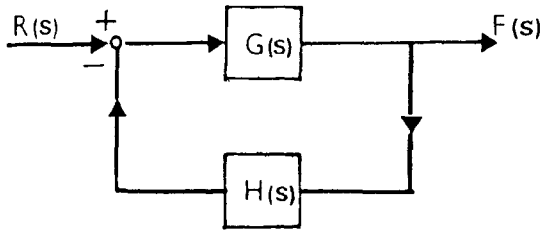

FIG 4 8 GENERAL FORM OF A CLOSED LOOP SYSTEM

where G(s) and H(s) represent two arbitary transfer functions. The closed-loop relation is:

$$F(s) = \frac{G(s)}{1+G(s)H(s)} R(s) \qquad (4.2.1)$$

For stability, all roots of the characteristic equation, $F(s)=1+G(s)H(s)=0$, must lie in the left-half S plane. By

mapping theorem, the number of encirclements of the origin of the F(s) plane depends on the closed contour in the S plane. Nevertheless, the expression of F(s)=1+G(s)H(s) is equivalent to encirclement of the -1+0j point by just the G(s)H(s) axis. Thus, stability of a closed-loop system can be investigated by examining encirclements of the -1+0j point by the locus of G(s)H(s); i.e., open-loop system. Locus of G(s)H(s) can be found by replacing s with jω and let ω vary from 0 to ∞ .

For the closed-loop system on Fig. 4.7, its open loop transfer function is:

$$e^{-ST_c} * (Kpro + \frac{Kint}{S})(K_g)(\frac{1}{S})(1-e^{-sT_r})(K_d*a) \qquad (4.2.2)$$

Schematically, Eq.(4.2.2) is represented in Fig. 4.9 .

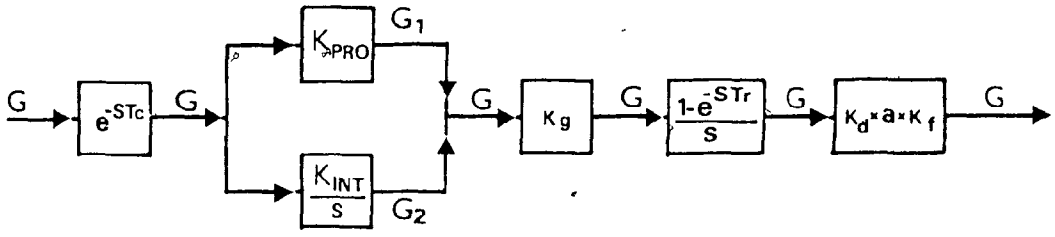

FIG 4.9 THE OPEN TF OF THE CLOSED LOOP AC SYSTEM IN CONTINUOUS MODE

In Fig. 4.9, for a certain depth-of-cut, the stability limits of Kpro and Kint are found by fixing Kpro and adjusting Kint until the magnitude of $G(j\omega)H(j\omega)$ is close to 1 at a phase angle of -180^0; i.e., the relationship between the limits of Kpro and Kint is found by trial and error. The calculation is done by computer. The program and results are collected in Appendix K. The computer results are plotted in Fig. 4.10 for three different depth-of-cuts, 0.03", 0.06", and 0.09".

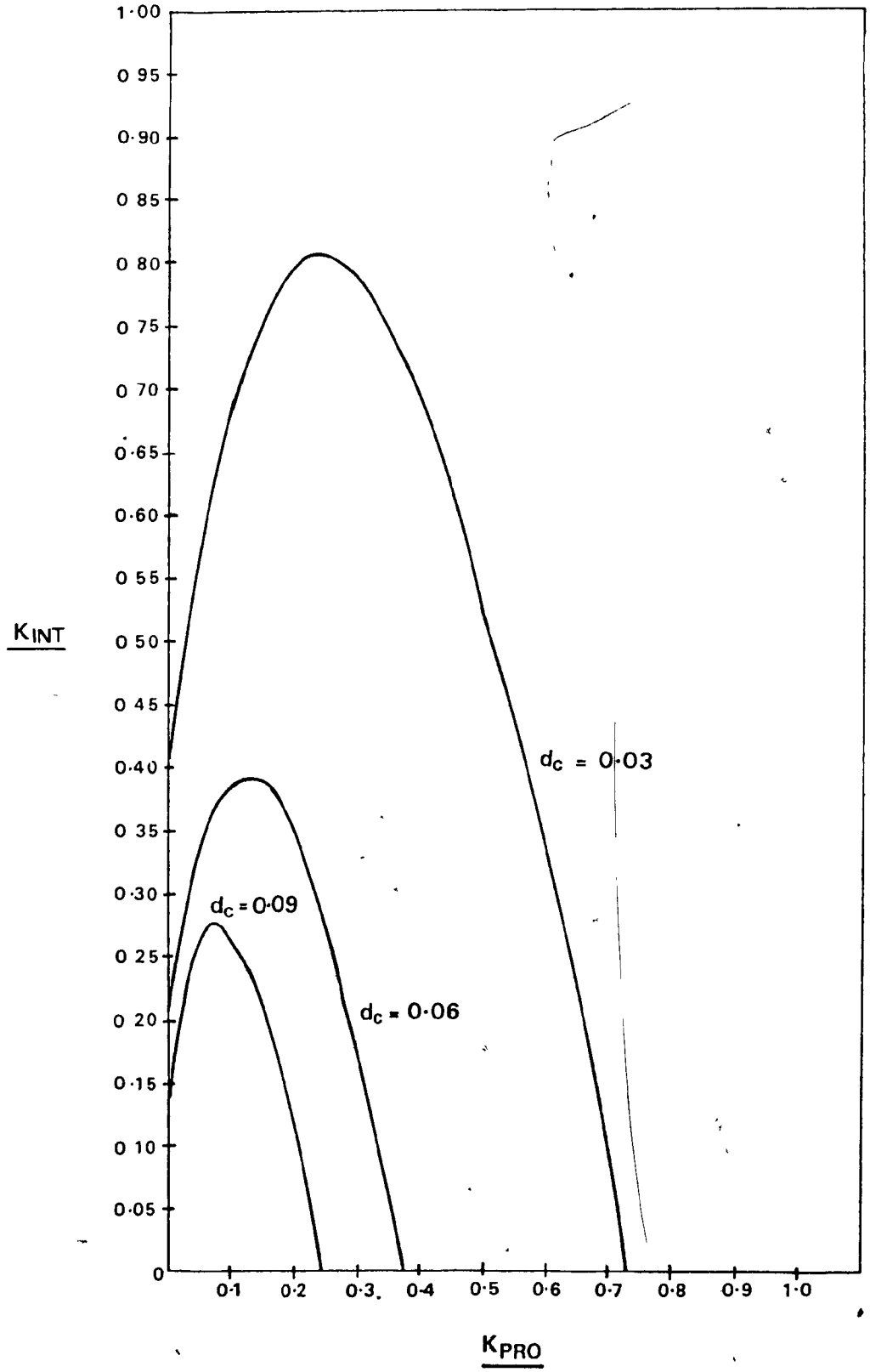

FIG 4·10 PLOT OF THE STABILITY LIMITS OF K_{PRO} & K_{INT}

4.2.2 Stability Analysis on the Eccentric Turning with a PI Controller

The system to be analyzed here is the same as previous one, except that the workpiece is eccentrically mounted. Under such a configuration of set-up, the depth-of-cut becomes a time-varying function (e.g., $a(t)=b+d*\cos(\omega t)$) and an external disturbance to the system. The entire closed-loop system is illustrated in Fig.4.11 .

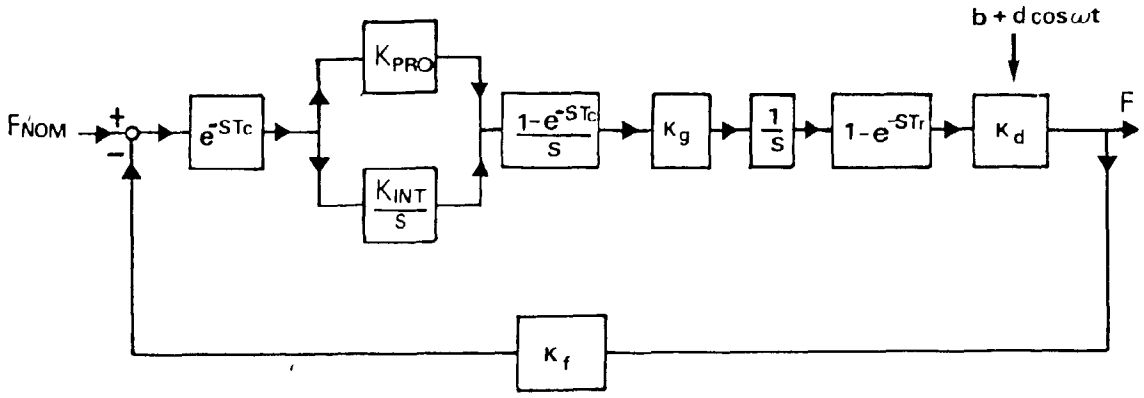

FIG 4.11 SYSTEM TO BE ANALYSED FOR THE ECCENTRIC CUTTING

Unlike an ordinary closed-loop system in which the disturbance comes in at the summation junction, the depth-of-cut here comes in the system as a multiplication term and therefore, the system stability depends on the depth-of-cut. This complicates the problem so much that there is apparently no straightforward way to solve the stability analysis problem; i.e., it precludes the use of ordinary

methods such as Nyquist plot, Bode plot, and Routh criteria to predict the stability.

An alternative way of predicting the stability is to simulate the system by computer and observe the transient behaviour of the cutting force. Such simulation can be used to evaluate the stability of the closed-loop systems for various parameter sets.

The system shown in Fig. 4.11 was simulated by a digital computer. The IBM system /360 Continuous System Modeling Program (CSMP) is used to handle the programming of this time-varying problem. The output of the simulation is a print-plotting of the cutting force with the feedrate, and chip thickness to be printed adjacent to it.

There are three runs in the program with three different parameter sets of Kpro and Kint. The three sets of values are: Kpro=0.05, Kint=0.003; Kpro=0.1, Kint=0.002; and Kpro=0.35, Kint=0.003. The selection of these values enables us to compare the simulated results with those of experimental for a large variety of gains in next chapter. The first set of output is collected in the following figure for reference . The last two outputs and the computer listings are assembled in Appendix L.1 .

MINIMUM 0.0 — FORCE VERSUS TIME — MAXIMUM 1.3929E+02

TIME	FORCE	FECRAT	CHIP
0.0	0.0	0.0	0.0
5.0000E-02	0.0	1.4A2BE-02	0.0
1.0000E-01	0.0	1.5456E-02	0.0
1.5000E-01	0.0	1.628AE-02	0.0
2.0000E-01	0.0	1.7112E-02	0.0
2.5000E-01	0.0	1.725CE-02	0.0
3.0000E-01	0.0	1.725CE-02	0.0
3.5000E-01	0.0	1.725CE-02	0.0
4.0000E-01	0.0	1.725CE-02	0.0
4.5000E-01	0.0	1.725CE-02	0.0
5.0000E-01	0.0	1.725CE-02	0.0
5.5000E-01	0.0	1.725CE-02	0.0
6.0000E-01	0.0	1.725CE-02	0.0
6.5000E-01	0.0	1.725CE-02	0.0
7.0000E-01	0.0	1.725CE-02	0.0
7.5000E-01	0.0	1.725CE-02	0.0
8.0000E-01	0.0	1.725CE-02	0.0
8.5000E-01	0.0	1.725CE-02	0.0
9.0000E-01	0.0	1.725CE-02	0.0
9.5000E-01	0.0	1.725CE-02	0.0
1.0000E+00	0.0	1.725CE-02	0.0
1.0500E+00	0.0	1.725CE-02	0.0
1.1000E+00	0.0	1.725CE-02	0.0
1.1500E+00	0.0	1.725CE-02	0.0
1.2000E+00	0.0	1.725CE-02	0.0
1.2500E+00	1.6246E+00	1.725CE-02	4.2360E-04
1.3000E+00	4.5859E+00	1.725CE-02	1.2861E-03
1.3500E+00	8.0703E+00	1.725CE-02	2.1486E-03
1.4000E+00	1.3159E+01	1.725CE-02	3.0110E-03
1.4500E+00	2.0771E+01	1.725CE-02	3.8735E-03
1.5000E+00	3.1115E+01	1.725CE-02	4.7360E-03
1.5500E+00	4.3952E+01	1.725CE-02	5.5985E-03
1.6000E+00	5.9329E+01	1.725CE-02	6.4609E-03
1.6500E+00	7.3074E+01	1.725CE-02	7.3234E-03
1.7000E+00	8.6836E+01	1.725CE-02	8.1859E-03
1.7500E+00	9.6646E+01	1.60B1E-02	9.0484E-03
1.8000E+00	1.0200E+02	1.4135E-02	9.8524E-03
1.8500E+00	1.0114E+02	1.2984E-02	1.0559E-02
1.9000E+00	9.5757E+01	1.2856E-02	1.1209E-02
1.9500E+00	8.4484E+01	1.3676E-02	1.1851E-02
2.0000E+00	7.6543E+01	1.5212E-02	1.2535E-02
2.0500E+00	6.5142E+01	1.7142E-02	1.3205E-02
2.1000E+00	5.7111E+01	1.725CE-02	1.4066E-02
2.1500E+00	5.0875E+01	1.725CE-02	1.4066E-02
2.2000E+00	5.1021E+01	1.725CE-02	1.4066E-02
2.2500E+00	5.7526E+01	1.725CE-02	1.4066E-02
2.3000E+00	6.9522E+01	1.725CE-02	1.4066E-02
2.3500E+00	8.4564E+01	1.725CE-02	1.4066E-02
2.4000E+00	1.0341E+02	1.6163E-02	1.4066E-02
2.4500E+00	1.2043E+02	1.2635E-02	1.4012E-02
2.5000E+00	1.3326E+02	9.4813E-03	1.3791E-02
2.5500E+00	1.3907E+02	6.7531E-03	1.3403E-02
2.6000E+00	1.3760E+02	5.1045E-03	1.2878E-02
2.6500E+00	1.2944E+02	4.7624E-03	1.2306E-02
2.7000E+00	1.1724E+02	5.6219E-03	1.1800E-02
2.7500E+00	1.0285E+02	7.3579E-03	1.1409E-02
2.8000E+00	8.6779E+01	9.6719E-03	1.1132E-02
2.8500E+00	7.1285E+01	1.2329E-02	1.0947E-02
2.9000E+00	5.7564E+01	1.5081E-02	1.0833E-02
2.9500E+00	4.6902E+01	1.725CE-02	1.0766E-02
3.0000E+00	4.0226E+01	1.725CE-02	1.0770E-02
3.0500E+00	3.8427E+01	1.725CE-02	1.0770E-02
3.1000E+00	4.1541E+01	1.725CE-02	1.0770E-02
3.1500E+00	4.9204E+01	1.725CE-02	1.0770E-02
3.2000E+00	6.0426E+01	1.725CE-02	1.0770E-02
3.2500E+00	7.3759E+01	1.725CE-02	1.0770E-02
3.3000E+00	8.7747E+01	1.7062E-02	1.0903E-02
3.3500E+00	1.0145E+02	1.4566E-02	1.0940E-02
3.4000E+00	1.1291E+02	1.1978E-02	1.1138E-02
3.4500E+00	1.2047E+02	9.6657E-03	1.1346E-02
3.5000E+00	1.2220E+02	7.9424E-03	1.1542E-02
3.5500E+00	1.1954E+02	7.0798E-03	1.1696E-02
3.6000E+00	1.1377E+02	7.2466E-03	1.1784E-02
3.6500E+00	1.0581E+02	8.4445E-03	1.1812E-02
3.7000E+00	9.7834E+01	1.0491E-02	1.1796E-02
3.7500E+00	8.9771E+01	1.3062E-02	1.1756E-02
3.8000E+00	8.2766E+01	1.5776E-02	1.1709E-02
3.8500E+00	7.6964E+01	1.725CE-02	1.1678E-02
3.9000E+00	7.2582E+01	1.725CE-02	1.1678E-02
3.9500E+00	7.0188E+01	1.725CE-02	1.1678E-02
4.0000E+00	6.9557E+01	1.725CE-02	1.1678E-02
4.0500E+00	7.0362E+01	1.725CE-02	1.1678E-02
4.1000E+00	7.2414E+01	1.725CE-02	1.1678E-02
4.1500E+00	7.5177E+01	1.6641E-02	1.1678E-02
4.2000E+00	8.0307E+01	1.3665E-02	1.1653E-02
4.2500E+00	8.7267E+01	1.1321E-02	1.1574E-02
4.3000E+00	9.4043E+01	9.1084E-03	1.1490E-02
4.3500E+00	9.8855E+01	7.5577E-03	1.1417E-02
4.4000E+00	1.0067E+02	6.8405E-03	1.1363E-02
4.4500E+00	9.9037E+01	7.0290E-03	1.1334E-02
4.5000E+00	9.5220E+01	8.0895E-03	1.1326E-02
4.5500E+00	8.9075E+01	9.8947E-03	1.1331E-02
4.6000E+00	8.1966E+01	1.2231E-02	1.1342E-02
4.6500E+00	7.5744E+01	1.4812E-02	1.1350E-02
4.7000E+00	7.0746E+01	1.725CE-02	1.1355E-02
4.7500E+00	6.7270E+01	1.725CE-02	1.1384E-02
4.8000E+00	6.5268E+01	1.725CE-02	1.1384E-02
4.8500E+00	6.4529E+01	1.725CE-02	1.1384E-02
4.9000E+00	6.4916E+01	1.725CE-02	1.1384E-02
4.9500E+00	6.6796E+01	1.725CE-02	1.1384E-02
5.0000E+00	6.9114E+01	1.725CE-02	1.1384E-02
5.0500E+00	7.1950E+01	1.5145E-02	1.1402E-02
5.1000E+00	7.5842E+01	1.2483E-02	1.1409E-02
5.1500E+00	8.0422E+02	1.0022E-02	1.1416E-02
5.2000E+00	1.0172E+02	8.0632E-03	1.1418E-02
5.2500E+00	1.2176E+02	6.8667E-03	1.1413E-02
5.3000E+00	1.2959E+02	6.5910E-03	1.1401E-02
5.3500E+00	1.1867E+02	7.2705E-03	1.1382E-02
5.4000E+00	1.0444E+02	8.8134E-03	1.1362E-02
5.4500E+00	9.1107E+01	1.1011E-02	1.1343E-02
5.5000E+00	7.8416E+01	1.3574E-02	1.1328E-02
5.5500E+00	6.7813E+01	1.6171E-02	1.1316E-02
5.6000E+00	5.9835E+01	1.725CE-02	1.1310E-02
5.6500E+00	5.4318E+01	1.725CE-02	1.1310E-02
5.7000E+00	5.0918E+01	1.725CE-02	1.1310E-02
5.7500E+00	4.9269E+01	1.725CE-02	1.1310E-02
5.8000E+00	4.9966E+01	1.725CE-02	1.1310E-02
5.8500E+00	5.1158E+01	1.725CE-02	1.1310E-02
5.9000E+00	5.4527E+01	1.725CE-02	1.1310E-02
5.9500E+00	5.9411E+01	1.6045E-02	1.1310E-02
6.0000E+00	6.5238E+01	1.3455E-02	1.1314E-02
6.0500E+00	7.1325E+01	1.0917E-02	1.1310E-02
6.1000E+00	7.6447E+01	8.7667E-03	1.1306E-02

FIG 4-12 SIMULATION OUTPUT OF FIG 4 11 WITH K_{PRO}=0 05 & K_{INT}=0 003

4.2.3 Stability Analysis on the Eccentric Turning with a PI Controller and Peak-Value Memory

It is obvious that the peak-value memory is a highly non-linear function. This non-linearity hinders the use of any approximate methods such as describing function or linearization to estimate the behavior of the system. Digital computer simulation again becomes the simplest and the most versatile way to obtain the necessary information about the system. The block diagram of the entire system with the peak-value memory to be simulated is shown in the following diagram.

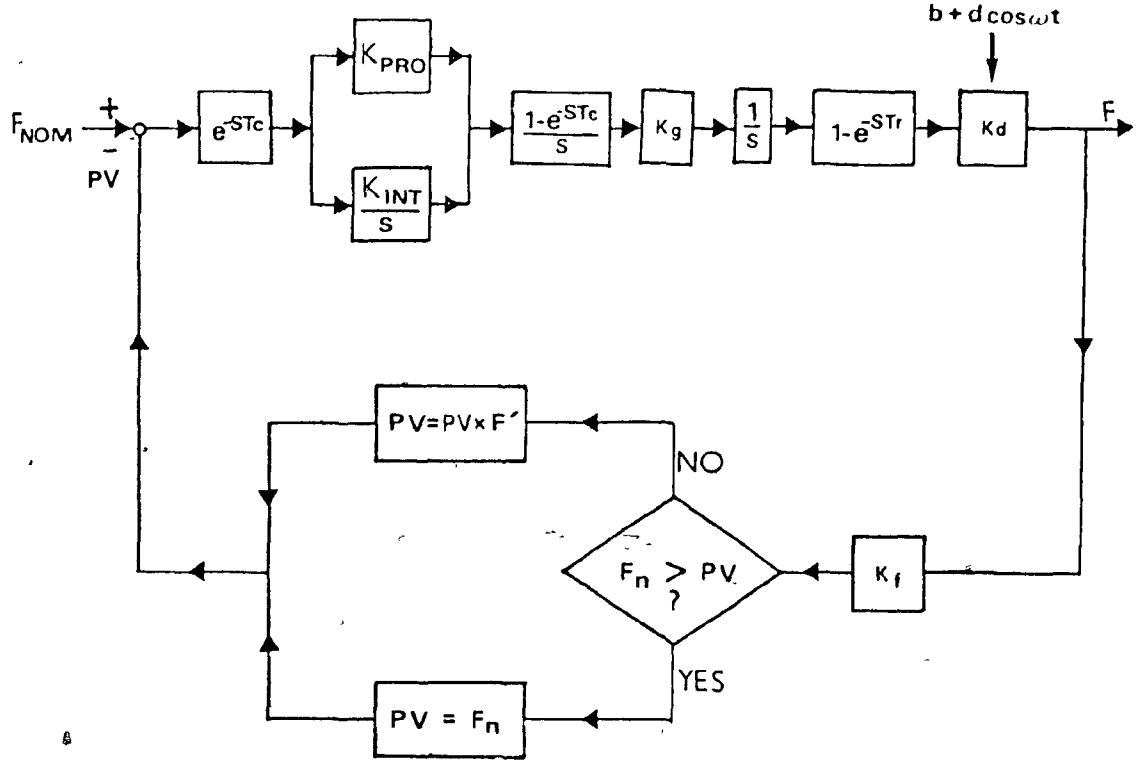

FIG 4·13 BLOCK DIAGRAM OF THE CLOSED LOOP SYSTEM WITH A PI & PV MEMORY CONTROLLER

Similar to the previous program, this one also consists of three runs with the same parameter sets. The first computer result with Kpro=0.05 and Kint=0.003 is collected in Fig. 4.14 . The last two outputs and the computer listings are collected in Appendix L.2.

MINIMUM FORCE VERSUS TIME MAXIMUM
0.0 1.21766E+02

TIME	FORCE		FECRAT	CHIP
0.0	0.0	1	0.0	0.0
5.0000E-02	0.0	+	1.4628E-02	0.0
1.0000E-01	0.0	+	1.5456E-02	0.0
1.5000E-01	0.0	+	1.6284E-02	0.0
2.0000E-01	0.0	+	1.7112E-02	0.0
2.5000E-01	0.0	+	1.7250E-02	0.0
3.0000E-01	0.0	+	1.7250E-02	0.0
3.5000E-01	0.0	+	1.7250E-02	0.0
4.0000E-01	0.0	+	1.7250E-02	0.0
4.5000E-01	0.0	+	1.7250E-02	0.0
5.0000E-01	0.0	+	1.7250E-02	0.0
5.5000E-01	0.0	+	1.7250E-02	0.0
6.0000E-01	0.0	+	1.7250E-02	0.0
6.5000E-01	0.0	+	1.7250E-02	0.0
7.0000E-01	0.0	+	1.7250E-02	0.0
7.5000E-01	0.0	+	1.7250E-02	0.0
8.0000E-01	0.0	+	1.7250E-02	0.0
8.5000E-01	0.0	+	1.7250E-02	0.0
9.0000E-01	0.0	+	1.7250E-02	0.0
9.5000E-01	0.0	+	1.7250E-02	0.0
1.0000E+00	0.0	+	1.7250E-02	0.0
1.0500E+00	0.0	+	1.7250E-02	0.0
1.1000E+00	0.0	+	1.7250E-02	0.0
1.1500E+00	0.0	+	1.7250E-02	0.0
1.2000E+00	1.6246E+00	+	1.7250E-02	4.2360E-04
1.2500E+00	4.5845E+00	-+	1.7250E-02	1.2661E-03
1.3000E+00	8.0703E+00	---+	1.7250E-02	2.1486E-03
1.3500E+00	1.2154E+01	-----+	1.7250E-02	3.0110E-03
1.4000E+00	2.0771E+01	---------+	1.7250E-02	3.8735E-03
1.4500E+00	3.1118E+01	------------+	1.7250E-02	4.7360E-03
1.5000E+00	4.3952E+01	----------------+	1.7250E-02	5.5985E-03
1.5500E+00	5.8356E+01	---------------------+	1.7250E-02	6.4609E-03
1.6000E+00	7.3074E+01	------------------------------+	1.7250E-02	7.3234E-03
1.6500E+00	8.6266E+01	----------------------------------+	1.7250E-02	8.1859E-03
1.7000E+00	9.6646E+01	------------------------------------+	1.6081E-02	9.0484E-03
1.7500E+00	1.0203E+02	--------------------------------------+	1.4135E-02	9.8524E-03
1.8000E+00	1.0145E+02	--------------------------------------+	1.2984E-02	1.0659E-02
1.8500E+00	9.5778E+01	------------------------------------+	1.2971E-02	1.1208E-02
1.9000E+00	8.6505E+01	----------------------------------+	1.2967E-02	1.1857E-02
1.9500E+00	7.5264E+01	------------------------------+	1.2973E-02	1.2505E-02
2.0000E+00	6.4448E+01	--------------------------+	1.2985E-02	1.3154E-02
2.0500E+00	5.5695E+01	----------------------+	1.3013E-02	1.3717E-02
2.1000E+00	4.8955E+01	--------------------+	1.3047E-02	1.3505E-02
2.1500E+00	4.4223E+01	-------------------+	1.3091E-02	1.3295E-02
2.2000E+00	5.3516E+01	---------------------+	1.3143E-02	1.3087E-02
2.2500E+00	6.7663E+01	--------------------------+	1.3204E-02	1.2882E-02
2.3000E+00	7.7052E+01	------------------------------+	1.3274E-02	1.2680E-02
2.3500E+00	9.1756E+01	------------------------------------+	1.3353E-02	1.2481E-02
2.4000E+00	1.0559E+02	--+	1.2896E-02	1.2286E-02
2.4500E+00	1.1644E+02	--+	1.0244E-02	1.2068E-02
2.5000E+00	1.2159E+02	--+	7.9966E-03	1.1718E-02
2.5500E+00	1.2026E+02	---+	6.6775E-03	1.1255E-02
2.6000E+00	1.1327E+02	--+	6.5027E-03	1.0762E-02
2.6500E+00	1.0265E+02	--+	6.3395E-03	1.0342E-02
2.7000E+00	8.9791E+01	------------------------------------+	6.1877E-03	9.9877E-03
2.7500E+00	7.5216E+01	------------------------------+	6.0471E-03	9.6483E-03
2.8000E+00	6.0606E+01	------------------------+	5.9177E-03	9.3022E-03
2.8500E+00	4.7956E+01	--------------------+	5.7993E-03	8.9456E-03
2.9000E+00	3.7339E+01	---------------+	5.6917E-03	8.5904E-03
2.9500E+00	3.0748E+01	-------------+	5.5950E-03	8.2248E-03
3.0000E+00	2.9019E+01	------------+	5.5088E-03	7.8529E-03
3.0500E+00	2.8801E+01	------------+	5.4332E-03	7.4746E-03
3.1000E+00	3.2392E+01	--------------+	5.3680E-03	7.0902E-03
3.1500E+00	3.9888E+01	----------------+	5.3130E-03	6.6995E-03
3.2000E+00	4.3116E+01	-----------------+	5.2682E-03	6.3028E-03
3.2500E+00	4.7923E+01	-------------------+	5.2334E-03	5.9001E-03
3.3000E+00	5.1049E+01	--------------------+	5.2086E-03	5.5081E-03
3.3500E+00	5.2758E+01	---------------------+	5.1938E-03	5.2044E-03
3.4000E+00	5.2305E+01	---------------------+	5.1882E-03	5.0203E-03
3.4500E+00	5.0838E+01	---------------------+	5.1924E-03	4.9200E-03
3.5000E+00	4.9556E+01	--------------------+	5.2061E-03	4.8511E-03
3.5500E+00	4.5006E+01	------------------+	5.2292E-03	4.7913E-03
3.6000E+00	3.9262E+01	----------------+	5.2615E-03	4.7404E-03
3.6500E+00	3.2966E+01	-------------+	5.3030E-03	4.6983E-03
3.7000E+00	2.6885E+01	----------+	5.3536E-03	4.6651E-03
3.7500E+00	2.1755E+01	--------+	5.4130E-03	4.6405E-03
3.8000E+00	1.8142E+01	-------+	5.4813E-03	4.6244E-03
3.8500E+00	1.6527E+01	------+	5.5584E-03	4.6168E-03
3.9000E+00	1.7041E+01	------+	5.6441E-03	4.6177E-03
3.9500E+00	1.9625E+01	--------+	5.7383E-03	4.6267E-03
4.0000E+00	2.4016E+01	----------+	5.8409E-03	4.6440E-03
4.0500E+00	2.9625E+01	------------+	5.9519E-03	4.6693E-03
4.1000E+00	3.5986E+01	--------------+	6.0712E-03	4.7026E-03
4.1500E+00	4.1959E+01	----------------+	6.1986E-03	4.7438E-03
4.2000E+00	4.7142E+01	------------------+	6.3340E-03	4.7928E-03
4.2500E+00	5.0836E+01	--------------------+	6.4774E-03	4.8496E-03
4.3000E+00	5.2557E+01	---------------------+	6.6287E-03	4.9139E-03
4.3500E+00	5.2065E+01	---------------------+	6.7878E-03	4.9858E-03
4.4000E+00	4.9845E+01	-------------------+	6.9545E-03	5.0651E-03
4.4500E+00	4.5058E+01	------------------+	7.1289E-03	5.1519E-03
4.5000E+00	3.9444E+01	----------------+	7.3108E-03	5.2459E-03
4.5500E+00	3.3336E+01	-------------+	7.5001E-03	5.3471E-03
4.6000E+00	2.7706E+01	----------+	7.6968E-03	5.4554E-03
4.6500E+00	2.3287E+01	---------+	7.9007E-03	5.5708E-03
4.7000E+00	2.0851E+01	--------+	8.1118E-03	5.6931E-03
4.7500E+00	2.0914E+01	--------+	8.3300E-03	5.8223E-03
4.8000E+00	2.3704E+01	---------+	8.5552E-03	5.9582E-03
4.8500E+00	2.9109E+01	-----------+	8.7873E-03	6.1009E-03
4.9000E+00	3.6679E+01	--------------+	9.0263E-03	6.2503E-03
4.9500E+00	4.5664E+01	----------------+	9.2720E-03	6.4062E-03
5.0000E+00	5.5096E+01	---------------------+	9.5245E-03	6.5685E-03
5.0500E+00	6.3904E+01	------------------------+	9.7836E-03	6.7373E-03
5.1000E+00	7.1048E+01	---------------------------+	1.0049E-02	6.9125E-03
5.1500E+00	7.5648E+01	-----------------------------+	9.5142E-03	7.0938E-03
5.2000E+00	7.6870E+01	-----------------------------+	8.7652E-03	7.2811E-03
5.2500E+00	7.3066E+01	----------------------------+	8.6164E-03	7.2431E-03
5.3000E+00	6.8151E+01	--------------------------+	8.8117E-03	7.4294E-03
5.3500E+00	6.2428E+01	------------------------+	9.0144E-03	7.5169E-03
5.4000E+00	5.1237E+01	--------------------+	9.2242E-03	7.6056E-03
5.4500E+00	4.2401E+01	----------------+	9.4411E-03	7.6956E-03
5.5000E+00	3.4976E+01	--------------+	9.6651E-03	7.7866E-03
5.5500E+00	3.0052E+01	------------+	9.8960E-03	7.8788E-03
5.6000E+00	2.8816E+01	------------+	1.0134E-02	7.9722E-03
5.6500E+00	3.0456E+01	------------+	1.0378E-02	8.0666E-03
5.7000E+00	3.6021E+01	--------------+	1.0630E-02	8.1622E-03
5.7500E+00	4.4695E+01	----------------+	1.0888E-02	8.2588E-03
5.8000E+00	5.5269E+01	---------------------+	1.1152E-02	8.3564E-03
5.8500E+00	6.6162E+01	-------------------------+	1.1422E-02	8.4549E-03
5.9000E+00	7.7218E+01	-----------------------------+	1.1546E-02	8.5547E-03
5.9500E+00	8.6674E+01	--------------------------------+	9.6936E-03	8.6475E-03
6.0000E+00	9.1[illegible]4E+01	---------------------------------+	8.0981E-03	8.7349E-03
			7.1780E-03	8.5574E-03

FIG 4.14 SIMULATION OUTPUT OF FIG 4.13 WITH KPRO=0.05 & KINT=0.003

4.3 DISCUSSIONS

It has to be emphasized again that the actual dynamic interaction of the entire closed-loop system is very complex. It is almost impossible to find a nice, neat, and exact model to describe the exact behaviour of the closed-loop system. Chapter 2 has already demonstrated the difficulties of analyzing only a part of the overall closed-loop system, which is the physical process (turning operation). Moreover, the backlash of the tool due to the reaction of feed force is ignored in the closed-loop model, though its effect is extremely small for a rigidly mounted tool. Thus, the block diagram of Fig. 4.5 which was developed to model the entire adaptive system, is only a crude approximation of the real process. However, the major dynamic elements are all taken into consideration in the model. Consequently, results obtained in this chapter can only provide a general idea about the stability of the system.

As to the stability relationship between Kpro and Kint, the results shown in Fig. 4.10 are quite reasonable. Since the depth-of-cut, a, acts as a constant in open-loop equation, a small depth-of-cut naturally allows larger values of Kpro and Kint and vice versa. Indeed, this is true in our case. By the same token, it is also expected to obtain three curves of similar shape as in Fig. 4.10 .

The programs to simulate the eccentric turning are

carefully designed in order to match as closely to the experimental conditions as possible. Many special features have been put in both of the programs in Appendices L.1 and L.2 . For example, the integral action is programmed as a summation of the error signals rather than as a continuous mode function because of the discrete nature of the experimental system (refer to Section 3.3.3 for details). To avoid the phenomenon of reset windup, the integrators in the simulation programs are further checked for saturated mode in the same say as the integrator in the micro-computer program (refer to Section 3.3.3) . Due to the discrete nature of the real system, a fixed-step integration method, RKSFX, is used to ensure that an integration is performed only at the sampling time. In the simulation program, the function "KEEP" further ensures that the statements of the procedure function cannot be executed except when an integration is performed. Finally, since fixed-step integration method is used , the statement - "IF (PULSE. NE. 1.0) GOTO 10" - is needed to allow for the procedure function to be executed at sampling instants only.

The simulation of Fig. 4.12 is quite sucessful. Firstly, because of the eccentricity imposed on the problem, it is expected to obtain sinusoidal cutting force signals as in Fig. 4.12 and Appendix L.1. Secondly, from any of the above output, it is easy to see that a complete cycle indicated by the computer is 0.85 seconds which is very close to the actual

one of 0.869 seconds. Their difference comes actually from the desired increment for the print-plot output in the program. Since OUTDEL is specified to be 0.05 seconds in the program, the force is print-plotted for every such a time interval. As a result, the output gives an apparent revolution time of 0.85 seconds.

Two observations have been made from Fig. 4.12 and Appendix L.1. The first one is that, regardless of the controller gains, the force always overshoots the nominal value which is 80 lbf. The second observation is that there is no essential difference among all the outputs. This suggests that for eccentric turning, one can arbitrarily choose the proportional and integral gains.

The overall effect of the PVM is explicitly depicted by a comparison between Figs. 4.12 and 4.14 . The latter figure shows that with the same parameter set, the program with PVM lowers the cutting force below the nominal value at steady state. However, the outputs in Appendix L.2 indicates that precaution is needed in the use of PVM. An improper combination of Kpro and Kint may result an undesirable irregular cyclic cutting force with large difference between its extreme values, as shown in the last output in Appendix L.1 . Therefore, the simulation indicates that if PVM is used in the control algorithm, the controller gains should be chosen carefully. Finally, a comparison between the

corresponding outputs of same parameter sets in Appendices L.1 and L.2 indicates that the cutting forces have the same values right before their first maximum values. This illustrates the success of simulating the function PVM.

Of course, the above conclusions and discussions concerned the stability analysis have to be verified and checked by experiments which are described in next chapter.

CHAPTER 5

EXPERIMENTS AND DISCUSSIONS

This chapter has three main sections. The first section, Section 5.1, describes how the experiments were conducted. It is concluded with a sub-section, Section 5.1.1, concerning the experimental aspects in general. The last two sections discuss the experimental results where Section 5.2 deals with non-eccentric turning and Section 5.3 with eccentric turning.

5.1 THE EXPERIMENTS

The main purposes of the experiments are to examine and evaluate the performance of three common controllers; namely, the P, I, and PI controls, and to investigate the desirability of the peak-value memory (PVM) function. Also, through the experiment, it is hoped to demonstrate the structure and modelling of any micro-computer adaptive control system.

The experiments were carried out for both eccentric and non-eccentric turning. Each cutting condition was tested for both with and without PVM in the control algorithm.

In all of the tests, the spindle speed and feedrate are manually set to be 69 RPM and 0.015 IPR respectively. The reason for selecting such a low RPM is to ensure there are adequate number of samples in every spindle revolution. Since

the computational time of the micro-computer for the developed algorithm was measured to be about 50 milli-seconds (refer to Appendix J), the selection of 69 RPM will give approximately 18 samples for every revolution, which is a reasonable sample size. Also, the selection of a moderate feedrate, 0.015 IPR, provides safety and ease in handling of the experiments.

In the experiments, a straight edge carbide tool is used as a cutter in order to match the cutting conditions imposed on the problem as described in Chapter 2.

There are two workpieces in the experiments; one for eccentric and the other for non-eccentric turning. They are both aluminum cylinders of about 3" in diameter. The only difference between them is in their lengths. One is 8" and the other 18". The shorter workpiece is used for the eccentric turning tests since a tailstock support is not used during the eccentric experiments. For both cutting conditions, the desired depth-of-cut, b, is set to be 0.06". In eccentric turning, the workpiece is eccentrically mounted by inserting a shim on one of the jaws of the lathe chuck. The thickness of the shim (i.e., eccentricity) is 0.03" giving a resulting depth-of-cut, a, varying in the range of $0.03" \leq a \leq 0.09"$ during one workpiece revolution.

To run the experiments, the workpiece and the tool are first mounted on the chuck and the tool holder. Then the digital adaptive control unit is properly set with the computer

controlled signal connected to the feedrate override switch at the control panel. The Assembler program is then loaded to the computer through the teletype. After activating the program, the desired values of different variables (e.g., Kpro, kint, F, RPM, ... etc) are input interactively to the computer by means of the teletype. To take actual measurements of data, the NC lathe is first programmed manually. A simple linear motion to turn the workpiece to a constant diameter was always used. The spindle speed is then selected. Once the NC lathe is started, the digital adaptive control unit is activated to take on-line measurements and control action. The cutting force and feedrate override signal are then recorded by a storage tube oscilloscope. To stop the experiments, the micro-computer is stopped by pushing the "BREAK" button and the NC lathe is put in a feed hold condition. In order to have a permanent record of results, the behavior of the cutting force and feedrate signals are then recorded by taking instant photos from the oscilloscope.

Therefore, on all of the photos, there are two signals. The upper one is the trace of the main cutting force whereas the lower one is that of the computer feedrate command signal. The sensivities are 80 lbf/div and 5.0 volts/div respectively. The feedrate command in the range of 0.0 to +5.0 volts corresponds to a feedrate in the range of 0.0 to 0.015 inches per revolution. Horizontal time swift for all pictures is 2.0

sec/div.

Attention is then drawn to the computer controlled signal. This signal on each photo always starts at -5.0 volts, which then abruptly jumps to +5.0 volts when computer algorithm is started. This phenomenon is caused by the micro-computer hardware and the analog-to-digital converter at the beginning of data conversion.

All results are collected in Appendices M and N. All photos labelled with subscript 'a' such as 1a, 2a, ... etc, are the results from the program without PVM. Likewise, those labelled with subscript 'b' are from the program with PVM.

Since there are numerous parameters in the system, it is almost impossible to find all the effects and relationships between them. The present research so far has concentrated on the effects of Kpro and Kint. This is due to the time and resource limitations of the project. The reason for selecting the two parameters of Kpro and Kint in this research is that they are the prime control factors in an adaptive system. In all of the experiments, the nominal force, nominal voltage, spindle speed, and decaying factor are set to be 80 lbf, 2.5 volts, 69 RPM, and 0.8 per revolution respectively.

5.1.1 Discussion on the General Aspects of the Experiments

The extent of this research is limited extensively by the physical capabilities of the experimental system. For example, if the NC lathe could provide an on-line continuous mode of changing RPM and depth-of-cut, research on the influence of these parameters can be included as well.

Since the micro-computer adaptive unit is an electronic system, it is extremely sensitive to environmental influences. One of the influences is the noise that it picks up during experiment. Although floating ground method is used to minimize the noise level, the system somehow still picks electrical noise from its surrounding metal cutting machines. Thus, there is considerable variation in the quality of the experimental records from experiment to experiment.

Also, it was observed that the oscilloscope employed in this project drifted slightly with time. To minimize this drift, the electronic equipment was allowed to warm up for several hours before experimentation. However, there is still some drift evidence in the experimental results on the photographs.

The accuracy of the cutting force measurements is actually quite low and the resolution of the oscilloscope display of the real-time force is about ± 10 lbf. Therefore, the following discussion has emphasized on the observable and general features only.

5.2 DISCUSSIONS OF THE RESULTS ON THE NON-ECCENTRIC TURNING

This section summarizes the experimental results of non-eccentric turning only. It has four sub-sections. The first sub-section is a discussion of the performance of a pure proportional (P) controller working along with and without a PVM. The following two sub-sections are the same as the first one except their differences in controllers. One is a pure integral (I) control and the other one is a proportional-plus-integral (PI) control. The last sub-section compares the experimental results with the theoretical prediction of the system stability by using Nyquist plot method.

5.2.1 Proportional Control

Photos for non-eccentric turning with P control are collected in Appendix M.1 . Pictures 1a, 2a, 3a, and 4a in this appendix show that, without PVM, the system behaves like a second-order system. This characteristic is particularly demonstrated by Photos 1a and 2a, which show that the larger the proportional gain, Kpro, the more oscillation there is before settling to a steady value and the less the steady-state error. To know the amount of steady-state error, one first has to have the nominal force signal, which can be found by having a run with a pure integral control. Then, the amount of difference between the nominal force and that from a P control

is the steady-state error.

Pictures 3a and 4a also indicate the stability limit of the proportional gain, Kpro, for P control of the system is between 0.24 and 0.35. This is revealed by Photo 4a for which, when Kpro equals 0.35, the cutting force keeps on oscillating without settling to a fixed value - an indication of the system instability. To understand the instability, the basic proportional control law (i.e., Eq.(3.3.5)) is recalled for explanation: Vout = Vnom+Kint*Int+Kpro*(Fnom-Data).

Because it is a pure proportional controller (i.e., Kint=0) and there is no PVM in the control algorithm, Eq.(3.3.5) becomes: Vout=Vnom+Kpro*(Fnom-Data). At the start up, there is no cutting force; hence, the difference between Fnom and Data is positive, and Vout is boosted up to 5.0 volts. This generates the initial jump to 5.0 volts of the controlling signal. As a result, the tool travels with a full programmed speed and the cutting forces increases. Eventually, the cutting force (i.e., the data) will become larger than Fnom and generates a negative error. This error may be well less than Vnom, so the computer will send out a zero volt commanded feedrate override signal. This is what happens for the first cycle of the controlling signal on Photos 2a, 3a, and 4a. However, if Kpro is large as in the case of Photo 4a, the rate of speeding up and slowing down the tool is so drastic that a full 5.0 volts or a 0.0 volt output always results.

Consequently, oscillation of the cutting force is produced; i.e., the system is unstable.

For the same control action, program with PVM gives rise to two distinct features. But when the gain is small, regardless of the presence of PVM, there is virtually no difference in both the controlling action and output force (compare Photos 1a and 1b). The reason is that a small Kpro in Eq.(3.3.2) implies a trivial control action.

However, once the Kpro is large enough to have significant effects on Vout, the feature resulted from PVM is the reduction of oscillation in the transient period (compare Photos 2a with 2b, 3a with 3b). This is a consequence of the time delay characteristic of the function. Since program with PVM results in a slower control action change with respect to a negative rate of force change, the whole system is driven with a lower speed than that without PVM. Thus, less oscillation is expected. Another advantage with the PVM is a slightly shorter settling time (compare Photos 2a with 2b, and 3a with 3b).

5.2.2 Integral Control

Results in Appendix M.2 show that under a pure integral controller, the system also behaves like a second-order system. As the integral gain, Kint, is increased there are more oscillations and higher overshooting before settling to a steady-state value (compare Photos 1a, 2a, 3a, and 4a in

Appendix M.2)

It is obvious, from Photos 3a and 4a, that when there is no PVM action the stability limit for Kint is in between 0.0055 and 0.008. Below the stability limit, the steady-state value of the cutting force is of course equal to the nominal value, Fnom (i.e. 80 lbf) because of the characteristic of an integral controller. Furthermore, when the steady-state values of the cutting force are compared with those from a pure P control, their values are higher for an I control. This verifies the general features of a pure P and a pure I controller: for a P controller there always exists steady-state error, whereas for an I controller there is no steady-state error regardless of the disturbances.

For integral control, advantage of having PVM in the control algorithm is solely in the transient behavior. There are three such aspects. Comparison of adjacent pictures in Appendix M.2 for corresponding Kint shows that less oscillations of the cutting force is resulted from the PVM. Best of all, program with such function gives a shorter settling time than that one without, and this is distinctly shown by Photo 3b when it compared with 3a. Photos 1b and 2b also indicate that for a small integral gain, overshooting can be avoided and the system behaves like a first-order system as a result of the PVM.

If the stability limit is exceeded, however, Photo 4b

reveals that the tool will suffer substantially from an intermittant triangular force with large peak values. At this stage, one cannot conclude and compare from Photos 4a and 4b the degree of tool damage between the programs without and with PVM in the absence of further detailed investigation.

5.2.3 Proportional-Plus-Integral Control

The merit of a PI controller is demonstrated explicitly by the results in Appendix M.3, which is the combination of the desirable transient characteristic of a proportional controller and the feature of no steady-state error of an integral controller (compare Photos 1a in Appendix M.3 with 3a and 2a in both appendices of M.1 and M.2). Indeed, results show that there is less overshooting and a smaller difference between the maximun and minimum forces with a PI controller.

One can also see that the Kint stability limits on Kpro and Kint acting together may be larger than the limits on Kint when Kpro=0. Photo 4a in Appendix M.3 shows that although Kint equals 0.008, which is an unstable value for a pure integral controller, the system is still stable. On the contrary, Photo 3a in the same appendix shows the instability of the system when it is under a stable value of Kint 0.004 but an unstable value of Kpro 0.35.

With the inclusion of PVM, the dynamic behavior of the system is also dominated by the P action for a PI control. The

above statement is supported by the Photos 1b, 2b, 3b, and 4b in Appendix M.3. They all show that when Kpro exceeds the stability limit, the integral control is incapable of improving the stability (refer to Photos 3b and 4b in the appendix). On the other hand, with PVM the steady-state behavior of the system with PI control resembles more to that with pure P control than with pure I control, and it fluctuates with respect to the nominal value. Fortunately, the fluctuation is small as can be seen from Photos 1b and 2b. Furthermore, these two photos show that for the same Kpro, the experimental system with a small Kint can reach the steady state faster than that with a larger Kint. The prime cause is the dominance of the integral control action on the transient behavior (compare Photos 3b in Appendix M.2 and 2b in Appendix M.3). A close examination of Photos 1a with 1b and 2a with 2b also reveals that with PVM, the PI controller gives a small steady-state value and a smoother controlling action than it does without PVM.

5.2.4 Comparison of the Experimental Results and the Theroetical Prediction of the System Stability by using Nyquist Plot Method

A comparison between Fig. 4.10 and Appendices M.1, M.2, and M.3, shows there is a substantial difference in between the experimental and analytical results. For example, Photo 4a in

Appendix M.1 indicates clearly that for a pure proportional control the stability limit of the experimental system is less than 0.35. However, for the same value of $\dot{K}pro$, Fig. 4.10 shows that it is still within the stability limit. Same disagreement takes place in between Photo 3a in both appendices of M.2 and M.3 and Fig. 4.10 .

The possible reason is that even though a digital system can be approximated as a continuous one in some cases, Nyquist plot is still not an appropriate method in predicting its stability.

5.3 DISCUSSIONS OF THE RESULTS ON ECCENTRIC TURNING

This section discusses the experimental results of eccentric turning only. It has also four sub-sections and its organization is the same as the previous one, Section 5.2 .

5.3.1 Proportional Control

The results for eccentric turning with a pure P controller are collected in Appendix N.1 . Because the workpiece is eccentrically mounted, the cutting force is always oscillating and therefore it is hard to decide whether or not the adaptive loop is stable. In fact the actual definition of stability is somewhat ambiguous. For our purposes we will define the system to be unstable when the control signal oscillations saturate at both the 0.0 and +5.0 volts limits;

e.g., as occurs in Photo 7a .

Due to the eccentricity, it is more difficult to visualize the interaction between the controlling action and the cutting force. For a small proportional gain of 0.005, Photo 1a indicates that very little control action is taking place. The commanded feedrate override signal in the picture is almost equal to Vnom. The explanation is the same as that one described in Section 5.2.1 . It is clear that the sinusoidal form of the cutting force solely comes from the eccentricity. For proportional gains of larger value, what the computer does basically is sending a commanded signal which is proportional to the difference between Fnom and the actual cutting force at each particular sampling instant.

In the experiments no attempt was made to always synchronize the starting of the tool motion with the workpiece angular position. Therefore, the transient behavior of each run is dependent on the initial depth-of-cut that the tool encounters with the workpiece. A photo with a high initial peak value of cutting force implies that the tool encountered a deep depth-of-cut at the start up motion. This is the case in Photo 7a . Therefore, it is not surprising to have photos with different transient behavior in the appendix. However, the steady-state behavior, which is sinusoidal, is independent of the transient state. It would seem reasonable that, at the steady state, what the computer "sees" and responses to is some

average value of the maximum and minimum values of the cutting force. From Photos 1a, 2a, 3a, ... 7a, it is obvious that, with a pure proportional control action, a larger gain gives a larger average value of cutting force.

The outstanding advantages of implemeting the PVM are readily seen from the Photos 1b to 7b in the same Appendix N.1 . For a P controller, two merits are obtained. The first one is the generation of a smaller maximum and a smaller minimum steady-state cutting force. In other words, the average cutting force is smaller. The second advantage is the acquirement of a smoother controlling signal (compare Photos 4a with 4b, 6a with 6b, and 7a with 7b).

Photos 3b, 4b, and 5b indicate that when the proportional gain is larger, the peak values between two successive forces are not equal at steady state. A close examination notices that most of the peak values are always within the limit of the nominal value. Therefore, for the same gain, even though the cutting force ripples more irregularly than the one resulted from the program without PVM, the PVM control action is still more desirable from the point of view of safety. But large peaks of cutting force may result from the PVM when instability is reached as shown in Photo 7b . The picture clearly shows there is a severe interaction between the workpiece and the tool. However, the degree of damage on the tool, when Photos 7a and 7b are compared, is still open for investigation.

5.3.2 Integral Control

Casual observation of Appendix N.2 suggests similar results for an integral controller when the photos in the appendix are compared with those from a proportional controller. They are both sinusoidal with an irregular transient behavior. A detailed examination, however, shows that they are actually different in several aspects. First of all, regardless of the integral gain, at steady state all the cutting forces ripple with the same maximum and minimum values for an I controller. On the other hand, under a P control the extreme values depend on the value of proportional gain.

Again, it is believed that the integral control takes the average of the extremities as the nominal value. The ripples of the commanded override signal are a result of the difference between the instantaneous and average values of the cutting force. This is why if a line joining the average value is drawn for any photo from 1a, 2a, ... to 5a in Appendix N.2, its magnitude is very close to that cutting force signal in any photo in Appendix M.2 .

For integral gain, the program with PVM improves at least two steady-state phenomena in eccentric turning. The first improvement is on the smoothness of the controlling signal (compare Photos 2a with 2b, 3a with 3b, and 4a with 4b in Appendix N.2). Although one may not necessary care about the smoothness of the controlling signal as long as it does what is

wanted, the smoothness does indicate the potential vigorousness of a dynamic system. The second improvement is again on the aspect of safety. The PVM lowers the maximum steady-state value within the desirable range, Fnom.

Despite the above merits, one drawback which is the long settling time may hinders the use of PVM for a pure integral control (compare all the adjacent photos in Appendix N.2). The long settling time is a consequence of the time delay character of the PVM.

5.3.3 Proportional-Plus-Integral Control

In Appendix N.3, the results for PI control are collected. In terms of cutting force signals, the program with PI control gives very similar results to those of pure I control. The co-operation with the P controller, however, eliminates the irregularity in the transient period that characterizes a pure P and a pure I control in eccentric turning (compare Photos 2a, 3a, and 4a in Appendices N.1, N.2, and N.3 respectively).

On the other hand, regardless of the values of Kpro and Kint, the cutting force steady-state behavior for all results are very similar. They all have the same maximum and minimum values and all the maximum values are greater than Fnom; i.e., 80 lbf. The similarity comes from the integral action which has been explained in previous section.

The proportional controller in the PI control acts like an amplifier to the integral signal. The results in Appendix N.2 show that, without PVM, all the integral controlling signals are ripples with small amplitudes. The addition of the P controller increases the amplitudes and hence, evens out the irregularity at the transient state (compare Photos 8a with 5a in Appendices N.3 and N.2 respectively).

Furthermore, Photo 9a in Appendix N.3 shows that even though the stability limits are exceeded, the cutting force is not affected and looks like those of other results. This suggests that one can arbitarily choose the gains of Kpro and Kint for a PI control in eccentric turning operation.

When the PVM is implemented in the control algorithm, the stability of the system is also indicated by the controlling signal. If the controlling signal regularly reaches the extreme values (i.e., 0.0 and 5.0 volts), the system is considered to be unstable (see Photo 9b in Appendix N.3). Within the stability limit, the basic character of PVM, which is the lowering of the maximum steady-state value, is shown clearly by photos 1b, 2b, ... to 7b in the same appendix. Therefore, the advantage of PVM is that the maximum cutting force is less, which should contribute toward a longer tool life - an important economic factor in metal machining operation.

The benefit from PVM may also be well seen in the transient period immediately after the cutting force has

reached the first peak value. Photos 1b to 6b in Appendix N.3 clearly show that the feedrate override signal always rapidly chops to a low value after the cutting force reaches its initial peak value. Then it increases gradually until the force reaches steady-state cyclic behavior with a maximum value equivalent to Fnom. As a result, program with PVM eliminates the perilous overshooting within this period of transient as compared to the program without PVM (compare Photos 1a with 1b, 2a with 2b, ... 6a with 6b in Appendix N.3). It is pointed out that such a benefit is not included in that period of time prior to the first initial peak. The reason is that the function PVM in this research does not check the rate of increasing but rather the rate of decreasing of data. Furthermore, since the synchronization of the starting of the tool motion with the workpiece angular position is not done, definite conclusion concerning the first peak of cutting force is not made.

In spite of the advantages, the PVM does have some imperfection. The choice of the proportional and integral gains is quite crucial. Inappropriate combination of Kpro and Kint may result in an undesirable surface finish, although in a rough cut this is of little concern. This can be depicted by Photos 4b, 5b, 7b, and 8b in Appendix N.3. In these cases the cutting force has a fairly irregular cyclic behavior in the steady state. This implies a varying cutting speed and hence,

poor surface finish results. Furthermore, if the stability limit is once exceeded, the PVM may generate periodic cutting force with large maximum amplitude as shown in Photo 9b . Therefore, if instability is reached, the program without PVM may be more preferable than that with this function.

5.3.4 Discussion of the Experimental and Simulation Results

In general, the experimental and simulation results match closely to each other for eccentric turning. For example, when Photos 2a, 4a, and 9a in Appendix N.3 are compared with Fig. 4.12 and the output in Appendix L.2 respectively, it is observed that all the cutting forces behave sinusoidally and overshoot the nominal value at steady state. Actually, within the accuracy which one can measure from the photo, the amount of overshooting is approximately the same for both results. The only significant difference between the experimental and simulation results is in their transient behaviors (compare Photos 2a, and 9a in Appendix N.3 with Fig. 4.12 and the last output in Appendix L.1) . The reason for the difference is that in the experiments, the initial depth-of-cut that the tool encounters with the workpiece is not synchronized. In the simulation, it is always the same for every run of the program.

The simulation results of the program with PVM also match closely to the experimental results. For example, Photo 2b in Appendix N.3 and Fig. 4.14 both show that there is a sharp

suppression and then a gradual increase of the cutting force right after its first maximum value. Furthermore, when Photo 4b and 9b in Appendix N.3 are compared with the two outputs in Appendix L.2 respectively, they look similar to each other with irregular cyclic cutting forces. This indicates that the simulations are successful.

CHAPTER 6

CONCLUSIONS AND RECOMMENDATIONS

6.1 CONCLUSIONS

The following conclusions may be drawn from the investigation of the dynamics and control of eccentric turning:

1) The natural frequencies of an eccentric turning process are more sensitive to the angular velocity (i.e. RPM) than to the feedrate (i.e. IPR). Within the scope of investigation, the experimental eccentric turning operation is a stable process. Although there is a small degree of instability indicated by the real part of the assumed solution, its value is so small compared with the imaginary part that it is believed to come from computational round-off error. Moreover, the structural damping, which has been neglected in the analysis, will contribute as a stability factor in a real process.

2) This research demonstrates that an adaptive control system can really work, and the proposed digital adaptive control NC lathe system is valid and useful. With further development and modification, it could be applied in practical turning operation.

3) The function of peak-value memory (PVM) generally tends to control turning operation with a conservative action by

driving the process with less oscillation and decreasing the peak values of the cutting force. Hence, the tool life is expected to be prolonged by the program with such function. Therefore, PVM is desirable not only from the point of view of safety but also of economy.

4) When PVM is used along with a P, I, or PI controller, the values of Kpro and Kint should be selected carefully. If they are too large, instability may result with high peak values of the cutting forces.

5) Digital simulation is a very flexible and versatile way of obtaining necessary information about non-linear systems. To have good results, the simulation program has to be designed carefully in order to match as close as possible to the actual system.

6) Even though a digital system sometimes can be approximated as a continuous one, Nyquist plot is still not an appropriate method in predicting its stability.

6.2 RECOMMENDATIONS FOR FUTURE WORK

Before the ideas of this research could actually be used in practice, many physical problems would have to be resolved first. One of the problems is the way of measuring the force signal. In practice, it is very difficult, time-consuming, and expensive to mount each tool on a dynamometer especially for the case of a turret lathe. Research on new methods of

measuring cutting forces should be carried out.

Research on how to speed up the computational rate of micro-computer is also essential because in practice the RPM's would usually be larger than that used in these experiments. For the control algorithms developed in this study it is essential that there be enough samples per revolution. Future work on the improvement of computational rate can concentrate at the designs of micro-computer and floating point package.

To fully implement the experimental idea, the NC lathe has to be improved so that the problem of transition from rapid traverse to feedrate can be solved. In practice, the NC lathe should have a very fast, responsive, and reliable servo to stop the feedrate without tool breakage when the tool hits the tool workpiece at rapid traverse. An alternative way to accomplish such an aim is the design of a tool/workpiece proximity sensor.

It is also obvious that the experiments carried out were limited to very specific cutting conditions. Different cutting conditions with different workpiece materials should be tested in future to fully evaluate the proposed system.

In this research, the selection of controller gains is still not really resolved because the depth-of-cut is a multiplication factor in the loop gain. What is needed is some sort of automatic compensation for the depth-of-cut in the adaptive control system.

Finally in this study the adaptive control system was

retrofitted to a conventional NC lathe. The peak-value memory feature required the operator to manually enter the workpiece RPM. One effective way to apply adaptive control in practice would be to implement it directly in in the executive software of a computer numerical control (CNC) controller.

REFERENCES

[1] M.M. Barash, "Computerized Systems in the Scheme of Things.", AIIE Conference, November 13-16, 1979.

[2] S.A. Tobias and W. Fishwick, "The Chatter of Lathe Tools under Orthogonal Cutting Conditions", Trans. Amer. Soc. Mech. Engrs., Vol 80, p 1079, 1958.

[3] J. Tlusty and M. Polacek, "Drittes Forschungs und Konstruktionskolloquium Werkzeugmaschinen", FoKoMa, Vogel Verlag, Coburg, Vol 3, p 131, 1957.

[4] C. Andrew and S.A. Tobias, "A Critical Comparison of Two Current Theories of Machine Tool Chatter", Int. J. Mach. Tool Des. Res., Vol 1, p 325-335, 1961.

[5] W.A. Knight, "Chatter in Turning: Some Effects of Tool Geometry and Cutting Conditions", Int. J. Mach. Des. Res., Vol 12, p 201-220, 1972.

[6] G. Sweeney and S.A. Tobias, "Survey of Basic Machine Tool Chatter Research", Int. J. Mach. Des. Res., Vol 9, p 217-238, 1969.

[7] W.A. Knight, "Application of the Universal Machinability Chart to the Prediction of Machine Tool Stability", Int. J. Mach. Des. Res., Vol 8, p 1-14, 1968.

[8] R.B. Bhat and T.S. Sankar, "Effect of Spatially Moving Random Tool Loads on the Response of Workpiece in Turning", Proceeding of the Eighth Canadian Congress of Applied Mechanics, Moncton, New Brunswick, Canada, June 7-12, Vol 1, p 407-408, 1981.

[9] S. Doi and S. Kato, "Chatter Vibration of Lathe Tools", Trans. Amer. Soc. Mech. Engrs., Vol 78, p 1127, 1956.

[10] L. Fine, "Off Centre Turning", Int. J. Mach. Tool Des. Res., Vol 10, p 15-24, 1970.

[11] M. Weck and K. Schaefer, "Digitale Adaptive Regelung Fuer Die Drehbearbeitung", Ind-Anz, vol 98, n 34, Apr 28, 1976.

[12] G. Stute, Van Brussel, J. Dinsdale, and J.G. Bollinger, "Digital Controls and Feed Drives: State-Of-The-Art and New Developments", Ann CIRP, Vol 29, n 2, p 497-506, 1980.

[13] C.H. Lee and J. Hoh, "Mini-Computer Application on Adaptive Control System for Turning Process", Published by SME, Dearborn, Mich., p 419-424, 1980.

[14] B. K. Kim and Z. Bien, "An Efficient Algorithm for a Time-Suboptional Regulator Problem for Systems with Delay in State", Int. J. Control, Vol 33, n 5, p 871-889, 1981.

[15] D. Carlucci and M. Vallauri, "Feed Back Control Linear Multivariable Systems with Uncertain Description in the Frequency Domain", Int. J. Control, Vol 33, n 5, p 903-912, 1981.

[16] C. Boer, M.C. De Malherbe, and R. Venter, "Adaptive Control Optimization for a Numerically Controlled Milling Process", Proceeding of the 18th Int. Mach. Tool Des and Res. Conference held in London, Sept. 14-16, 1977.

[17] S.R. Atre and V.P. Lele, "Analytic Application of Tsypkin's Method Relay with Hysteresis and Dead Zone", Proc Instr Electr Eng (London), Vol 124, n 12, p 1241-1242, 1977.

[18] G. Stute and F.R. Goetz, "Adaptive Control System for Variable Gain in ACC System", Proceeding of the 16th Int. Mach. Tool Des and Res. Conference held in Manchester, Sept. 10-12, 1975.

[19] A. J. Rushing, "Modify a PI Controller for Fast Response without Overshoot", ISA Trans., Vol 16, n 2, p 21-25, 1977.

[20] M. Weck and K. Schafer, "Direct Digital Control for Turning Operations", Proceeding of the 17th Int. Mach. Tool Des and Res. Conference, Vol 1: Met. Cutting Mach Tools, Sept 20-24, 1976.

[21] L. Meirvoith, "Analytical Methods in Vibration", McGraw Hill, N.Y., N.Y., p 130, 1970.

[22] E.J.A. Armarego, "The Machining of Metals", Prentice-Hall Inc., N.J., p 39, 1969.

[23] F. Koenigsberger, "Design Principles of Metal-Cutting Machine Tools", Pergamon Press Book, Macmillan Co., p 4-5, 1964.

[24] J. Kaczmarek, "Principles of Machining by Cutting, Abrasion, and Erosion", Peter Peregrinus Ltd., Stevenage, p 182-183, 1976.

[25] J.E. Shigley, "Mechanical Engineering Design", 3rd edition, McGraw Hill, N.Y., N.Y., p 636, 1978.

[26] M. Leung, "Micro-processor based Adaptive Control of an NC lathe", McGill University Thesis, Mechanical Eng., Montreal, Canada, 1982.

[27] P. Zsombor-Murray, "Floating Point Arithmetic Package", McGill University, Mechanical Eng., Data Lab., Montreal, Canada, 1979.

[28] Machinability Data Center, 2nd edition, Metcut Research Associates Inc., Cincinnati, Ohio, p 874, 1976.

APPENDIX A

DERIVATION OF THE VELOCITY EXPRESSION OF ANY POINT A W.R.T. THE ORIGIN:

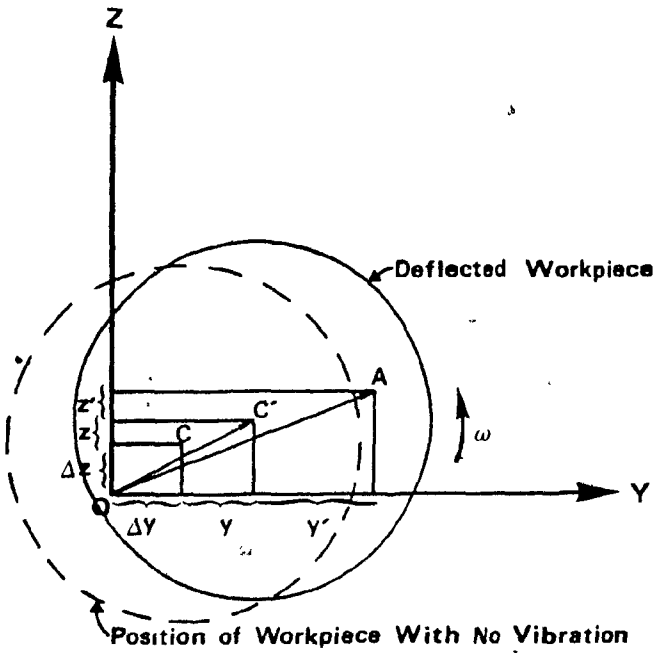

FIG A·1 END VIEW OF THE BEAM WITH VIBRATION

Denote:

$V_{A/O}$ = Velocity of A w.r.t.O

$V_{A/C'}$ = " " A w.r.t.C'

$V_{C'/O}$ = " " C'w.r.t.O

$V^{R}_{C'}$ = Radial velocity of C' w.r.t.O

$\vec{\omega} \times \vec{r}_i$ = Transverse velocity of C' w.r.t.O

$V_{A/C'}$ = Transverse velocity of a w.r.t.C'

$$V_{A/O} = V_{A/C'} + V_{C'/O}$$

But $V_{C'/O} = \left(\vec{V}_{C'}\right)^R + \vec{\omega} \times (\vec{r}_{C'})$ and $V_{A/C'} = \vec{\omega} \times \vec{r}_{C'A}$

$\vec{r}_{C'} = (\Delta y + y)\vec{j} + (\Delta z + z)\vec{k}$ where $\Delta y = d \cos\theta = d \cos \omega t$

$\vec{r}_{C'A} = y'\vec{j} + z'\vec{k}$ $\Delta z = d \sin\theta = d \sin \omega t$

$$V_{C'/O} = (\dot{y}\vec{j} + \dot{z}\vec{k}) + \omega\vec{i} \times ((\Delta y + y)\vec{j} + (\Delta z + z)\vec{k})$$

$$= \dot{y}\vec{j} + \dot{z}\vec{k} + \omega(\Delta y + y)\vec{k} - \omega(\Delta z + z)\vec{j}$$

$$V_{A/C'} = \omega\vec{i} \times (y'\vec{j} + z'\vec{k}) = \omega y'\vec{k} - \omega z'\vec{k}$$

$$V_{A/O} = (\dot{y} - \omega(\Delta z + y) - \omega z')\vec{j} + (\dot{z} + \omega(\Delta y + y) + \omega y')\vec{k}$$

APPENDIX B

INTERMEDIATE STEPS OF INTEGRATION FOR EQUATION (2.1.6) and (2.1.7)

Integration Properties:

i) $$\int_{t_1}^{t_2} \dot{y}\delta\dot{y}dt = \int_{t_1}^{t_2} \frac{\partial y}{\partial t}\delta\left(\frac{\partial y}{\partial t}\right)dt = \frac{\partial y}{\partial t}\delta y\Big|_{t_1}^{t_2} - \int_{t_1}^{t_2} \frac{\partial^2 y}{\partial t^2}\delta y dt$$

$$= \underline{\underline{-\int_{t_1}^{t_2} \frac{\partial^2 y}{\partial t^2}\delta y dt}}$$

ii) $$\int_{t_1}^{t_2} \dot{z}\delta\dot{z}dt = \underline{\underline{-\int_{t_1}^{t_2} \frac{\partial^2 z}{\partial t^2}\delta z dt}}$$

iii) $$\int_{t_1}^{t_2} -\omega\Delta z\delta\dot{y}dt = \int_{t_1}^{t_2} -\omega d \sin \omega t \frac{\partial}{\partial t}\delta y dt = -\omega d \sin \omega t\ \delta y\Big|_{t_1}^{t_2} +$$

$$\int_{t_1}^{t_2} \omega d\frac{\partial}{\partial t}(\sin \omega t)\delta y dt = \underline{\underline{\int_{t_1}^{t_2} \omega^2 d \cos \omega t\ \delta y dt}}$$

iv) $$\int_{t_1}^{t_2} \omega\Delta y\delta\dot{z}dt = \int_{t_1}^{t_2} \omega d \cos \omega t \frac{\partial}{\partial t}\delta z dt = \omega d \cos \omega t\ \delta z\Big|_{t_1}^{t_2} -$$

$$\int_{t_1}^{t_2} \omega d\frac{\partial}{\partial t}(\cos \omega t)\delta z dt = \underline{\underline{\int_{t_1}^{t_2} \omega^2 d \sin \omega t\ \delta z dt}}$$

v) $$-\int_{t_1}^{t_2} \omega z \delta \dot{y} dt = \int_{t_1}^{t_2} -\omega z \frac{\partial}{\partial t} \delta y dt = -\omega z \delta y \Big|_{t_1}^{t_2} + \int_{t_1}^{t_2} \omega \frac{\partial z}{\partial t} \delta y dt$$

$$= \underline{\underline{\int_{t_1}^{t_2} \omega \dot{z} \delta y dt}}$$

vi) $$\int_{t_1}^{t_2} \omega y \delta \dot{z} dt = \underline{\underline{-\int_{t_1}^{t_2} \omega \dot{y} \delta z dt}}$$

vii) $$\int_0^{\ell} -\frac{EI}{\rho A}\left(\frac{\partial^2 z}{\partial x^2}\right) \delta\left(\frac{\partial^2 z}{\partial x^2}\right) dx = -\frac{EI}{\rho A}\left(\frac{\partial^2 z}{\partial x^2}\right) \frac{\partial}{\partial x}(\delta z) \Big|_0^{\ell} + \int_0^{\ell} \frac{EI}{\rho A} \frac{\partial^3 z}{\partial x^3} \delta\left(\frac{\partial z}{\partial x}\right) dx$$

$$= \underline{\underline{-\frac{EI}{\rho A}\left(\frac{\partial^2 z}{\partial x^2}\right) \delta\left(\frac{\partial z}{\partial x}\right) \Big|_0^{\ell} + \frac{EI}{\rho A} \frac{\partial^3 z}{\partial x^3} \delta z \Big|_0^{\ell}}}$$

$$\underline{\underline{-\int_0^{\ell} \frac{EI}{\rho A} \frac{\partial^4 z}{\partial x^4} \delta z dx}}$$

viii) $$\int_0^{\ell} -\frac{EI}{\rho A}\left(\frac{\partial^2 y}{\partial x^2}\right) \delta\left(\frac{\partial^2 y}{\partial x^2}\right) dx = \underline{\underline{-\frac{EI}{\rho A}\left(\frac{\partial^2 y}{\partial x^2}\right) \delta\left(\frac{\partial y}{\partial x}\right) \Big|_0^{\ell} + \frac{EI}{\rho A} \frac{\partial^3 y}{\partial x^3} \delta y \Big|_0^{\ell}}}$$

$$\underline{\underline{-\int_0^{\ell} \frac{EI}{\rho A} \frac{\partial^4 y}{\partial x^4} \delta y dx}}$$

APPENDIX C

REDUCED ORDER METHOD IN OBTAINING THE SOLUTION FOR $[M]\{\ddot{q}\}+[C]\{\dot{q}\}+[k]\{q\}=\{Q\}$

THE MATRIX WE HAVE = (2.1.12):
$$\begin{bmatrix} \ell & 0 \\ 0 & \ell \end{bmatrix}\begin{Bmatrix} \ddot{A}_k \\ \ddot{B}_k \end{Bmatrix}+\begin{bmatrix} 0 & 2\omega \\ -2\omega & 0 \end{bmatrix}\begin{Bmatrix} \dot{A}_k \\ \dot{B}_k \end{Bmatrix} + \begin{bmatrix} K_k & 0 \\ 0 & K_k \end{bmatrix}\begin{Bmatrix} A_k \\ B_k \end{Bmatrix} = \begin{Bmatrix} f_k(t) \\ g_k(t) \end{Bmatrix}$$

Let $\{y\} = \begin{Bmatrix} \{\dot{q}\} \\ \{q\} \end{Bmatrix} = \begin{Bmatrix} \dot{A}_k \\ \dot{B}_k \\ A_k \\ B_k \end{Bmatrix}$ in our case.

Subsitute $\{y\}$ and $\{\dot{y}\}$ into above matrix equation: then it can be written as:

$$[M]\{\dot{y}\} + [K]\{y\} = \{Y\} \qquad [C.1]$$

where
$$[M] = \begin{bmatrix} [C] & [M] \\ [M] & [C] \end{bmatrix} = \begin{bmatrix} 0 & 0 & \ell & 0 \\ 0 & 0 & 0 & \ell \\ \ell & 0 & 0 & 2\omega\ell \\ 0 & \ell & -2\omega\ell & 0 \end{bmatrix} \quad \& \quad [M]^{-1} = \begin{bmatrix} 0 & -2\omega/\ell & 1/\ell & 0 \\ 2\omega/\ell & 0 & 0 & 1/\ell \\ 1/\ell & 0 & 0 & 0 \\ 0 & 1/\ell & 0 & 0 \end{bmatrix}$$

$$[K] = \begin{bmatrix} -[M] & [0] \\ [0] & [k] \end{bmatrix} = \begin{bmatrix} -\ell & 0 & 0 & 0 \\ 0 & -\ell & 0 & 0 \\ 0 & 0 & K_k & 0 \\ 0 & 0 & 0 & K_k \end{bmatrix}$$

$$[Y] = \begin{bmatrix} [0] \\ [Q] \end{bmatrix} = \begin{bmatrix} 0 \\ 0 \\ f_k(t) \\ g_k(t) \end{bmatrix}$$

Homogeneous solution for [C.1] :

$$[M]\{\dot{y}\} + [K]\{y\} = \{0\}$$

Let $\{y\} = \{\Phi\}e^{\lambda t}$

$$\lambda[M]\{\Phi\} + [K]\{\Phi\} = \{0\}$$

$$\lambda[I]\{\Phi\} + [D]\{\Phi\} = \{0\} \quad \text{where} \quad [D] = [M]^{-1}[K]$$

$$[\lambda[I] + [D]]\{\Phi\} = 0$$

For eigenvalues: $\det |\lambda[I] + [D]| = 0$

$$[D] = \begin{bmatrix} 0 & -2\omega/\ell & 1/\ell & 0 \\ 2\omega/\ell & 0 & 0 & 1/\ell \\ 1/\ell & 0 & 0 & 0 \\ 0 & 1 & 0 & 0 \end{bmatrix}\begin{bmatrix} -1 & 0 & 0 & 0 \\ 0 & -1 & 0 & 0 \\ 0 & 0 & K_k & 0 \\ 0 & 0 & 0 & K_k \end{bmatrix} = \begin{bmatrix} 0 & 2\omega/\ell & K_k/\ell & 0 \\ -2\omega/\ell & 0 & 0 & K_k/\ell \\ -1/\ell & 0 & 0 & 0 \\ 0 & -1/\ell & 0 & 0 \end{bmatrix}$$

$$\therefore \quad [I] + [D] = \begin{bmatrix} \lambda & 2\omega/\ell & K_k/\ell & 0 \\ -2\omega & \lambda & 0 & K_k/\ell \\ -1/\ell & 0 & \lambda & 0 \\ 0 & -1/\ell & 0 & \lambda \end{bmatrix}$$

$\det |\lambda[I] + [D]| = 0$

$$\rightarrow \quad \lambda \begin{vmatrix} \lambda & 0 & K_k/\ell \\ 0 & \lambda & 0 \\ -1/\ell & 0 & \lambda \end{vmatrix} - \frac{2\omega}{\ell} \begin{vmatrix} -2\omega & 0 & K_k/\ell \\ -1/\ell & \lambda & 0 \\ 0 & 0 & \lambda \end{vmatrix} + \frac{K_k}{\ell} \begin{vmatrix} -2\omega & \lambda & K_k/\ell \\ -1/\ell & 0 & 0 \\ 0 & -1/\ell & \alpha \end{vmatrix}$$

$$- 0 \begin{vmatrix} -2\omega & \lambda & 0 \\ -/1\ell & 0 & \lambda \\ 0 & -1/\ell & 0 \end{vmatrix} = 0$$

$$\rightarrow \quad \lambda^4 + \lambda^2 \left(\frac{2K_k}{\ell^2} + \frac{4\omega^2}{\ell^2}\right) + \frac{K_k^2}{\ell^4} = 0$$

$$\rightarrow \quad \lambda^2 = -\left(\frac{2K_k}{\ell^2} + \frac{4\omega^2}{\ell^2}\right) \pm \sqrt{4\left(\frac{K_k}{\ell^2} + \frac{2\omega^2}{\ell^2}\right)^2 - \frac{4K_k^2}{\ell^4}} \Big/ 2$$

$$\rightarrow \quad \lambda^2 = -2\left(\frac{K_k}{\ell^2} + \frac{2\omega^2}{\ell^2}\right) \pm \sqrt{4\left(\frac{K_k^2}{\ell^4} + \frac{4K_k\omega^2}{\ell^4} + \frac{4\omega^4}{\ell^4}\right) - \frac{4K_k^2}{\ell^4}} \Big/ 2$$

$$\rightarrow \quad \lambda^2 = -\left(\frac{K_k}{\ell^2} + \frac{2\omega^2}{\ell^2}\right) \pm \frac{1}{\ell^2}\sqrt{\frac{16}{4} K_k\omega^2 + \frac{16}{4} \omega^4}$$

$$\rightarrow \quad \lambda^2 = \frac{1}{\ell^2}\left[-(K_k + 2\omega^2) \pm 2\sqrt{K_k\omega^2 + \omega^4}\right]$$

$$\rightarrow \quad \lambda^2 = \frac{1}{\ell^2}\left[-(K_k + 2\omega^2) \pm 2\omega\sqrt{\omega^2 + K_k}\right]$$

APPENDIX D

DETERMINATION OF THE RELATIONSHIP BETWEEN THE CUTTING FORCE (P_1) AND THE PRODUCT OF DEPTH-OF-CUT & FEEDRATE (a.s) AS FOUND BY F. KOENIGSBERGER

The 2 points picked up for evaluation are: $A_1 = (300, 0.0035)$
$A_2 = (80, 0.0006)$

Denote F by y and (a.s) be x so we have:

$$\frac{\ln y - \ln 80.0}{\ln x - \ln 0.0006} = \frac{\ln 300.0 - \ln 80.0}{\ln 0.0035 - \ln 0.0006}$$

$$\Rightarrow (\ln 0.0035 - \ln 0.0006) * (\ln y - \ln 80) = (\ln 300 - \ln 80) * (\ln x - \ln 0.0006)$$

$$\Rightarrow \ln y - \ln 80 = 0.749(\ln x - \ln 0.0006)$$

$$\Rightarrow \ln y - 4.328 = 0.749(\ln x - (-7.418))$$

$$\Rightarrow \ln y = 0.749 * \ln x + 9.942$$

$$\Rightarrow y = e^{(0.749 \ln x + 9.942)}$$

$$\Rightarrow y = 20786 * x^{0.749}$$

$$\Rightarrow F = \underline{20786 (a.s)^{0.75}}$$

APPENDIX E

DETERMINATION OF THE DEPTH-OF-CUT IN ECCENTRIC TURNING WITH CONSIDERATION OF THE DISPALCEMENT DUE TO VIBRATION

Since the workpiece is eccentric and subject to vibration, the depth-of-cut (a) changes with time which alternatively changes the force magnitudes, hence, depth-of-cut has to be determined.

Consider the beam under deflection:

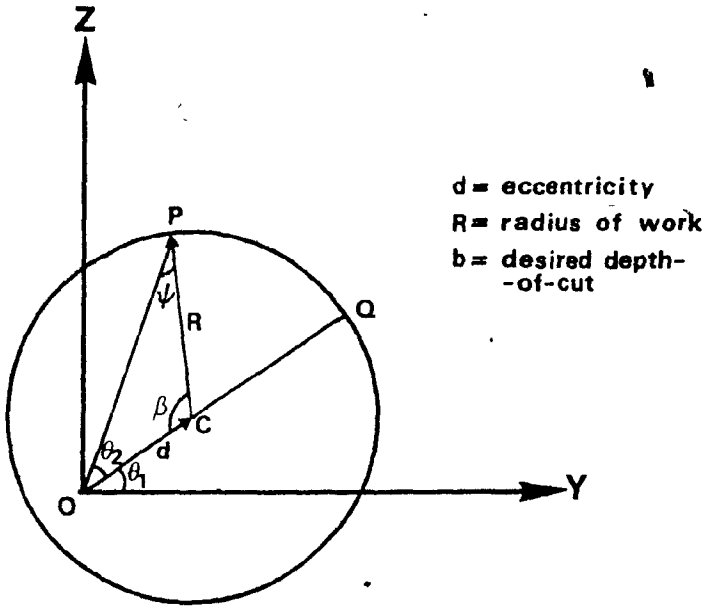

FIG E·1 END VIEW OF THE DEFLECTED BEAM WITH DEFINED ANGLES

where d = eccentricity
R = radius of work
b = desired depth-of-cut
OQ = summation of eccentricity and radius of work
OP = radial length that the workpiece crosses the y-axis at any time

By Sine Law: $\frac{R}{\sin\theta_2} = \frac{d}{\sin\psi} = \frac{OP}{\sin\beta}$

$$\Rightarrow \quad \sin\psi = \frac{d}{R}*(\sin\theta_2)$$

$$\Rightarrow \quad \psi = \sin^{-1}\left(\frac{d}{R}*\sin\theta_2\right)$$

$$\beta = 180^0 - \psi - \theta_2$$

$$\Rightarrow \quad \beta = 180^0 - \theta_2 - \sin^{-1}\left(\frac{d}{R}*\sin\theta_2\right)$$

Since $OP = \frac{R}{\sin\theta_2} * \sin\beta$

$$OP = \frac{R}{\sin\theta_2} * \sin\left(180^0 - \theta_2 - \sin^{-1}\left(\frac{d}{R}*\sin\theta_2\right)\right)$$

$$OP = \frac{R}{\sin\theta_2} * \sin\left(\theta_2 + \sin^{-1}\left(\frac{d}{R}*\sin\theta_2\right)\right)$$

But $\theta_2 = \omega t - \theta_1$ where θ_1 is the initial angle that the maximum radial length (OQ) makes with the horizontal axis as shown in Fig. E.1 .

Since OQ = R+d, OP can be expressed as:

$$OP = \frac{R}{\sin(\omega t-\theta_1)} * \sin((\omega t-\theta_1)+\sin^{-1}(\frac{d}{R}*\sin(\omega t-\theta_1))$$

If set $\theta_1 = 0.0$

$$OP = \frac{R}{\sin \omega t} * \sin(\omega t+\sin^{-1}(\frac{d}{R}*\sin \omega t)$$

$$OP = \frac{R}{\sin \omega t} *\{ \sin \omega t\cos(\sin^{-1}(\frac{d}{R} \sin \omega t))+\cos(\omega t)\frac{d}{R} \sin \omega t\}$$

Physically, d/R is a small ratio so that d*sin ωt/R will be even smaller. Hence OP can be approximated as:

$$OP \simeq \frac{R*}{\sin \omega t}(\sin \omega t+\cos \omega t*\frac{d}{R}*\sin \omega t)$$

$$=> OP \simeq R + d \cos \omega t$$

Therefore, if initially OQ is on the y-axis, i.e. $\theta_1=0^0$, and the desired depth-of-cut is b (refer to Fig. E.2 on next page), the actual depth-of-cut (a) with time is:

$$a = OP-OB = OP-(R+d-b)$$

$$=> a = R+d \cos \omega t-R-d+b$$

$$=> a = \underline{\underline{d(\cos \omega t-1)+b}}$$

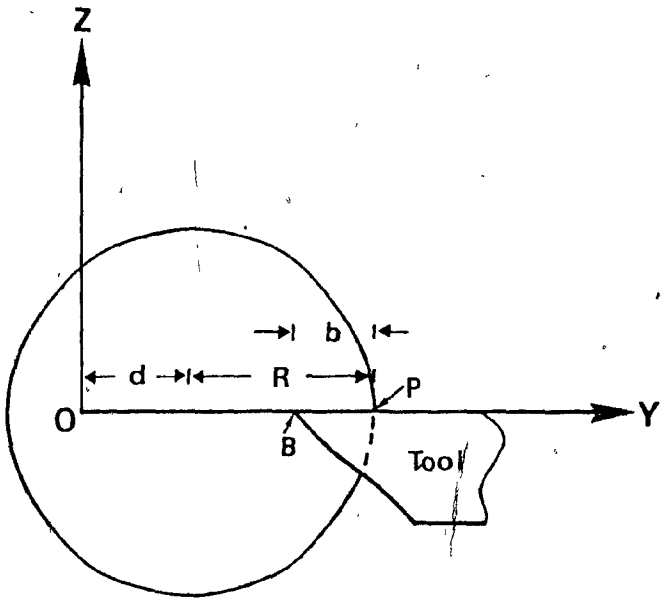

FIG E·2 DIAGRAM SHOWING THE PARAMETERS DEFINED IN THIS APPENDIX

APPENDIX F

RELATIONSHIP BETWEEN $20786(as)^{0.75}$[ℓbf] and $191\ as^{0.75}$[Kg].

a		s		$P_1=20786(as)^{0.75}$[ℓbf]	$P_1^*=P_1*\frac{4.45}{9.81}$ [Kg]	$P'_1=191\ as^{0.75}$[Kg]	$\frac{P_1^*}{P'_1}$
in	mm	in/rev	mm/rev	a [in]; s [in/rev]		a [mm]; s [mm/rev]	
0.03	0.762	0.015	0.381	64.221	29.132	70.580	0.413
		0.020	0.508	79.686	36.147	87.576	0.413
		0.030	0.762	108.007	48.994	118.701	0.413
		0.050	1.270	158.430	71.867	174.117	0.413
		0.100	2.54	266.447	120.866	292.829	0.413
		0.500	12.7	890.921	404.138	979.132	0.413
0.06	1.524	0.015	0.381	108.007	48.994	141.160	0.347
		0.020	0.508	134.016	60.792	175.152	0.347
		0.030	0.762	181.646	82.398	237.402	0.347
		0.050	1.270	266.448	120.866	348.234	0.347
		0.100	2.54	448.109	203.271	585.657	0.347
		0.500	12.7	1498.345	679.677	1958.264	0.347
0.09	2.286	0.0150	0.381	146.393	66.407	211.740	0.314
		0.02	0.508	181.646	82.398	262.729	0.314
		0.030	0.762	246.203	111.682	356.103	0.314
		0.050	1.270	361.143	163.821	522.351	0.314
		0.100	2.54	607.369	275.514	878.486	0.314
		0.500	12.7	2030.861	921.237	2937.395	0.314

∴ For a fixed depth cut the expression $20786(as)^{0.75}$ can be expressed as a fraction multiplied by $191\ as^{0.75}$, i.e. $K*191\ as^{0.75}$, particularly for a = 0.06" K = 0.347.

APPENDIX G

DETERMINATION OF THE VALUE OF THE FUNCTION: $\phi_n|_{x=L}=\phi_n(\ell)=?$ INTEGRATION FOR $\int \phi_k \delta(x-\ell)\phi_n(\ell)\,dx=?$

For clamped-free beam, the mode shape is:

$$\phi_n = \cosh \beta_n x - \cos \beta_n x - C_n(\sinh \beta_n x - \sin \beta_n x)$$

where $$C_n = \frac{\cosh \beta_n L + \cos \beta_n L}{\sinh \beta_n L + \sin \beta_n L} = \frac{\sinh \beta_n L - \sin \beta_n L}{\cosh \beta_n L + \cos \beta_n L} .$$

which leads to the transcendental equation for β_n:

$$\cosh \beta_n L \cos \beta_n L + 1 = 0 .$$

Since we want to find $\phi_n|_{x=L}$ or $\phi_n(\ell)$

$$\phi_n|_{x=L} = \phi_n(\ell) = \cosh \beta_n L - \cos \beta_n L - \frac{(\sinh \beta_n L - \sin \beta_n L)^2}{\cosh \beta_n L + \cos \beta_n L}$$

$$= \frac{\cosh^2 \beta_n L - \cos^2 \beta_n L - \sinh^2 \beta_n L - \sin^2 \beta_n L + 2 \sinh \beta_n L \sin \beta_n L}{\cosh \beta_n L + \cos \beta_n L}$$

$$\phi_n|_{x=L} = \frac{2 \sinh \beta_n L \sin \beta_n L}{\cosh \beta_n L + \cos \beta_n L} \qquad [G.1]$$

Squaring [G.1]:

$$\left((\phi_n)|_{x=L}\right)^2 = \frac{4 \sinh^2 \beta_n L \sin^2 \beta_n L}{\cosh^2 \beta_n L + \cos^2 \beta_n L + 2 \cosh \beta_n L \cos \beta_n L}$$

$$\left(\phi_n\Big|_{x=L}\right)^2 = \frac{4(\cosh^2 \beta_n L - 1)(1-\cos^2 \beta_n L)}{\cosh^2 \beta_n L + \cos^2 \beta_n L - 2} \quad \because \cosh \beta_n L \cos \beta_n L + 1 = 0$$

$$\left(\phi_n\Big|_{x=L}\right)^2 = \frac{4(\cosh^2 \beta_n L - \cosh^2 \beta_n L \cos^2 \beta_n L + \cos^2 \beta_n L - 1)}{\cosh^2 \beta_n L + \cos^2 \beta_n L - 2}$$

$$\left(\phi_n\Big|_{x=L}\right)^2 = \frac{4(\cosh^2 \beta_n L + \cos \beta_n L - 2)}{\cosh^2 \beta_n L + \cos^2 \beta_n L - 2}$$

$$\left(\phi_n\Big|_{x=L}\right)^2 = 4$$

From observation, the sign of $\phi_n\Big|_{x=L}$ alternatively changes

$$\phi_n\Big|_{x=L} = \phi_n(\ell) = (-1)^{n+1}.2$$

APPENDIX H

EVALUATION OF EQUATION (2.3.6) BY REDUCED METHOD AND ITS COMPUTER RESULTS FOR 3 DIFFERENT ω's.

$$\begin{bmatrix} \ell & 0 & 0 & 0 \\ 0 & \ell & 0 & 0 \\ 0 & 0 & \ell & 0 \\ 0 & 0 & 0 & \ell \end{bmatrix} \begin{Bmatrix} \ddot{A}_1 \\ \ddot{A}_2 \\ \ddot{B}_1 \\ \ddot{B}_2 \end{Bmatrix} + \begin{bmatrix} 0 & 0 & 2\omega\ell & 0 \\ 0 & 0 & 0 & 2\omega\ell \\ -2\omega\ell & 0 & 0 & 0 \\ 0 & -2\omega\ell & 0 & 0 \end{bmatrix} \begin{Bmatrix} \dot{A}_1 \\ \dot{A}_2 \\ B_1 \\ B_2 \end{Bmatrix}$$

$$+ \begin{bmatrix} (\frac{EI}{\rho A}\beta_1^4 - \omega^2)\ell & 0 & -4S_1 & 4S_1 \\ 0 & (\frac{EI}{\rho A}\beta_2^4 - \omega^2)\ell & 4S_1 & -4S_1 \\ 0 & 0 & (\frac{EI}{\rho A}\beta_1^4 - \omega^2)\ell - 4S_2 & 4S_2 \\ 0 & 0 & 4S_2 & (\frac{EI}{\rho A}\beta_2^4 - \omega^2)\ell - 4S_2 \end{bmatrix} \begin{Bmatrix} A_1 \\ A_2 \\ B_1 \\ B_2 \end{Bmatrix}$$

$$= \begin{Bmatrix} \langle F_z \rangle \int_0^\ell \phi_1 dx \\ \langle F_z \rangle \int_0^\ell \phi_2 dx \\ \langle F_y \rangle \int_0^\ell \phi_1 dx \\ \langle F_y \rangle \int_0^\ell \phi_2 dx \end{Bmatrix} \qquad (2.3.9)$$

For homogeneous solution, let L.H.s. be {0} .

Denote: $\{y\} = \begin{Bmatrix}\{\dot{q}\}\\ \{q\}\end{Bmatrix} = \begin{Bmatrix}\dot{A}_1\\ \dot{A}_2\\ \dot{B}_1\\ \dot{B}_2\\ A_1\\ A_2\\ B_1\\ B_2\end{Bmatrix}$ in our case (2.3.9) can be written as:

$$\left[\begin{array}{cccc|c|ccc} 0&0&0&0&\ell&0&0&0\\ 0&0&0&0&0&\ell&0&0\\ 0&0&0&0&0&0&\ell&0\\ 0&0&0&0&0&0&0&\ell\\ \hline \ell&0&0&0&0&0&2\omega\ell&0\\ 0&\ell&0&0&0&0&0&2\omega\ell\\ 0&0&\ell&0&-2\omega\ell&0&0&0\\ 0&0&0&\ell&0&-2\omega\ell&0&0 \end{array}\right] \begin{Bmatrix}\ddot{A}_1\\ \ddot{A}_2\\ \ddot{B}_1\\ \ddot{B}_2\\ \dot{A}_1\\ \dot{A}_2\\ \dot{B}_1\\ \dot{B}_2\end{Bmatrix} +$$

$$\left[\begin{array}{cccc|cccc} -\ell&0&0&0&0&0&0&0\\ 0&-\ell&0&0&0&0&0&0\\ 0&0&-\ell&0&0&0&0&0\\ 0&0&0&-\ell&0&0&0&0\\ \hline 0&0&0&0&(\frac{EI}{\rho A}\beta_1^4-\omega^2)\ell&0&-4S_1&4S_1\\ 0&0&0&0&0&(\frac{EI}{\rho A}\beta_2^4-\omega^2)\ell&4S_1&-4S_1\\ 0&0&0&0&0&0&(\frac{EI}{\rho A}\beta_1^4-\omega^2)\ell-4S_1&4S_2\\ 0&0&0&0&0&0&4S_2&(\frac{EI}{\rho A}\beta_2^2-\omega^2)\ell-4S_2 \end{array}\right] \begin{Bmatrix}\dot{A}_1\\ \dot{A}_2\\ \dot{B}_1\\ \dot{B}_2\\ A_1\\ A_2\\ B_1\\ B_2\end{Bmatrix}$$

$$= \begin{Bmatrix}0\\0\\0\\0\\0\\0\\0\\0\end{Bmatrix}$$

which is in the form $[M]\{\dot{X}\} + [K]\{X\} = \{0\}$.
Assume $\{\dot{X}\} = e^{\lambda t}$ and substitute the solution into above equation.

$$\lambda[M]\{\Phi\} + [K]\{\Phi\} = 0$$

$-[K]\{\Phi\} = \lambda[M]\{\Phi\}$ which is solved by the computer program as shown behind. Note that the subroutine EIGZF is used in the program to solve and find the λ's for system (2.3.9) .

```
*BATCH WATFIV ME39001 HEMAN C.H. HUI
*****************************************************

$WATFIV ,NOEXT
C     ***************************************************************
C     *                                                             *
C     *                                                             *
C     *    THIS PROGRAM FINDS THE EIGENVALUES OF A DYNAMIC SYSTEM   *
C     *                                                             *
C     *    WHICH IS IN THE FOLLOWING FORM:                          *
C     *                                                             *
C     *                                                             *
C     ***************************************************************
      IMPLICIT REAL*8(A-Z)
      DIMENSION M(8,8),K(8,8),ALFA(8),BETA(8),Z(8,8),WK(128)
      COMPLEX*16 ALFA,Z,OMEGA,NATFRE
      INTEGER I,J,N,IJOB,IER,CHECK1,CHECK2
      READ(5,*) RPM
9     WRITE(6,111) RPM
111   FORMAT('1',2(/),2X,'THE SPINDLE SPEED OF THE NC LATHE IS:',D11.4,
     $1X,'RPM')
      READ(5,*,END=99) SIN
      S = SIN*2.54D-02
      WRITE(6,555) SIN,S
555   FORMAT(2(/),T20,'THE FEEDRATE IN IN/REV :',D13.6,3X,'IN M/REV
     $ :',D13.6)
C
      N = 8
      IJOB = 2
C
      E = 71.0D09
      DENSIT = 26.6D03/9.8D0
      DIA = 3.0D0*2.54D-02
      MODE1 = 1.87516407D0
      MODE2 = 4.69409113D0
      PI = 3.141593D0
C
      W = RPM/60.0D0*2.0D0*PI
      LENGTH = 8.0D0*2.54D-02
      R = DIA/2.0D0
      AREA =(R**2.0D0)*PI
      IO = PI*(R**4.0D0)/4.0D0
      B1 = MODE1/LENGTH
      B2 = MODE2/LENGTH
      CONST = E*IO/(DENSIT*AREA)
      K1 = (CONST*(B1**4.0D0)-(W**2.0D0))*LENGTH
      K2 = (CONST*(B2**4.0D0)-(W**2.0D0))*LENGTH
      S1 = 650.177D0/(DENSIT*AREA)*(S**0.75D0)
      S2 = 390.106D0/(DENSIT*AREA)*(S**0.75D0)
C
      DO 10 I=1,8
      DO 10 J=1,8
      CHECK1 = J-I
      CHECK2 = I-J
      M(I,J) = 0.0D0
      IF(I.LE.4.AND.J.GE.4.AND.CHECK1.EQ.4) M(I,J)=LENGTH
      IF(I.GE.4.AND.J.LE.4.AND.CHECK2.EQ.4) M(I,J)=LENGTH
10    CONTINUE
      M(5,7) = 2.0D0*W*LENGTH
      M(6,8) = 2.0D0*W*LENGTH
      M(7,5) = -2.0D0*W*LENGTH
      M(8,6) = -2.0D0*W*LENGTH
C
```

```
      WRITE(6,222)
222   FORMAT(' ',2(/),T20,'THE MASS MATRIX OF THE SYSTEM IS:')
      DO 11 I=1,8
11    WRITE(6,20) (M(I,J),J=1,8)
20    FORMAT(' ',T10,8D13.6)
C
      DO 100 I=1,8
      DO 100 J=1,8
      K(I,J) = 0.0D0
      IF(I.LE.4.AND.J.LE.4.AND.I.EQ.J) K(I,J)=LENGTH
100   CONTINUE
      K(5,5) = -1.0D0*K1
      K(5,7) = 4.0D0*S1
      K(5,8) = -4.0D0*S1
      K(6,6) = -1.0D0*K2
      K(6,7) = -4.0D0*S1
      K(6,8) = 4.0D0*S1
      K(7,7) = -K1+4.0D0*S2
      K(7,8) = -4.0D0*S2
      K(8,7) = -4.0D0*S2
      K(8,8) = -K2+4.0D0*S2
C
      WRITE(6,333)
333   FORMAT(' ',2(/),T20,'THE STIFFNESS MATRIX OF THE SYSTEM IS:')
      DO 101 I=1,8
101   WRITE(6,30) (K(I,J),J=1,8)
30    FORMAT(' ',T10,8D13.6)
C
      CALL EIGZF(K,N,M,N,N,IJOB,ALFA,BETA,Z,N,WK,IER)
C
      WRITE(6,444)
444   FORMAT(' ',2(/),10X,'THE FIRST 8TH  NATURAL FREQUENCIES ARE:',
     &2(/),22X,'NATURAL FREQUENCIES')
      DO 200 I=1,8
      OMEGA = ALFA(I)/BETA(I)
200   WRITE(6,40) OMEGA
40    FORMAT(/,10X,D18.11,2X,D18.11)
      GOTO 9
C
99    WRITE(6,999)
999   FORMAT('1')
      STOP
      END

$DATA
```

SPINDLE SPEED OF THE NC LATHE IS: 0.6900D 02 RPM

THE FEEDRATE IN IN/REV : 0.0000000D 00 IN M/REV : 0.0000000D 00

THE MASS MATRIX OF THE SYSTEM IS:

0.0000000	00	0.0000000D	00	0.0000000D	00	0.0000000D	00	0.2032000D	00	0.0000000D	00	0.0000000D	00	0.0000000D	00
0.0000000	00	0.0000000D	00	0.0000000D	00	0.0000000D	00	0.0000000D	00	0.2032000D	00	0.0000000D	00	0.0000000D	00
0.0000000	00	0.0000000D	00	0.0000000D	00	0.0000000D	00	0.0000000D	00	0.0000000D	00	-0.2032000D	00	0.0000000D	00
0.0000000	00	0.0000000D	00	0.0000000D	00	0.0000000D	00	0.0000000D	00	0.0000000D	00	0.0000000D	00	0.2032000D	00
0.2032000	00	0.0000000D	00	0.0000000D	00	0.0000000D	00	0.0000000D	00	0.0000000D	00	0.2936510	01	0.0000000D	00
0.0000000	00	0.2032000	00	0.0000000D	00	0.0000000D	00	0.0000000D	00	0.0000000D	00	0.0000000D	00	0.2936510	01
0.0000000	00	0.0000000D	00	0.2032000	00	0.0000000D	00	-0.2936510	01	0.0000000D	00	0.0000000D	00	0.0000000D	00
0.0000000	00	0.0000000D	00	0.0000000D	00	0.2032000D	00	0.0000000D	00	-0.2936510	01	0.0000000D	00	0.0000000D	00

THE STIFFNESS MATRIX OF THE SYSTEM IS:

0.2032000	00	0.0000000D	00	0.0000000D	00	0.0000000D	00	0.0000000D	00	0.0000000D	00	0.0000000D	00	0.0000000D	00
0.0000000	00	0.2032000	00	0.0000000D	00	0.0000000D	00	0.0000000D	00	0.0000000D	00	0.0000000D	00	0.0000000D	00
0.0000000	00	0.0000000D	00	0.2032000	00	0.0000000D	00	0.0000000D	00	0.0000000D	00	0.0000000D	00	0.0000000D	00
0.0000000	00	0.0000000D	00	0.0000000D	00	0.2032000D	00	0.0000000D	00	0.0000000D	00	0.0000000D	00	0.0000000D	00
0.0000000	00	0.0000000D	00	0.0000000D	00	0.0000000D	00	-0.1398870	08	0.0000000D	00	0.0000000D	00	0.0000000D	00
0.0000000	00	0.0000000D	00	0.0000000D	00	0.0000000D	00	0.0000000D	00	-0.5493230	09	0.0000000D	00	0.0000000D	00
0.0000000	00	0.0000000D	00	0.0000000D	00	0.0000000D	00	0.0000000D	00	0.0000000D	00	-0.1398870	08	0.0000000D	00
0.0000000	00	0.0000000D	00	0.0000000D	00	0.0000000D	00	0.0000000D	00	0.0000000D	00	0.0000000D	00	-0.5493230	09

THE FIRST 8TH NATURAL FREQUENCIES ARE:

NATURAL FREQUENCIES	
0.247307432610-08	0.830434835300 04
0.247307432610-08	-0.830434835300 04
0.245065536360-08	0.828989702520 04
0.245065536360-08	-0.828989702520 04
0.271704761430-06	0.520010763640 05
0.271704761430-06	-0.520010763640 05
0.270604717550-06	0.519866255370 05
0.270604717550-06	-0.519866255370 05

SPINDLE SPEED OF THE NC LATHE IS: 0.6900D 02 RPM

THE FEEDRATE IN IN/REV : 0.1500000-01 IN M/REV : 0.3810000-03

THE MASS MATRIX OF THE SYSTEM IS:

0.0000000 00	0.0000000 00	0.0000000 00	0.0000000 00	0.2032000 00	0.0000000 00	0.0000000 00	0.0000000 00
0.0000000 00	0.0000000 00	0.0000000 00	0.0000000 00	0.0000000 00	0.2032000 00	0.0000000 00	0.0000000 00
0.0000000 00	0.0000000 00	0.0000000 00	0.0000000 00	0.0000000 00	0.0000000 00	0.2032000 00	0.0000000 00
0.0000000 00	0.0000000 00	0.0000000 00	0.0000000 00	0.0000000 00	0.0000000 00	0.0000000 00	0.2032000 00
0.2032000 00	0.0000000 00	0.0000000 00	0.0000000 00	0.0000000 00	0.0000000 00	0.2936510 01	0.0000000 00
0.0000000 00	0.2032000 00	0.0000000 00	0.0000000 00	0.0000000 00	0.0000000 00	0.0000000 00	0.2936510 01
0.0000000 00	0.0000000 00	0.2032000 00	0.0000000 00	-0.2936510 01	0.0000000 00	0.0000000 00	0.0000000 00
0.0000000 00	0.0000000 00	0.0000000 00	0.2032000 00	0.0000000 00	-0.2936510 01	0.0000000 00	0.0000000 00

THE STIFFNESS MATRIX OF THE SYSTEM IS:

0.2032000 00	0.0000000 00	0.0000000 00	0.0000000 00	0.0000000 00	0.0000000 00	0.0000000 00	0.0000000 00
0.0000000 00	0.2032000 00	0.0000000 00	0.0000000 00	0.0000000 00	0.0000000 00	0.0000000 00	0.0000000 00
0.0000000 00	0.0000000 00	0.2032000 00	0.0000000 00	0.0000000 00	0.0000000 00	0.0000000 00	0.0000000 00
0.0000000 00	0.0000000 00	0.0000000 00	0.2032000 00	0.0000000 00	0.0000000 00	0.0000000 00	0.0000000 00
0.0000000 00	0.0000000 00	0.0000000 00	0.0000000 00	-0.1398870 08	0.0000000 00	0.5729670 00	-0.5729670 00
0.0000000 00	0.0000000 00	0.0000000 00	0.0000000 00	0.0000000 00	-0.5493230 09	-0.5729670 00	0.5729670 00
0.0000000 00	0.0000000 00	0.0000000 00	0.0000000 00	0.0000000 00	0.0000000 00	-0.1398870 08	-0.3437800 00
0.0000000 00	0.0000000 00	0.0000000 00	0.0000000 00	0.0000000 00	0.0000000 00	-0.3437800 00	-0.5493230 09

THE FIRST 8TH NATURAL FREQUENCIES ARE:

NATURAL FREQUENCIES	
-0.8826993112 8D-04	0.8304348258 7D 04
-0.8826993112 8D-04	-0.8304348258 7D 04
0.8826279415 5D-04	0.8289896931 1D 04
0.8826279415 5D-04	-0.8289896931 1D 04
0.1463680965 8D-03	0.5200107849 6D 05
0.1463680965 8D-03	-0.5200107849 6D 05
-0.1454193814 5D-03	0.5198662716 8D 05
-0.1454193814 5D-03	-0.5198662716 8D 05

SPINDLE SPEED OF THE NC LATHE IS: 0.6900D 02 RPM

THE FEEDRATE IN IN/REV : 0.5000000-02 IN M/REV : 0.1270000D-03

THE MASS MATRIX OF THE SYSTEM IS:

0.0000000 00	0.0000000 00	0.0000000 00	0.0000000 00	0.2032000 00	0.0000000 00	0.0000000 00	0.0000000 00
0.0000000 00	0.0000000 00	0.0000000 00	0.0000000 00	0.0000000 00	0.2032000 00	0.0000000 00	0.0000000 00
0.0000000 00	0.0000000 00	0.0000000 00	0.0000000 00	0.0000000 00	0.0000000 00	0.2032000 00	0.0000000 00
0.0000000 00	0.0000000 00	0.0000000 00	0.0000000 00	0.0000000 00	0.0000000 00	0.0000000 00	0.2032000 00
0.2032000 00	0.0000000 00	0.0000000 00	0.0000000 00	0.0000000 00	0.0000000 00	0.2936510 01	0.0000000 00
0.0000000 00	0.2032000 00	0.0000000 00	0.0000000 00	0.0000000 00	0.0000000 00	0.0000000 00	0.2936510 01
0.0000000 00	0.0000000 00	0.2032000 00	0.0000000 00	-0.2936510 01	0.0000000 00	0.0000000 00	0.0000000 00
0.0000000 00	0.0000000 00	0.0000000 00	0.2032000 00	0.0000000 00	-0.2936510 01	0.0000000 00	0.0000000 00

THE STIFFNESS MATRIX OF THE SYSTEM IS:

0.2032000 00	0.0000000 00	0.0000000 00	0.0000000 00	0.0000000 00	0.0000000 00	0.0000000 00	0.0000000 00
0.0000000 00	0.2032000 00	0.0000000 00	0.0000000 00	0.0000000 00	0.0000000 00	0.0000000 00	0.0000000 00
0.0000000 00	0.0000000 00	0.2032000 00	0.0000000 00	0.0000000 00	0.0000000 00	0.0000000 00	0.0000000 00
0.0000000 00	0.0000000 00	0.0000000 00	0.2032000 00	0.0000000 00	0.0000000 00	0.0000000 00	0.0000000 00
0.0000000 00	0.0000000 00	0.0000000 00	0.0000000 00	-0.1398870 08	0.0000000 00	0.2513560 00	-0.2513560 00
0.0000000 00	0.0000000 00	0.0000000 00	0.0000000 00	0.0000000 00	-0.5493230 09	-0.2513560 00	0.2513560 00
0.0000000 00	0.0000000 00	0.0000000 00	0.0000000 00	0.0000000 00	0.0000000 00	-0.1398870 08	-0.1508130 00
0.0000000 00	0.0000000 00	0.0000000 00	0.0000000 00	0.0000000 00	0.0000000 00	-0.1508130 00	-0.5493230 09

THE FIRST 8TH NATURAL FREQUENCIES ARE:

NATURAL FREQUENCIES	
-0.3726916 3897D-04	0.8304348 3306D 04
-0.3726916 3897D-04	-0.8304348 3306D 04
0.3727337 1720D-04	0.8289897 0029D 04
0.3727337 1720D-04	-0.8289897 0029D 04
-0.1112021 4803D-04	0.5200107 8397D 05
-0.1112021 4803D-04	-0.5200107 8397D 05
0.1180593 2497D-04	0.5198662 7069D 05
0.1180593 2497D-04	-0.5198662 7069D 05

SPINDLE SPEED OF THE NC LATHE IS: 0.6900D 02 RPM

THE FEEDRATE IN IN/REV : 0.300000D-01 IN M/REV : 0.762000D-03

THE MASS MATRIX OF THE SYSTEM IS:

0.0000000 00	0.0000000 00	0.0000000 00	0.0000000 00	0.2032000 00	0.0000000 00	0.0000000 00	0.0000000 00
0.0000000 00	0.0000000 00	0.0000000 00	0.0000000 00	0.0000000 00	0.2032000 00	0.0000000 00	0.0000000 00
0.0000000 00	0.0000000 00	0.0000000 00	0.0000000 00	0.0000000 00	0.0000000 00	0.2032000 00	0.0000000 00
0.0000000 00	0.0000000 00	0.0000000 00	0.0000000 00	0.0000000 00	0.0000000 00	0.0000000 00	0.2032000 00
0.2032000 00	0.0000000 00	0.0000000 00	0.0000000 00	0.0000000 00	0.0000000 00	0.2936510 01	0.0000000 00
0.0000000 00	0.2032000 00	0.0000000 00	0.0000000 00	0.0000000 00	0.0000000 00	0.0000000 00	0.2936510 01
0.0000000 00	0.0000000 00	0.2032000 00	0.0000000 00	-0.2936510 01	0.0000000 00	0.0000000 00	0.0000000 00
0.0000000 00	0.0000000 00	0.0000000 00	0.2032000 00	0.0000000 00	-0.2936510 01	0.0000000 00	0.0000000 00

THE STIFFNESS MATRIX OF THE SYSTEM IS:

0.2032000 00	0.0000000 00	0.0000000 00	0.0000000 00	0.0000000 00	0.0000000 00	0.0000000 00	0.0000000 00
0.0000000 00	0.2032000 00	0.0000000 00	0.0000000 00	0.0000000 00	0.0000000 00	0.0000000 00	0.0000000 00
0.0000000 00	0.0000000 00	0.2032000 00	0.0000000 00	0.0000000 00	0.0000000 00	0.0000000 00	0.0000000 00
0.0000000 00	0.0000000 00	0.0000000 00	0.2032000 00	0.0000000 00	0.0000000 00	0.0000000 00	0.0000000 00
0.0000000 00	0.0000000 00	0.0000000 00	0.0000000 00	-0.1398870 08	0.0000000 00	0.9636120 00	-0.9636120 00
0.0000000 00	0.0000000 00	0.0000000 00	0.0000000 00	0.0000000 00	-0.5493230 09	-0.9636120 00	0.9636120 00
0.0000000 00	0.0000000 00	0.0000000 00	0.0000000 00	0.0000000 00	0.0000000 00	-0.1398870 08	-0.5781670 00
0.0000000 00	0.0000000 00	0.0000000 00	0.0000000 00	0.0000000 00	0.0000000 00	-0.5781670 00	-0.5493230 09

THE FIRST 8TH NATURAL FREQUENCIES ARE:

NATURAL FREQUENCIES	
-0.14239833361D-03	0.83043482232D 04
-0.14239833361D-03	-0.83043482232D 04
0.14240478544D-03	0.82898968955D 04
0.14240478544D-03	-0.82898968955D 04
-0.20530290422D-04	0.52001078392D 05
-0.20530290422D-04	-0.52001078392D 05
0.21248381231D-04	0.51986627064D 05
0.21248381231D-04	-0.51986627064D 05

SPINDLE SPEED OF THE NC LATHE IS: 0.1800D 03 RPM

THE FEEDRATE IN IN/REV : 0.000000D 00 IN M/REV : 0.000000D 00

THE MASS MATRIX OF THE SYSTEM IS:

0.0000000 00	0.0000000 00	0.0000000 00	0.0000000 00	0.2032000 00	0.0000000 00	0.0000000 00	0.0000000 00
0.0000000 00	0.0000000 00	0.0000000 00	0.0000000 00	0.0000000 00	0.2032000 00	0.0000000 00	0.0000000 00
0.0000000 00	0.0000000 00	0.0000000 00	0.0000000 00	0.0000000 00	0.0000000 00	0.2032000 00	0.0000000 00
0.0000000 00	0.0000000 00	0.0000000 00	0.0000000 00	0.0000000 00	0.0000000 00	0.0000000 00	0.2032000 00
0.2032000 00	0.0000000 00	0.0000000 00	0.0000000 00	0.0000000 00	0.0000000 00	0.7660460 01	0.0000000 00
0.0000000 00	0.2032000 00	0.0000000 00	0.0000000 00	0.0000000 00	0.0000000 00	0.0000000 00	0.7660460 01
0.0000000 00	0.0000000 00	0.2032000 00	0.0000000 00	0.0000000 00	-0.7660460 01	0.0000000 00	0.0000000 00
0.0000000 00	0.0000000 00	0.0000000 00	0.2032000 00	0.0000000 00	0.0000000 00	-0.7660460 01	0.0000000 00

THE STIFFNESS MATRIX OF THE SYSTEM IS:

0.2032000 00	0.0000000 00	0.0000000 00	0.0000000 00	0.0000000 00	0.0000000 00	0.0000000 00	0.0000000 00
0.0000000 00	0.2032000 00	0.0000000 00	0.0000000 00	0.0000000 00	0.0000000 00	0.0000000 00	0.0000000 00
0.0000000 00	0.0000000 00	0.2032000 00	0.0000000 00	0.0000000 00	0.0000000 00	0.0000000 00	0.0000000 00
0.0000000 00	0.0000000 00	0.0000000 00	0.2032000 00	0.0000000 00	0.0000000 00	0.0000000 00	0.0000000 00
0.0000000 00	0.0000000 00	0.0000000 00	0.0000000 00	-0.1398870 08	0.0000000 00	0.0000000 00	0.0000000 00
0.0000000 00	0.0000000 00	0.0000000 00	0.0000000 00	0.0000000 00	-0.5493230 09	0.0000000 00	0.0000000 00
0.0000000 00	0.0000000 00	0.0000000 00	0.0000000 00	0.0000000 00	0.0000000 00	-0.1398870 08	0.0000000 00
0.0000000 00	0.0000000 00	0.0000000 00	0.0000000 00	0.0000000 00	0.0000000 00	0.0000000 00	-0.5493230 09

THE FIRST 8TH NATURAL FREQUENCIES ARE:

NATURAL FREQUENCIES	
0.3291063304380-08	0.83159722556D 04
0.3291063304380-08	-0.83159722556D 04
0.3239956121500-08	0.82782731396D 04
0.3239956121500-08	-0.82782731396D 04
0.3390980037800-06	0.52012702055D 05
0.3390980037800-06	-0.52012702055D 05
0.3385859537600-06	0.51975002939D 05
0.3385859537600-06	-0.51975002939D 05

SPINDLE SPEED OF THE NC LATHE IS: 0.1800D 03 RPM

THE FEEDRATE IN IN/REV : 0.5000000D-02 IN M/REV : 0.1270000D-03

THE MASS MATRIX OF THE SYSTEM IS:

0.0000000 00	0.0000000D 00	0.0000000D 00	0.0000000D 00	0.2032000D 00	0.0000000D 00	0.0000000D 00	0.0000000D 00
0.0000000 00	0.0000000D 00	0.0000000D 00	0.0000000D 00	0.0000000D 00	0.2032000D 00	0.0000000D 00	0.0000000D 00
0.0000000 00	0.0000000D 00	0.0000000D 00	0.0000000D 00	0.0000000D 00	0.0000000D 00	0.2032000D 00	0.0000000D 00
0.0000000 00	0.0000000D 00	0.0000000D 00	0.0000000D 00	0.0000000D 00	0.0000000D 00	0.0000000D 00	0.2032000D 00
0.2032000 00	0.0000000D 00	0.0000000D 00	0.0000000D 00	0.0000000D 00	0.0000000D 00	0.7660460 01	0.0000000D 00
0.0000000 00	0.2032000D 00	0.0000000D 00	0.0000000D 00	0.0000000D 00	0.0000000D 00	0.0000000D 00	0.7660460 01
0.0000000 00	0.0000000D 00	0.2032000D 00	0.0000000D 00	-0.7660460 01	0.0000000D 00	0.0000000D 00	0.0000000D 00
0.0000000 00	0.0000000D 00	0.0000000D 00	0.2032000D 00	0.0000000D 00	-0.7660460 01	0.0000000D 00	0.0000000D 00

THE STIFFNESS MATRIX OF THE SYSTEM IS:

0.2032000 00	0.0000000 00	0.0000000D 00	0.0000000D 00	0.0000000D 00	0.0000000D 00	0.0000000D 00	0.0000000D 00
0.0000000 00	0.2032000D 00	0.0000000D 00	0.0000000D 00	0.0000000D 00	0.0000000D 00	0.0000000D 00	0.0000000D 00
0.0000000 00	0.0000000D 00	0.2032000D 00	0.0000000D 00	0.0000000D 00	0.0000000D 00	0.0000000D 00	0.0000000D 00
0.0000000 00	0.0000000D 00	0.0000000D 00	0.2032000D 00	0.0000000D 00	0.0000000D 00	0.0000000D 00	0.0000000D 00
0.0000000 00	0.0000000D 00	0.0000000D 00	0.0000000D 00	-0.1398870 08	0.0000000D 00	0.2513560 00	-0.2513560 00
0.0000000 00	0.0000000D 00	0.0000000D 00	0.0000000D 00	0.0000000D 00	-0.5493230 09	-0.2513560 00	0.2513560 00
0.0000000 00	0.0000000D 00	0.0000000D 00	0.0000000D 00	0.0000000D 00	0.0000000D 00	-0.1398870 08	-0.1508130 00
0.0000000 00	0.0000000D 00	0.0000000D 00	0.0000000D 00	0.0000000D 00	0.0000000D 00	-0.1508130 00	-0.5493230 09

THE FIRST 8TH NATURAL FREQUENCIES ARE:

NATURAL FREQUENCIES	
-0.372601801120-04	0.831597223030 04
-0.372601361120-04	-0.831597223030 04
0.372667510130-04	0.827827311430 04
0.372667510130-04	-0.827827311430 04
-0.907257554650-04	0.520126971620 05
-0.907257554650-04	-0.520126971620 05
0.911172746320-04	0.519749980530 05
0.911172746320-04	-0.519749980530 05

SPINDLE SPEED OF THE NC LATHE IS: 0.1800D 03 RPM

THE FEEDRATE IN IN/REV : 0.1500000D-01 IN M/REV : 0.3810000D-03

THE MASS MATRIX OF THE SYSTEM IS:

0.0000000	00	0.0000000	00	0.0000000	00	0.0000000	00	0.2032000	00	0.0000000	00	0.0000000	00	0.0000000	00
0.0000000	00	0.0000000	00	0.0000000	00	0.0000000	00	0.0000000	00	0.2032000	00	0.0000000	00	0.0000000	00
0.0000000	00	0.0000000	00	0.0000000	00	0.0000000	00	0.0000000	00	0.0000000	00	0.2032000	00	0.0000000	00
0.0000000	00	0.0000000	00	0.0000000	00	0.0000000	00	0.0000000	00	0.0000000	00	0.0000000	00	0.2032000	00
0.2032000	00	0.0000000	00	0.0000000	00	0.0000000	00	0.0000000	00	0.0000000	00	0.0000000	00	0.7660460	01
0.0000000	00	0.2032000	00	0.0000000	00	0.0000000	00	0.0000000	00	0.0000000	00	0.0000000	00	0.7660460	01
0.0000000	00	0.0000000	00	0.2032000	00	0.0000000	00	-0.7660460	01	0.0000000	00	0.0000000	00	0.0000000	00
0.0000000	00	0.0000000	00	0.0000000	00	0.2032000	00	0.0000000	00	-0.7660460	01	0.0000000	00	0.0000000	00

THE STIFFNESS MATRIX OF THE SYSTEM IS:

0.2032000	00	0.0000000	00	0.0000000	00	0.0000000	00	0.0000000	00	0.0000000	00	0.0000000	00	0.0000000	00
0.0000000	00	0.2032000	00	0.0000000	00	0.0000000	00	0.0000000	00	0.0000000	00	0.0000000	00	0.0000000	00
0.0000000	00	0.0000000	00	0.2032000	00	0.0000000	00	0.0000000	00	0.0000000	00	0.0000000	00	0.0000000	00
0.0000000	00	0.0000000	00	0.0000000	00	0.2032000	00	0.0000000	00	0.0000000	00	0.0000000	00	0.0000000	00
0.0000000	00	0.0000000	00	0.0000000	00	0.0000000	00	-0.1398870	08	0.0000000	00	0.5729670	00	-0.5729670	00
0.0000000	00	0.0000000	00	0.0000000	00	0.0000000	00	0.0000000	00	-0.5493230	09	-0.5729670	00	0.5729670	00
0.0000000	00	0.0000000	00	0.0000000	00	0.0000000	00	0.0000000	00	0.0000000	00	-0.1398870	08	-0.3437800	00
0.0000000	00	0.0000000	00	0.0000000	00	0.0000000	00	0.0000000	00	0.0000000	00	-0.3437800	00	-0.5493230	09

THE FIRST 8TH NATURAL FREQUENCIES ARE:

NATURAL FREQUENCIES	
-0.84897847286D-04	0.83159721995D 04
-0.84897847286D-04	-0.83159721995D 04
0.84904517219D-04	0.82782730836D 04
0.84904517219D-04	-0.82782730836D 04
-0.30951165497D-03	0.52012697037D 05
-0.30951165497D-03	-0.52012697037D 05
0.30987688458D-03	0.51974997927D 05
0.30987688458D-03	-0.51974997927D 05

SPINDLE SPEED OF THE NC LATHE IS: 0.1800D 03 RPM

THE FEEDRATE IN IN/REV : 0.3000000D-01 IN M/REV : 0.7620000D-03

THE MASS MATRIX OF THE SYSTEM IS:

0.0000000	00	0.0000000	00	0.0000000	00	0.0000000	00	0.2032000	00	0.0000000	00	0.0000000	00	0.0000000	00
0.0000000	00	0.0000000	00	0.0000000	00	0.0000000	00	0.0000000	00	0.2032000	00	0.0000000	00	0.0000000	00
0.0000000	00	0.0000000	00	0.0000000	00	0.0000000	00	0.0000000	00	0.0000000	00	0.2032000	00	0.0000000	00
0.0000000	00	0.0000000	00	0.0000000	00	0.0000000	00	0.0000000	00	0.0000000	00	0.0000000	00	0.2032000	00
0.2032000	00	0.0000000	00	0.0000000	00	0.0000000	00	0.0000000	00	0.0000000	00	0.7660460	01	0.0000000	00
0.0000000	00	0.2032000	00	0.0000000	00	0.0000000	00	0.0000000	00	0.0000000	00	0.0000000	00	0.7660460	01
0.0000000	00	0.0000000	00	0.2032000	00	0.0000000	00	-0.7660460	01	0.0000000	00	0.0000000	00	0.0000000	00
0.0000000	00	0.0000000	00	0.0000000	00	0.2032000	00	0.0000000	00	-0.7660460	01	0.0000000	00	0.0000000	00

THE STIFFNESS MATRIX OF THE SYSTEM IS:

0.2032000	00	0.0000000	00	0.0000000	00	0.0000000	00	0.0000000	00	0.0000000	00	0.0000000	00	0.0000000	00
0.0000000	00	0.2032000	00	0.0000000	00	0.0000000	00	0.0000000	00	0.0000000	00	0.0000000	00	0.0000000	00
0.0000000	00	0.0000000	00	0.2032000	00	0.0000000	00	0.0000000	00	0.0000000	00	0.0000000	00	0.0000000	00
0.0000000	00	0.0000000	00	0.0000000	00	0.2032000	00	0.0000000	00	0.0000000	00	0.0000000	00	0.0000000	00
0.0000000	00	0.0000000	00	0.0000000	00	0.0000000	00	-0.1398870	08	0.0000000	00	0.9636120	00	-0.9636120	00
0.0000000	00	0.0000000	00	0.0000000	00	0.0000000	00	0.0000000	00	-0.5493230	09	-0.9636120	00	0.9636120	00
0.0000000	00	0.0000000	00	0.0000000	00	0.0000000	00	0.0000000	00	0.0000000	00	-0.1398670	08	-0.5781670	00
0.0000000	00	0.0000000	00	0.0000000	00	0.0000000	00	0.0000000	00	0.0000000	00	-0.5781670	00	-0.5493230	09

THE FIRST 8TH NATURAL FREQUENCIES ARE:

NATURAL FREQUENCIES	
-0.14278910779D-03	0.83159721648D 04
-0.14278910779D-03	-0.83159721648D 04
0.14279710376D-03	0.82782730488D 04
0.14279710376D-03	-0.82782730488D 04
-0.49112380828D-03	0.52012696937D 05
-0.49112380828D-03	-0.52012696937D 05
0.49133004739D-03	0.51974997827D 05
0.49133004739D-03	-0.51974997827D 05

SPINDLE SPEED OF THE NC LATHE IS: 0.1800D 04 RPM

THE FEEDRATE IN IN/REV : 0.000000D 00 IN M/REV : 0.000000D 00

THE MASS MATRIX OF THE SYSTEM IS:

0.000000D 00	0.000000D 00	0.000000D 00	0.000000D 00	0.203200D 00	0.000000D 00	0.000000D 00	0.000000D 00
0.000000D 00	0.000000D 00	0.000000D 00	0.000000D 00	0.000000D 00	0.203200D 00	0.000000D 00	0.000000D 00
0.000000D 00	0.000000D 00	0.000000D 00	0.000000D 00	0.000000D 00	0.000000D 00	0.203200D 00	0.000000D 00
0.000000D 00	0.000000D 00	0.000000D 00	0.000000D 00	0.000000D 00	0.000000D 00	0.000000D 00	0.203200D 00
0.203200D 00	0.000000D 00	0.000000D 00	0.000000D 00	0.000000D 00	0.000000D 00	0.766046D 02	0.000000D 00
0.000000D 00	0.203200D 00	0.000000D 00	0.000000D 00	0.000000D 00	0.000000D 00	0.000000D 00	0.766046D 02
0.000000D 00	0.000000D 00	0.203200D 00	0.000000D 00	-0.766046D 02	0.000000D 00	0.000000D 00	0.000000D 00
0.000000D 00	0.000000D 00	0.000000D 00	0.203200D 00	0.000000D 00	-0.766046D 02	0.000000D 00	0.000000D 00

THE STIFFNESS MATRIX OF THE SYSTEM IS:

0.203200D 00	0.000000D 00	0.000000D 00	0.000000D 00	0.000000D 00	0.000000D 00	0.000000D 00	0.000000D 00
0.000000D 00	0.203200D 00	0.000000D 00	0.000000D 00	0.000000D 00	0.000000D 00	0.000000D 00	0.000000D 00
0.000000D 00	0.000000D 00	0.203200D 00	0.000000D 00	0.000000D 00	0.000000D 00	0.000000D 00	0.000000D 00
0.000000D 00	0.000000D 00	0.000000D 00	0.203200D 00	0.000000D 00	0.000000D 00	0.000000D 00	0.000000D 00
0.000000D 00	0.000000D 00	0.000000D 00	0.000000D 00	-0.139815D 08	0.000000D 00	0.000000D 00	0.000000D 00
0.000000D 00	0.000000D 00	0.000000D 00	0.000000D 00	0.000000D 00	-0.549316D 09	0.000000D 00	0.000000D 00
0.000000D 00	0.000000D 00	0.000000D 00	0.000000D 00	0.000000D 00	0.000000D 00	-0.139815D 08	0.000000D 00
0.000000D 00	0.000000D 00	0.000000D 00	0.000000D 00	0.000000D 00	0.000000D 00	0.000000D 00	-0.549316D 09

THE FIRST 8TH NATURAL FREQUENCIES ARE:

NATURAL FREQUENCIES	
0.311098049710-08	0.848561827790 04
0.311098049710-08	-0.848561827790 04
0.268915044580-08	0.810862711790 04
0.268915044580-08	-0.810862711790 04
0.288617421300-06	0.521823482010 05
0.288617421300-06	-0.521823482010 05
0.284715066170-06	0.518053570430 05
0.284715066170-06	-0.518053570430 05

SPINDLE SPEED OF THE NC LATHE IS: 0.1800D 04 RPM

THE FEEDRATE IN IN/REV : 0.500000D-02 IN M/REV : 0.127000D-03

THE MASS MATRIX OF THE SYSTEM IS:

0.0000000 00	0.0000000 00	0.0000000 00	0.0000000 00	0.2032000 00	0.0000000 00	0.0000000 00	0.0000000 00
0.0000000 00	0.0000000 00	0.0000000 00	0.0000000 00	0.0000000 00	0.2032000 00	0.0000000 00	0.0000000 00
0.0000000 00	0.0000000 00	0.0000000 00	0.0000000 00	0.0000000 00	0.0000000 00	0.2032000 00	0.0000000 00
0.0000000 00	0.0000000 00	0.0000000 00	0.0000000 00	0.0000000 00	0.0000000 00	0.0000000 00	0.2032000 00
0.2032000 00	0.0000000 00	0.0000000 00	0.0000000 00	0.0000000 00	0.0000000 00	0.7660460 02	0.0000000 00
0.0000000 00	0.2032000 00	0.0000000 00	0.0000000 00	0.0000000 00	0.0000000 00	0.0000000 00	0.7660460 02
0.0000000 00	0.0000000 00	0.2032000 00	0.0000000 00	-0.7660460 02	0.0000000 00	0.0000000 00	0.0000000 00
0.0000000 00	0.0000000 00	0.0000000 00	0.2032000 00	0.0000000 00	-0.7660460 02	0.0000000 00	0.0000000 00

THE STIFFNESS MATRIX OF THE SYSTEM IS:

0.2032000 00	0.0000000 00	0.0000000 00	0.0000000 00	0.0000000 00	0.0000000 00	0.0000000 00	0.0000000 00
0.0000000 00	0.2032000 00	0.0000000 00	0.0000000 00	0.0000000 00	0.0000000 00	0.0000000 00	0.0000000 00
0.0000000 00	0.0000000 00	0.2032000 00	0.0000000 00	0.0000000 00	0.0000000 00	0.0000000 00	0.0000000 00
0.0000000 00	0.0000000 00	0.0000000 00	0.2032000 00	0.0000000 00	0.0000000 00	0.0000000 00	0.0000000 00
0.0000000 00	0.0000000 00	0.0000000 00	0.0000000 00	-0.1398150 08	0.0000000 00	0.2513560 00	-0.2513560 00
0.0000000 00	0.0000000 00	0.0000000 00	0.0000000 00	0.0000000 00	-0.5493160 09	-0.2513560 00	0.2513560 00
0.0000000 00	0.0000000 00	0.0000000 00	0.0000000 00	0.0000000 00	0.0000000 00	-0.1398150 08	-0.1508130 00
0.0000000 00	0.0000000 00	0.0000000 00	0.0000000 00	0.0000000 00	0.0000000 00	-0.1508130 00	-0.5493160 09

THE FIRST 8TH NATURAL FREQUENCIES ARE:

NATURAL FREQUENCIES.	
-0.372685213910-04	0.848561825340 04
-0.372685213910-04	-0.848561825340 04
0.372742843840-04	0.810862709360 04
0.372742343840-04	-0.810862709360 04
0.116884241030-04	0.521823427540 05
0.116884241030-04	-0.521823427540 05
-0.107823396890-04	0.518053516740 05
-0.107823396890-04	-0.518053516740 05

SPINDLE SPEED OF THE NC LATHE IS: 0.1800D 04 RPM

THE FEEDRATE IN IN/REV : 0.150000D-01 IN M/REV : 0.381000D-03

THE MASS MATRIX OF THE SYSTEM IS:

0.0000000 00	0.0000000 00	0.0000000 00	0.0000000 00	0.2032000 00	0.0000000 00	0.0000000 00	0.0000000 00
0.0000000 00	0.0000000 00	0.0000000 00	0.0000000 00	0.0000000 00	0.2032000 00	0.0000000 00	0.0000000 00
0.0000000 00	0.0000000 00	0.0000000 00	0.0000000 00	0.0000000 00	0.0000000 00	0.2032000 00	0.0000000 00
0.0000000 00	0.0000000 00	0.0000000 00	0.0000000 00	0.0000000 00	0.0000000 00	0.0000000 00	0.2032000 00
0.2032000 00	0.0000000 00	0.0000000 00	0.0000000 00	0.0000000 00	0.0000000 00	0.7660460 02	0.0000000 00
0.0000000 00	0.2032000 00	0.0000000 00	0.0000000 00	0.0000000 00	0.0000000 00	0.0000000 00	0.7660460 02
0.0000000 00	0.0000000 00	0.2032000 00	0.0000000 00	-0.7660460 02	0.0000000 00	0.0000000 00	0.0000000 00
0.0000000 00	0.0000000 00	0.0000000 00	0.2032000 00	0.0000000 00	-0.7660460 02	0.0000000 00	0.0000000 00

THE STIFFNESS MATRIX OF THE SYSTEM IS:

0.2032000 00	0.0000000 00	0.0000000 00	0.0000000 00	0.0000000 00	0.0000000 00	0.0000000 00	0.0000000 00
0.0000000 00	0.2032000 00	0.0000000 00	0.0000000 00	0.0000000 00	0.0000000 00	0.0000000 00	0.0000000 00
0.0000000 00	0.0000000 00	0.2032000 00	0.0000000 00	0.0000000 00	0.0000000 00	0.0000000 00	0.0000000 00
0.0000000 00	0.0000000 00	0.0000000 00	0.2032000 00	0.0000000 00	0.0000000 00	0.0000000 00	0.0000000 00
0.0000000 00	0.0000000 00	0.0000000 00	0.0000000 00	-0.1398150 08	0.0000000 00	0.5729670 00	-0.5729670 00
0.0000000 00	0.0000000 00	0.0000000 00	0.0000000 00	0.0000000 00	-0.5493160 09	-0.5729670 00	0.5729670 00
0.0000000 00	0.0000000 00	0.0000000 00	0.0000000 00	0.0000000 00	0.0000000 00	-0.1398150 08	-0.3437800 00
0.0000000 00	0.0000000 00	0.0000000 00	0.0000000 00	0.0000000 00	0.0000000 00	-0.3437800 00	-0.5493160 09

THE FIRST 8TH NATURAL FREQUENCIES ARE:

NATURAL FREQUENCIES	
-0.8495775481 4D-04	0.8485618224 8D 04
-0.8495775481 4D-04	-0.8485618224 8D 04
0.8496336028 6D-04	0.8108627064 9D 04
0.8496336028 6D-04	-0.8108627064 9D 04
-0.1421643391 4D-04	0.5218234273 8D 05
-0.1421643391 4D-04	-0.5218234273 8D 05
0.1494210298 4D-04	0.5180533516 9D 05
0.1494210298 4D-04	-0.5180533516 9D 05

SPINDLE SPEED OF THE NC LATHE IS: 0.1800D 04 RPM

THE FEEDRATE IN IN/REV : 0.300000D-01 IN M/REV : 0.762000D-03

THE MASS MATRIX OF THE SYSTEM IS:

0.0000000 00	0.0000000D 00	0.0000000D 00	0.0000000D 00	0.2032000D 00	0.0000000D 00	0.0000000D 00	0.0000000D 00
0.0000000 00	0.0000000D 00	0.0000000D 00	0.0000000D 00	0.0000000D 00	0.2032000D 00	0.0000000D 00	0.0000000D 00
0.0000000 00	0.0000000D 00	0.0000000D 00	0.0000000D 00	0.0000000D 00	0.0000000D 00	0.2032000D 00	0.0000000D 00
0.0000000D 00	0.0000000D 00	0.0000000D 00	0.0000000D 00	0.0000000D 00	0.0000000D 00	0.0000000D 00	0.2032000D 00
0.2032000 00	0.0000000D 00	0.0000000D 00	0.0000000D 00	0.0000000D 00	0.0000000D 00	0.7660460 02	0.0000000D 00
0.0000000 00	0.2032000D 00	0.0000000D 00	0.0000000D 00	0.0000000D 00	0.0000000D 00	0.0000000D 00	0.7660460 02
0.0000000 00	0.0000000D 00	0.2032000D 00	0.0000000D 00-0.7660460 02	0.0000000D 00	0.0000000D 00	0.0000000D 00	
0.0000000D 00	0.0000000D 00	0.0000000D 00	0.2032000D 00	0.0000000D 00-0.7660460 02	0.0000000D 00	0.0000000D 00	

THE STIFFNESS MATRIX OF THE SYSTEM IS:

0.2032000 00	0.0000000D 00	0.0000000D 00	0.0000000D 00	0.0000000D 00	0.0000000D 00	0.0000000D 00	0.0000000D 00
0.0000000 00	0.2032000D 00	0.0000000D 00	0.0000000D 00	0.0000000D 00	0.0000000D 00	0.0000000D 00	0.0000000D 00
0.0000000 00	0.0000000D 00	0.2032000D 00	0.0000000D 00	0.0000000D 00	0.0000000D 00	0.0000000D 00	0.0000000D 00
0.0000000D 00	0.0000000D 00	0.0000000D 00	0.2032000D 00	0.0000000D 00	0.0000000D 00	0.0000000D 00	0.0000000D 00
0.0000000 00	0.0000000D 00	0.0000000D 00	0.0000000D 00-0.1398150 08	0.0000000D 00	0.9636120 00-0.9636120 00		
0.0000000 00	0.0000000D 00	0.0000000D 00	0.0000000D 00	0.0000000D 00-0.5493160 09-0.9636120 00	0.9636120 00		
0.0000000 00	0.0000000D 00	0.0000000D 00	0.0000000D 00	0.0000000D 00	0.0000000D 00-0.1398150 08-0.5781670 00		
0.0000000 00	0.0000000D 00	0.0000000D 00	0.0000000D 00	0.0000000D 00	0.0000000D 00-0.5781670 00-0.5493160 09		

THE FIRST 8TH NATURAL FREQUENCIES ARE:

NATURAL FREQUENCIES	
-0.142382710080-03	0.848561819000 04
-0.142882710080-03	-0.848561819000 04
0.142889711600-03	0.810862703020 04
0.142889711600-03	-0.810862703020 04
-0.163765315900-04	0.521823427370 05
-0.163765315900-04	-0.521823427370 05
0.170409404510-04	0.518053516570 05
0.170409404510-04	-0.518053516570 05

MOTOROLA M6800AM CROSS-ASSEMBLER

```
M6800AM IS THE PROPERTY OF MOTOROLA SPD, INC
        COPYRIGHT 1974 BY MOTOROLA INC

MOTOROLA M6800 CROSS ASSEMBLER, RELEASE 1 1

00001                       NAM   EXPERINMENT
00002                 ***************************************************
00003                 *                                                 *
00004                 *                                                 *
00005                 *    PROPORTIONAL + INTEGRAL CONTROL ALOGRITHM     *
00006                 *                                                 *
00007                 *    WITH PEAK-VALUE INPUT DESIRE                 *
00008                 *                                                 *
00009                 *                                                 *
00010                 ***************************************************
00011   8009          ADCCTL  EQU     $8009
00012   0307          BNTODC  EQU     $0307
00013   E0E3          CONTEL  EQU     $E0E3
00014   800B          DACCTL  EQU     $800B
00015   CB18          DECONV  EQU     $CB18
00016   C2C7          DIP     EQU     $C2C7
00017   0035          DPPLC   EQU     $0035
00018   0034          FLDDEF  EQU     $0034
00019   009F          FPOP    EQU     $009F
00020   0097          FPACC   EQU     $0097
00021   C889          FPADD   EQU     $C889
00022   CA73          FPCONV  EQU     $CA73
00023   C9C0          FPDIV   EQU     $C9C0
00024   C916          FPMULT  EQU     $C916
00025   C90B          FPSUB   EQU     $C90B
00026   E0AA          INHEX   EQU     $E0AA
00027   8011          LINCTL  EQU     $8011
00028   8010          LSBIN   EQU     $8010
00029   800E          LSBOUT  EQU     $800E
00030   800F          LSDCTL  EQU     $800F
00031   000A          LSZC    EQU     $000A
00032   CA61          MOVEIT  EQU     $CA61
00033   800D          MPLCTL  EQU     $800D
00034   800C          MPLXOR  EQU     $800C
00035   8008          MSBIN   EQU     $8008
00036   800A          MSBOUT  EQU     $800A
00037   0033          OUTFLG  EQU     $0033
00038   E07E          PDATA1  EQU     $E07E
00039   0000          SUMNUM  EQU     $0000
00040   0093          TEMP2   EQU     $0093
00041   C202          XDOT    EQU     $C202
00042 1000                    ORG     $1000
00043                 *
```

```
00044                    *    INPUT DESIRE OF P V
00045                    *
00046 1000 OF                 SEI
00047 1001 CE 1407            LDX     #DESIPV   PRINT  INPUT 0 FOR NO P V  W
00048                    *                               1 FOR P V  WANTED
00049                    *
00050 1004 BD E07E            JSR     PDATA1
00051 1007 BD E0AA            JSR     INHEX
00052 100A B7 1516            STA A   YENOPV    STORE THE DESIRE IN  YENOPV
00053                    *
00054                    *    INPUT PARAMETERS   VNOM, K INT, K PRO, KNOM, RPM
00055                    *
00056                    *    FIRST INPUT VNOM - NOMINAL VOLTAGE
00057                    *
00058 100D CE 142A            LDX     #TEXT1    PRINT  VNOM=
00059 1010 BD E07E            JSR     PDATA1
00060 1013 BD C2C7            JSR     DIP
00061 1016 CE 0000            LDX     #SUMNUM
00062 1019 D6 0A              LDA B   LSZC
00063 101D BD CA73            JSR     FPCONV    VNOM IS CONVERTED TO F P  NO
00064 101E CE 0080            LDX     #$0080    PUT CONVERSION FACTOR BECAUSE
00065 1021 DF 9F              STX     FPOP      MSB + LSB EACH IS 8 BITS SO
00066 1023 CE 6566            LDX     #$6566    2 EXP 15=32767=10 VOLTS
00067 1026 DF A1              STX     FPOP+2
00068 1028 86 0C              LDA A   #$0C      32767/10=3276 7=1VOLT
00069 102A 97 A3              STA A   FPOP+4    3276 7=00 80 65 66 0C
00070 102C BD C916            JSR     FPMULT    (BASE 10)  (HEX F P )
00071 102F CE 1549            LDX     #VNOM     STORE IN  VNOM
00072 1032 BD 139D            JSR     FFPACC
00073                    *
00074                    *    INPUT K INT - INTEGRAL GAIN
00075                    *
00076 1035 CE 1459            LDX     #TEXT2    PRINT  K INT=
00077 1038 BD E07E            JSR     PDATA1
00078 103B BD C2C7            JSR     DIP
00079 103E CE 0000            LDX     #SUMNUM
00080 1041 D6 0A              LDA B   LSZC
00081 1043 BD CA73            JSR     FPCONV
00082 1046 CE 0060            LDX     #$0060    PUT CONVERSION FACTOR
00083 1049 DF 9F              STX     FPOP      32767/107=468 1(BASE 10)
00084 104B CE 0675            LDX     #$0675    = 00 60 06 75 09(HEX  F P  )
00085 104E DF A1              STX     FPOP+2    7 IS THE FACTOR OBTAINED FROM
00086 1050 86 09              LDA A   #$09      DYNAMOMETER CALIBRATION CURVE
00087 1052 97 A3              STA A   FPOP+4
00088 1054 BD C916            JSR     FPMULT
00089 1057 CE 1535            LDX     #K.INT    STORE IN  K INT
00090 105A BD 139D            JSR     FFPACC
00091                    *
```

```
00092                    *    INPUT FPRO - PROPORTIONAL GAIN
00093                    *
00094 105D CE 1461       *       LDX     #TEXT3    PRINT  FPRO=
00095 1060 BD E07E       *       JSR     PDATA1
00096 1063 BD C2C7       *       JSR     DIP
00097 1066 CE 0000       *       LDX     #SUMNUM
00098 1069 D6 0A         *       LDA B   LSZC
00099 106B BD CA73       *       JSR     FPCONV
00100 106E CE 0060       *       LDX     #$0060    PUT CONVERSION FACTOR. 468.1
00101 1071 DF 9F         *       STX     FPOP
00102 1073 CE 0675       *       LDX     #$0675
00103 1076 DF A1         *       STX     FPOP+2
00104 1078 86 09         *       LDA A   #$09
00105 107A 97 A3         *       STA A   FPOP+4
00106 107C BD C916       *       JSR     FPMULT
00107 107F CE 153A       *       LDX     #FPRO     STORE IN  FPRO
00108 1082 BD 139D       *       JSR     FFPACC
00109                    *
00110                    *    INPUT FNOM - NOMINAL FORCE
00111                    *
00112 1085 CE 1469       *       LDX     #TEXT4    PRINT. FNOM=
00113 1088 BD E07E       *       JSR     PDATA1
00114 108B BD C2C7       *       JSR     DIP
00115 108E CE 0000       *       LDX     #SUMNUM
00116 1091 D6 0A         *       LDA B   LSZC
00117 1093 BD CA73       *       JSR     FPCONV
00118 1096 CE 0000       *       LDX     #$0000    PUT CONVERSION FACTOR 7
00119 1099 DF 9F         *       STX     FPOP      7     =   00 00 00 70 03
00120 109B CE 0070       *       LDX     #$0070    (BASE 10).    (HEX  F P  )
00121 109E DF A1         *       STX     FPOP+2
00122 10A0 86 03         *       LDA A   #$03
00123 10A2 97 A3         *       STA A   FPOP+4
00124 10A4 BD C916       *       JSR     FPMULT
00125 10A7 CE 1526       *       LDX     #FNOM     STORE IN  FNOM
00126 10AA BD 139D       *       JSR     FFPACC
00127                    *
00128                    *    TEST WHETHER P V  WANTED
00129                    *
00130 10AD 7D 1516       *       TST     YENOPV
00131 10B0 26 03         *       BNE     MORE
00132 10B2 7E 1142       *       JMP     NOPV      TO PRINT DESIRED
00133                    *
00134                    *    INPUT INITIAL PEAK VALUE - PEAKVAL
00135                    *
00136 10B5 CE 14A4 MORE  *       LDX     #TEXT8    PRINT  INITIAL PEAKVAL=
00137 10B8 BD E07E       *       JSR     PDATA1
00138 10BB BD C2C7       *       JSR     DIP
00139 10BE CE 0000       *       LDX     #SUMNUM
```

```
00140 10C1 D6 0A          LDA B  LSZC
00141 10C3 BD CA73        JSR    FPCONV
00142 10C6 CE 153F        LDX    #PEP VAL
00143 10C9 BD 139D        JSR    FFPACC
00144                *
00145                *    INPUT DESIRED DECAYING FACTOR(F) + RPM
00146                *
00147                *    SO THAT THE DECAYING FACTOR PER REVOLUTION
00148                *    F  IS CALCULATED AS FOLLOWS.
00149                *   LET TR/TC = N SO F  EXP(N) = F
00150                *    F  = F EXP(1/N)
00151                *    FROM SERIES EXPANSION, FOR FIRST 2 TERMS
00152                *    F  = 1 0-(1.0-F)/TR/TC
00153                *    F  = 1 0-(1 0-F)/(60/RPM)/0 05
00154                *    F  = 1 0-(1.0-F)*RPM/1200
00155                *    NOTE  1) TC IS ASSUMED TO APPROX 50 MSEC
00156                *             FROM OSCILLOSCOPE
00157                *
00158 10CC CE 14B6        LDX    #TEXT9   PRINT  F =
00159 10CF BD E07E        JSR    PDATA1
00160 10D2 BD C2C7        JSR    DIP
00161 10D5 CE 0000        LDX    #SUMNUM
00162 10D8 D6 0A          LDA B  LSZC
00163 10DA BD CA73        JSR    FPCONV   F IS AT FPACC
00164 10DD CE 0000        LDX    #$0000   LOAD FPOP WITH 1 0
00165 10E0 DF 9F          STX    FPOP
00166 10E2 CE 0040        LDX    #$0040
00167 10E5 DF A1          STX    FPOP+2
00168 10E7 86 01          LDA A  #$01
00169 10E9 97 A3          STA A  FPOP+4
00170 10EB BD C90B        JSR    FPSUB    FPACC = 1.0-F
00171 10EE CE 1521        LDX    #F       STORE (1 0-F) IN ADDRESS 'F'
00172 10F1 DD 139D        JSR    FFPACC
00173                *
00174 10F4 CE 1471        LDX    #TEXT5   PRINT  RPM=
00175 10F7 BD E07E        JSR    PDATA1
00176 10FA BD C2C7        JSR    DIP
00177 10FD CE 0000        LDX    #SUMNUM
00178 1100 D6 0A          LDA B  LSZC
00179 1102 BD CA73        JSR    FPCONV
00180 1105 CE 1544        LDX    #RPM
00181 1108 BD 139D        JSR    FFPACC
00182 110B CE 1544        LDX    #RPM     PUT RPM INTO FPOP
00183 110E BD 138C        JSR    TOFPOP
00184 1111 CE 0000        LDX    #$0000   LOAD FPACC WITH 1200
00185 1114 DF 97          STX    FPACC    =00 00 00 4B 0B (HEX F P )
00186 1116 CE 004B        LDX    #$004D
00187 1119 DF 99          STX    FPACC+2
```

```
00188 111B 86 0B          LDA A  #$0B
00189 111D 97 9B          STA A  FPACC+4
00190 111F BD C9C0        JSR    FPDIV      RPM(FPOP)/1200=RPM*8.333E-4
00191                *
00192 1122 CE 1521        LDX    #F
00193 1125 BD 138C        JSR    TOFPOP     LOAD FPOP WITH (1.0-F)
00194 1128 BD C916        JSR    FPMULT     FPACC=(1.0-F)*RPM/1200
00195                *
00196 112B CE 0000        LDX    #$0000     LOAD FPOP WITH 1.0
00197 112E DF 9F          STX    FPOP
00198 1130 CE 0040        LDX    #$0040
00199 1133 DF A1          STX    FPOP+2
00200 1135 86 01          LDA A  #$01
00201 1137 97 A3          STA A  FPOP+4
00202 1139 BD C90B        JSR    FPSUB      F=1.0-(1.0-F)*RPM/1200
00203 113C CE 152B        LDX    #FPI       STORE IN FPI
00204 113F BD 139D        JSR    FFPACC
00205                *
00206                *    INPUT PRINT DESIRE
00207                *
00208 1142 CE 14BB NOPV   LDX    #TEXTW     PRINT  INPUT 1 FOR PRINT OUT
00209 1145 BD E07E        JSR    PDATA1     0 FOR NO PRINT OUT
00210 1148 BD E0AA        JSR    INHEX
00211 114B B7 1513        STA A  PRT
00212 114E 7D 1513        TST    PRT
00213 1151 27 5A          BEQ    NOPRNT
00214 1153 CE 1478        LDX    #TEXT6     PRINT  PRINTING INTERVAL
00215 1156 BD E07E        JSR    PDATA1
00216 1159 BD C2C7        JSR    DIP
00217 115C CE 0000        LDX    #SUMNUM
00218 115F D6 0A          LDA B  LSZC
00219 1161 BD CA73        JSR    FPCONV
00220 1164 86 17          LDA A  #23        SHIFT BITS IN FPACC
00221 1166 90 9B          SUB A  FPACC+4
00222 1168 B7 1515        STA A  SCOUNT
00223 116B 77 009A BSHIFT ASR    FPACC+3
00224 116E 76 0099        ROR    FPACC+2
00225 1171 76 0098        ROR    FPACC+1
00226 1174 7A 1515        DEC    SCOUNT
00227 1177 26 F2          BNE    BSHIFT
00228 1179 96 98          LDA A  FPACC+1    EXTRACT LSB FROM FPACC
00229 117B B7 1514        STA A  PRINT
00230 117E CE 149C        LDX    #TEXT7     PRINT. VOUT=
00231 1181 BD E07E        JSR    PDATA1
00232                *
00233                *    SET UP TIMER NOTE TIMER IS ON B SIDE OF PIA.
00234                *    IT IS PHYSICALLY FIXED AT PORT =4 WITH ADDRESSES
00235                *    8010 TO 8013 NOTE  WE USE ONLY B SIDE I.E.
```

```
00236                    *    8012 - PDDB , 8013 - DDRD
00237                    *
00238 1184 4F            *        CLR A
00239 1185 B7 8013       *        STA A  $8013
00240 1188 86 FF         *        LDA A  #$FF     SETTING B SIDE AS OUTPUT
00241 118A B7 8012       *        STA A  $8012
00242 118D 86 05         *        LDA A  #$05     RETURN TO CR WITH BIT 2=1
00243 118F B7 8013       *        STA A  $8013    SET CB1 RESPONSE TO -VE IDGE
00244 1192 86 14         *        LDA A  #$14     LOADING THE STARTING ADDRESS
00245 1194 B7 A000       *        STA A  $A000    OF INTERRUPT SERVICE
00246 1197 86 00         *        LDA A  #$00     I E  $1400
00247 1199 B7 A001       *        STA A  $A001
00248 119C 86 80         *        LDA A  #$80     RESET THE OSCILLATOR
00249 119E B7 8012       *        STA A  $8012
00250 11A1 86 06         *        LDA A  #$06     SET TIMER TO 1 SECOND INTERVA
00251 11A3 B7 8012       *        STA A  $8012
00252 11A6 C6 00         *        LDA B  #$00
00253 11A8 F7 1511       *        STA B  COUNT
00254 11AB 20 06         *        BRA    CLINT
00255                    *
00256 11AD CE 14F2 NOPRNT *        LDX    #TEXTNP   PRINT  NO RRINT IS REQUIRED
00257 11B0 BD E07E       *        JSR    PDATA1    PROGRAM IS ACTIVATED NOW
00258                    *
00259 11B3 CE 0000 CLINT  *        LDX    #$0000    CLEAR INTEGRAL
00260 11B6 FF 1530        *        STX    INT
00261 11B9 FF 1532        *        STX    INT+2
00262 11BC FF 1533        *        STX    INT+3
00263 11BF 7F 1512        *        CLR    INTFLG    CLEAR INTEGRAL FLAG INITIALLY
00264                    *                           SO THAT IT WILL DO INTEGRATI
00265                    *                           AT FIRST TIME REGARDLESS OF
00266                    *                           SIGN OF ERROR LATER ON
00267                    *
00268                    *    SET UP CONVERTERS
00269                    *
00270 11C2 4F            *        CLR A
00271 11C3 B7 8009       *        STA A  ADCCTL    SETTING ALL CONTROL REGISTERS
00272 11C6 B7 800B       *        STA A  DACCTL    WITH BIT 2 = 0
00273 11C9 B7 800D       *        STA A  MPLCTL
00274 11CC B7 800F       *        STA A  LSDCTL
00275 11CF B7 8011       *        STA A  LINCTL
00276 11D2 B7 8008       *        STA A  MSBIN     SET A SIDES FOR ADC DATA
00277 11D5 B7 8010       *        STA A  LSBIN     LINES AS INPUTS TO PIA
00278 11D8 86 FF         *        LDA A  #$FF
00279 11DA B7 800A       *        STA A  MSBOUT    SET B SIDES FOR ADC DATA
00280 11DD B7 800E       *        STA A  LSBOUT    LINES AS OUTPUTS FROM PIA
00281 11E0 B7 800C       *        STA A  MPLXOR    SET MPLXOR LINES AS PUTPUT LI
00282                    *
00283                    *    SET BIT 2 OF CONTROL REGISTER SO LET MPU
```

```
00284                    *    COMMUNICATE WITH PDR
00285                    *
00286 11E3 86 04              LDA A  #$04
00287 11E5 B7 8009            STA A  ADCCTL
00288 11E8 B7 800B            STA A  DACCTL
00289 11EB B7 800D            STA A  MPLCTL
00290 11EE B7 800F            STA A  LSOCTL
00291 11F1 B7 8011            STA A. LINCTL
00292                    *
00293                    *    SET UP PULSE MODE OF ADCCTL
00294                    *
00295 11F4 86 2C              LDA A  #$2C
00296 11F6 B7 8009            STA A  ADCCTL
00297                    *
00298                    *    SET MULTIPLEXOR FOR CHANNEL NO 3
00299                    *
00300 11F9 86 03              LDA A  #$03
00301 11FB B7 800C            STA A  MPLXOR
00302                    *
00303                    *    PREPARE INPUT ON ADC
00304                    *
00305 11FE 7D 1513            TST    PRT
00306 1201 27 05              BEQ    SCONV     IF PRT=0, BY PASS IRQ
00307 1203 02                 NOP              THIS IS REQUIRED BY MANUAL.
00308 1204 0E                 CLI
00309 1205 B6 8012            LDA A  $8012
00310                    *
00311                    *    START CHECKING BIT 7 UNTIL IT IS SET
00312                    *
00313 1208 B6 8008 SCONV  LDA A  MSBIN     CAUSE AN SOC PULSE TO.GENERAT
00314 120B B6 8009 CHECK  LDA A  ADCCTL    CHECK IF BIT 7 OF DDR IS SET
00315 120E 2A FB          BPL    CHECK     I E  WAIT UNTIL ADC FINISHES
00316                    *
00317                    *    DATA INPUT
00318                    *
00319 1210 4F                 CLR A
00320 1211 97 0A              STA A  LSZC
00321 1213 86 FF              LDA A  #$FF      OFFSET ADJUST
00322 1215 B0 8010            SUB A  LSBIN     AND
00323 1218 97 04              STA A  SUMNUM+4    TRANSFER DATA
00324 121A 86 7F              LDA A  #$7F      TO
00325 121C B2 8008            SBC A  MSBIN     SUMNUM
00326 121F 97 03              STA A  SUMNUM+3
00327 1221 2C 0A              BGE    POSIGN
00328 1223 C6 FF              LDA B  #$FF
00329 1225 D7 00    SETSUM    STA B  SUMNUM
00330 1227 D7 01              STA B  SUMNUM+1
00331 1229 D7 02              STA B  SUMNUM+2
```

```
00332 122B 20 03          BRA     CONV
00333 122D 5F       POSIGN CLR B
00334 122E 20 F5          BRA     SETSUM
00335 1230 CE 0000  CONV  LDX     #SUMNUM
00336 1233 D6 0A          LDA B   LSZC
00337 1235 BD CA73        JSR     FPCONV   THE DATA IS CONVERTED TO F P.
00338                *
00339 1238 CE 1517        LDX     #DATA    STORE DATA IN ADDRESS DATA
00340 123B BD 139D        JSR     FFPACC
00341                *
00342                *    TEST HOW TO HANDLE THE DATA BY KNOWING THE
00343                *    P V  DESIRE
00344                *
00345 123E 7D 1516        TST     YENOPV
00346 1241 27 3D          BEQ     SIMPLE
00347                *
00348 1243 CE 153F        LDX     #PERVAL   LOAD PEAK VALUE IN FPOP
00349 1246 BD 138C        JSR     TOFPOP
00350 1249 BD C90B        JSR     FPSUB    FPACC = P V  - DATA
00351 124C 7D 009A        TST     FPACC+3   TEST THE RESULT
00352 124F 2F 11          BLE     NEWPV    IF DATA GE.  P V  BRANCH TO
00353                *                      NEW PEAK VALUE( NEWPV )
00354                *
00355 1251 CE 152D        LDX     #FPI     LOAD F  FACTOR TO FPACC
00356 1254 BD 137B        JSR     TFPACC
00357 1257 BD C916        JSR     FPMULT   DECAY THE PEAK VALUE BY F
00358 125A CE 153F        LDX     #PERVAL  REPLACE OLD P V.  WITH
00359 125D BD 139D        JSR     FFPACC   DECAYED ONE
00360 1260 20 0D          BRA     EROR
00361                *
00362 1262 CE 153F  NEWPV LDX     #PERVAL   REPLACE PERVAL BY DATA
00363 1265 DF 93          STX     TEMP2
00364 1267 CE 1517        LDX     #DATA
00365 126A C6 05          LDA B   #5
00366 126C BD CA61        JSR     MOVEIT
00367                *
00368 126F CE 1526  EROR  LDX     #FNOM    LOAD FNOM IN FPOP
00369 1272 BD 138C        JSR     TOFPOP
00370                *
00371 1275 CE 153F        LDX     #PERVAL   LOAD PERVAL IN FPACC
00372 1278 BD 137B        JSR     TFPACC
00373                *
00374 127B BD C90B        JSR     FPSUB    ERROR( FPACC )=FNOM-P. V.
00375                *
00376 127E 20 09          BRA     LDEROR
00377                *
00378 1280 CE 1526  SIMPLE LDX    #FNOM
00379 1283 BD 138C        JSR     TOFPOP   LOAD FNOM IN FPOP
```

```
00380 1286 BD C90B          J$R     FPSUB    ERROR(FPACC)=FNOM-DATA
00381                *
00382 1289 CE 151C LDERROR  LDX     #ERROR   STORE THE DIFFERENCE IN ERROR
00383 128C BD 139D          J$R     FFPACC
00384                *
00385 128F 7D 151F          T$T     ERROR+3   TEST DATA IS GT  OR LT  FNOM
00386 1292 2B 07            BMI     NEGTST   IF -VE BRANCH TO NEGTST
00387                *
00388 1294 7D 1512          T$T     INTFLG   TEST INTFLG, IF VOUT GT  5VT
00389 1297 2E 18            B$T     OLDINT   THEN BRANCH TO OLDINT
00390                *
00391 1299 20 05            BRA     DOINT    OR PERFORM INTEGRATION
00392                *
00393 129D 7D 1512 NEGTST   TST     INTFLG   TEST INTFLG, IF VOUT LT  0VT
00394 129E 2D 11            BLT     OLDINT   BRANCH TO OLDINT
00395                *
00396 12A0 CE 1530 DOINT    LDX     #INT     LOAD FPOP WITH INT
00397 12A3 BD 138C          JSR     TOFPOP
00398                *
00399 12A6 BD C889          JSR     FPADD    INT(FPACC)=INT(FPOP)+ERROR
00400                *
00401 12A9 CE 1530          LDX     #INT     REPLACE INT WITH NEW VALUE
00402 12AC BD 139D          JSR     FFPACC
00403 12AF 20 12            BRA     LDKINT   GOTO LOAD KINT
00404                *
00405 12B1 7F 1512 OLDINT   CLR     INTFLG   CLEAR INTFLAG
00406 12B4 FE 1530          LDX     INT      RETRIVE OLD INT
00407 12B7 DF 97            STX     FPACC    AND PUT INTO FPACC
00408 12B9 FE 1532          LDX     INT+2
00409 12BC DF 99            STX     FPACC+2
00410 12BE B6 1534          LDA A   INT+4
00411 12C1 97 9B            STA A   FPACC+4
00412                *
00413 12C3 CE 1535 LDKINT   LDX     #KINT    LOAD FPOP WITH KINT
00414 12C6 BD 138C          JSR     TOFPOP
00415                *
00416 12C9 BD C916          JSR     FPMULT   KINT*INT = FPACC
00417                *
00418 12CC CE 1549          LDX     #VNOM    LOAD VNOM IN FPOP
00419 12CF BD 138C          JSR     TOFPOP
00420                *
00421 12D2 BD C889          JSR     FPADD    VNOM+KINT*INT = FPACC
00422                *
00423 12D5 CE 154E          LDX     #WRKSP   STORE RESULT IN WORKSPACE
00424 12D8 BD 139D          JSR     FFPACC
00425                *
00426 12DB CE 153A          LDX     #KPRO    LOAD FPACC WITH KPRO
00427 12DE BD 137B          JSR     TFPACC
```

```
00428                    *
00429 12E1 CE 151C       LDX    #ERROR   LOAD FPOP WITH ERROR
00430 12E4 BD 138C       JSR    TOFPOP
00431                    *
00432 12E7 BD C916       JSR    FPMULT   FPRO*ERROR = FPACC
00433                    *
00434 12EA CE 154E       LDX    #WRKSP   LOAD WRKSP INTO FPOP
00435 12ED BD 138C       JSR    TOFPOP
00436                    *
00437 12F0 BD C889       JSR    FPADD    VNOM+INT*INT+FPRO*ERROR=VOUT
00438                    *
00439 12F3 7D 1513       TST    PRT      IF NO PRINT IS NEEDED BRANCH
00440 12F6 27 35         BEQ    CONOFF
00441 12F8 7D 1511       TST    COUNT    TEST WHETHER COUNT IS SET OR
00442 12FB 2A 30         BPL    CONOFF
00443                    *
00444                    *  PRINT OUTPUT
00445                    *
00446 12FD CE 150D       LDX    #TEXTP   START PRINTING
00447 1300 BD E07E       JSR    PDATA1
00448 1303 4F            CLR A           PUT CONVERSION FACTOR 5/32767
00449 1304 97 9F         STA A  FPOP     NOTE THAT DAC RANGE IS 5VLT
00450 1306 97 A1         STA A  FPOP+2   SO 5/32767=1.5259E-4
00451 1308 86 A0         LDA A  #$A0     1.5259E-4=00 A0 00 50 F4
00452 130A 97 A0         STA A  FPOP+1   (BASE 10)    (HEX  F P )
00453 130C 86 50         LDA A  #$50
00454 130E 97 A2         STA A  FPOP+3
00455 1310 86 F4         LDA A  #$F4
00456 1312 97 A3         STA A  FPOP+4
00457 1314 BD C916       JSR    FPMULT   VOUT IN VOLTS
00458 1317 BD CB18       JSR    DECONV   CONVERT TO DECEMIAL
00459 131A 96 34         LDA A  FLDDEF
00460 131C D6 35         LDA B  DPPLC
00461 131E CE 0000       LDX    #SUMNUM
00462 1321 BD C202       JSR    XDOT
00463 1324 F6 1514       LDA B  PRINT    SET UP INTERVAL
00464 1327 F7 1511       STA B  COUNT    OF INTERRUPT TIMER
00465 132A 7E 120B       JMP    CHECK
00466                    *
00467 132D 7D 009A CONOFF TST   FPACC+3   TEST SIGN
00468 1330 2B 29         BMI    ZEVOLT
00469 1332 86 17         LDA A  #23
00470 1334 90 9B         SUB A  FPACC+4
00471 1336 B7 1515       STA A  SCOUNT
00472 1339 80 07         SUB A  #07
00473 133B 2F 2F         BLE    PLSVLT   SATURATE WITH + VOLTS
00474 133D 77 009A SHIFTB ASR   FPACC+3
00475 1340 76 0099       ROR    FPACC+2
```

```
00476 1343 76 0098          ROR     FPACC+1
00477 1346 7A 1515          DEC     SCOUNT
00478 1349 26 F2            BNE     SHIFTB
00479 134B 86 FF            LDA A   #$FF        OFFSET ADJUST
00480 134D 90 98            SUB A   FPACC+1
00481 134F B7 800E          STA A   LSDOUT
00482 1352 86 7F            LDA A   #$7F
00483 1354 92 99            SBC A   FPACC+2
00484 1356 B7 800A          STA A   MSBOUT
00485 1359 20 1D            BRA     FIN
00486                       *
00487 135D 86 FF    ZEVOLT  LDA A   #$FF
00488 135D B7 800E          STA A   LSDOUT
00489 1360 86 7F            LDA A   #$7F
00490 1362 B7 800A          STA A   MSBOUT
00491 1365 86 FF            LDA A   #$FF        SET INTFLG TO AN ARBITARY
00492 1367 B7 1512          STA A   INTFLG      VALUE S T  TO SET UP A LOGIC
00493 136A 20 0C            BRA     FIN         CHECKING POINT OF SHIPPING
00494                       *                   INTEGRAT  WHEN ERROR IS -VE
00495                       *
00496 136C 4F       PLSVLT  CLR A
00497 136D B7 800E          STA A   LSDOUT
00498 1370 B7 800A          STA A   MSBOUT
00499 1373 86 01            LDA A   #$01        SET INTFLG TO AN ARBITARY
00500 1375 B7 1512          STA A   INTFLG      VALUE S T  TO SET UP A LOGIC
00501 1378 7E 120B  FIN     JMP     CHECK       CHECKING POINT OF SHIPPING
00502                       *                   INTEGRATION WHEN ERROR IS +VE
00503                       *
00504                       *   SUBPROGRAM TFPACC -  TO LOAD A DATA TO FPACC
00505                       *
00506 137B FF 1553  TFPACC  STX     TEMPLY
00507 137E CE 0097          LDX     #FPACC
00508 1381 DF 93            STX     TEMP2
00509 1383 FE 1553          LDX     TEMPLY
00510 1386 C6 05            LDA B   #5
00511 1388 BD CA61          JSR     MOVEIT
00512 138B 39               RTS
00513                       *
00514                       *   SUBPROGRAM TOFPOP - TO LOAD A DATA TO FPOP
00515                       *
00516 138C FF 1553  TOFPOP  STX     TEMPLY
00517 138F CE 009F          LDX     #FPOP
00518 1392 DF 93            STX     TEMP2
00519 1394 FE 1553          LDX     TEMPLY
00520 1397 C6 05            LDA B   #5
00521 1399 BD CA61          JSR     MOVEIT
00522 139C 39               RTS
00523                       *
```

```
00524                    *    SUBPROGRAM FFPACC - TO LOAD A DATA FROM FPACC
00525                    *
00526 139D DF 93         FFPACC STX     TEMP2
00527 139F CE 0097             LDX     #FPACC
00528 13A2 C6 05               LDA B   #5
00529 13A4 BD CA61             JSR     MOVEIT
00530 13A7 39                  RTS
00531                    *
00532                    *    SUBPROGRAM FFPOP - TO LOAD A DATA FROM FPOP
00533                    *
00534 13A8 DF 93         FFPOP  STX     TEMP2
00535 13AA CE 009F             LDX     #FPOP
00536 13AD C6 05               LDA B   #5
00537 13AF BD CA61             JSR     MOVEIT
00538 13B2 39                  RTS
00539                    *
00540                    *    TIMER INTERRUPT SERVICE ROUTINE
00541                    *
00542 1400                     ORG     $1400
00543 1400 7A 1511             DEC     COUNT
00544 1403 B6 8012             LDA A   $8012
00545 1406 3B                  RTI
00546                    *
00547 1407 0D            DESIPV FCB     $0D,$0A
      1408 0A
00548 1409 49                  FCC     /INPUT 0 FOR NO PV, 1 FOR PV     /
      140A 4E
      140B 50
      140C 55
      140D 54
      140E 20
      140F 30
      1410 20
      1411 46
      1412 4F
      1413 52
      1414 20
      1415 4E
      1416 4F
      1417 20
      1418 50
      1419 56
      141A 3B
      141B 20
      141C 31
      141D 20
      141E 46
      141F 4F
```

```
                1420 52
                1421 20
                1422 50
                1423 56
                1424 20
                1425 2E
                1426 2E
                1427 2E
                1428 20
00549           1429 04             FCB     4
00550                       *
00551           142A 0D     TEXT1   FCB     $0D, $0A, $0A, $0A
                142B 0A
                142C 0A
                142D 0A
00552           142E 56             FCC     /VOUT=VNOM+KINT*INTEGRAL+KPRO*ERROR/
                142F 4F
                1430 55
                1431 54
                1432 3D
                1433 56
                1434 4E
                1435 4F
                1436 4D
                1437 2B
                1438 4B
                1439 49
                143A 4E
                143B 54
                143C 2A
                143D 49
                143E 4E
                143F 54
                1440 45
                1441 47
                1442 52
                1443 41
                1444 4C
                1445 2B
                1446 4B
                1447 50
                1448 52
                1449 4F
                144A 2A
                144B 45
                144C 52
                144D 52
                144E 4F
```

```
                144F 52
00553           1450 0D             FCB     $0D,$0A,$0A
                1451 0A
                1452 0A
00554           1453 56             FCC     /VNOM=/
                1454 4E
                1455 4F
                1456 4D
                1457 3D
00555           1458 04             FCB     4
00556                       *
00557           1459 0D     TEXT2   FCB     $0D,$0A
                145A 0A
00558           145B 4B             FCC     /KINT=/
                145C 49
                145D 4E
                145E 54
                145F 3D
00559           1460 04             FCB     4
00560                       *
00561           1461 0D     TEXT3   FCB     $0D,$0A
                1462 0A
00562           1463 4B             FCC     /KPRO=/
                1464 50
                1465 52
                1466 4F
                1467 3D
00563           1468 04             FCB     4
00564                       *
00565           1469 0D     TEXT4   FCB     $0D,$0A
                146A 0A
00566           146B 46             FCC     /FNOM=/
                146C 4E
                146D 4F
                146E 4D
                146F 3D
00567           1470 04             FCB     4
00568                       *
00569           1471 0D     TEXT5   FCB     $0D,$0A
                1472 0A
00570           1473 52             FCC     /RPM=/
                1474 50
                1475 4D
                1476 3D
00571           1477 04             FCB     4
00572                       *
00573           1478 0D     TEXT6   FCB     $0D,$0A,$0A
                1479 0A
```

```
                147A 0A
00574           147B 50             FCC     /PRINTING INTERVAL ( 1-127 SEC ) = /
                147C 52
                147D 49
                147E 4E
                147F 54
                1480 49
                1481 4E
                1482 47
                1483 20
                1484 49
                1485 4E
                1486 54
                1487 45
                1488 52
                1489 56
                148A 41
                148B 4C
                148C 20
                148D 28
                148E 31
                148F 2D
                1490 31
                1491 32
                1492 37
                1493 20
                1494 53
                1495 45
                1496 43
                1497 29
                1498 20
                1499 3D
                149A 20
00575           149B 04             FCB     4
00576                       *
00577           149C 0D     TEXT7   FCB     $0D,$0A
                149D 0A
00578           149E 56             FCC     /VOUT=/
                149F 4F
                14A0 55
                14A1 54
                14A2 3D
00579           14A3 04             FCB     4
00580                       *
00581           14A4 0D     TEXT8   FCB     $0D,$0A
                14A5 0A
00582           14A6 49             FCC     /INITIAL PERVAL=/
                14A7 4E
```

```
                14A8 49
                14A9 54
                14AA 49
                14AB 41
                14AC 4C
                14AD 20
                14AE 50
                14AF 45
                14B0 4B
                14B1 56
                14B2 41
                14B3 4C
                14B4 3D
00583           14B5 04             FCB     4
00584                       *
00585           14B6 0D     TEXT9   FCB     $0D,$0A
                14B7 0A
00586           14B8 46             FCC     /F=/
                14B9 3D
00587           14BA 04             FCB     4
00588                       *
00589           14BB 0D     TEXTW   FCB     $0D,$0A
                14BC 0A
00590           14BD 49             FCC     /INPUT "1" FOR PRINTOUT OR /
                14BE 4E
                14BF 50
                14C0 55
                14C1 54
                14C2 20
                14C3 22
                14C4 31
                14C5 22
                14C6 20
                14C7 46
                14C8 4F
                14C9 52
                14CA 20
                14CB 50
                14CC 52
                14CD 49
                14CE 4E
                14CF 54
                14D0 4F
                14D1 55
                14D2 54
                14D3 20
                14D4 4F
                14D5 52
```

```
                14D6 20
00591           14D7 22             FCC     /"O" FOR NO PRINTOUT ----- /
                14D8 30
                14D9 22
                14DA 20
                14DB 46
                14DC 4F
                14DD 52
                14DE 20
                14DF 4E
                14E0 4F
                14E1 20
                14E2 50
                14E3 52
                14E4 49
                14E5 4E
                14E6 54
                14E7 4F
                14E8 55
                14E9 54
                14EA 20
                14EB 2D
                14EC 2D
                14ED 2D
                14EE 2D
                14EF 2D
                14F0 20
00592           14F1 04             FCB     4
00593                       *
00594           14F2 0D     TEXTNP  FCB     $0D,$0A
                14F3 0A
00595           14F4 50             FCC     /PROGRAM IS ACTIVATED NOW/
                14F5 52
                14F6 4F
                14F7 47
                14F8 52
                14F9 41
                14FA 4D
                14FB 20
                14FC 49
                14FD 53
                14FE 20
                14FF 41
                1500 43
                1501 54
                1502 49
                1503 56
                1504 41
```

```
                1505 54
                1506 45
                1507 44
                1508 20
                1509 4E
                150A 4F
                150B 57
00596           150C 04             FCB     4
00597                       *
00598           150D 0D     TEXTP   FCB     $0D, $0A, 00, 04
                150E 0A
                150F 00
                1510 04
00599                       *
00600           1511 0001   COUNT   RMB     1
00601           1512 0001   INTFLG  RMB     1
00602           1513 0001   PRT     RMB     1
00603           1514 0001   PRINT   RMB     1
00604           1515 0001   SCOUNT  RMB     1
00605           1516 0001   YENDFV  RMB     1
00606           1517 0005   DATA    RMB     5
00607           151C 0005   ERROR   RMB     5
00608           1521 0005   F       RMB     5
00609           1526 0005   FNOM    RMB     5
00610           152B 0005   FFI     RMB     5
00611           1530 0005   INT     RMB     5
00612           1535 0005   FINT    RMB     5
00613           153A 0005   FPRO    RMB     5
00614           153F 0005   PERVAL  RMB     5
00615           1544 0005   RPM     RMB     5
00616           1549 0005   VNOM    RMB     5
00617           154E 0005   WRKSP   RMB     5
00618           1553 0005   TEMPLY  RMB     5
00619                       END
```

SYMBOL TABLE

ADCCTL	8009	BNTODC	0307	CONTEL	E0E3	DACCTL	800B
DECONV	CB18	DIP	C2C7	DPPLC	0035	FLDDEF	0034
FPOP	009F	FPACC	0097	FPADD	C889	FPCONV	CA73
FPDIV	C9C0	FPMULT	C916	FPSUB	C90B	INHEX	E0AA
LINCTL	8011	LSBIN	8010	LSBOUT	800E	LSDCTL	800F
LSZC	000A	MOVEIT	CA61	MPLCTL	800D	MPLXOR	800C
MSBIN	8008	MSBOUT	800A	OUTFLG	0033	PDATA1	E07E
SUMNUM	0000	TEMPZ	0093	XDOT	C202	MORE	10D5
NOPV	1142	BSHIFT	116B	NOPRNT	11AD	CLINT	11B3
SCONV	1208	CHECK	120B	SETSUM	1225	POSIGN	122D
CONV	1230	NEWPV	1262	ERDR	126F	SIMPLE	1280
LDERDR	1289	NEGTST	129B	DOINT	12A0	OLDINT	12B1
LDKINT	12C3	CONOFF	132D	SHIFTD	133D	ZEVOLT	135B
PLSVLT	136C	FIN	1378	TFPACC	137B	TOFPOP	138C
FFPACC	139D	FFPOP	13A8	DESIPV	1407	TEXT1	142A
TEXT2	1459	TEXT3	1461	TEXT4	1469	TEXT5	1471
TEXT6	1478	TEXT7	149C	TEXT8	14A4	TEXT9	14B6
TEXTW	14BB	TEXTNP	14F2	TEXTP	150D	COUNT	1511
INTFLG	1512	PRT	1513	PRINT	1514	SCOUNT	1515
YENOPV	1516	DATA	1517	ERROR	151C	F.	1521
FNOM	1526	FPI	152B	INT	1530	FINT	1535
FPRO	153A	PERVAL	153F	RPM	1544	VNOM	1549
WRKSP	154E	TEMPLY	1553				

151935 12-16-81 JOB, END

973 SECONDS

151937 12-16-81 JOB, HALT

APPENDIX J

PHYSICAL UNITS AND CONVERSION FACTORS OF THE CLOSED-LOOP SYSTEM

The physical units and dimensions at each stage of the close-loop system is shown in the following figure.

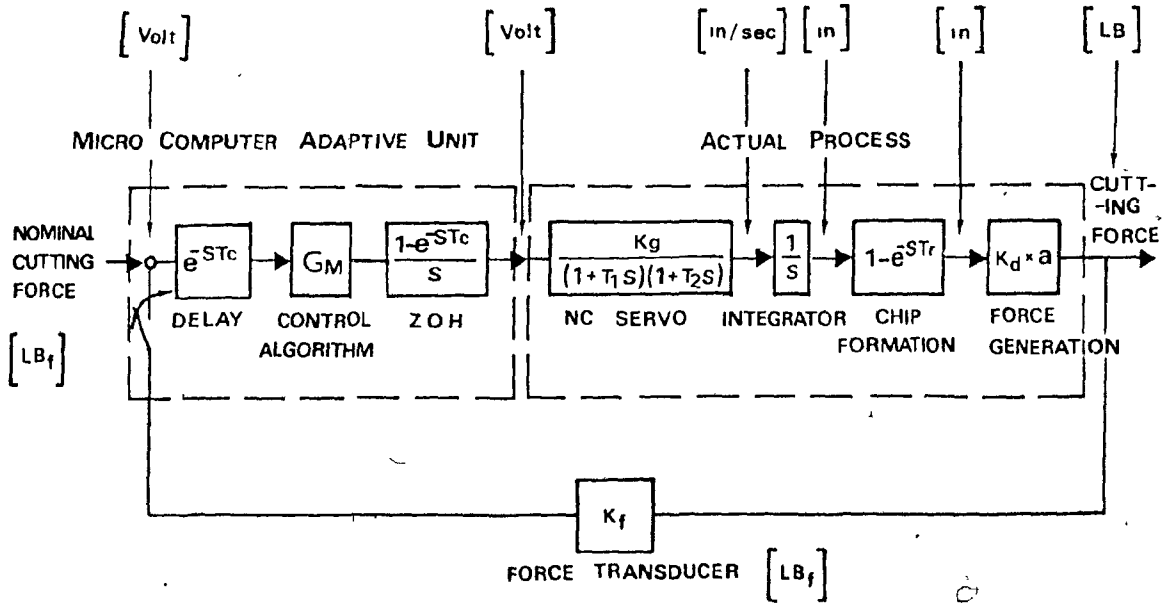

FIG J-1 RE-DRAW OF THE CLOSED LOOP WITH PROPER UNITS AT DIFFERENT STAGES

Though unit of Fnom is in lbf, it is converted and stored in the computer as a binary number. This number represents a certain voltage according to the range of A/D converter. For the feed back signal, same token is applied. Therefore, since the computer adaptive unit is also a voltage signal, there is

no units or dimensions changes as far as it is concerned. Hence, the time delay and ZOH have simply the unit of time.

To find T_c, a sinusoidal signal is input to the micro-computer adaptive unit only. By an osciloscope measuring at the D/A converter output, the sampling time is recorded. It is found that, T_c, is approximately 50 milli-seconds or 0.05 second.

Through the NC servo, the feedrate override signal, 0.0 to 5.0 volts range, is converted to a tool velocity command which also depends on the program feedrate and RPM. Hence, the K_g has a value of:

$$K_g = \frac{\text{FEED [in/rev]} * \text{RPM [rev/min]} * 1/60 \text{ [min/sec]}}{5 \text{ [volt]}}$$

For the experiment to carried out, the selected feed and RPM are 0.015 in/rev and 69 RPM respectively, so by substituting these values into the expression of K_g, K_g becomes:

$$K_g = \frac{0.015 \text{ [in/rev]} * 69 \text{ [rev/min]} * 1/60 \text{ [min/sec]}}{5 \text{ [volt]}}$$

$$K_g = 0.00345 \text{ [in/sec.volt]}$$

For integrator, 1/s, the unit is second.

The delay function from the chip formation is a pure time delay unit (T_r) and since the selected RPM equals to 69, the

T_r = 60/69 [sec/min]/[rev/min] ≈ 0.87 [sec/rev]

From the chip thickness and depth-of-cut, the cutting force is generated. Hence, K_d converts a chip cross-sectional area [in^2] into a force unit [lbf]. Hence K_d should have a unit of [lbf/in^2] by itself. Also as mentioned previously, K_d represents the properties of the workpiece material as well. From the reference "Machining Data Handbook" [28], the specific cutting energy for aluminum with a carbide tool is found to be 0.3 hp per cub inch per minute, i.e. 0.3 [hp]/[in^3 /min]. Hence K_d equals to:

$$K_d = 0.3 \left[\frac{hp}{in^3/min}\right] * 550 \left[\frac{lbf.ft}{hp.sec}\right] * 60 \left[\frac{sec}{min}\right] * 12 \left[\frac{in}{ft}\right].$$

$$K_d = 118800 \left[\frac{lbf}{in^2}\right]$$

Furthermore, since the force transducer transposes 1.0 lbf of measured cutting force to 1.0 lbf force signal, so the dimension for K_f is unity.

APPENDIX K

PROGRAM FOR FINDING THE MAGNITUDE AND PHASE ANGLE OF THE CONTINUOUS MODE OUTPUT ; THE RESULTS ARE COLLECTED IN TABLE K.1

Depth-Of-Cut					
0.03	[in]	0.06	[in]	0.09	[in]
Kpro	Kint	Kpro	Kint	Kpro	Kint
0.0000	0.423	0.0000	0.211	0.0000	0.141
0.0500	0.575	0.0250	0.290	0.0125	0.180
0.1000	0.690	0.0687	0.370	0.0250	0.214
0.1500	0.760	0.1375	0.397	0.0500	0.255
0.2750	0.800	0.1750	0.379	0.0750	0.270
0.3500	0.750	0.2063	0.345	0.1000	0.260
0.4000	0.695	0.2250	0.300	0.1250	0.238
0.4500	0.620	0.2500	0.259	0.1400	0.223
0.5000	0.520	0.2750	0.212	0.1500	0.200
0.5500	0.423	0.2900	0.200	0.1750	0.163
0.6000	0.357	0.3063	0.175	0.1930	0.141
0.6500	0.225	0.3069	0.140	0.2000	0.119
0.7000	0.097	0.3255	0.105	0.2100	0.098
0.7372	0.000	0.3455	0.070	0.2250	0.065
/	/	0.3685	0.035	0.2457	0.000
/	/	0.3686	0.000	/	/

TABLE K.1 COLLECTIVE RESULTS OF APPENDIX K

```
*BATCH WATFIV ME39001 HEMAN HUI
**********

$WATFIV ,NOEXT
C  ***********************************************************
C  *                                                         *
C  *     THIS PROGRAM FINDS THE FREQUENCY RESPONSE OF THE    *
C  *                                                         *
C  *     TRANSFER FUNCTION OF PROJECT IN CONTINUOUS MODE     *
C  *                                                         *
C  ***********************************************************
C
      REAL START,END,DELTA,KD,KG,TR,TC,W, IMAG,REALG,ANGG,MAGG
      REAL KPRO,KINT,DC
      INTEGER J
      COMPLEX G,S,G1,G2
999   READ(5,*,END=99) DC,KPRO,KINT,START,END,DELTA
      WRITE(6,70) DC,KPRO,KINT
70    FORMAT('0',/,10X,'DEPTH OF CUT=',F6.2,5X,'KPRO=',F8.5,5X,'KINT=',
     $F8.5)
      WRITE(6,20) START,END,DELTA
20    FORMAT('0',10X,'THE STARTING, ENDING, & DECREMENT FREQ. ARE:',
     $3F10.5)
      WRITE(6,60)
60    FORMAT(' ',//,T2,'FREQ(RAD/SEC)',T22,'REAL(G)',T37,'IMAG(G)',T53,
     $'MAG(G)',T66,'ANGLE(C)',/)
C
      KD = 118800.0
      KF = 1.0
      KG = 0.00345
      TR = 0.869
      TC = 0.053
      W = START
      J = (END-START)/DELTA+3
C
      DO 30 I=1,J
      S = CMPLX(0.0,W)
      G = CEXP(-S*TC)
      G1 = G*KPRO
      G2 = (G*KINT)/S
      G = G1+G2
      G = G*(1-CEXP(-S*TR))/S
      G = G*KG*KD*DC*KF
      REALG = REAL(G)
      IMAG = AIMAG(G)
      MAGG = CABS(G)
      ANGG = ATAN2(IMAG,REALG)*180.0/3.14159
      WRITE(6,40) W,REALG,IMAG,MAGG,ANGG
40    FORMAT(T2,F10.5,T20,F10.5,T35,F10.5,T50,F10.5,T65,F10.5)
      W = W+DELTA
30    CONTINUE
      GOTO 999
99    WRITE(6,50)
50    FORMAT('1')
      STOP
      END

$DATA
```

DEPTH OF CUT= 0.03 KPRO= 0.00000 KINT= 0.42330

THE STARTING, ENDING, & DECREMENT FREQ. ARE: 3.10000 3.30000 0.05000

FREQ(RAD/SEC)	REAL(G)	IMAG(G)	MAG(G)	ANGLE(G)
3.10000	-1.05431	-0.06285	1.05618	-176.58820
3.15000	-1.02710	-0.03614	1.02773	-177.98480
3.20000	-1.00001	-0.01080	1.00007	-179.38140
3.25000	-0.97306	0.01321	0.97315	179.22210
3.30000	-0.94626	0.03593	0.94694	177.82550
3.35000	-0.91963	0.05739	0.92142	176.42890

DEPTH OF CUT= 0.03 KPRO= 0.05000 KINT= 0.57500

THE STARTING, ENDING, & DECREMENT FREQ. ARE: 3.75000 3.95000 0.05000

FREQ(RAD/SEC)	REAL(G)	IMAG(G)	MAG(G)	ANGLE(G)
3.75000	-1.05405	-0.06108	1.05582	-176.68340
3.80000	-1.02727	-0.03848	1.02799	-177.85500
3.85000	-1.00063	-0.01699	1.00077	-179.02730
3.90000	-0.97415	0.00340	0.97416	179.79990
3.95000	-0.94785	0.02273	0.94812	178.62640
4.00000	-0.92173	0.04101	0.92265	177.45230

DEPTH OF CUT= 0.03 KPRO= 0.10000 KINT= 0.69000

THE STARTING, ENDING, & DECREMENT FREQ. ARE: 4.20000 4.40000 0.05000

FREQ(RAD/SEC)	REAL(G)	IMAG(G)	MAG(G)	ANGLE(G)
4.20000	-1.08727	-0.07633	1.08994	-175.98440
4.25000	-1.06023	-0.05410	1.06161	-177.07910
4.30000	-1.03327	-0.03291	1.03379	-178.17550
4.35000	-1.00639	-0.01275	1.00647	-179.27410
4.40000	-0.97962	0.00640	0.97964	179.62560
4.45000	-0.95296	0.02457	0.95327	178.52310

DEPTH OF CUT= 0.03 KPRO= 0.15000 KINT= 0.76000

THE STARTING, ENDING, & DECREMENT FREQ. ARE: 4.65000 4.85000 0.05000

FREQ(RAD/SEC)	REAL(G)	IMAG(G)	MAG(G)	ANGLE(G)
4.65000	-1.05546	-0.04908	1.05659	-177.33790
4.70000	-1.02781	-0.02819	1.02819	-178.42900
4.75000	-1.00015	-0.00832	1.00019	-179.52310
4.80000	-0.97252	0.01053	0.97257	179.37980
4.85000	-0.94492	0.02838	0.94534	178.27970
4.90000	-0.91737	0.04524	0.91848	177.17680
4.95000	-0.88989	0.06112	0.89199	176.07100

DEPTH OF CUT= 0.03 KPRO= 0.27500 KINT= 0.80000

THE STARTING, ENDING, & DECREMENT FREQ. ARE: 5.30000 5.50000 0.05000

FREQ(RAD/SEC)	REAL(G)	IMAG(G)	MAG(G)	ANGLE(G)
5.30000	-1.08095	-0.06044	1.08264	-176.79970
5.35000	-1.04841	-0.03716	1.04907	-177.96990
5.40000	-1.01566	-0.01519	1.01577	-179.14340
5.45000	-0.98274	0.00549	0.98276	179.68000
5.50000	-0.94970	0.02486	0.95002	178.50030
5.55000	-0.91656	0.04294	0.91756	177.31750

DEPTH OF CUT= 0.03 KPRO= 0.35000 KINT= 0.75000

THE STARTING, ENDING, & DECREMENT FREQ. ARE: 5.60000 5.80000 0.05000

FREQ(RAD/SEC)	REAL(G)	IMAG(G)	MAG(G)	ANGLE(G)
5.60000	-1.06955	-0.04937	1.07069	-177.35700
5.65000	-1.03257	-0.02552	1.03289	-178.58410
5.70000	-0.99536	-0.00323	0.99536	-179.81390
5.75000	-0.95795	0.01749	0.95811	178.95390
5.80000	-0.92040	0.03666	0.92113	177.71910
5.85000	-0.88277	0.05427	0.88444	176.48190

DEPTH OF CUT= 0.03 KPRO= 0.40000 KINT= 0.69500

THE STARTING, ENDING, & DECREMENT FREQ. ARE: 5.75000 5.95000 0.05000

FREQ(RAD/SEC)	REAL(G)	IMAG(G)	MAG(G)	ANGLE(G)
5.75000	-1.07078	-0.04824	1.07186	-177.42070
5.80000	-1.03056	-0.02374	1.03083	-178.68030
5.85000	-0.99009	-0.00100	0.99009	-179.94220
5.90000	-0.94942	0.01999	0.94963	178.79390
5.95000	-0.90862	0.03923	0.90946	177.52790
6.00000	-0.86775	0.05673	0.86960	176.25980

DEPTH OF CUT= 0.03 KPRO= 0.45000 KINT= 0.62000

THE STARTING, ENDING, & DECREMENT FREQ. ARE: 5.85000 6.05000 0.05000

FREQ(RAD/SEC)	REAL(G)	IMAG(G)	MAG(G)	ANGLE(G)
5.85000	-1.09509	-0.06404	1.09696	-176.65310
5.90000	-1.05171	-0.03781	1.05239	-177.94120
5.95000	-1.00802	-0.01353	1.00811	-179.23110
6.00000	-0.96411	0.00880	0.96415	179.47730
6.05000	-0.92003	0.02917	0.92049	178.18420
6.10000	-0.87587	0.04760	0.87716	176.88920

DEPTH OF CUT= 0.03 KPRO= 0.50000 KINT= 0.52000

THE STARTING, ENDING, & DECREMENT FREQ. ARE: 5.95000 6.15000 0.05000

FREQ(RAD/SEC)	REAL(G)	IMAG(G)	MAG(G)	ANGLE(G)
5.95000	-1.10524	-0.07519	1.10779	-176.10810
6.00000	-1.05860	-0.04763	1.05967	-177.42370
6.05000	-1.01162	-0.02224	1.01186	-178.74050
6.10000	-0.96439	0.00099	0.96439	179.94130
6.15000	-0.91700	0.02206	0.91727	178.62200
6.20000	-0.86953	0.04099	0.87049	177.30140

DEPTH OF CUT= 0.03 KPRO= 0.55000 KINT= 0.42330

THE STARTING, ENDING, & DECREMENT FREQ. ARE: 6.05000 6.25000 0.05000

FREQ(RAD/SEC)	REAL(G)	IMAG(G)	MAG(G)	ANGLE(G)
6.05000	-1.10341	-0.07258	1.10580	-176.23660
6.10000	-1.05309	-0.04461	1.05403	-177.57430
6.15000	-1.00245	-0.01902	1.00263	-178.91300
6.20000	-0.95159	0.00420	0.95160	179.74740
6.25000	-0.90060	0.02505	0.90095	178.40690
6.30000	-0.84958	0.04355	0.85070	177.06550

DEPTH OF CUT= 0.03 KPRO= 0.60000 KINT= 0.35700

THE STARTING, ENDING, & DECREMENT FREQ. ARE: 6.15000 6.35000 0.05000

FREQ(RAD/SEC)	REAL(G)	IMAG(G)	MAG(G)	ANGLE(G)
6.15000	-1.08917	-0.05125	1.09038	-177.30600
6.20000	-1.03465	-0.02423	1.03493	-178.65820
6.25000	-0.97990	0.00019	0.97990	179.98890
6.30000	-0.92502	0.02204	0.92529	178.63520
6.35000	-0.87013	0.04133	0.87111	177.28090
6.40000	-0.81531	0.05807	0.81738	175.92590
6.45000	-0.76068	0.07230	0.76411	174.57030

DEPTH OF CUT= 0.03 KPRO= 0.65000 KINT= 0.22500

THE STARTING, ENDING, & DECREMENT FREQ. ARE: 6.20000 6.40000 0.05000

FREQ(RAD/SEC)	REAL(G)	IMAG(G)	MAG(G)	ANGLE(G)
6.20000	-1.11555	-0.07073	1.11778	-176.37210
6.25000	-1.05757	-0.04168	1.05839	-177.74310
6.30000	-0.99934	-0.01544	0.99946	-179.11460
6.35000	-0.94095	0.00799	0.94098	179.51370
6.40000	-0.88251	0.02864	0.88298	178.14140
6.45000	-0.82415	0.04653	0.82547	176.76880

DEPTH OF CUT= 0.03 KPRC= 0.70000 KINT= 0.09700

THE STARTING, ENDING, & DECREMENT FREQ. ARE: 6.25000 6.45000 0.05000

FREQ(RAD/SEC)	REAL(G)	IMAG(G)	MAG(G)	ANGLE(G)
6.25000	-1.13535	-0.08251	1.13834	-175.84320
6.30000	-1.07372	-0.05196	1.07497	-177.22970
6.35000	-1.01180	-0.02444	1.01210	-178.61630
6.40000	-0.94973	0.00005	0.94973	179.99690
6.45000	-0.88763	0.02154	0.88789	178.60990
6.50000	-0.82561	0.04005	0.82658	177.22290

DEPTH OF CUT= 0.03 KPRC= 0.73720 KINT= 0.00000

THE STARTING, ENDING, & DECREMENT FREQ. ARE: 6.30000 6.50000 0.05000

FREQ(RAD/SEC)	REAL(G)	IMAG(G)	MAG(G)	ANGLE(G)
6.30000	-1.12903	-0.07955	1.13183	-175.96970
6.35000	-1.06450	-0.04897	1.06563	-177.36620
6.40000	-0.99974	-0.02159	0.99997	-178.76280
6.45000	-0.93485	0.00260	0.93486	179.84070
6.50000	-0.86999	0.02363	0.87031	178.44410
6.55000	-0.80527	0.04153	0.80634	177.04760

DEPTH OF CUT= 0.06 KPRO= 0.00000 KINT= 0.21163

THE STARTING, ENDING, & DECREMENT FREQ. ARE: 3.10000 3.30000 0.05000

FREQ(RAD/SEC)	REAL(G)	IMAG(G)	MAG(G)	ANGLE(G)
3.10000	-1.05421	-0.06285	1.05608	-176.58820
3.15000	-1.02700	-0.03614	1.02764	-177.98480
3.20000	-0.99992	-0.01080	0.99997	-179.38140
3.25000	-0.97296	0.01321	0.97305	179.22210
3.30000	-0.94617	0.03593	0.94685	177.82550
3.35000	-0.91954	0.05739	0.92133	176.42890

DEPTH OF CUT= 0.06 KPRO= 0.02500 KINT= 0.29000

THE STARTING, ENDING, & DECREMENT FREQ. ARE: 3.75000 3.95000 0.05000

FREQ(RAD/SEC)	REAL(G)	IMAG(G)	MAG(G)	ANGLE(G)
3.75000	-1.06249	-0.05886	1.06412	-176.82910
3.80000	-1.03542	-0.03612	1.03605	-178.00240
3.85000	-1.00850	-0.01450	1.00860	-179.17610
3.90000	-0.98174	0.00601	0.98176	179.64950
3.95000	-0.95516	0.02544	0.95550	178.47460
4.00000	-0.92877	0.04382	0.92981	177.29900

DEPTH OF CUT= 0.06 KPRO= 0.06875 KINT= 0.37000

THE STARTING, ENDING, & DECREMENT FREQ. ARE: 4.55000 4.75000 0.05000

FREQ(RAD/SEC)	REAL(G)	IMAG(G)	MAG(G)	ANGLE(G)
4.55000	-1.05583	-0.05761	1.05740	-176.87670
4.60000	-1.02869	-0.03657	1.02934	-177.96430
4.65000	-1.00156	-0.01653	1.00170	-179.05470
4.70000	-0.97446	0.00251	0.97446	179.85220
4.75000	-0.94740	0.02057	0.94762	178.75620
4.80000	-0.92040	0.03765	0.92117	177.65760

DEPTH OF CUT= 0.06 KPFC= 0.13750 KINT= 0.39175

THE STARTING, ENDING, & DECREMENT FREQ. ARE: 5.30000 5.50000 0.05000

FREQ(RAD/SEC)	REAL(G)	IMAG(G)	MAG(G)	ANGLE(G)
5.30000	-1.07527	-0.06956	1.07751	-176.29880
5.35000	-1.04315	-0.04606	1.04417	-177.47170
5.40000	-1.01082	-0.02386	1.01110	-178.64770
5.45000	-0.97830	-0.00296	0.97830	-179.82680
5.50000	-0.94563	0.01666	0.94577	178.99090
5.55000	-0.91285	0.03498	0.91352	177.80550

DEPTH OF CUT= 0.06 KPRO= 0.17500 KINT= 0.37900

THE STARTING, ENDING, & DECREMENT FREQ. ARE: 5.55000 5.75000 0.05000

FREQ(RAD/SEC)	REAL(G)	IMAG(G)	MAG(G)	ANGLE(G)
5.55000	-1.10802	-0.07092	1.11029	-176.33760
5.60000	-1.07118	-0.04563	1.07215	-177.56070
5.65000	-1.03405	-0.02191	1.03428	-178.78640
5.70000	-0.99668	0.00026	0.99668	179.98510
5.75000	-0.95913	0.02086	0.95936	178.75420
5.80000	-0.92145	0.03990	0.92232	177.52080

DEPTH OF CUT= 0.06 KPRO= 0.20625 KINT= 0.34500

THE STARTING, ENDING, & DECREMENT FREQ. ARE: 5.75000 5.95000 0.05000

FREQ(RAD/SEC)	REAL(G)	IMAG(G)	MAG(G)	ANGLE(G)
5.75000	-1.10028	-0.06099	1.10197	-176.82740
5.80000	-1.05925	-0.03530	1.05984	-178.09140
5.85000	-1.01793	-0.01142	1.01800	-179.35750
5.90000	-0.97638	0.01066	0.97644	179.37440
5.95000	-0.93467	0.03094	0.93519	178.10430
6.00000	-0.89287	0.04942	0.89423	176.83220

DEPTH OF CUT= 0.06 KPRO= 0.22500 KINT= 0.30000

THE STARTING, ENDING, & DECREMENT FREQ. ARE: 5.85000 6.05000 0.05000

FREQ(RAD/SEC)	REAL(G)	IMAG(G)	MAG(G)	ANGLE(G)
5.85000	-1.09277	-0.07182	1.09513	-176.23990
5.90000	-1.04968	-0.04526	1.05066	-177.53130
5.95000	-1.00627	-0.02065	1.00648	-178.82430
6.00000	-0.96261	0.00200	0.96261	179.88110
6.05000	-0.91877	0.02270	0.91905	178.58490
6.10000	-0.87483	0.04145	0.87581	177.28700

DEPTH OF CUT= 0.06 KPRO= 0.25000 KINT= 0.25900

THE STARTING, ENDING, & DECREMENT FREQ. ARE: 5.85000 6.05000 0.05000

FREQ(RAD/SEC)	REAL(G)	IMAG(G)	MAG(G)	ANGLE(G)
5.85000	-1.19697	-0.13758	1.20485	-173.44300
5.90000	-1.15127	-0.10566	1.15611	-174.75620
5.95000	-1.10507	-0.07590	1.10767	-176.07070
6.00000	-1.05845	-0.04831	1.05955	-177.38660
6.05000	-1.01149	-0.02289	1.01175	-178.70370
6.10000	-0.96429	0.00037	0.96429	179.97790

DEPTH OF CUT= 0.06 KPRO= 0.27500 KINT= 0.21163

THE STARTING, ENDING, & DECREMENT FREQ. ARE: 6.05000 6.15000 0.05000

FREQ(RAD/SEC)	REAL(G)	IMAG(G)	MAG(G)	ANGLE(G)
6.05000	-1.10341	-0.07260	1.10580	-176.23590
6.10000	-1.05308	-0.04462	1.05403	-177.57360
6.15000	-1.00245	-0.01903	1.00263	-178.91240
6.20000	-0.95159	0.00418	0.95160	179.74800

DEPTH OF CUT= 0.06 KPRO= 0.29000 KINT= 0.20000

THE STARTING, ENDING, & DECREMENT FREQ. ARE: 6.10000 6.30000 0.05000

FREQ(RAD/SEC)	REAL(G)	IMAG(G)	MAG(G)	ANGLE(G)
6.10000	-1.10811	-0.06130	1.10981	-176.83370
6.15000	-1.05517	-0.03356	1.05571	-178.17820
6.20000	-1.00197	-0.00833	1.00200	-179.52370
6.25000	-0.94859	0.01440	0.94869	179.13020
6.30000	-0.89513	0.03465	0.89580	177.78320
6.35000	-0.84170	0.05243	0.84333	176.43550

DEPTH OF CUT= 0.06 KPRO= 0.30630 KINT= 0.17500

THE STARTING, ENDING, & DECREMENT FREQ. ARE: 6.15000 6.35000 0.05000

FREQ(RAD/SEC)	REAL(G)	IMAG(G)	MAG(G)	ANGLE(G)
6.15000	-1.11143	-0.05655	1.11287	-177.08740
6.20000	-1.05590	-0.02873	1.05629	-178.44140
6.25000	-1.00012	-0.00356	1.00012	-179.79610
6.30000	-0.94420	0.01898	0.94439	178.84860
6.35000	-0.88825	0.03890	0.88910	177.49260
6.40000	-0.83237	0.05622	0.83427	176.13600
6.45000	-0.77666	0.07097	0.77990	174.77880

DEPTH OF CUT= 0.06 KPRO= 0.30690 KINT= 0.14000

THE STARTING, ENDING, & DECREMENT FREQ. ARE: 6.15000 6.35000 0.05000

FREQ(RAD/SEC)	REAL(G)	IMAG(G)	MAG(G)	ANGLE(G)
6.15000	-1.11064	-0.07724	1.11332	-176.02200
6.20000	-1.05564	-0.04822	1.05674	-177.38450
6.25000	-1.00034	-0.02187	1.00058	-178.74750
6.30000	-0.94484	0.00183	0.94484	179.88900
6.35000	-0.88925	0.02290	0.88954	178.52490
6.40000	-0.83368	0.04135	0.83470	177.16040
6.45000	-0.77822	0.05721	0.78032	175.79530

DEPTH OF CUT= 0.06 KPRO= 0.32550 KINT= 0.10550

THE STARTING, ENDING, & DECREMENT FREQ. ARE: 6.20000 6.40000 0.05000

FREQ(RAD/SEC)	REAL(G)	IMAG(G)	MAG(G)	ANGLE(G)
6.20000	-1.11679	-0.07478	1.11929	-176.16900
6.25000	-1.05885	-0.04546	1.05982	-177.54160
6.30000	-1.00063	-0.01896	1.00081	-178.91470
6.35000	-0.94224	0.00474	0.94226	179.71190
6.40000	-0.88381	0.02564	0.88418	178.33820
6.45000	-0.82543	0.04378	0.82659	176.96400

DEPTH OF CUT= 0.06 KPRO= 0.34550 KINT= 0.07000

THE STARTING, ENDING, & DECREMENT FREQ. ARE: 6.25000 6.45000 0.05000

FREQ(RAD/SEC)	REAL(G)	IMAG(G)	MAG(G)	ANGLE(G)
6.25000	-1.12184	-0.07000	1.12402	-176.42980
6.30000	-1.06067	-0.04053	1.06144	-177.81160
6.35000	-0.99926	-0.01406	0.99936	-179.19360
6.40000	-0.93773	0.00943	0.93777	179.42410
6.45000	-0.87619	0.02996	0.87670	178.04150
6.50000	-0.81478	0.04757	0.81617	176.65880

DEPTH OF CUT= 0.06 KPRO= 0.36850 KINT= 0.03500

THE STARTING, ENDING, & DECREMENT FREQ. ARE: 6.30000 6.50000 0.05000

FREQ(RAD/SEC)	REAL(G)	IMAG(G)	MAG(G)	ANGLE(G)
6.30000	-1.12992	-0.06251	1.13165	-176.83340
6.35000	-1.06495	-0.03304	1.06546	-178.22320
6.40000	-0.99979	-0.00675	0.99981	-179.61300
6.45000	-0.93456	0.01636	0.93471	178.99700
6.50000	-0.86941	0.03633	0.87017	177.60690
6.55000	-0.80445	0.05320	0.80621	176.21680

DEPTH OF CUT= 0.06 KPFO= 0.36860 KINI= 0.00000

THE STARTING, ENDING, & DECREMENT FREQ. ARE: 6.30000 6.50000 0.05000

FREQ(RAD/SEC)	REAL(G)	IMAG(G)	MAG(G)	ANGLE(G)
6.30000	-1.12903	-0.07955	1.13183	-175.96970
6.35000	-1.06450	-0.04897	1.06563	-177.36620
6.40000	-0.99974	-0.02159	0.99997	-178.76280
6.45000	-0.93486	0.00260	0.93486	179.84070
6.50000	-0.86999	0.02363	0.87031	178.44410
6.55000	-0.80527	0.04153	0.80634	177.04760

DEPTH OF CUT= 0.09 KPRO= 0.00000 KINT= 0.14110

THE STARTING, ENDING, & DECREMENT FREQ. ARE: 3.10000 3.30000 0.05000

FREQ(RAD/SEC)	REAL(G)	IMAG(G)	MAG(G)	ANGLE(G)
3.10000	-1.05431	-0.06285	1.05618	-176.58820
3.15000	-1.02710	-0.03614	1.02773	-177.98480
3.20000	-1.00001	-0.01080	1.00007	-179.38140
3.25000	-0.97306	0.01321	0.97315	179.22210
3.30000	-0.94626	0.03593	0.94694	177.82550
3.35000	-0.91963	0.05739	0.92142	176.42890

DEPTH OF CUT= 0.09 KPRO= 0.01250 KINT= 0.18000

THE STARTING, ENDING, & DECREMENT FREQ. ARE: 3.60000 3.80000 0.05000

FREQ(RAD/SEC)	REAL(G)	IMAG(G)	MAG(G)	ANGLE(G)
3.60000	-1.05421	-0.06415	1.05616	-176.51780
3.65000	-1.02736	-0.04077	1.02817	-177.72740
3.70000	-1.00067	-0.01857	1.00084	-178.93710
3.75000	-0.97414	0.00250	0.97414	179.85280
3.80000	-0.94778	0.02246	0.94805	178.64240
3.85000	-0.92162	0.04134	0.92254	177.43170

DEPTH OF CUT= 0.09 KPRO= 0.02500 KINT= 0.21400

THE STARTING, ENDING, & DECREMENT FREQ. ARE: 4.00000 4.20000 0.05000

FREQ(RAD/SEC)	REAL(G)	IMAG(G)	MAG(G)	ANGLE(G)
4.00000	-1.07216	-0.06219	1.07396	-176.68060
4.05000	-1.04513	-0.04009	1.04587	-177.80310
4.10000	-1.01817	-0.01907	1.01834	-178.92680
4.15000	-0.99136	0.00090	0.99136	179.94830
4.20000	-0.96471	0.01984	0.96492	178.82210
4.25000	-0.93822	0.03777	0.93898	177.69460

DEPTH OF CUT= 0.09 KPRC= 0.05000 KINT= 0.25500

THE STARTING, ENDING, & DECREMENT FREQ. ARE: 4.65000 4.85000 0.05000

FREQ(RAD/SEC)	REAL(G)	IMAG(G)	MAG(G)	ANGLE(G)
4.65000	-1.05939	-0.04579	1.06037	-177.52490
4.70000	-1.03153	-0.02492	1.03183	-178.61620
4.75000	-1.00368	-0.00507	1.00370	-179.71050
4.80000	-0.97586	0.01376	0.97595	179.19230
4.85000	-0.94807	0.03158	0.94859	178.09210
4.90000	-0.92034	0.04841	0.92161	176.98910
4.95000	-0.89268	0.06425	0.89499	175.88320

DEPTH OF CUT= 0.09 KPRC= 0.07500 KINT= 0.27000

THE STARTING, ENDING, & DECREMENT FREQ. ARE: 5.10000 5.30000 0.05000

FREQ(RAD/SEC)	REAL(G)	IMAG(G)	MAG(G)	ANGLE(G)
5.10000	-1.06019	-0.04315	1.06107	-177.66930
5.15000	-1.02979	-0.02152	1.03001	-178.80290
5.20000	-0.99927	-0.00105	0.99927	-179.94000
5.25000	-0.96867	0.01827	0.96884	178.91970
5.30000	-0.93800	0.03643	0.93871	177.77590
5.35000	-0.90731	0.05344	0.90889	176.62900

DEPTH OF CUT= 0.09 KPRC= 0.10000 KINT= 0.26000

THE STARTING, ENDING, & DECREMENT FREQ. ARE: 5.40000 5.60000 0.05000

FREQ(RAD/SEC)	REAL(G)	IMAG(G)	MAG(G)	ANGLE(G)
5.40000	-1.08078	-0.06533	1.08275	-176.54110
5.45000	-1.04709	-0.04147	1.04791	-177.73190
5.50000	-1.01316	-0.01900	1.01334	-178.92570
5.55000	-0.97903	0.00209	0.97903	179.87760
5.60000	-0.94475	0.02180	0.94500	178.67790
5.65000	-0.91036	0.04014	0.91124	177.47530
5.70000	-0.87590	0.05710	0.87776	176.26990

DEPTH OF CUT= 0.09 KPRO= 0.12500 KINT= 0.23750

THE STARTING, ENDING, & DECREMENT FREQ. ARE: 5.65000 5.85000 0.05000

FREQ(RAD/SEC)	REAL(G)	IMAG(G)	MAG(G)	ANGLE(G)
5.65000	-1.08953	-0.06853	1.09169	-176.40100
5.70000	-1.05136	-0.04323	1.05224	-177.64560
5.75000	-1.01288	-0.01958	1.01307	-178.89260
5.80000	-0.97417	0.00241	0.97417	179.85820
5.85000	-0.93527	0.02275	0.93555	178.60670
5.90000	-0.89625	0.04144	0.89721	177.35280
5.95000	-0.85716	0.05848	0.85916	176.09690

DEPTH OF CUT= 0.09 KPRO= 0.14000 KINT= 0.22300

THE STARTING, ENDING, & DECREMENT FREQ. ARE: 5.75000 5.95000 0.05000

FREQ(RAD/SEC)	REAL(G)	IMAG(G)	MAG(G)	ANGLE(G)
5.75000	-1.11532	-0.07621	1.11792	-176.09100
5.80000	-1.07410	-0.04952	1.07524	-177.36040
5.85000	-1.03255	-0.02466	1.03285	-178.63180
5.90000	-0.99074	-0.00164	0.99074	-179.90520
5.95000	-0.94873	0.01955	0.94893	178.81950
6.00000	-0.90659	0.03891	0.90743	177.54230

DEPTH OF CUT= 0.09 KPRO= 0.15000 KINT= 0.20000

THE STARTING, ENDING, & DECREMENT FREQ. ARE: 5.85000 6.05000 0.05000

FREQ(RAD/SEC)	REAL(G)	IMAG(G)	MAG(G)	ANGLE(G)
5.85000	-1.09277	-0.07182	1.09513	-176.23990
5.90000	-1.04968	-0.04526	1.05066	-177.53130
5.95000	-1.00627	-0.02065	1.00648	-178.82430
6.00000	-0.96261	0.00200	0.96261	179.88110
6.05000	-0.91877	0.02270	0.91905	178.58490
6.10000	-0.87483	0.04145	0.87581	177.28700

DEPTH OF CUT= 0.09 KPRO= 0.17500 KINT= 0.16250

THE STARTING, ENDING, & DECREMENT FREQ. ARE: 6.00000 6.20000 0.05000

FREQ(RAD/SEC)	REAL(G)	IMAG(G)	MAG(G)	ANGLE(G)
6.00000	-1.10715	-0.06990	1.10935	-176.38750
6.05000	-1.05851	-0.04228	1.05936	-177.71260
6.10000	-1.00957	-0.01694	1.00971	-179.03870
6.15000	-0.96039	0.00613	0.96041	179.63410
6.20000	-0.91108	0.02695	0.91148	178.30580
6.25000	-0.86172	0.04552	0.86292	176.97630

DEPTH OF CUT= 0.09 KPRO= 0.19300 KINT= 0.14110

THE STARTING, ENDING, & DECREMENT FREQ. ARE: 6.10000 6.30000 0.05000

FREQ(RAD/SEC)	REAL(G)	IMAG(G)	MAG(G)	ANGLE(G)
6.10000	-1.10745	-0.05382	1.10876	-177.21760
6.15000	-1.05437	-0.02652	1.05470	-178.55920
6.20000	-1.00103	-0.00172	1.00103	-179.90160
6.25000	-0.94754	0.02059	0.94776	178.75530
6.30000	-0.89400	0.04042	0.89491	177.41110
6.35000	-0.84050	0.05780	0.84248	176.06620

DEPTH OF CUT= 0.09 KPRO= 0.20000 KINT= 0.11850

THE STARTING, ENDING, & DECREMENT FREQ. ARE: 6.15000 6.35000 0.05000

FREQ(RAD/SEC)	REAL(G)	IMAG(G)	MAG(G)	ANGLE(G)
6.15000	-1.08911	-0.05169	1.09033	-177.28280
6.20000	-1.03460	-0.02465	1.03489	-178.63530
6.25000	-0.97986	-0.00020	0.97986	-179.98850
6.30000	-0.92500	0.02167	0.92525	178.65770
6.35000	-0.87011	0.04098	0.87108	177.30320
6.40000	-0.81531	0.05775	0.81735	175.94810
6.45000	-0.76068	0.07201	0.76408	174.59230

DEPTH OF CUT= 0.09 KPRO= 0.21000 KINT= 0.09800

THE STARTING, ENDING, & DECREMENT FREQ. ARE: 6.15000 6.35000 0.05000

FREQ(RAD/SEC)	REAL(G)	IMAG(G)	MAG(G)	ANGLE(G)
6.15000	-1.14023	-0.07735	1.14285	-176.11920
6.20000	-1.08372	-0.04768	1.08477	-177.48090
6.25000	-1.02690	-0.02074	1.02711	-178.84320
6.30000	-0.96989	0.00349	0.96990	179.79400
6.35000	-0.91279	0.02501	0.91313	178.43070
6.40000	-0.85571	0.04384	0.85683	177.06690
6.45000	-0.79876	0.06002	0.80101	175.70260

DEPTH OF CUT= 0.09 KPRO= 0.22500 KINT= 0.06500

THE STARTING, ENDING, & DECREMENT FREQ. ARE: 6.25000 6.45000 0.05000

FREQ(RAD/SEC)	REAL(G)	IMAG(G)	MAG(G)	ANGLE(G)
6.25000	-1.09730	-0.05329	1.09859	-177.21950
6.30000	-1.03711	-0.02543	1.03742	-178.59510
6.35000	-0.97673	-0.00049	0.97673	-179.97110
6.40000	-0.91628	0.02155	0.91653	178.65280
6.45000	-0.85587	0.04072	0.85684	177.27610
6.50000	-0.79563	0.05704	0.79767	175.89930

DEPTH OF CUT= 0.09 KPRO= 0.23500 KINT= 0.03500

THE STARTING, ENDING, & DECREMENT FREQ. ARE: 6.25000 6.45000 0.05000

FREQ(RAD/SEC)	REAL(G)	IMAG(G)	MAG(G)	ANGLE(G)
6.25000	-1.14364	-0.08121	1.14652	-175.93820
6.30000	-1.08151	-0.05055	1.08269	-177.32390
6.35000	-1.01911	-0.02295	1.01937	-178.70980
6.40000	-0.95655	0.00160	0.95655	179.90420
6.45000	-0.89397	0.02313	0.89426	178.51790
6.50000	-0.83147	0.04166	0.83252	177.13150

DEPTH OF CUT= 0.09 KPFO= 0.24570 KINT= 0.00000

THE STARTING, ENDING, & DECREMENT FREQ. ARE: 6.30000 6.50000 0.05000

FREQ(RAD/SEC)	REAL(G)	IMAG(G)	MAG(G)	ANGLE(G)
6.30000	-1.12887	-0.07954	1.13167	-175.96970
6.35000	-1.06436	-0.04896	1.06549	-177.36620
6.40000	-0.99960	-0.02159	0.99983	-178.76280
6.45000	-0.93473	0.00260	0.93473	179.84070
6.50000	-0.86987	0.02363	0.87019	178.44410
6.55000	-0.80516	0.04153	0.80623	177.04760

APPENDIX L

DIGITAL COMPUTER SIMULATION LISTINGS AND OUTPUTS

This appendix is the listings of two digital computer simulation programs. It has two sub-appendices. The first one, Appendix L.1, is the program listing and simulation results of the closed-loop system shown in Fig. 4.11 . The second one, Appendix L.2, is the simulation of Fig. 4.13 .

APPENDIX L.1

SIMULATION LISTINGS AND RESULTS OF FIG. 4.11

```
                *** CONTINUOUS SYSTEM MODELING PROGRAM ***
                      *** VERSION 1.3 ***
*********************************************************************
*                                                                   *
*    SIMULATION OF THE ECCENTRIC TURNING WITH A P-I CONTROLLER      *
*                                                                   *
*    FOLLOWING FEATURES ARE ADDED IN THE PROGRAM:                   *
*                                                                   *
*    1) FIXED STEP SIZE INTEGRATION METHOD I.E. RKSFX               *
*    2) LIMIT ON FEEDRATE (0.01<FEED<0.0)IN/SEC                     *
*    3) NO PEAK-VALUE MEMORY (PVV)                                  *
*    4) ECCENTRICITY S.T. DEPTH OF CUT IS: 0.09>DC>0.03 IN          *
*    5) "RESET WINDUPCUT-OUT" FEATURE FOR SATURATED MODE            *
*    6) CONDITION IS SAME AS THAT IF REAL EXPERIMENT                *
*       ========================================                    *
*                                                                   *
*********************************************************************
INITIAL
      PARAM KPRO=0.05,KINT=0.003
      INCON LIMIC=0.0
      TIMER DELT=0.005,FINTIM=12.0,OUTDEL=0.05,PRDEL=0.05
      METHOD RKSFX
      PRTPLOT FORCE(FEDRAT,CHIP)
      LABEL SIMULATION OF FIG.4.11 WITH KPRO=0.05, KINT=0.003
      RPM = 60.0
      OMEGA = 2*3.1416*RPM/60.0
      TR = 60.0/RPM
      TC = 0.05
      KC = 0.00345
      KF = 1.0
      KD = 1.0E+06
      B = 0.06
      D = 0.03
      MSTART = 0.02
      C = 0.0
      SUM = 0.0
      TEST = 0.0
      FDIFFC = 0.0
      CLOSUM = 0.0
DYNAMIC
      FNOM = 20.0
      FEDRAT = FEED*KC
      POSIT = INTGRL(LIMIC,FEDRAT)
      DELAY = DELAY(100,TR,POSIT)
      MNOW = AMAX1(MSTART,DELAY)
      CHIPT = POSIT-MNOW
      CHIP = LIMIT(0.0,1000.0,CHIPT)
      FORCE = CHIP*KD*(B+D-COS(OMEGA*TIME))
      F = FORCE*KF
      FEED = ZHOLD(PULSE,ZOFIN)
      PULSE = IMPULS(0.0,TC)
   PROCEDURE  ZOFIN,FDIFF=DUMMY(KPRO,KINT,FNOM,F,PULSE, ...
              FDIFFO,SUM,C,CLOSUM,TEST)
      IF (PULSE.NE.1.0) GOTO 10
      IF (KEEP.NE.1.  ) GOTO 10
      FDIFF = FNOM-F
      SUM = SUM+KINT*FDIFFC
```

```
      TEST = (SUM-0.0)*(5.0-SUM)
      IF (TEST.LE.0.0) GOTO 11
      C = SUM+KPRO*EDIFF0
      CLDSUM = SUM
      GOTO 22
11    C = CLDSUM+KPRO*EDIFF0
      SUM = CLDSUM
22    ZOPIN = LIMIT(0.0,5.0,C)
      EDIFF0 = EDIFF
10    CONTINUE
   ENDPROCEDURE
TERMINAL
END
      PARAM KPRO=0.1,KINT=0.002
      RESET LABEL
      LABEL SIMULATION OF FIG.4.11 WITH KPRO=0.1, KINT=0.002
END
      PARAM  KPRO=0.35,KINT=0.003
      RESET LABEL
      LABEL SIMULATION OF FIG.4.11 WITH KPRO=0.35, KINT=0.003
END
STOP
```

SIMULATION OF FIG.4.11 WITH KPRO=0.1, KINT=0.002 PAGE 1

FORCE VERSUS TIME

TIME	FORCE	MINIMUM 0.0 / MAXIMUM 1.2775E+02	FEDRAT	CHIP
0.0	0.0	+	0.0	0.0
5.0000E-02	0.0	+	1.7250E-02	0.0
1.0000E-01	0.0	+	1.7250E-02	0.0
1.5000E-01	0.0	+	1.7250E-02	0.0
2.0000E-01	0.0	+	1.7250E-02	0.0
2.5000E-01	0.0	+	1.7250E-02	0.0
3.0000E-01	0.0	+	1.7250E-02	0.0
3.5000E-01	0.0	+	1.7250E-02	0.0
4.0000E-01	0.0	+	1.7250E-02	0.0
4.5000E-01	0.0	+	1.7250E-02	0.0
5.0000E-01	0.0	+	1.7250E-02	0.0
5.5000E-01	0.0	+	1.7250E-02	0.0
6.0000E-01	0.0	+	1.7250E-02	0.0
6.5000E-01	0.0	+	1.7250E-02	0.0
7.0000E-01	0.0	+	1.7250E-02	0.0
7.5000E-01	0.0	+	1.7250E-02	0.0
8.0000E-01	0.0	+	1.7250E-02	0.0
8.5000E-01	0.0	+	1.7250E-02	0.0
9.0000E-01	0.0	+	1.7250E-02	0.0
9.5000E-01	0.0	+	1.7250E-02	0.0
1.0000E+00	0.0	+	1.7250E-02	0.0
1.0500E+00	0.0	+	1.7250E-02	0.0
1.1000E+00	0.0	+	1.7250E-02	0.0
1.1500E+00	0.0	+	1.7250E-02	0.0
1.2000E+00	0.0	+	1.7250E-02	0.0
1.2500E+00	2.6831E+00	-+	1.7250E-02	6.9959E-04
1.3000E+00	5.5699E+00	--+	1.7250E-02	1.5621E-03
1.3500E+00	9.1070E+00	---+	1.7250E-02	2.4245E-03
1.4000E+00	1.4403E+01	-----+	1.7250E-02	3.2870E-03
1.4500E+00	2.2251E+01	---------+	1.7250E-02	4.1495E-03
1.5000E+00	3.2931E+01	------------+	1.7250E-02	5.0120E-03
1.5500E+00	4.6119E+01	------------------+	1.7250E-02	5.8745E-03
1.6000E+00	6.0887E+01	------------------------+	1.7250E-02	6.7369E-03
1.6500E+00	7.5828E+01	------------------------------+	1.7250E-02	7.5994E-03
1.7000E+00	8.9277E+01	----------------------------------+	1.7250E-02	8.4619E-03
1.7500E+00	9.9594E+01	---------------------------------------+	1.3642E-02	9.3244E-03
1.8000E+00	1.0359E+02	---+	9.9475E-03	1.0006E-02
1.8500E+00	1.0092E+02	--+	8.4044E-03	1.0504E-02
1.9000E+00	9.3328E+01	--------------------------------------+	9.1818E-03	1.0924E-02
1.9500E+00	8.3049E+01	------------------------------------+	1.1710E-02	1.1383E-02
2.0000E+00	7.2130E+01	----------------------------+	1.5235E-02	1.1969E-02
2.0500E+00	6.2373E+01	------------------------+	1.7250E-02	1.2730E-02
2.1000E+00	5.3720E+01	----------------------+	1.7250E-02	1.3231E-02
2.1500E+00	4.7856E+01	--------------------+	1.7250E-02	1.3231E-02
2.2000E+00	4.7990E+01	--------------------+	1.7250E-02	1.3231E-02
2.2500E+00	5.4103E+01	----------------------+	1.7250E-02	1.3231E-02
2.3000E+00	6.5408E+01	--------------------------+	1.7250E-02	1.3231E-02
2.3500E+00	8.0444E+01	----------+----------------------+	1.7250E-02	1.3231E-02
2.4000E+00	9.7270E+01	---------------------------------------+	1.7032E-02	1.3231E-02
2.4500E+00	1.1362E+02	---+	1.1107E-02	1.3220E-02
2.5000E+00	1.2458E+02	---+	5.2348E-03	1.2913E-02

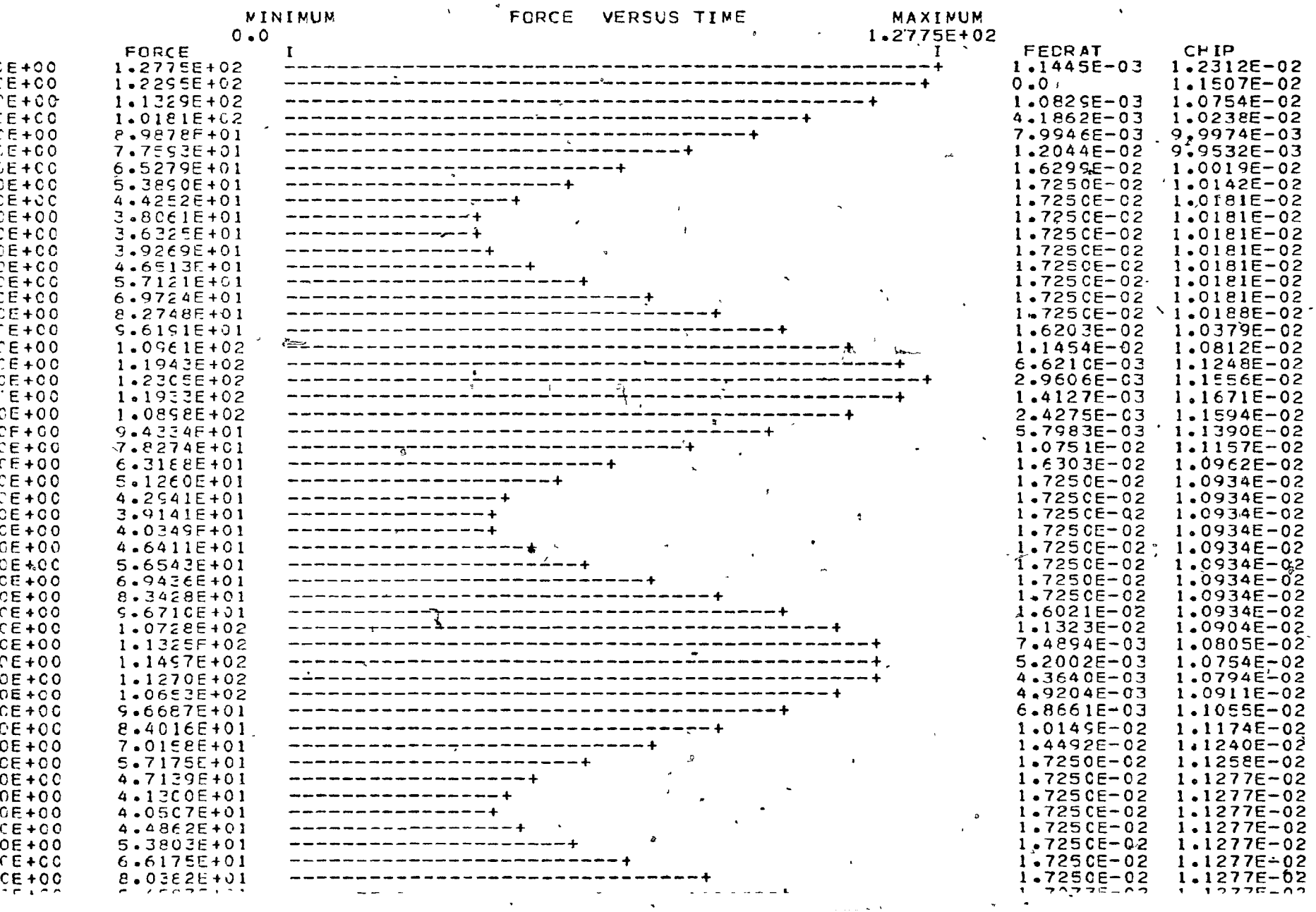

TIME	FORCE	FEDRAT	CHIP
2.550CE+00	1.2775E+02	1.1445E-03	1.2312E-02
2.600CE+00	1.2295E+02	0.0	1.1507E-02
2.650CE+00	1.1329E+02	1.0829E-03	1.0754E-02
2.700CE+00	1.0181E+02	4.1862E-03	1.0238E-02
2.750CE+00	8.9878E+01	7.9946E-03	9.9974E-03
2.800CE+00	7.7593E+01	1.2044E-02	9.9532E-03
2.850CE+00	6.5279E+01	1.6299E-02	1.0019E-02
2.900CE+00	5.3890E+01	1.7250E-02	1.0142E-02
2.950CE+00	4.4252E+01	1.7250E-02	1.0181E-02
3.000CE+00	3.8061E+01	1.7250E-02	1.0181E-02
3.050CE+00	3.6325E+01	1.7250E-02	1.0181E-02
3.100CE+00	3.9269E+01	1.7250E-02	1.0181E-02
3.150CE+00	4.6513E+01	1.7250E-02	1.0181E-02
3.200CE+00	5.7121E+01	1.7250E-02	1.0181E-02
3.250CE+00	6.9724E+01	1.7250E-02	1.0181E-02
3.300CE+00	8.2748E+01	1.7250E-02	1.0188E-02
3.350CE+00	9.6191E+01	1.6203E-02	1.0379E-02
3.400CE+00	1.0961E+02	1.1454E-02	1.0812E-02
3.450CE+00	1.1943E+02	6.6210E-03	1.1248E-02
3.500CE+00	1.2305E+02	2.9606E-03	1.1556E-02
3.550CE+00	1.1933E+02	1.4127E-03	1.1671E-02
3.600CE+00	1.0898E+02	2.4275E-03	1.1594E-02
3.650CE+00	9.4334E+01	5.7983E-03	1.1390E-02
3.700CE+00	7.8274E+01	1.0751E-02	1.1157E-02
3.750CE+00	6.3188E+01	1.6303E-02	1.0962E-02
3.800CE+00	5.1260E+01	1.7250E-02	1.0934E-02
3.850CE+00	4.2941E+01	1.7250E-02	1.0934E-02
3.900CE+00	3.9141E+01	1.7250E-02	1.0934E-02
3.950CE+00	4.0349E+01	1.7250E-02	1.0934E-02
4.000CE+00	4.6411E+01	1.7250E-02	1.0934E-02
4.050CE+00	5.6543E+01	1.7250E-02	1.0934E-02
4.100CE+00	6.9436E+01	1.7250E-02	1.0934E-02
4.150CE+00	8.3428E+01	1.7250E-02	1.0934E-02
4.200CE+00	9.6710E+01	1.6021E-02	1.0934E-02
4.250CE+00	1.0728E+02	1.1323E-02	1.0904E-02
4.300CE+00	1.1325E+02	7.4894E-03	1.0805E-02
4.350CE+00	1.1497E+02	5.2002E-03	1.0754E-02
4.400CE+00	1.1270E+02	4.3640E-03	1.0794E-02
4.450CE+00	1.0653E+02	4.9204E-03	1.0911E-02
4.500CE+00	9.6687E+01	6.8661E-03	1.1055E-02
4.550CE+00	8.4016E+01	1.0149E-02	1.1174E-02
4.600CE+00	7.0158E+01	1.4492E-02	1.1240E-02
4.650CE+00	5.7175E+01	1.7250E-02	1.1258E-02
4.700CE+00	4.7139E+01	1.7250E-02	1.1277E-02
4.750CE+00	4.1300E+01	1.7250E-02	1.1277E-02
4.800CE+00	4.0507E+01	1.7250E-02	1.1277E-02
4.850CE+00	4.4862E+01	1.7250E-02	1.1277E-02
4.900CE+00	5.3803E+01	1.7250E-02	1.1277E-02
4.950CE+00	6.6175E+01	1.7250E-02	1.1277E-02
5.000CE+00	8.0382E+01	1.7250E-02	1.1277E-02

SIMULATION OF FIG.4.11 WITH KPRO=0.1, KINT=0.002 PAGE 3

FORCE VERSUS TIME

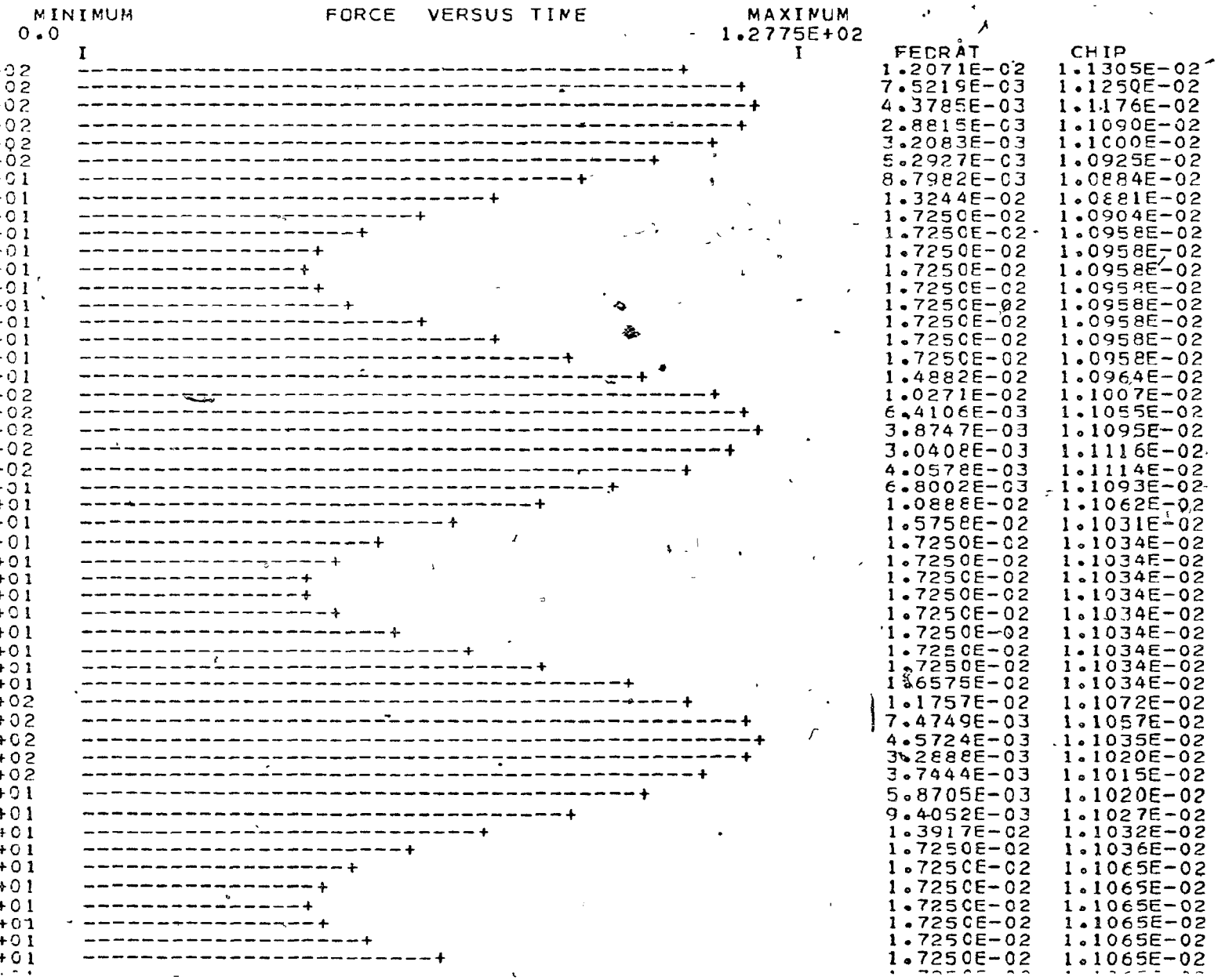

TIME	FORCE	FEDRAT	CHIP
5.1000E+00	1.0723E+02	1.2071E-02	1.1305E-02
5.1500E+00	1.1563E+02	7.5219E-03	1.1250E-02
5.2000E+00	1.1918E+02	4.3785E-03	1.1176E-02
5.2500E+00	1.1749E+02	2.8815E-03	1.1090E-02
5.3000E+00	1.1083E+02	3.2083E-03	1.1000E-02
5.3500E+00	1.0026E+02	5.2927E-03	1.0925E-02
5.4000E+00	8.7230E+01	8.7982E-03	1.0884E-02
5.4500E+00	7.3306E+01	1.3244E-02	1.0881E-02
5.5000E+00	6.0081E+01	1.7250E-02	1.0904E-02
5.5500E+00	4.9224E+01	1.7250E-02	1.0958E-02
5.6000E+00	4.1798E+01	1.7250E-02	1.0958E-02
5.6500E+00	3.9061E+01	1.7250E-02	1.0958E-02
5.7000E+00	4.1366E+01	1.7250E-02	1.0958E-02
5.7500E+00	4.8415E+01	1.7250E-02	1.0958E-02
5.8000E+00	5.9298E+01	1.7250E-02	1.0958E-02
5.8500E+00	7.2611E+01	1.7250E-02	1.0958E-02
5.9000E+00	8.6634E+01	1.7250E-02	1.0958E-02
5.9500E+00	9.9605E+01	1.4882E-02	1.0964E-02
6.0000E+00	1.1019E+02	1.0271E-02	1.1007E-02
6.0500E+00	1.1681E+02	6.4106E-03	1.1055E-02
6.1000E+00	1.1845E+02	3.8747E-03	1.1095E-02
6.1500E+00	1.1481E+02	3.0408E-03	1.1116E-02
6.2000E+00	1.0633E+02	4.0578E-03	1.1114E-02
6.2500E+00	9.4201E+01	6.8002E-03	1.1093E-02
6.3000E+00	8.0086E+01	1.0888E-02	1.1062E-02
6.3500E+00	6.5892E+01	1.5758E-02	1.1031E-02
6.4000E+00	5.3583E+01	1.7250E-02	1.1034E-02
6.4500E+00	4.4491E+01	1.7250E-02	1.1034E-02
6.5000E+00	3.9810E+01	1.7250E-02	1.1034E-02
6.5500E+00	4.0143E+01	1.7250E-02	1.1034E-02
6.6000E+00	4.5449E+01	1.7250E-02	1.1034E-02
6.6500E+00	5.5041E+01	1.7250E-02	1.1034E-02
6.7000E+00	6.7682E+01	1.7250E-02	1.1034E-02
6.7500E+00	8.1739E+01	1.7250E-02	1.1034E-02
6.8000E+00	9.5398E+01	1.6575E-02	1.1034E-02
6.8500E+00	1.0726E+02	1.1757E-02	1.1072E-02
6.9000E+00	1.1498E+02	7.4749E-03	1.1057E-02
6.9500E+00	1.1794E+02	4.5724E-03	1.1035E-02
7.0000E+00	1.1590E+02	3.2888E-03	1.1020E-02
7.0500E+00	1.0916E+02	3.7444E-03	1.1015E-02
7.1000E+00	9.8539E+01	5.8705E-03	1.1020E-02
7.1500E+00	8.5355E+01	9.4052E-03	1.1027E-02
7.2000E+00	7.1269E+01	1.3917E-02	1.1032E-02
7.2500E+00	5.8110E+01	1.7250E-02	1.1036E-02
7.3000E+00	4.7710E+01	1.7250E-02	1.1065E-02
7.3500E+00	4.1179E+01	1.7250E-02	1.1065E-02
7.4000E+00	3.9514E+01	1.7250E-02	1.1065E-02
7.4500E+00	4.2931E+01	1.7250E-02	1.1065E-02
7.5000E+00	5.0989E+01	1.7250E-02	1.1065E-02
7.5500E+00	6.2646E+01	1.7250E-02	1.1065E-02

FORCE VERSUS TIME

MINIMUM 0.0 MAXIMUM 1.2775E+02

TIME	FORCE	FEDRAT	CHIP
7.6500E+00	9.0471E+01	1.7250E-02	1.1065E-02
7.7000E+00	1.0324E+02	1.3542E-02	1.1086E-02
7.7500E+00	1.1265E+02	8.9767E-03	1.1080E-02
7.8000E+00	1.1768E+02	5.5027E-03	1.1072E-02
7.8500E+00	1.1768E+02	3.5084E-03	1.1061E-02
7.9000E+00	1.1264E+02	3.2486E-03	1.1048E-02
7.9500E+00	1.0321E+02	4.7639E-03	1.1032E-02
8.0000E+00	9.0666E+01	7.8545E-03	1.1018E-02
8.0500E+00	7.6623E+01	1.2110E-02	1.1009E-02
8.1000E+00	6.2876E+01	1.6978E-02	1.1007E-02
8.1500E+00	5.1396E+01	1.7250E-02	1.1059E-02
8.2000E+00	4.3163E+01	1.7250E-02	1.1059E-02
8.2500E+00	3.9534E+01	1.7250E-02	1.1059E-02
8.3000E+00	4.0979E+01	1.7250E-02	1.1059E-02
8.3500E+00	4.7309E+01	1.7250E-02	1.1059E-02
8.4000E+00	5.7710E+01	1.7250E-02	1.1059E-02
8.4500E+00	7.0836E+01	1.7250E-02	1.1059E-02
8.5000E+00	8.4994E+01	1.7250E-02	1.1059E-02
8.5500E+00	9.8356E+01	1.5462E-02	1.1059E-02
8.6000E+00	1.0943E+02	1.0726E-02	1.1082E-02
8.6500E+00	1.1634E+02	6.7019E-03	1.1080E-02
8.7000E+00	1.1837E+02	4.0665E-03	1.1072E-02
8.7500E+00	1.1527E+02	3.1036E-03	1.1061E-02
8.8000E+00	1.0746E+02	3.9294E-03	1.1049E-02
8.8500E+00	9.5976E+01	6.4324E-03	1.1037E-02
8.9000E+00	8.2292E+01	1.0285E-02	1.1027E-02
8.9500E+00	6.8175E+01	1.4990E-02	1.1019E-02
9.0000E+00	5.5435E+01	1.7250E-02	1.1015E-02
9.0500E+00	4.5722E+01	1.7250E-02	1.1020E-02
9.1000E+00	4.0220E+01	1.7250E-02	1.1020E-02
9.1500E+00	3.9667E+01	1.7250E-02	1.1020E-02
9.2000E+00	4.4134E+01	1.7250E-02	1.1020E-02
9.2500E+00	5.3045E+01	1.7250E-02	1.1020E-02
9.3000E+00	6.5249E+01	1.7250E-02	1.1020E-02
9.3500E+00	7.9170E+01	1.7250E-02	1.1020E-02
9.4000E+00	9.3011E+01	1.7250E-02	1.1020E-02
9.4500E+00	1.0550E+02	1.2598E-02	1.1074E-02
9.5000E+00	1.1411E+02	8.1121E-03	1.1075E-02
9.5500E+00	1.1809E+02	4.9062E-03	1.1067E-02
9.6000E+00	1.1698E+02	3.2721E-03	1.1057E-02
9.6500E+00	1.1095E+02	3.3985E-03	1.1046E-02
9.7000E+00	1.0077E+02	5.2672E-03	1.1036E-02
9.7500E+00	8.7770E+01	8.6340E-03	1.1027E-02
9.8000E+00	7.3624E+01	1.3066E-02	1.1020E-02
9.8500E+00	6.0148E+01	1.7250E-02	1.1016E-02
9.9000E+00	4.9268E+01	1.7250E-02	1.1060E-02
9.9500E+00	4.1963E+01	1.7250E-02	1.1060E-02
1.0000E+01	3.9419E+01	1.7250E-02	1.1060E-02
1.0050E+01	4.1965E+01	1.7250E-02	1.1060E-02
1.0100E+01	4.9272E+01	1.7250E-02	1.1060E-02
1.0150E+01	6.0766E+01	1.7250E-02	1.1060E-02

SIMULATION OF FIG.4.11 WITH KPRO=0.1, KINT=0.002 PAGE 5

FORCE VERSUS TIME

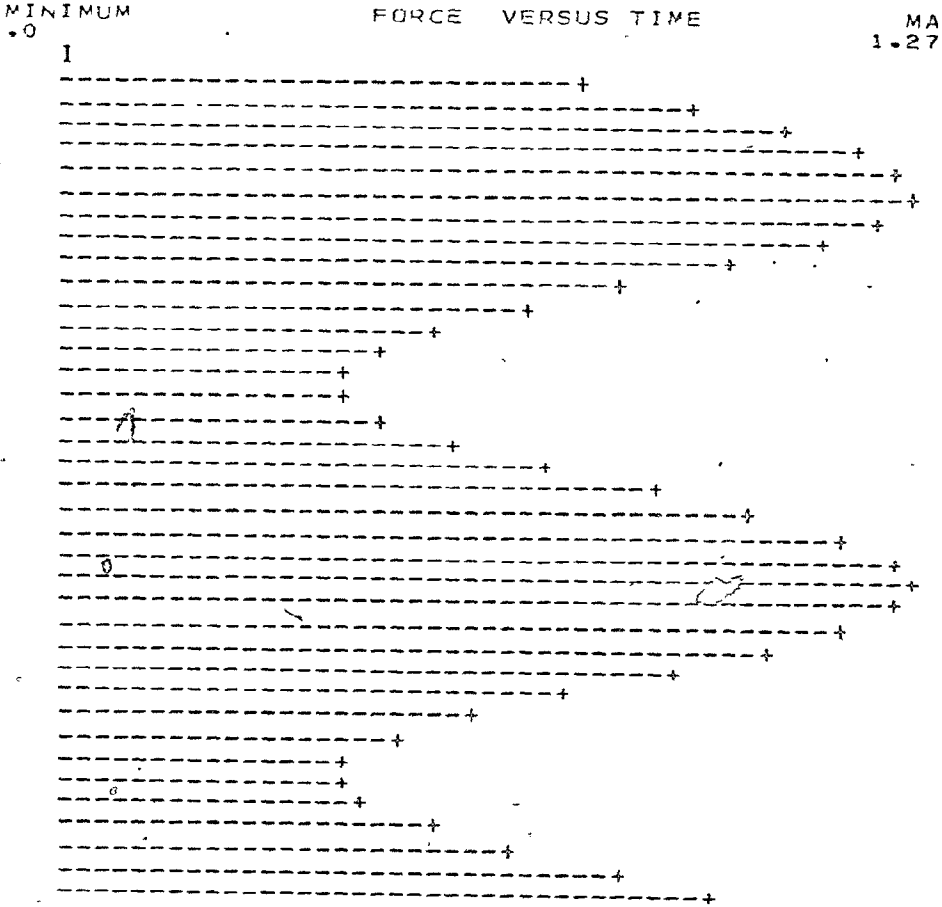

TIME	FORCE	FECRAT	CHIP
1.020CE+01	7.39C2E+01	1.7250E-02	1.1060E-02
1.025CE+01	8.8044E+01	1.7250E-02	1.1060E-02
1.030CE+01	1.01C0E+02	1.4368E-02	1.1060E-02
1.035CE+01	1.1107E+02	9.7540E-03	1.1058E-02
1.040CE+01	1.1694E+02	6.0658E-03	1.1053E-02
1.045CE+01	1.1788E+02	3.7859E-03	1.1048E-02
1.050CE+01	1.1376E+02	3.1981E-03	1.1041E-02
1.055CE+01	1.0511E+02	4.3865E-03	1.1034E-02
1.060CE+01	9.3056E+01	7.1980E-03	1.1026E-02
1.065CE+01	7.9163E+01	1.1267E-02	1.1020E-02
1.070CE+01	6.5224E+01	1.6066E-02	1.1017E-02
1.075CE+01	5.3132E+01	1.7250E-02	1.1039E-02
1.080CE+01	4.4207E+01	1.7250E-02	1.1039E-02
1.085CE+01	3.9735E+01	1.7250E-02	1.1039E-02
1.090CE+01	4.0291E+01	1.7250E-02	1.1039E-02
1.095CE+01	4.5805E+01	1.7250E-02	1.1039E-02
1.100CE+01	5.5564E+01	1.7250E-02	1.1039E-02
1.105CE+01	6.8308E+01	1.7250E-02	1.1039E-02
1.110CE+01	8.2392E+01	1.7250E-02	1.1039E-02
1.115CE+01	9.5997E+01	1.7250E-02	1.1039E-02
1.120CE+01	1.0778E+02	1.6338E-02	1.1039E-02
1.125CE+01	1.1546E+02	1.1534E-02	1.1081E-02
1.130CE+01	1.1832E+02	7.2790E-03	1.1079E-02
1.135CE+01	1.1605E+02	4.3841E-03	1.1068E-02
1.140CE+01	1.0859E+02	3.1327E-03	1.1053E-02
1.145CE+01	9.8055E+01	3.6647E-03	1.1038E-02
1.150CE+01	8.4661E+01	5.9025E-03	1.1025E-02
1.155CE+01	7.0518E+01	9.5501E-03	1.1016E-02
1.160CE+01	5.7439E+01	1.4139E-02	1.1010E-02
1.165CE+01	4.7188E+01	1.7250E-02	1.1008E-02
1.170CE+01	4.0875E+01	1.7250E-02	1.1031E-02
1.175CE+01	3.9437E+01	1.7250E-02	1.1031E-02
1.180CE+01	4.3059E+01	1.7250E-02	1.1031E-02
1.185CE+01	5.1274E+01	1.7250E-02	1.1031E-02
1.190CE+01	6.3021E+01	1.7250E-02	1.1031E-02
1.195CE+01	7.6783E+01	1.7250E-02	1.1031E-02
1.200CE+01	9.0784E+01	1.7250E-02	1.1031E-02

SIMULATION OF FIG.4.11 WITH KPRO=0.35, KINT=0.003 PAGE 1

FORCE VERSUS TIME

MINIMUM 0.0 MAXIMUM 1.1400E+02

TIME	FORCE	FECRAT	CHIP
0.0	0.0	0.0	0.0
5.0000E-02	0.0	1.7250E-02	0.0
1.0000E-01	0.0	1.7250E-02	0.0
1.5000E-01	0.0	1.7250E-02	0.0
2.0000E-01	0.0	1.7250E-02	0.0
2.5000E-01	0.0	1.7250E-02	0.0
3.0000E-01	0.0	1.7250E-02	0.0
3.5000E-01	0.0	1.7250E-02	0.0
4.0000E-01	0.0	1.7250E-02	0.0
4.5000E-01	0.0	1.7250E-02	0.0
5.0000E-01	0.0	1.7250E-02	0.0
5.5000E-01	0.0	1.7250E-02	0.0
6.0000E-01	0.0	1.7250E-02	0.0
6.5000E-01	0.0	1.7250E-02	0.0
7.0000E-01	0.0	1.7250E-02	0.0
7.5000E-01	0.0	1.7250E-02	0.0
8.0000E-01	0.0	1.7250E-02	0.0
8.5000E-01	0.0	1.7250E-02	0.0
9.0000E-01	0.0	1.7250E-02	0.0
9.5000E-01	0.0	1.7250E-02	0.0
1.0000E+00	0.0	1.7250E-02	0.0
1.0500E+00	0.0	1.7250E-02	0.0
1.1000E+00	0.0	1.7250E-02	0.0
1.1500E+00	0.0	1.7250E-02	0.0
1.2000E+00	0.0	1.7250E-02	0.0
1.2500E+00	2.6831E+00	1.7250E-02	6.9959E-04
1.3000E+00	5.5699E+00	1.7250E-02	1.5621E-03
1.3500E+00	9.1070E+00	1.7250E-02	2.4245E-03
1.4000E+00	1.4403E+01	1.7250E-02	3.2870E-03
1.4500E+00	2.2251E+01	1.7250E-02	4.1495E-03
1.5000E+00	3.2931E+01	1.7250E-02	5.0120E-03
1.5500E+00	4.6119E+01	1.7250E-02	5.8745E-03
1.6000E+00	6.0887E+01	1.7250E-02	6.7369E-03
1.6500E+00	7.5828E+01	1.7250E-02	7.5994E-03
1.7000E+00	8.9277E+01	1.7250E-02	8.4619E-03
1.7500E+00	9.9594E+01	5.9406E-03	9.3244E-03
1.8000E+00	9.9608E+01	0.0	9.6214E-03
1.8500E+00	9.2444E+01	0.0	9.6214E-03
1.9000E+00	8.2199E+01	1.5820E-03	9.6214E-03
1.9500E+00	7.0773E+01	1.3930E-02	9.7005E-03
2.0000E+00	6.2658E+01	1.7250E-02	1.0397E-02
2.0500E+00	5.5167E+01	1.7250E-02	1.1259E-02
2.1000E+00	4.7748E+01	1.7250E-02	1.1760E-02
2.1500E+00	4.2536E+01	1.7250E-02	1.1760E-02
2.2000E+00	4.2655E+01	1.7250E-02	1.1760E-02
2.2500E+00	4.8088E+01	1.7250E-02	1.1760E-02
2.3000E+00	5.8136E+01	1.7250E-02	1.1760E-02
2.3500E+00	7.1501E+01	1.7250E-02	1.1760E-02
2.4000E+00	8.6456E+01	1.7250E-02	1.1760E-02
2.4500E+00	1.0107E+02	9.3430E-03	1.1760E-02

FORCE VERSUS TIME

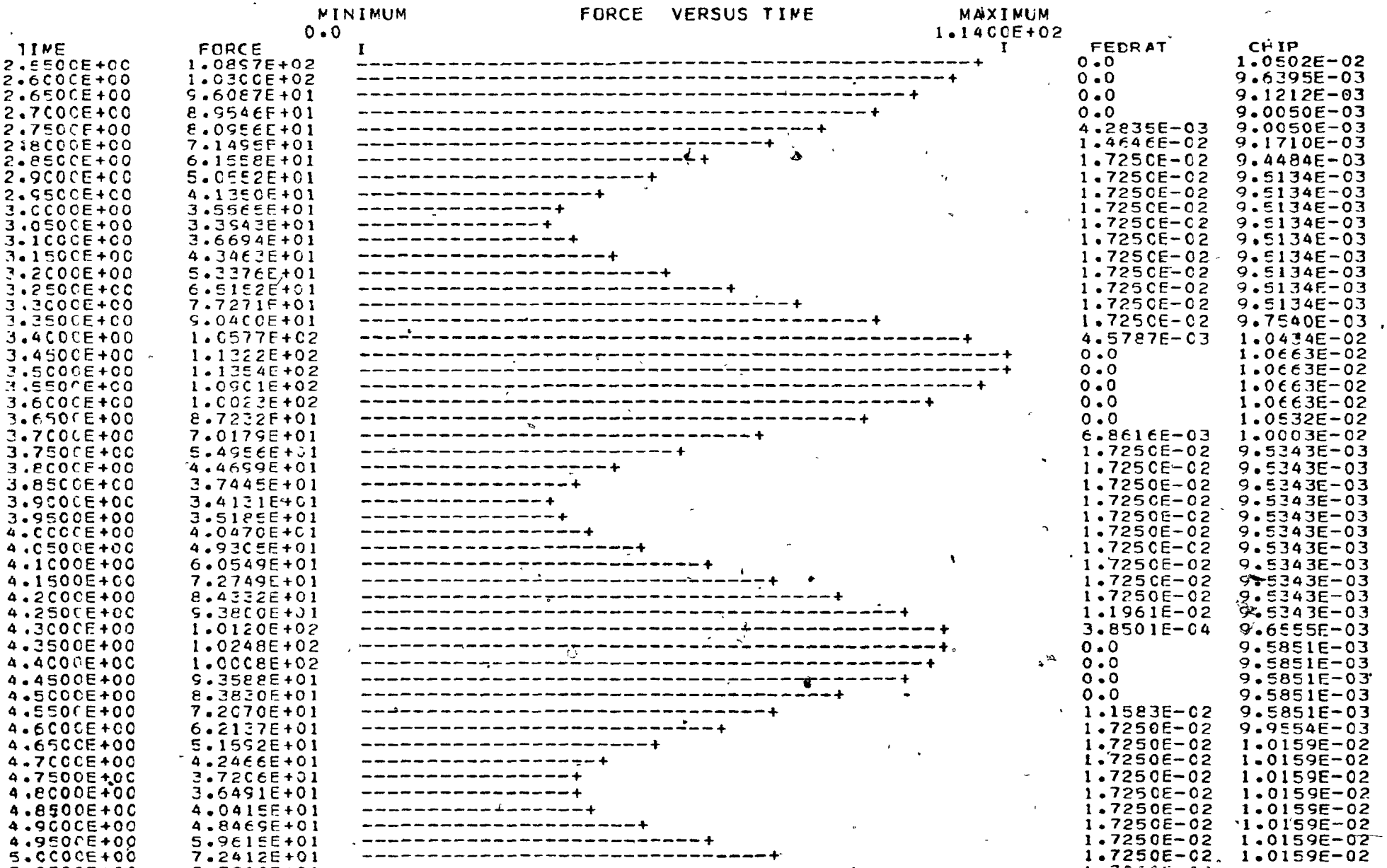

TIME	FORCE	FEDRAT	CHIP
2.5500E+00	1.0857E+02	0.0	1.0502E-02
2.6000E+00	1.0300E+02	0.0	9.6395E-03
2.6500E+00	9.6087E+01	0.0	9.1212E-03
2.7000E+00	8.9546E+01	0.0	9.0050E-03
2.7500E+00	8.0956E+01	4.2835E-03	9.0050E-03
2.8000E+00	7.1495E+01	1.4646E-02	9.1710E-03
2.8500E+00	6.1558E+01	1.7250E-02	9.4484E-03
2.9000E+00	5.0552E+01	1.7250E-02	9.5134E-03
2.9500E+00	4.1350E+01	1.7250E-02	9.5134E-03
3.0000E+00	3.5565E+01	1.7250E-02	9.5134E-03
3.0500E+00	3.3943E+01	1.7250E-02	9.5134E-03
3.1000E+00	3.6694E+01	1.7250E-02	9.5134E-03
3.1500E+00	4.3463E+01	1.7250E-02	9.5134E-03
3.2000E+00	5.3376E+01	1.7250E-02	9.5134E-03
3.2500E+00	6.5152E+01	1.7250E-02	9.5134E-03
3.3000E+00	7.7271E+01	1.7250E-02	9.5134E-03
3.3500E+00	9.0400E+01	1.7250E-02	9.7540E-03
3.4000E+00	1.0577E+02	4.5787E-03	1.0434E-02
3.4500E+00	1.1322E+02	0.0	1.0663E-02
3.5000E+00	1.1354E+02	0.0	1.0663E-02
3.5500E+00	1.0901E+02	0.0	1.0663E-02
3.6000E+00	1.0023E+02	0.0	1.0663E-02
3.6500E+00	8.7232E+01	0.0	1.0532E-02
3.7000E+00	7.0179E+01	6.8616E-03	1.0003E-02
3.7500E+00	5.4956E+01	1.7250E-02	9.5343E-03
3.8000E+00	4.4699E+01	1.7250E-02	9.5343E-03
3.8500E+00	3.7445E+01	1.7250E-02	9.5343E-03
3.9000E+00	3.4131E+01	1.7250E-02	9.5343E-03
3.9500E+00	3.5185E+01	1.7250E-02	9.5343E-03
4.0000E+00	4.0470E+01	1.7250E-02	9.5343E-03
4.0500E+00	4.9365E+01	1.7250E-02	9.5343E-03
4.1000E+00	6.0549E+01	1.7250E-02	9.5343E-03
4.1500E+00	7.2749E+01	1.7250E-02	9.5343E-03
4.2000E+00	8.4332E+01	1.7250E-02	9.5343E-03
4.2500E+00	9.3800E+01	1.1961E-02	9.5343E-03
4.3000E+00	1.0120E+02	3.8501E-04	9.6555E-03
4.3500E+00	1.0248E+02	0.0	9.5851E-03
4.4000E+00	1.0008E+02	0.0	9.5851E-03
4.4500E+00	9.3588E+01	0.0	9.5851E-03
4.5000E+00	8.3830E+01	0.0	9.5851E-03
4.5500E+00	7.2070E+01	1.1583E-02	9.5851E-03
4.6000E+00	6.2137E+01	1.7250E-02	9.9554E-03
4.6500E+00	5.1592E+01	1.7250E-02	1.0159E-02
4.7000E+00	4.2466E+01	1.7250E-02	1.0159E-02
4.7500E+00	3.7206E+01	1.7250E-02	1.0159E-02
4.8000E+00	3.6491E+01	1.7250E-02	1.0159E-02
4.8500E+00	4.0415E+01	1.7250E-02	1.0159E-02
4.9000E+00	4.8469E+01	1.7250E-02	1.0159E-02
4.9500E+00	5.9615E+01	1.7250E-02	1.0159E-02
5.0000E+00	7.2412E+01	1.7250E-02	1.0159E-02
5.0500E+00	8.5210E+01		

SIMULATION OF FIG.4.11 WITH KPRO=0.35, KINT=0.003 PAGE 3

FORCE VERSUS TIME

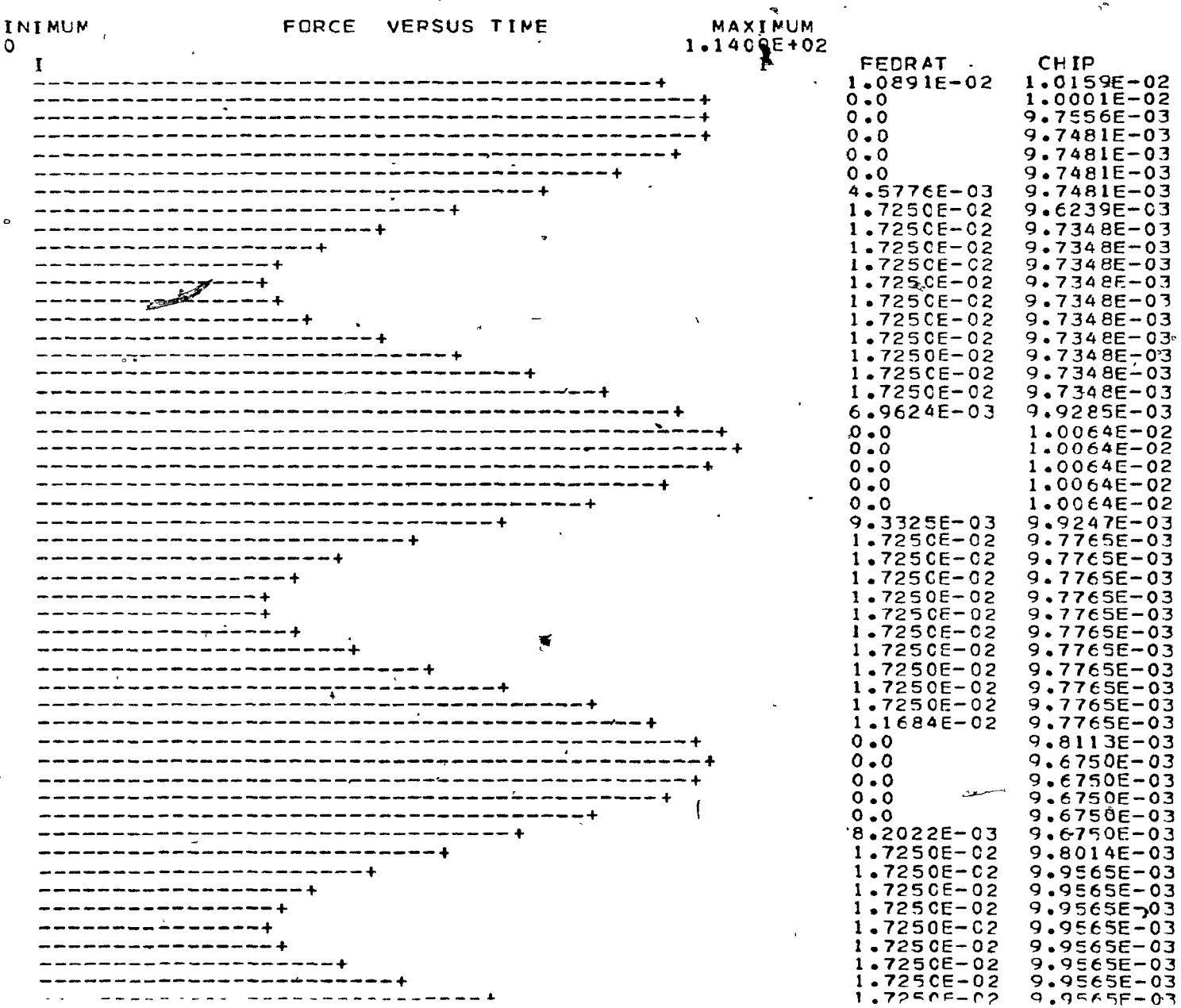

TIME	FORCE	FEDRAT	CHIP
5.1000E+00	9.6355E+01	1.0891E-02	1.0159E-02
5.1500E+00	1.0279E+02	0.0	1.0001E-02
5.2000E+00	1.0403E+02	0.0	9.7556E-03
5.2500E+00	1.0327E+02	0.0	9.7481E-03
5.3000E+00	9.8218E+01	0.0	9.7481E-03
5.3500E+00	8.9460E+01	0.0	9.7481E-03
5.4000E+00	7.8123E+01	4.5776E-03	9.7481E-03
5.4500E+00	6.4833E+01	1.7250E-02	9.6239E-03
5.5000E+00	5.3637E+01	1.7250E-02	9.7348E-03
5.5500E+00	4.3727E+01	1.7250E-02	9.7348E-03
5.6000E+00	3.7130E+01	1.7250E-02	9.7348E-03
5.6500E+00	3.4699E+01	1.7250E-02	9.7348E-03
5.7000E+00	3.6747E+01	1.7250E-02	9.7348E-03
5.7500E+00	4.3009E+01	1.7250E-02	9.7348E-03
5.8000E+00	5.2677E+01	1.7250E-02	9.7348E-03
5.8500E+00	6.4503E+01	1.7250E-02	9.7348E-03
5.9000E+00	7.6960E+01	1.7250E-02	9.7348E-03
5.9500E+00	8.8439E+01	1.7250E-02	9.7348E-03
6.0000E+00	9.9399E+01	6.9624E-03	9.9285E-03
6.0500E+00	1.0633E+02	0.0	1.0064E-02
6.1000E+00	1.0744E+02	0.0	1.0064E-02
6.1500E+00	1.0394E+02	0.0	1.0064E-02
6.2000E+00	9.6285E+01	0.0	1.0064E-02
6.2500E+00	8.5458E+01	0.0	1.0064E-02
6.3000E+00	7.1853E+01	9.3325E-03	9.9247E-03
6.3500E+00	5.8399E+01	1.7250E-02	9.7765E-03
6.4000E+00	4.7476E+01	1.7250E-02	9.7765E-03
6.4500E+00	3.9420E+01	1.7250E-02	9.7765E-03
6.5000E+00	3.5272E+01	1.7250E-02	9.7765E-03
6.5500E+00	3.5568E+01	1.7250E-02	9.7765E-03
6.6000E+00	4.0269E+01	1.7250E-02	9.7765E-03
6.6500E+00	4.8768E+01	1.7250E-02	9.7765E-03
6.7000E+00	5.9968E+01	1.7250E-02	9.7765E-03
6.7500E+00	7.2423E+01	1.7250E-02	9.7765E-03
6.8000E+00	8.4528E+01	1.7250E-02	9.7765E-03
6.8500E+00	9.4711E+01	1.1684E-02	9.7765E-03
6.9000E+00	1.0203E+02	0.0	9.8113E-03
6.9500E+00	1.0341E+02	0.0	9.6750E-03
7.0000E+00	1.0176E+02	0.0	9.6750E-03
7.0500E+00	9.5873E+01	0.0	9.6750E-03
7.1000E+00	8.6514E+01	0.0	9.6750E-03
7.1500E+00	7.4850E+01	8.2022E-03	9.6750E-03
7.2000E+00	6.3317E+01	1.7250E-02	9.8014E-03
7.2500E+00	5.2427E+01	1.7250E-02	9.9565E-03
7.3000E+00	4.2930E+01	1.7250E-02	9.9565E-03
7.3500E+00	3.7053E+01	1.7250E-02	9.9565E-03
7.4000E+00	3.5565E+01	1.7250E-02	9.9565E-03
7.4500E+00	3.8630E+01	1.7250E-02	9.9565E-03
7.5000E+00	4.5880E+01	1.7250E-02	9.9565E-03
7.5500E+00	5.6370E+01	1.7250E-02	9.9565E-03

FORCE VERSUS TIME

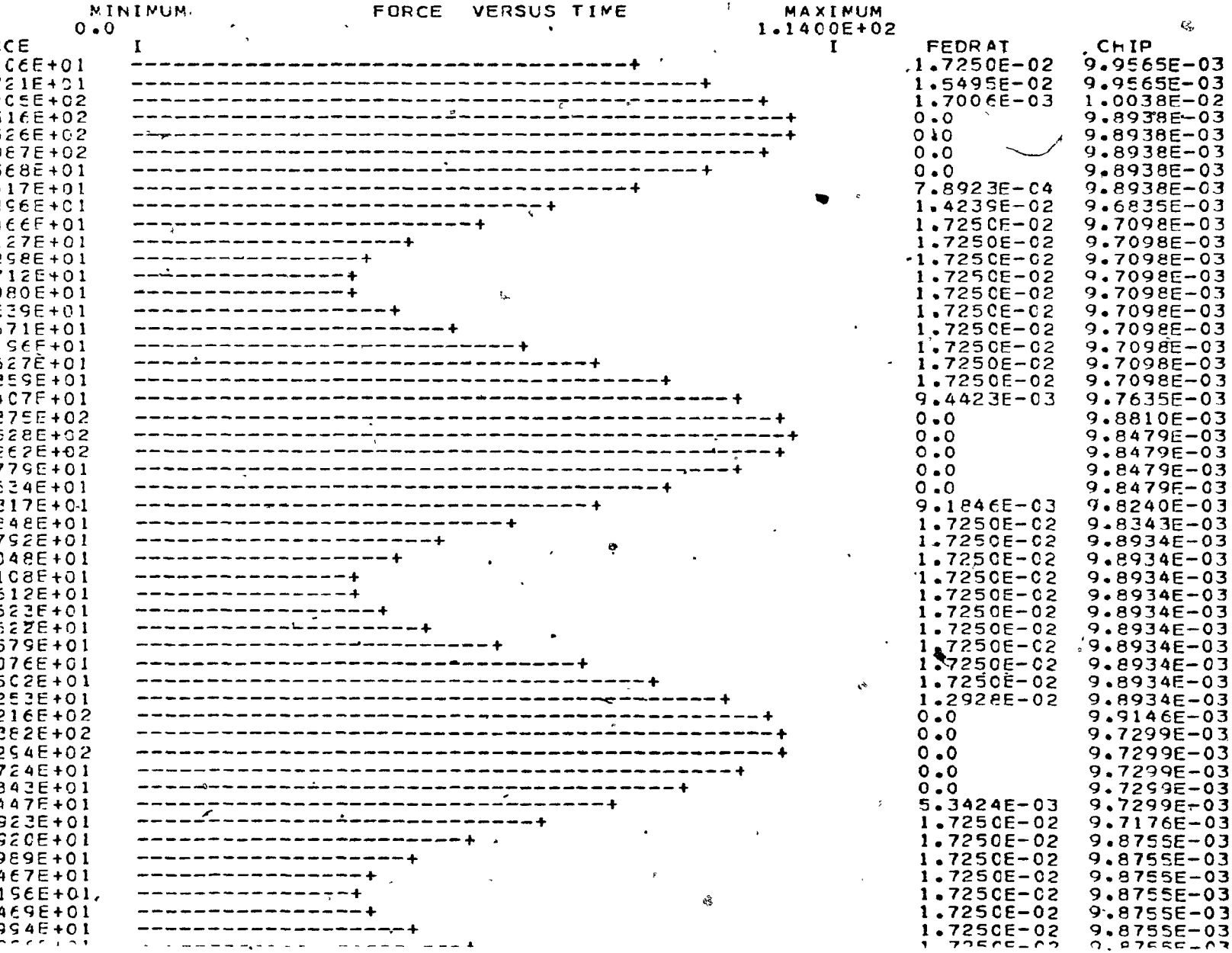

TIME	FORCE	FEDRAT	CHIP
7.6500E+00	8.1406E+01	1.7250E-02	9.9565E-03
7.7000E+00	9.2721E+01	1.5495E-02	9.9565E-03
7.7500E+00	1.0205E+02	1.7006E-03	1.0038E-02
7.8000E+00	1.0516E+02	0.0	9.8938E-03
7.8500E+00	1.0526E+02	0.0	9.8938E-03
7.9000E+00	1.0087E+02	0.0	9.8938E-03
7.9500E+00	9.2568E+01	0.0	9.8938E-03
8.0000E+00	8.1417E+01	7.8923E-04	9.8938E-03
8.0500E+00	6.7396E+01	1.4239E-02	9.6835E-03
8.1000E+00	5.5466E+01	1.7250E-02	9.7098E-03
8.1500E+00	4.5127E+01	1.7250E-02	9.7098E-03
8.2000E+00	3.7858E+01	1.7250E-02	9.7098E-03
8.2500E+00	3.4712E+01	1.7250E-02	9.7098E-03
8.3000E+00	3.5980E+01	1.7250E-02	9.7098E-03
8.3500E+00	4.1539E+01	1.7250E-02	9.7098E-03
8.4000E+00	5.0671E+01	1.7250E-02	9.7098E-03
8.4500E+00	6.2196E+01	1.7250E-02	9.7098E-03
8.5000E+00	7.4627E+01	1.7250E-02	9.7098E-03
8.5500E+00	8.6359E+01	1.7250E-02	9.7098E-03
8.6000E+00	9.6407E+01	9.4423E-03	9.7635E-03
8.6500E+00	1.0375E+02	0.0	9.8810E-03
8.7000E+00	1.0528E+02	0.0	9.8479E-03
8.7500E+00	1.0262E+02	0.0	9.8479E-03
8.8000E+00	9.5779E+01	0.0	9.8479E-03
8.8500E+00	8.5634E+01	0.0	9.8479E-03
8.9000E+00	7.3317E+01	9.1846E-03	9.8240E-03
8.9500E+00	6.0848E+01	1.7250E-02	9.8343E-03
9.0000E+00	4.9792E+01	1.7250E-02	9.8934E-03
9.0500E+00	4.1048E+01	1.7250E-02	9.8934E-03
9.1000E+00	3.6108E+01	1.7250E-02	9.8934E-03
9.1500E+00	3.5612E+01	1.7250E-02	9.8934E-03
9.2000E+00	3.9623E+01	1.7250E-02	9.8934E-03
9.2500E+00	4.7622E+01	1.7250E-02	9.8934E-03
9.3000E+00	5.8579E+01	1.7250E-02	9.8934E-03
9.3500E+00	7.1076E+01	1.7250E-02	9.8934E-03
9.4000E+00	8.3502E+01	1.7250E-02	9.8934E-03
9.4500E+00	9.4253E+01	1.2928E-02	9.8934E-03
9.5000E+00	1.0216E+02	0.0	9.9146E-03
9.5500E+00	1.0382E+02	0.0	9.7299E-03
9.6000E+00	1.0294E+02	0.0	9.7299E-03
9.6500E+00	9.7724E+01	0.0	9.7299E-03
9.7000E+00	8.8843E+01	0.0	9.7299E-03
9.7500E+00	7.7447E+01	5.3424E-03	9.7299E-03
9.8000E+00	6.4923E+01	1.7250E-02	9.7176E-03
9.8500E+00	5.3920E+01	1.7250E-02	9.8755E-03
9.9000E+00	4.3989E+01	1.7250E-02	9.8755E-03
9.9500E+00	3.7467E+01	1.7250E-02	9.8755E-03
1.0000E+01	3.5196E+01	1.7250E-02	9.8755E-03
1.0050E+01	3.7469E+01	1.7250E-02	9.8755E-03
1.0100E+01	4.3994E+01	1.7250E-02	9.8755E-03

SIMULATION OF FIG.4.11 WITH KPRO=0.35, KINT=0.003 PAGE 5

FORCE VERSUS TIME

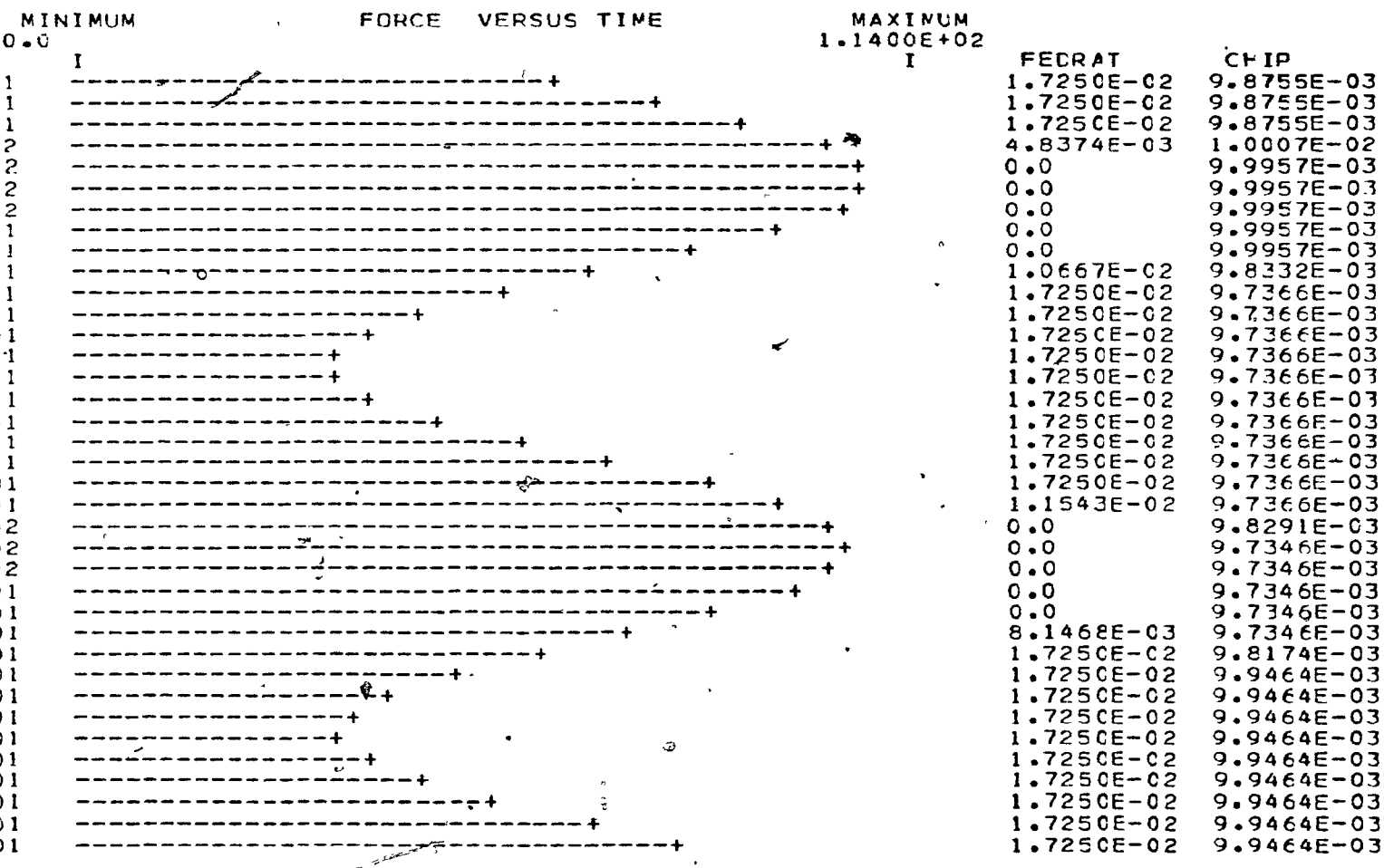

TIME	FORCE	FEDRAT	CHIP
1.0200E+01	6.5984E+01	1.7250E-02	9.8755E-03
1.0250E+01	7.8612E+01	1.7250E-02	9.8755E-03
1.0300E+01	9.0178E+01	1.7250E-02	9.8755E-03
1.0350E+01	1.0091E+02	4.8374E-03	1.0007E-02
1.0400E+01	1.0576E+02	0.0	9.9957E-03
1.0450E+01	1.0666E+02	0.0	9.9957E-03
1.0500E+01	1.0299E+02	0.0	9.9957E-03
1.0550E+01	9.5223E+01	0.0	9.9957E-03
1.0600E+01	8.4360E+01	0.0	9.9957E-03
1.0650E+01	7.0638E+01	1.0667E-02	9.8332E-03
1.0700E+01	5.7645E+01	1.7250E-02	9.7366E-03
1.0750E+01	4.6863E+01	1.7250E-02	9.7366E-03
1.0800E+01	3.8992E+01	1.7250E-02	9.7366E-03
1.0850E+01	3.5047E+01	1.7250E-02	9.7366E-03
1.0900E+01	3.5538E+01	1.7250E-02	9.7366E-03
1.0950E+01	4.0401E+01	1.7250E-02	9.7366E-03
1.1000E+01	4.9008E+01	1.7250E-02	9.7366E-03
1.1050E+01	6.0249E+01	1.7250E-02	9.7366E-03
1.1100E+01	7.2671E+01	1.7250E-02	9.7366E-03
1.1150E+01	8.4672E+01	1.7250E-02	9.7366E-03
1.1200E+01	9.4701E+01	1.1543E-02	9.7366E-03
1.1250E+01	1.0243E+02	0.0	9.8291E-03
1.1300E+01	1.0407E+02	0.0	9.7346E-03
1.1350E+01	1.0221E+02	0.0	9.7346E-03
1.1400E+01	9.6118E+01	0.0	9.7346E-03
1.1450E+01	8.6575E+01	0.0	9.7346E-03
1.1500E+01	7.4812E+01	8.1468E-03	9.7346E-03
1.1550E+01	6.2880E+01	1.7250E-02	9.8174E-03
1.1600E+01	5.1900E+01	1.7250E-02	9.9464E-03
1.1650E+01	4.2548E+01	1.7250E-02	9.9464E-03
1.1700E+01	3.6856E+01	1.7250E-02	9.9464E-03
1.1750E+01	3.5559E+01	1.7250E-02	9.9464E-03
1.1800E+01	3.8824E+01	1.7250E-02	9.9464E-03
1.1850E+01	4.6231E+01	1.7250E-02	9.9464E-03
1.1900E+01	5.6823E+01	1.7250E-02	9.9464E-03
1.1950E+01	6.9232E+01	1.7250E-02	9.9464E-03
1.2000E+01	8.1856E+01	1.7250E-02	9.9464E-03

APPENDIX L.2

SIMULATION LISTINGS AND RESULTS OF FIG. 4.13

```
        *** CONTINUOUS SYSTEM MODELING PROGRAM***
                    *** VERSION 1.3 ***
*********************************************************************
*                                                                   *
*    SIMULATION OF THE ECCENTRIC TURNING WITH A P-I CONTROLLER      *
*                                                                   *
*    FOLLOWING FEATURES ARE ADDED IN THE PROGRAM:                   *
*                                                                   *
*    1) FIXED STEP SIZE INTEGRATION METHOD I.E. RKSFX               *
*    2) LIMIT ON FEEDRATE (0.01>FEED>0.0)IN/SEC                     *
*    3) WITH PEAK-VALUE MEMORY (PV)                                 *
*    4) ECCENTRICITY S.T. DEPTH OF CUT IS: 0.09>DC>0.03 IN          *
*    5) "RESET WINDUP CUT-OUT" FEATURE FOR SATURATED MODE           *
*    6) CONDITION IS SAME AS THAT OF REAL EXPERIMENT                *
*       ========================================                    *
*                                                                   *
*********************************************************************
INITIAL
      PARAM KPRO=0.05,KINT=0.003
      INCON LIMIC=0.0
      TIMER DELT=0.005,FINTIM=12.4,CUTDEL=0.05,PPDEL=0.05
      METHOD RKSFX
      PRTPLOT FORCE(FEDRAT,CHIP)
      LABEL SIMULATION OF FIG.4.13 WITH KPRO=0.05, KINT=0.003
      RPM = 69.0
      OMEGA = 2*3.1416*RPM/60.0
      TR = 60.0/RPM
      TC = 0.05
      KG = 0.00345
      KF = 1.0
      KC = 118800.0
      E = 0.06
      D = 0.03
      DECAY = 0.8
      DEKAY = 1.0-(1.0-DECAY)*TC/TR
      MSTART = 0.02
      C = 0.0
      PV = 0.0
      SUM = 0.0
      TEST = 0.0
      PEAK = 0.0
      FDIFFO = 0.0
      CLOSUM = 0.0
DYNAMIC
      FNOM = 50.0
      FEDRAT = FEED*KG
      FDSIT = INTGRL(LIMIC,FEDRAT)
      DELAY = DELAY(100,TR,POSIT)
      MNOW = AMAX1(MSTART,DELAY)
      CHIPT = POSIT-MNOW
      CHIP = LIMIT(0.0,1000.0,CHIPT)
      FORCE = CHIP*KC*(P+D*COS(OMEGA*TIME))
      F = FORCE*KF
      FEED = ZHOLD(PULSE,ZCHIN)
      PULSE = IMPULS(0.0,TC)
PROCEDURE ZCHIN,FDIFF=DUMMY(KPRO,KINT,FNOM,F,PULSE,FDIFFO, ...
          SUM,C,PEAK,PV,CLOSUM,TEST)
      IF (PULSE.NE.1.0) GOTO 10
      IF (KEEP.NE.1.0) GOTO 10
      COMPAR = PEAK-F
      IF (COMPAR.GE.0.0) GOTO 1
      PV = F
```

```
      GOTO 2
1     PV = PEAK-DEKAY
2     PEAK = PV
      PDIFF = PNOW-PV
      SUM = SUM+KINT*PDIFFO
      TEST = (SUM-0.0)*(5.0-SUM)
      IF (TEST.LE.0.0) GOTO 11
      C = SUM+KPRO*PDIFFO
      CLDSUM = SUM
      GOTO 22
11    C = CLDSUM+KPRO*PDIFFO
      SUM = CLDSUM
22    ?CHIN = LIMIT(0.0,1.0,C)
      PDIFFO = PDIFF
10    CONTINU
      ENDPROCEDURE
TERMINAL
END
      PARAM KPRO=0.1,KINT=0.002
      RESET LABEL
      LABEL SIMULATION OF FIG.4.1  WITH KPRO=0.1, KINT=0.002
END
      PARAM KPRO=0.35,KINT=0.003
      RESET LABEL
      LABEL SIMULATION OF FIG.4.1 WITH KPRO=0.35, KINT=0.003
END
STOP
```

SIMULATION OF FIG.4.13 WITH KPRO=0.1, KINT=0.002 PAGE 1

MINIMUM FORCE VERSUS TIME MAXIMUM
0.0 1.1455E+02

TIME	FORCE		FEDRAT	CHIP
0.0	0.0	+	0.0	0.0
5.000E-02	0.0	+	1.7250E-02	0.0
1.0000E-01	0.0	+	1.7250E-02	0.0
1.5000E-01	0.0	+	1.7250E-02	0.0
2.0000E-01	0.0	+	1.7250E-02	0.0
2.5000E-01	0.0	+	1.7250E-02	0.0
3.0000E-01	0.0	+	1.7250E-02	0.0
3.5000E-01	0.0	+	1.7250E-02	0.0
4.0000E-01	0.0	+	1.7250E-02	0.0
4.5000E-01	0.0	+	1.7250E-02	0.0
5.0000E-01	0.0	+	1.7250E-02	0.0
5.5000E-01	0.0	+	1.7250E-02	0.0
6.0000E-01	0.0	+	1.7250E-02	0.0
6.5000E-01	0.0	+	1.7250E-02	0.0
7.0000E-01	0.0	+	1.7250E-02	0.0
7.5000E-01	0.0	+	1.7250E-02	0.0
8.0000E-01	0.0	+	1.7250E-02	0.0
8.5000E-01	0.0	+	1.7250E-02	0.0
9.0000E-01	0.0	+	1.7250E-02	0.0
9.5000E-01	0.0	+	1.7250E-02	0.0
1.0000E+00	0.0	+	1.7250E-02	0.0
1.0500E+00	0.0	+	1.7250E-02	0.0
1.1000E+00	0.0	+	1.7250E-02	0.0
1.1500E+00	0.0	+	1.7250E-02	0.0
1.2000E+00	0.0	+	1.7250E-02	0.0
1.2500E+00	2.6831E+00	-+	1.7250E-02	6.9959E-04
1.3000E+00	5.3699E+00	--+	1.7250E-02	1.5621E-03
1.3500E+00	9.1070E+00	---+	1.7250E-02	2.4245E-03
1.4000E+00	1.4403E+01	-------+	1.7250E-02	3.2870E-03
1.4500E+00	2.2251E+01	----------+	1.7250E-02	4.1495E-03
1.5000E+00	3.2931E+01	--------------+	1.7250E-02	5.0120E-03
1.5500E+00	4.6119E+01	----------------------+	1.7250E-02	5.8745E-03
1.6000E+00	6.0887E+01	----------------------------+	1.7250E-02	6.7369E-03
1.6500E+00	7.5828E+01	---------------------------------+	1.7250E-02	7.5994E-03
1.7000E+00	8.9277E+01	------------------------------------+	1.7250E-02	8.4619E-03
1.7500E+00	9.9594E+01	--+	1.3642E-02	9.3244E-03
1.8000E+00	1.0359E+02	--+	9.9475E-03	1.0006E-02
1.8500E+00	1.0092E+02	--+	8.4044E-03	1.0504E-02
1.9000E+00	9.3328E+01	--+	8.6608E-03	1.0924E-02
1.9500E+00	8.2859E+01	------------------------------------+	8.9206E-03	1.1357E-02
2.0000E+00	7.1133E+01	----------------------------+	9.1838E-03	1.1803E-02
2.0500E+00	6.0080E+01	------------------------+	9.4503E-03	1.2262E-02
2.1000E+00	5.0237E+01	----------------------+	9.7201E-03	1.2373E-02
2.1500E+00	4.3391E+01	------------------+	9.9932E-03	1.1996E-02
2.2000E+00	4.2196E+01	------------------+	1.0269E-02	1.1633E-02
2.2500E+00	4.6144E+01	--------------------+	1.0549E-02	1.1284E-02
2.3000E+00	5.4129E+01	------------------------+	1.0831E-02	1.0949E-02
2.3500E+00	6.4621E+01	--------------------------+	1.1117E-02	1.0628E-02
2.4000E+00	7.5883E+01	------------------------------+	1.1406E-02	1.0322E-02
2.4500E+00	8.6200E+01	----------------------------------+	1.1697E-02	1.0030E-02

FORCE VERSUS TIME

MINIMUM 0.0 MAXIMUM 1.1455E+02

TIME	FORCE	FEDRAT	CHIP
2.550 E+00	9.8461E+01	1.0185E-02	9.4890E-03
2.600 E+00	9.7616E+01	8.5492E-03	9.1358E-03
2.650 E+00	9.2814E+01	8.8203E-03	8.8106E-03
2.700 E+00	8.6334E+01	9.0946E-03	8.6819E-03
2.750 E+00	7.8099E+01	9.3721E-03	8.6862E-03
2.800 E+00	6.8032E+01	9.6528E-03	8.7268E-03
2.850 E+00	5.7128E+01	9.9366E-03	8.7685E-03
2.900 E+00	4.6821E+01	1.0223E-02	8.8113E-03
2.950 E+00	3.8489E+01	1.0513E-02	8.8551E-03
3.000 E+00	3.3272E+01	1.0806E-02	8.9000E-03
3.050 E+00	3.1919E+01	1.1102E-02	8.9460E-03
3.100 E+00	3.4687E+01	1.1401E-02	8.9931E-03
3.150 E+00	4.1306E+01	1.1703E-02	9.0411E-03
3.200 E+00	5.1002E+01	1.2007E-02	9.0903E-03
3.250 E+00	6.2597E+01	1.2315E-02	9.1404E-03
3.300 E+00	7.4697E+01	1.2625E-02	9.1915E-03
3.350 E+00	8.5669E+01	1.2938E-02	9.2436E-03
3.400 E+00	9.4242E+01	1.1902E-02	9.2966E-03
3.450 E+00	9.9247E+01	8.8457E-03	9.3471E-03
3.500 E+00	9.9346E+01	6.9866E-03	9.3299E-03
3.550 E+00	9.4503E+01	6.8185E-03	9.2435E-03
3.600 E+00	8.5867E+01	7.0870E-03	9.1351E-03
3.650 E+00	7.4759E+01	7.3588E-03	9.0262E-03
3.700 E+00	6.2561E+01	7.6339E-03	8.9170E-03
3.750 E+00	5.0766E+01	7.9121E-03	8.8074E-03
3.800 E+00	4.0776E+01	8.1934E-03	8.6975E-03
3.850 E+00	3.3725E+01	8.4779E-03	8.5872E-03
3.900 E+00	3.0344E+01	8.7655E-03	8.4765E-03
3.950 E+00	3.0871E+01	9.0561E-03	8.3654E-03
4.000 E+00	3.5036E+01	9.3497E-03	8.2540E-03
4.050 E+00	4.2106E+01	9.6462E-03	8.1422E-03
4.100 E+00	5.0996E+01	9.9457E-03	8.0301E-03
4.150 E+00	6.0414E+01	1.0248E-02	7.9177E-03
4.200 E+00	6.9035E+01	1.0553E-02	7.8049E-03
4.250 E+00	7.5673E+01	1.0862E-02	7.6917E-03
4.300 E+00	7.9862E+01	1.1172E-02	7.6194E-03
4.350 E+00	8.2068E+01	1.1486E-02	7.6760E-03
4.400 E+00	8.2120E+01	1.1803E-02	7.8646E-03
4.450 E+00	7.9191E+01	1.1613E-02	8.1106E-03
4.500 E+00	7.2959E+01	1.1931E-02	8.3421E-03
4.550 E+00	6.4483E+01	1.2251E-02	8.5760E-03
4.600 E+00	5.5002E+01	1.2574E-02	8.8122E-03
4.650 E+00	4.5965E+01	1.2900E-02	9.0508E-03
4.700 E+00	3.8841E+01	1.3228E-02	9.2916E-03
4.750 E+00	3.4926E+01	1.3559E-02	9.5346E-03
4.800 E+00	3.5131E+01	1.3892E-02	9.7800E-03
4.850 E+00	3.9893E+01	1.4228E-02	1.0027E-02
4.900 E+00	4.9034E+01	1.4567E-02	1.0277E-02
4.950 E+00	6.1786E+01	1.4907E-02	1.0529E-02
5.000 E+00	7.6858E+01	1.5251E-02	1.0782E-02

TIME	FORCE	FEDRAT	CHIP
5.1000E+00	1.0625E+02	8.1894E-03	1.1201E-02
5.1500E+00	1.1381E+02	3.2963E-03	1.1073E-02
5.2000E+00	1.1395E+02	4.5374E-04	1.0685E-02
5.2500E+00	1.0742E+02	1.7199E-04	1.0140E-02
5.3000E+00	9.6365E+01	3.9888E-04	9.5641E-03
5.3500E+00	8.2590E+01	6.2952E-04	8.9995E-03
5.4000E+00	6.7641E+01	8.6385E-04	8.4402E-03
5.4500E+00	5.3064E+01	1.1018E-03	7.8768E-03
5.5000E+00	4.0273E+01	1.3434E-03	7.3093E-03
5.5500E+00	3.0264E+01	1.5886E-03	6.7375E-03
5.6000E+00	2.3502E+01	1.8373E-03	6.1618E-03
5.6500E+00	1.9897E+01	2.0895E-03	5.5821E-03
5.7000E+00	1.8866E+01	2.3451E-03	4.9984E-03
5.7500E+00	1.9485E+01	2.6041E-03	4.4104E-03
5.8000E+00	2.0664E+01	2.8665E-03	3.8188E-03
5.8500E+00	2.1359E+01	3.1322E-03	3.2235E-03
5.9000E+00	2.0746E+01	3.4013E-03	2.6242E-03
5.9500E+00	1.8886E+01	3.6736E-03	2.0788E-03
6.0000E+00	1.7475E+01	3.9490E-03	1.7455E-03
6.0500E+00	1.7779E+01	4.2277E-03	1.6827E-03
6.1000E+00	1.9383E+01	4.5095E-03	1.8155E-03
6.1500E+00	2.0934E+01	4.7945E-03	2.0269E-03
6.2000E+00	2.1539E+01	5.0825E-03	2.2513E-03
6.2500E+00	2.1048E+01	5.3735E-03	2.4786E-03
6.3000E+00	1.9609E+01	5.6675E-03	2.7086E-03
6.3500E+00	1.7571E+01	5.9645E-03	2.9415E-03
6.4000E+00	1.5430E+01	6.2645E-03	3.1775E-03
6.4500E+00	1.3774E+01	6.5673E-03	3.4160E-03
6.5000E+00	1.3194E+01	6.8730E-03	3.6569E-03
6.5500E+00	1.4192E+01	7.1816E-03	3.9008E-03
6.6000E+00	1.7084E+01	7.4929E-03	4.1477E-03
6.6500E+00	2.1935E+01	7.8070E-03	4.3973E-03
6.7000E+00	2.8517E+01	8.1238E-03	4.6492E-03
6.7500E+00	3.6328E+01	8.4434E-03	4.9040E-03
6.8000E+00	4.4625E+01	8.7656E-03	5.1615E-03
6.8500E+00	5.2520E+01	9.0904E-03	5.4214E-03
6.9000E+00	5.9104E+01	9.4179E-03	5.6837E-03
6.9500E+00	6.3582E+01	9.7480E-03	5.9489E-03
7.0000E+00	6.5379E+01	1.0081E-02	6.2162E-03
7.0500E+00	6.4270E+01	1.0416E-02	6.4858E-03
7.1000E+00	6.0429E+01	1.0753E-02	6.7579E-03
7.1500E+00	5.4438E+01	1.1093E-02	7.0328E-03
7.2000E+00	4.7221E+01	1.1436E-02	7.3099E-03
7.2500E+00	3.9962E+01	1.1781E-02	7.5893E-03
7.3000E+00	3.3938E+01	1.2128E-02	7.8711E-03
7.3500E+00	3.0350E+01	1.2478E-02	8.1553E-03
7.4000E+00	3.0145E+01	1.2830E-02	8.4415E-03
7.4500E+00	3.3871E+01	1.3184E-02	8.7301E-03
7.5000E+00	4.1566E+01	1.3541E-02	9.0204E-03
7.5500E+00	5.2727E+01	1.3899E-02	9.3132E-03

FORCE VERSUS TIME

TIME	FORCE	FEDRAT	CHIP
7.650 E+00	8.0966E+01	1.4294E-02	9.9052E-03
7.700 E+00	9.4877E+01	9.2334E-03	1.0188E-02
7.750 E+00	1.0372E+02	4.3384E-03	1.0201E-02
7.800 E+00	1.0579E+02	1.1247E-03	9.9535E-03
7.850 E+00	1.0138E+02	2.3005E-04	9.5289E-03
7.900 E+00	9.2199E+01	4.8019E-04	9.0430E-03
7.950 E+00	8.0024E+01	7.3381E-04	8.5531E-03
8.000 E+00	6.6315E+01	9.9087E-04	8.0585E-03
8.050 E+00	5.2618E+01	1.2513E-03	7.5603E-03
8.100 E+00	4.0314E+01	1.5151E-03	7.0574E-03
8.150 E+00	3.0446E+01	1.7822E-03	6.5510E-03
8.200 E+00	2.3576E+01	2.0526E-03	6.0403E-03
8.250 E+00	1.9756E+01	2.3262E-03	5.5262E-03
8.300 E+00	1.8588E+01	2.6031E-03	5.0080E-03
8.350 E+00	1.9192E+01	2.8831E-03	4.4861E-03
8.400 E+00	2.0667E+01	3.1662E-03	3.9603E-03
8.450 E+00	2.1976E+01	3.4524E-03	3.4308E-03
8.500 E+00	2.2269E+01	3.7417E-03	2.8974E-03
8.550 E+00	2.1079E+01	4.0340E-03	2.3701E-03
8.600 E+00	1.9857E+01	4.3292E-03	2.0110E-03
8.650 E+00	2.0109E+01	4.6275E-03	1.9152E-03
8.700 E+00	2.1676E+01	4.9286E-03	2.0276E-03
8.750 E+00	2.3394E+01	5.2326E-03	2.2450E-03
8.800 E+00	2.4189E+01	5.5395E-03	2.4871E-03
8.850 E+00	2.3759E+01	5.8492E-03	2.7322E-03
8.900 E+00	2.2240E+01	6.1617E-03	2.9799E-03
8.950 E+00	1.9987E+01	6.4770E-03	3.2304E-03
9.000 E+00	1.7533E+01	6.7949E-03	3.4837E-03
9.050 E+00	1.5517E+01	7.1156E-03	3.7398E-03
9.100 E+00	1.4591E+01	7.4389E-03	3.9979E-03
9.150 E+00	1.5331E+01	7.7649E-03	4.2590E-03
9.200 E+00	1.8112E+01	8.0934E-03	4.5224E-03
9.250 E+00	2.3049E+01	8.4245E-03	4.7883E-03
9.300 E+00	2.9941E+01	8.7582E-03	5.0567E-03
9.350 E+00	3.8274E+01	9.0944E-03	5.3275E-03
9.400 E+00	4.7272E+01	9.4330E-03	5.6008E-03
9.450 E+00	5.5986E+01	9.7741E-03	5.8766E-03
9.500 E+00	6.3411E+01	1.0118E-02	6.1542E-03
9.550 E+00	6.8657E+01	1.0464E-02	6.4343E-03
9.600 E+00	7.1062E+01	1.0812E-02	6.7167E-03
9.650 E+00	7.0320E+01	1.0705E-02	7.0014E-03
9.700 E+00	6.6347E+01	1.1055E-02	7.2662E-03
9.750 E+00	5.9958E+01	1.1406E-02	7.5327E-03
9.800 E+00	5.2119E+01	1.1760E-02	7.8011E-03
9.850 E+00	4.4070E+01	1.2116E-02	8.0714E-03
9.900 E+00	3.7165E+01	1.2475E-02	8.3435E-03
9.950 E+00	3.2696E+01	1.2835E-02	8.6178E-03
1.000 E+01	3.1697E+01	1.3198E-02	8.8937E-03
1.005 E+01	3.4800E+01	1.3563E-02	9.1718E-03
1.010 E+01	4.2100E+01	1.3930E-02	9.4517E-03
1.015 E+01	5.3151E+01		

FORCE VERSUS TIME

MINIMUM 0.0 MAXIMUM 1.1455E+02

TIME	FORCE	FEDRAT	CHIP
1.020E+01	6.6932E+01	1.4671E-02	1.0017E-02
1.025E+01	8.2013E+01	1.3257E-02	1.0303E-02
1.030E+01	9.5889E+01	8.0400E-03	1.0501E-02
1.035E+01	1.0467E+02	3.1432E-03	1.0421E-02
1.040E+01	1.0664E+02	0.0	1.0079E-02
1.045E+01	1.0204E+02	0.0	9.5631E-03
1.050E+01	9.3038E+01	0.0	9.0299E-03
1.055E+01	8.0905E+01	0.0	8.4928E-03
1.060E+01	6.7070E+01	0.0	7.9470E-03
1.065E+01	5.3043E+01	9.2763E-05	7.3839E-03
1.070E+01	4.0303E+01	3.5427E-04	6.8074E-03
1.075E+01	2.9967E+01	6.1911E-04	6.2261E-03
1.080E+01	2.2586E+01	8.8725E-04	5.6400E-03
1.085E+01	1.8177E+01	1.1587E-03	5.0498E-03
1.090E+01	1.6260E+01	1.4333E-03	4.4550E-03
1.095E+01	1.5999E+01	1.7111E-03	3.8558E-03
1.100E+01	1.6369E+01	1.9921E-03	3.2521E-03
1.105E+01	1.6362E+01	2.2762E-03	2.6442E-03
1.110E+01	1.5163E+01	2.5634E-03	2.0316E-03
1.115E+01	1.2778E+01	2.8536E-03	1.4694E-03
1.120E+01	1.0776E+01	3.1468E-03	1.1079E-03
1.125E+01	1.0547E+01	3.4430E-03	1.0121E-03
1.130E+01	1.1998E+01	3.7422E-03	1.1224E-03
1.135E+01	1.3743E+01	4.0442E-03	1.3089E-03
1.140E+01	1.4919E+01	4.3492E-03	1.5110E-03
1.145E+01	1.5367E+01	4.6569E-03	1.7279E-03
1.150E+01	1.5065E+01	4.9675E-03	1.9604E-03
1.155E+01	1.4128E+01	5.2809E-03	2.2058E-03
1.160E+01	1.2821E+01	5.5970E-03	2.4571E-03
1.165E+01	1.1599E+01	5.9158E-03	2.7114E-03
1.170E+01	1.0999E+01	6.2373E-03	2.9683E-03
1.175E+01	1.1539E+01	6.5614E-03	3.2276E-03
1.180E+01	1.3620E+01	6.8882E-03	3.4893E-03
1.185E+01	1.7446E+01	7.2176E-03	3.7533E-03
1.190E+01	2.2966E+01	7.5495E-03	4.0200E-03
1.195E+01	2.9856E+01	7.8839E-03	4.2894E-03
1.200E+01	3.7536E+01	8.2209E-03	4.5611E-03

SIMULATION OF FIG.4.13 WITH KPRO=0.35, KINT=0.003 PAGE 1

FORCE VERSUS TIME

MINIMUM 0.0 MAXIMUM 1.2627E+02

TIME	FORCE	I	FEDRAT	CHIP
0.0	0.0	+	0.0	0.0
5.0000E-02	0.0	+	1.7250E-02	0.0
1.0000E-01	0.0	+	1.7250E-02	0.0
1.5000E-01	0.0	+	1.7250E-02	0.0
2.0000E-01	0.0	+	1.7250E-02	0.0
2.5000E-01	0.0	+	1.7250E-02	0.0
3.0000E-01	0.0	+	1.7250E-02	0.0
3.5000E-01	0.0	+	1.7250E-02	0.0
4.0000E-01	0.0	+	1.7250E-02	0.0
4.5000E-01	0.0	+	1.7250E-02	0.0
5.0000E-01	0.0	+	1.7250E-02	0.0
5.5000E-01	0.0	+	1.7250E-02	0.0
6.0000E-01	0.0	+	1.7250E-02	0.0
6.5000E-01	0.0	+	1.7250E-02	0.0
7.0000E-01	0.0	+	1.7250E-02	0.0
7.5000E-01	0.0	+	1.7250E-02	0.0
8.0000E-01	0.0	+	1.7250E-02	0.0
8.5000E-01	0.0	+	1.7250E-02	0.0
9.0000E-01	0.0	+	1.7250E-02	0.0
9.5000E-01	0.0	+	1.7250E-02	0.0
1.0000E+00	0.0	+	1.7250E-02	0.0
1.0500E+00	0.0	+	1.7250E-02	0.0
1.1000E+00	0.0	+	1.7250E-02	0.0
1.1500E+00	0.0	+	1.7250E-02	0.0
1.2000E+00	0.0	+	1.7250E-02	0.0
1.2500E+00	2.6831E+00	-+	1.7250E-02	6.9959E-04
1.3000E+00	5.5699E+00	--+	1.7250E-02	1.5621E-03
1.3500E+00	9.1070E+00	---+	1.7250E-02	2.4245E-03
1.4000E+00	1.4403E+01	-----+	1.7250E-02	3.2870E-03
1.4500E+00	2.2251E+01	--------+	1.7250E-02	4.1495E-03
1.5000E+00	3.2931E+01	----------+	1.7250E-02	5.0120E-03
1.5500E+00	4.6119E+01	----------+	1.7250E-02	5.8745E-03
1.6000E+00	6.0987E+01	----------+	1.7250E-02	6.7369E-03
1.6500E+00	7.5828E+01	----------+	1.7250E-02	7.5994E-03
1.7000E+00	8.9277E+01	----------+	1.7250E-02	8.4619E-03
1.7500E+00	9.9594E+01	----------+	5.9406E-03	9.3244E-03
1.8000E+00	9.9608E+01	----------+	0.0	9.6214E-03
1.8500E+00	9.2444E+01	----------+	0.0	9.6214E-03
1.9000E+00	8.2199E+01	----------+	0.0	9.6214E-03
1.9500E+00	7.0196E+01	----------+	0.0	9.6214E-03
2.0000E+00	5.7984E+01	----------+	0.0	9.6214E-03
2.0500E+00	4.7141E+01	----------+	0.0	9.6214E-03
2.1000E+00	3.7696E+01	----------+	0.0	9.2593E-03
2.1500E+00	3.0372E+01	----------+	1.5100E-04	8.3969E-03
2.2000E+00	2.7399E+01	----------+	1.3187E-03	7.5419E-03
2.2500E+00	2.7583E+01	----------+	2.4825E-03	6.7453E-03
2.3000E+00	2.9696E+01	----------+	3.6424E-03	6.0069E-03
2.3500E+00	3.2386E+01	----------+	4.7985E-03	5.3265E-03
2.4000E+00	3.4583E+01	----------+	5.9508E-03	4.7040E-03
2.4500E+00	3.5573E+01	----------+	7.0994E-03	4.1390E-03
[illegible]	[illegible]	----------+	8.2443E-03	3.6315E-03

FORCE VERSUS TIME

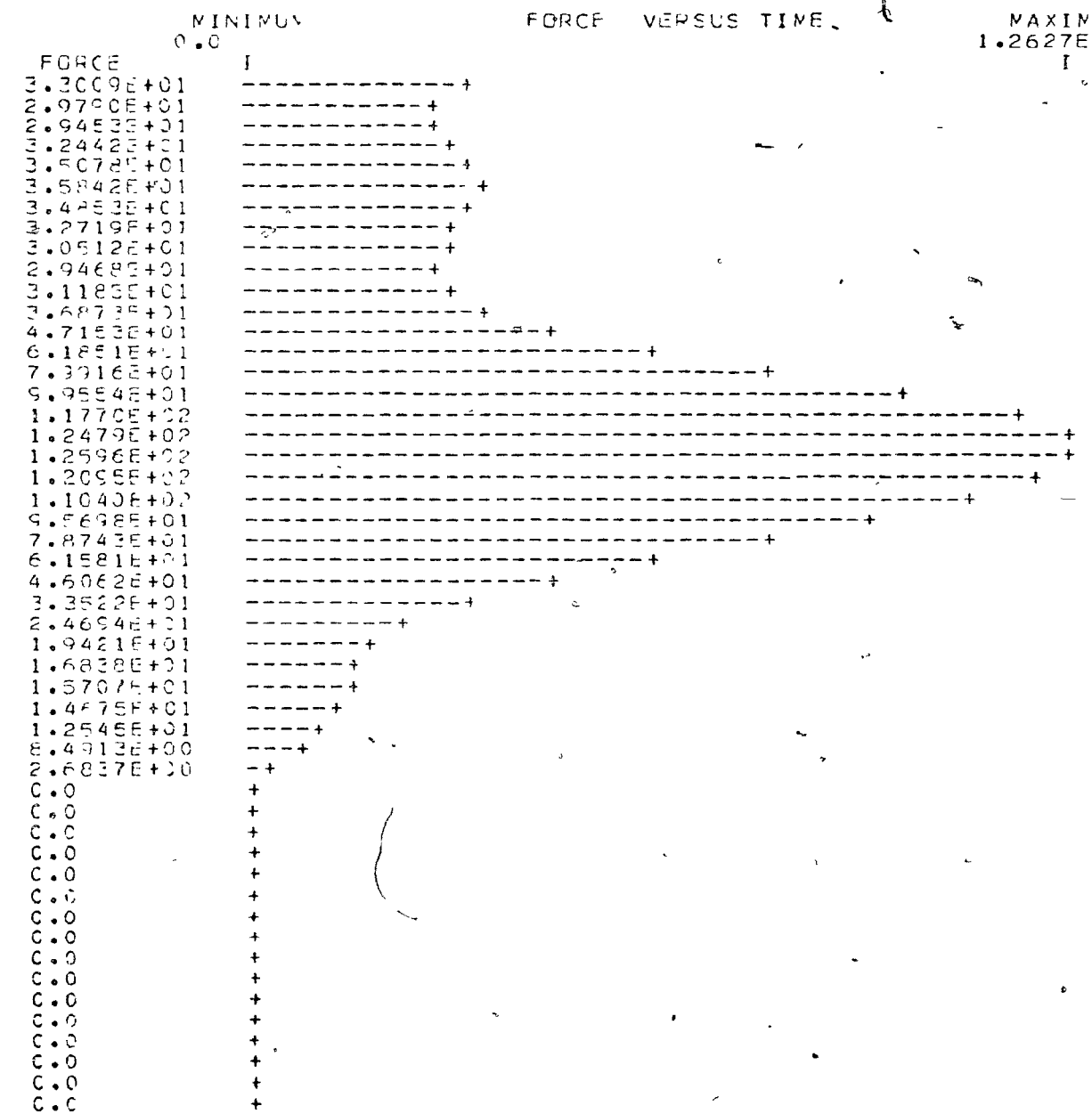

TIME	FORCE	FEDRAT	CHIP
2.550 E+00	3.3009E+01	9.3856E-03	3.1812E-03
2.600 E+00	2.9790E+01	1.0523E-02	2.7880E-03
2.650 E+00	2.9453E+01	1.1657E-02	2.7959E-03
2.700 E+00	3.2442E+01	1.2788E-02	3.2625E-03
2.750 E+00	3.5078E+01	1.3915E-02	3.9019E-03
2.800 E+00	3.5842E+01	1.5039E-02	4.5976E-03
2.850 E+00	3.4853E+01	1.6159E-02	5.3495E-03
2.900 E+00	3.2719E+01	1.7250E-02	6.1575E-03
2.950 E+00	3.0512E+01	1.7250E-02	7.0199E-03
3.000 E+00	2.9468E+01	1.7250E-02	7.8824E-03
3.050 E+00	3.1185E+01	1.7250E-02	8.7403E-03
3.100 E+00	3.6873E+01	1.7250E-02	9.5597E-03
3.150 E+00	4.7153E+01	1.7250E-02	1.0321E-02
3.200 E+00	6.1851E+01	1.7250E-02	1.1024E-02
3.250 E+00	7.9916E+01	1.7250E-02	1.1669E-02
3.300 E+00	9.9554E+01	1.5508E-02	1.2257E-02
3.350 E+00	1.1770E+02	0.0	1.2700E-02
3.400 E+00	1.2479E+02	0.0	1.2810E-02
3.450 E+00	1.2596E+02	0.0	1.1863E-02
3.500 E+00	1.2095E+02	0.0	1.1359E-02
3.550 E+00	1.1040E+02	0.0	1.0798E-02
3.600 E+00	9.5698E+01	0.0	1.0181E-02
3.650 E+00	7.8743E+01	0.0	9.5073E-03
3.700 E+00	6.1581E+01	0.0	8.7774E-03
3.750 E+00	4.6062E+01	0.0	7.9913E-03
3.800 E+00	3.3522E+01	0.0	7.1502E-03
3.850 E+00	2.4694E+01	0.0	6.2877E-03
3.900 E+00	1.9421E+01	0.0	5.4252E-03
3.950 E+00	1.6838E+01	0.0	4.5628E-03
4.000 E+00	1.5707E+01	0.0	3.7003E-03
4.050 E+00	1.4675E+01	0.0	2.8378E-03
4.100 E+00	1.2545E+01	0.0	1.9753E-03
4.150 E+00	8.4913E+00	0.0	1.1129E-03
4.200 E+00	2.6837E+00	0.0	3.0341E-04
4.250 E+00	0.0	0.0	0.0
4.300 E+00	0.0	0.0	0.0
4.350 E+00	0.0	0.0	0.0
4.400 E+00	0.0	0.0	0.0
4.450 E+00	0.0	0.0	0.0
4.500 E+00	0.0	0.0	0.0
4.550 E+00	0.0	0.0	0.0
4.600 E+00	0.0	0.0	0.0
4.650 E+00	0.0	0.0	0.0
4.700 E+00	0.0	0.0	0.0
4.750 E+00	0.0	0.0	0.0
4.800 E+00	0.0	0.0	0.0
4.850 E+00	0.0	0.0	0.0
4.900 E+00	0.0	0.0	0.0
4.950 E+00	0.0	0.0	0.0
5.000 E+00	0.0	0.0	0.0

SIMULATION OF FIG.4.13 WITH KPRO=0.35, KINT=0.003

FORCE VERSUS TIME

MINIMUM 0.0 — MAXIMUM 1.2627E+02

TIME	FORCE	I	FECRAT	CHIP
5.100 E+00	0.0	+	0.0	0.0
5.150 E+00	0.0	+	0.0	0.0
5.200 E+00	0.0	+	0.0	0.0
5.250 E+00	0.0	+	6.8754E-04	0.0
5.300 E+00	3.4607E-01	+	1.8227E-03	3.4347E-05
5.350 E+00	1.1514E+00	+	2.9543E-03	1.2547E-04
5.400 E+00	2.1893E+00	+	4.0824E-03	2.7318E-04
5.450 E+00	3.2153E+00	-+	5.2071E-03	4.7728E-04
5.500 E+00	4.0641E+00	-+	6.3283E-03	7.3761E-04
5.550 E+00	4.7344E+00	-+	7.4462E-03	1.0540E-03
5.600 E+00	5.4402E+00	--+	8.5607E-03	1.4263E-03
5.650 E+00	6.0097E+00	--+	9.6728E-03	1.8543E-03
5.700 E+00	8.8251E+00	---+	1.0780E-02	2.3379E-03
5.750 E+00	1.2710E+01	------+	1.1885E-02	2.8769E-03
5.800 E+00	1.9783E+01	-------+	1.2986E-02	3.4711E-03
5.850 E+00	2.7302E+01	----------+	1.4085E-02	4.1204E-03
5.900 E+00	3.8142E+01	--------------+	1.5180E-02	4.8246E-03
5.950 E+00	5.0726E+01	------------------+	1.6272E-02	5.5836E-03
6.000 E+00	6.4045E+01	------------------------+	1.7250E-02	6.3972E-03
6.050 E+00	7.6704E+01	----------------------------+	1.7250E-02	7.2597E-03
6.100 E+00	8.6714E+01	--------------------------------+	1.0181E-02	8.1222E-03
6.150 E+00	8.8931E+01	---------------------------------+	0.0	8.6103E-03
6.200 E+00	8.1720E+01	-------------------------------+	0.0	8.5414E-03
6.250 E+00	7.1465E+01	----------------------------+	0.0	8.4158E-03
6.300 E+00	5.9611E+01	------------------------+	0.0	8.2338E-03
6.350 E+00	4.7760E+01	---------------------+	0.0	7.9955E-03
6.400 E+00	3.7397E+01	--------------+	0.0	7.7010E-03
6.450 E+00	2.9638E+01	----------+	9.8283E-04	7.3506E-03
6.500 E+00	2.5231E+01	---------+	2.1176E-03	6.9935E-03
6.550 E+00	2.4148E+01	---------+	3.2489E-03	6.6375E-03
6.600 E+00	2.5878E+01	----------+	4.3767E-03	6.2827E-03
6.650 E+00	2.9575E+01	----------+	5.5011E-03	5.9289E-03
6.700 E+00	3.4204E+01	-------------+	6.6220E-03	5.5762E-03
6.750 E+00	3.8702E+01	--------------+	7.7396E-03	5.2245E-03
6.800 E+00	4.2138E+01	---------------+	8.8538E-03	4.8739E-03
6.850 E+00	4.3830E+01	----------------+	9.9643E-03	4.5243E-03
6.900 E+00	4.3459E+01	----------------+	1.1072E-02	4.1792E-03
6.950 E+00	4.1366E+01	---------------+	1.2177E-02	3.8703E-03
7.000 E+00	4.0301E+01	---------------+	1.3278E-02	3.8318E-03
7.050 E+00	4.2576E+01	----------------+	1.4376E-02	4.2965E-03
7.100 E+00	4.4847E+01	-----------------+	1.5471E-02	5.0153E-03
7.150 E+00	4.4809E+01	-----------------+	1.6563E-02	5.7889E-03
7.200 E+00	4.2745E+01	----------------+	1.7250E-02	6.6170E-03
7.250 E+00	3.9384E+01	---------------+	1.7250E-02	7.4795E-03
7.300 E+00	3.5968E+01	--------------+	1.7250E-02	8.3420E-03
7.350 E+00	3.4143E+01	--------------+	1.7250E-02	9.1745E-03
7.400 E+00	3.5644E+01	--------------+	1.7250E-02	9.9533E-03
7.450 E+00	4.1419E+01	----------------+	1.7250E-02	1.0676E-02
7.500 E+00	5.2261E+01	--------------------+	1.7250E-02	1.1341E-02
7.550 E+00	6.7660E+01	--------------------------+	1.7250E-02	1.1951E-02
7.600 E+00	8.6333E+01	---------------------------------+	1.7250E-02	1.2504E-02

FORCE VERSUS TIME

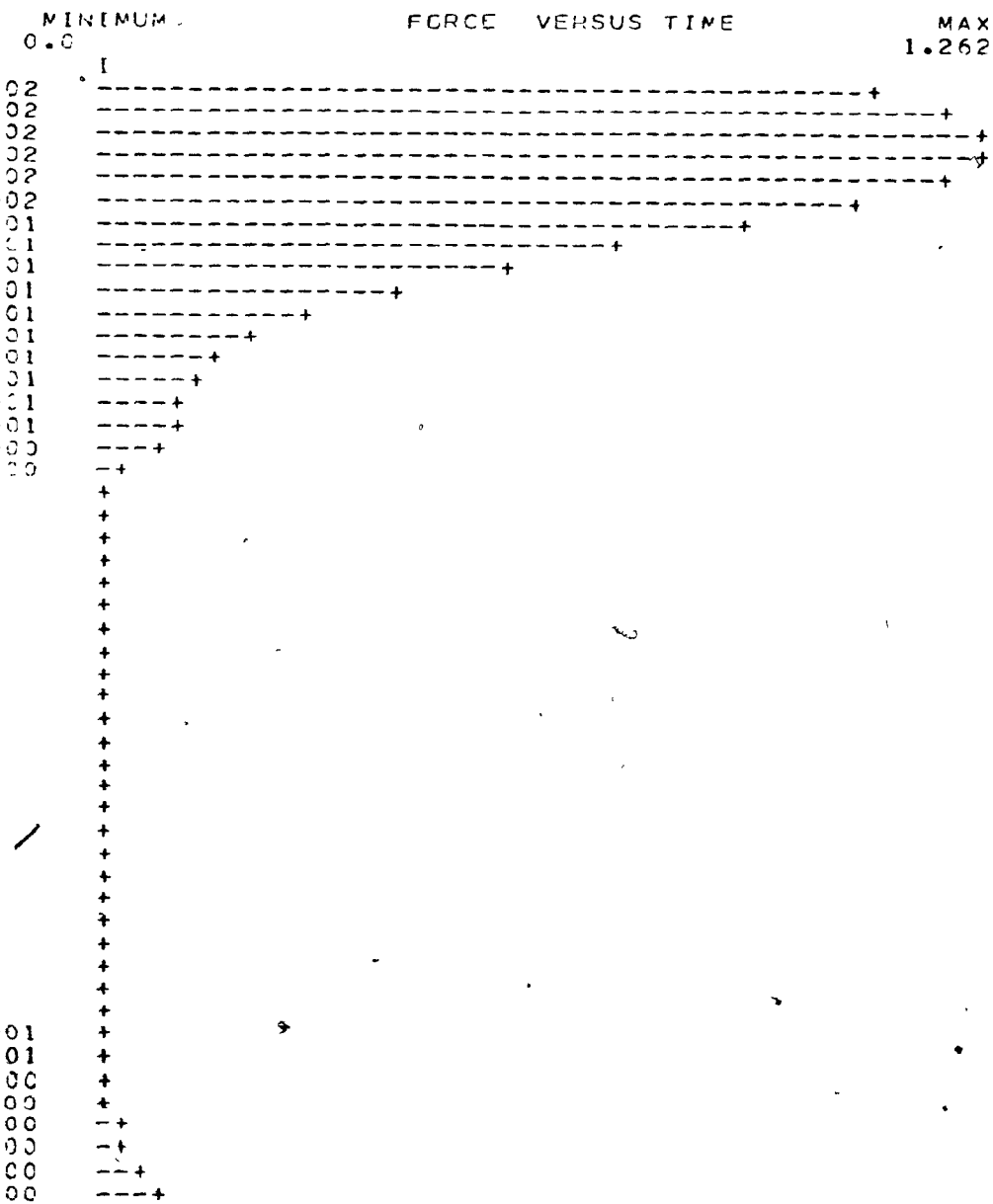

TIME	FORCE	FEDRAT	CHIP
7.650 E+00	1.0630E+02	0.0	1.3001E-02
7.700 E+00	1.1716E+02	0.0	1.2581E-02
7.750 E+00	1.2306E+02	0.0	1.2104E-02
7.800 E+00	1.2300E+02	0.0	1.1572E-02
7.850 E+00	1.1687E+02	0.0	1.0985E-02
7.900 E+00	1.0545E+02	0.0	1.0343E-02
7.950 E+00	9.0243E+01	0.0	9.6453E-03
8.000 E+00	7.3183E+01	0.0	8.8931E-03
8.050 E+00	5.6280E+01	0.0	8.0864E-03
8.100 E+00	4.1342E+01	0.0	7.2373E-03
8.150 E+00	2.9628E+01	0.0	6.3749E-03
8.200 E+00	2.1515E+01	0.0	5.5124E-03
8.250 E+00	1.6623E+01	0.0	4.6499E-03
8.300 E+00	1.4035E+01	0.0	3.7875E-03
8.350 E+00	1.2513E+01	0.0	2.9250E-03
8.400 E+00	1.0763E+01	0.0	2.0625E-03
8.450 E+00	7.6868E+00	0.0	1.2000E-03
8.500 E+00	2.5943E+00	0.0	3.3754E-04
8.550 E+00	0.0	0.0	0.0
8.600 E+00	0.0	0.0	0.0
8.650 E+00	0.0	0.0	0.0
8.700 E+00	0.0	0.0	0.0
8.750 E+00	0.0	0.0	0.0
8.800 E+00	0.0	0.0	0.0
8.850 E+00	0.0	0.0	0.0
8.900 E+00	0.0	0.0	0.0
8.950 E+00	0.0	0.0	0.0
9.000 E+00	0.0	0.0	0.0
9.050 E+00	0.0	0.0	0.0
9.100 E+00	0.0	0.0	0.0
9.150 E+00	0.0	0.0	0.0
9.200 E+00	0.0	0.0	0.0
9.250 E+00	0.0	0.0	0.0
9.300 E+00	0.0	0.0	0.0
9.350 E+00	0.0	0.0	0.0
9.400 E+00	0.0	0.0	0.0
9.450 E+00	0.0	0.0	0.0
9.500 E+00	0.0	0.0	0.0
9.550 E+00	0.0	0.0	0.0
9.600 E+00	0.0	0.0	0.0
9.650 E+00	0.0	0.0	0.0
9.700 E+00	0.0	0.0	0.0
9.750 E+00	3.4159E-01	8.6802E-04	0.0
9.800 E+00	9.4776E-01	1.9859E-03	4.2915E-05
9.850 E+00	1.6207E+00	3.1004E-03	1.4186E-04
9.900 E+00	2.2594E+00	4.2116E-03	2.9683E-04
9.950 E+00	2.9330E+00	5.3195E-03	5.0724E-04
1.000 E+01	3.8961E+00	6.4243E-03	7.7307E-04
1.050 E+01	5.5769E+00	7.5258E-03	1.0937E-03
1.010 E+01	8.4677E+00	8.6242E-03	1.4699E-03
1.015 E+01	1.2627E+02	9.7195E-03	1.9009E-03

FORCE VERSUS TIME

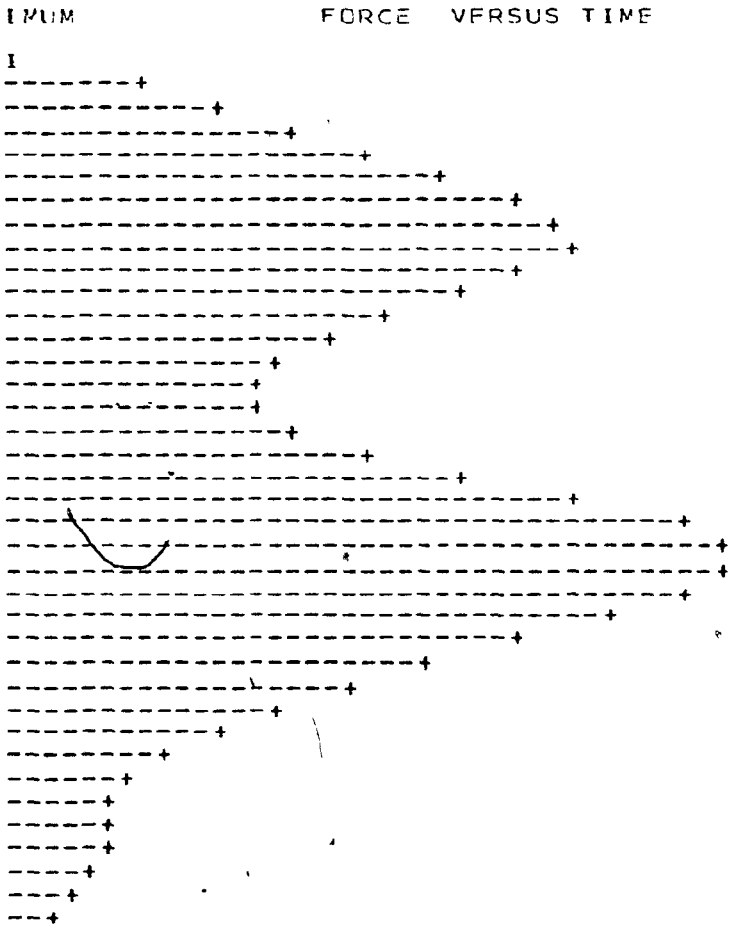

TIME	FORCE	FEDRAT	CHIP
1.0200E+01	1.9554E+01	1.1901E-02	2.9266E-03
1.0250E+01	2.8032E+01	1.2987E-02	3.5214E-03
1.0300E+01	3.8083E+01	1.4070E-02	4.1705E-03
1.0350E+01	4.8953E+01	1.5151E-02	4.8739E-03
1.0400E+01	5.9575E+01	1.6228E-02	5.6309E-03
1.0450E+01	6.8740E+01	1.7250E-02	6.4421E-03
1.0500E+01	7.5262E+01	1.4912E-02	7.3045E-03
1.0550E+01	7.6684E+01	7.0853E-03	8.0496E-03
1.0600E+01	7.0704E+01	5.4026E-03	8.3776E-03
1.0650E+01	6.1568E+01	6.5109E-03	8.5706E-03
1.0700E+01	5.1981E+01	7.6160E-03	8.7630E-03
1.0750E+01	4.3099E+01	8.7179E-03	8.9545E-03
1.0800E+01	3.6627E+01	9.8166E-03	9.1461E-03
1.0850E+01	3.3610E+01	1.0912E-02	9.3374E-03
1.0900E+01	3.4778E+01	1.2005E-02	9.5284E-03
1.0950E+01	4.0328E+01	1.3094E-02	9.7191E-03
1.1000E+01	4.9977E+01	1.4181E-02	9.9093E-03
1.1050E+01	6.2493E+01	1.5264E-02	1.0099E-02
1.1100E+01	7.6792E+01	1.6345E-02	1.0289E-02
1.1150E+01	9.1119E+01	6.1329E-03	1.0478E-02
1.1200E+01	9.8297E+01	0.0	1.0102E-02
1.1250E+01	9.7603E+01	0.0	9.3663E-03
1.1300E+01	9.1682E+01	0.0	8.5763E-03
1.1350E+01	8.1204E+01	0.0	7.7339E-03
1.1400E+01	6.8553E+01	0.0	6.9429E-03
1.1450E+01	5.7237E+01	0.0	6.4358E-03
1.1500E+01	4.7132E+01	0.0	6.1329E-03
1.1550E+01	3.7335E+01	0.0	5.8292E-03
1.1600E+01	2.8544E+01	0.0	5.4703E-03
1.1650E+01	2.1629E+01	0.0	5.0563E-03
1.1700E+01	1.6998E+01	0.0	4.5872E-03
1.1750E+01	1.4526E+01	0.0	4.0633E-03
1.1800E+01	1.3601E+01	0.0	3.4845E-03
1.1850E+01	1.3253E+01	0.0	2.8513E-03
1.1900E+01	1.2362E+01	0.0	2.1638E-03
1.1950E+01	9.8980E+00	0.0	1.4221E-03
1.2000E+01	5.1535E+00	0.0	6.2621E-04

APPENDIX M

NON-ECCENTRIC TURNING EXPERIMENTAL RESULTS FOR BOTH WITH AND WITHOUT PVM IN ALGORITHM

In this appendix the photos of non-eccentric turning are collected. results. It has three sub-appendices as follows:

Appendix M.1 - the experimental results of a P controller

Appendix M.2 - the experimental results of a I controller

Appendix M.3 - the experimental results of a PI controller

APPENDIX M.1 PROPORTIONAL (P) CONTROL

WITHOUT P.V.

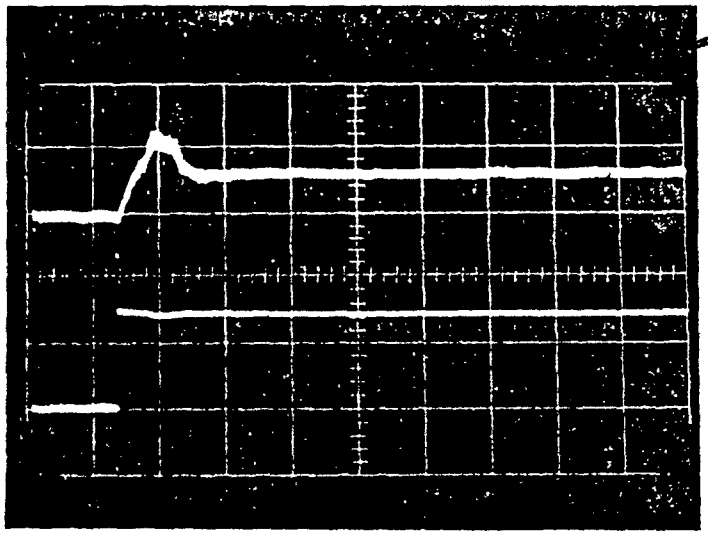

NO. 1a

K_{pro}: 0.005

WITH P.V.

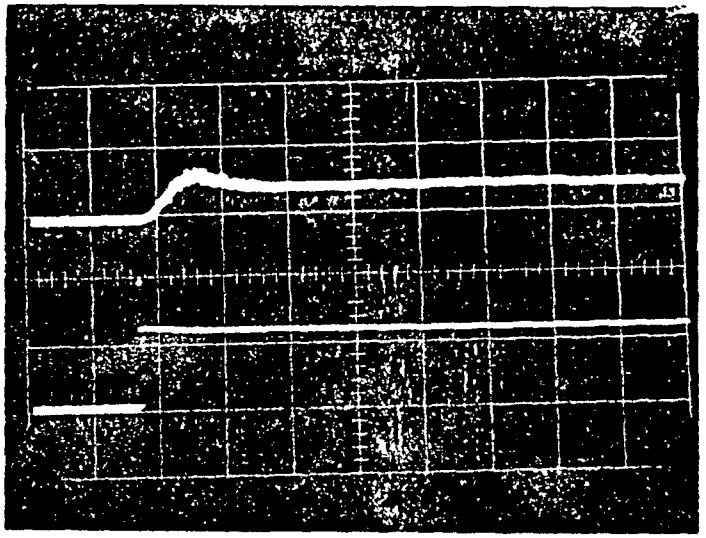

NO. 1b

K_{pro}: 0.005

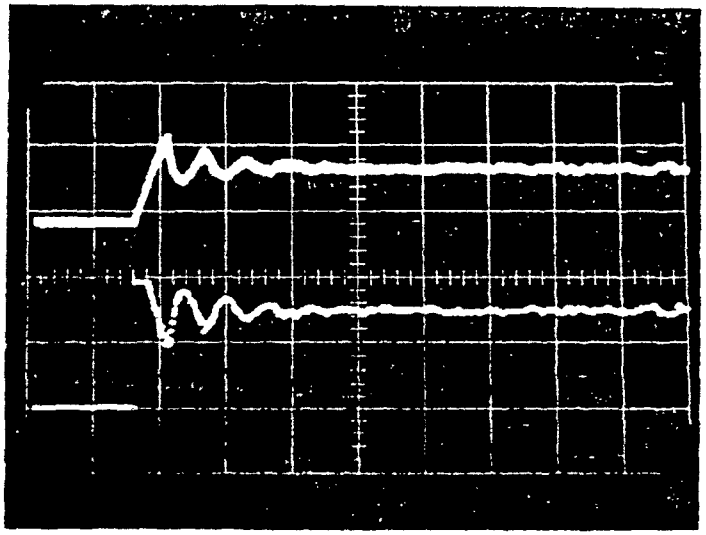

NO. 2a

K_{pro}: 0.15

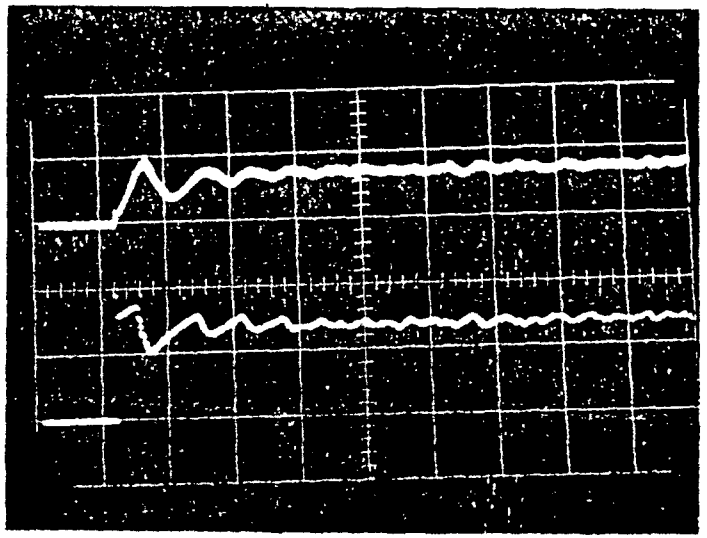

NO. 2b

K_{pro}: 0.22

WITHOUT P.V.

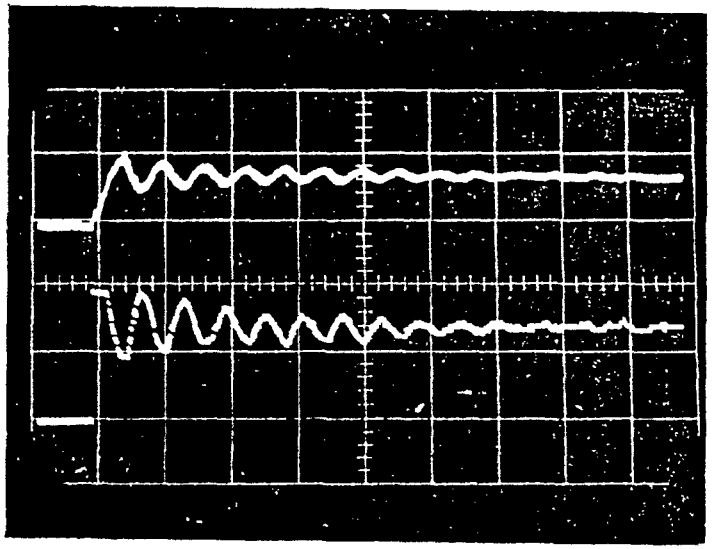

NO. 3a

K_{pro}: 0.24

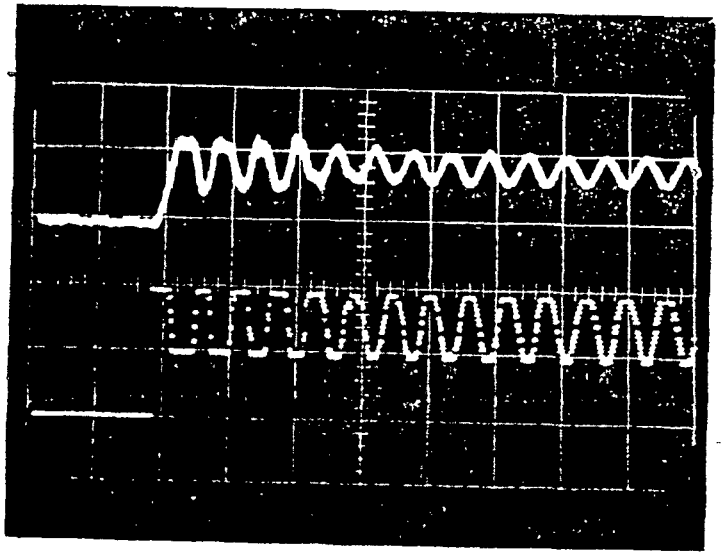

NO. 4a

K_{pro}: 0.35

WITH P.V.

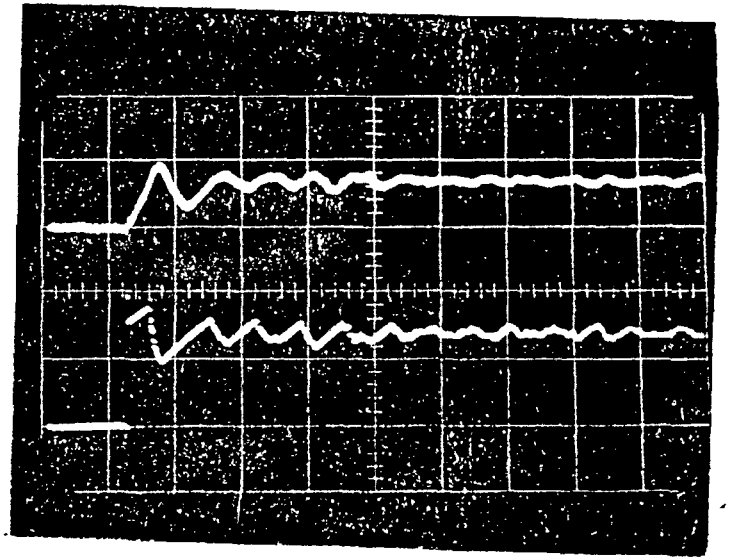

NO. 3b

K_{pro}: 0.23

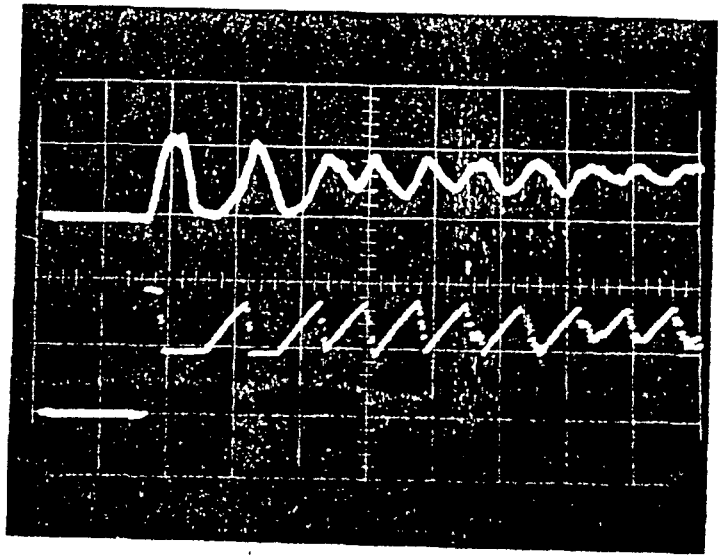

NO.4b

K_{pro}: 0.35

APPENDIX M.2 INTEGRAL (I) CONTROL

WITHOUT P.V.

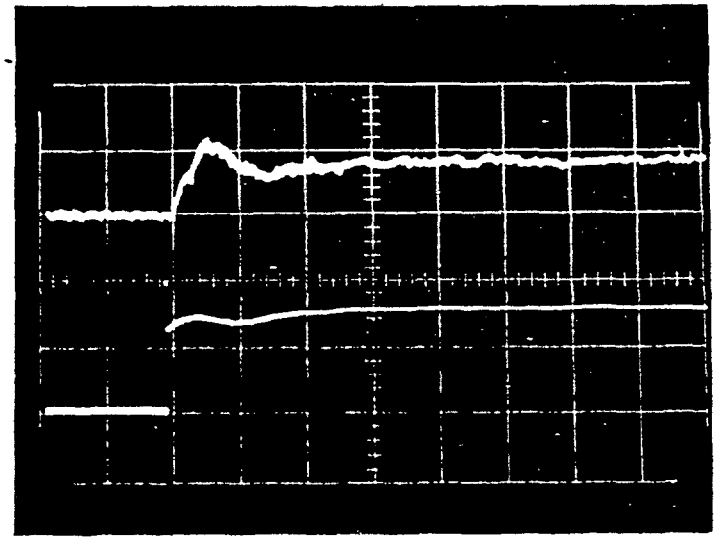

NO. 1a

K_{int}: 0.001

WITH P.V.

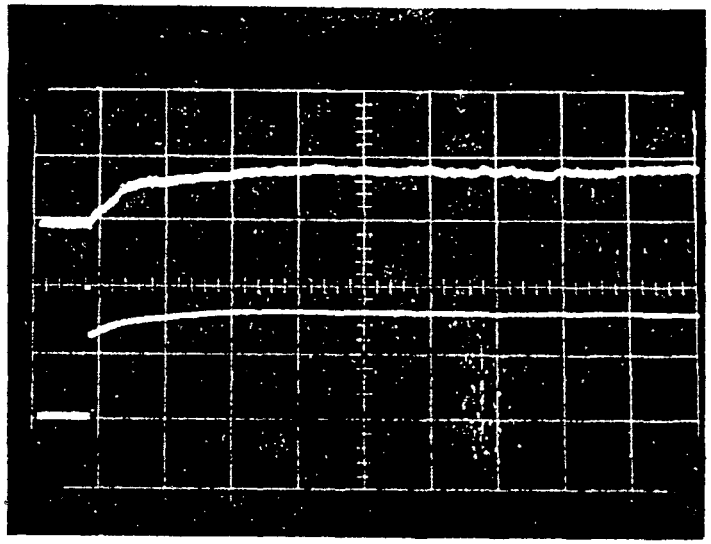

NO. 1b

K_{int}: 0.001

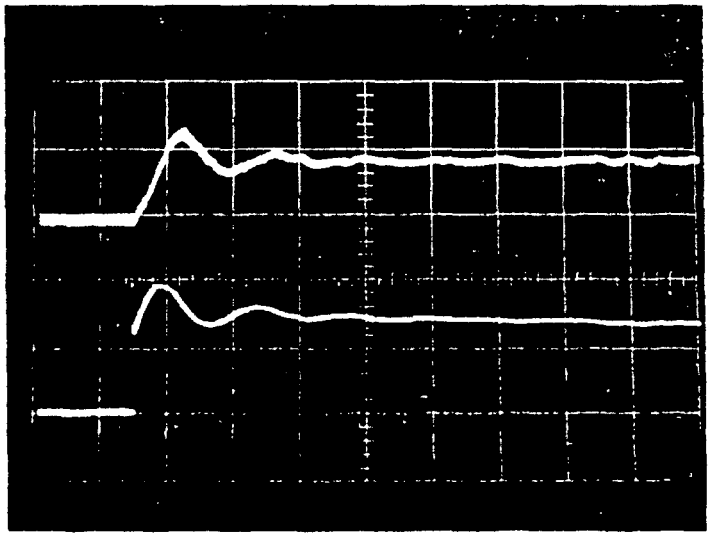

NO. 2a

K_{int}: 0.004

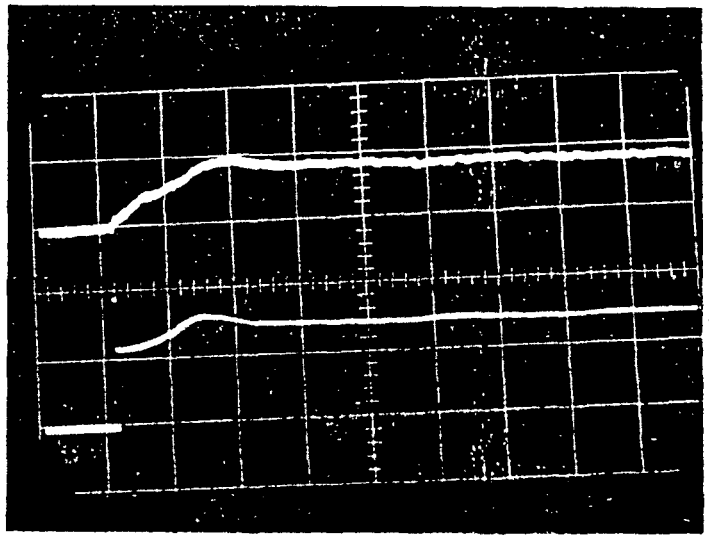

NO. 2b

K_{int}: 0.0035

WITHOUT P.V.

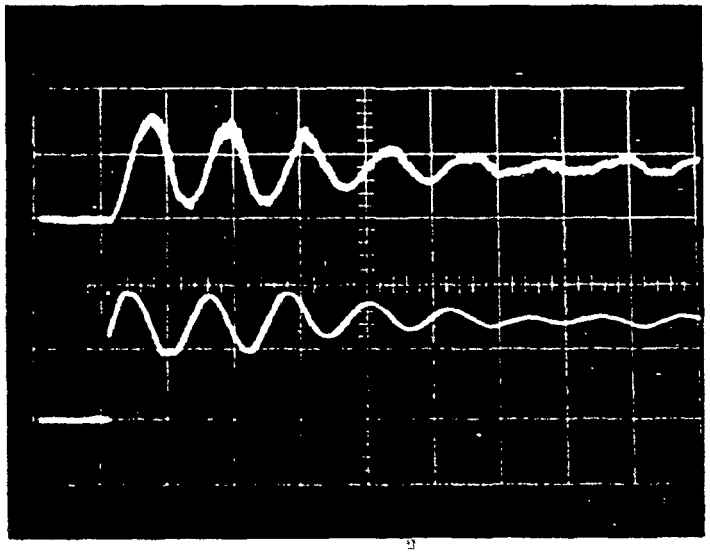

NO. 3a

K_{int}: 0.0055

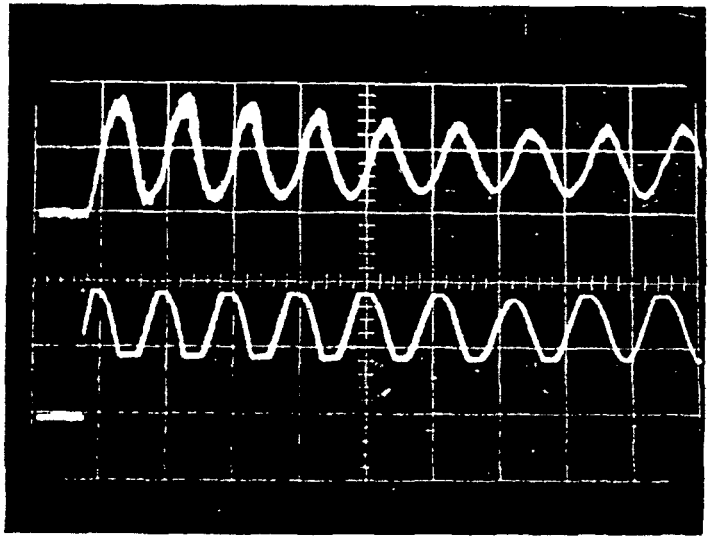

NO. 4a

K_{int}: 0.008

WITH P.V.

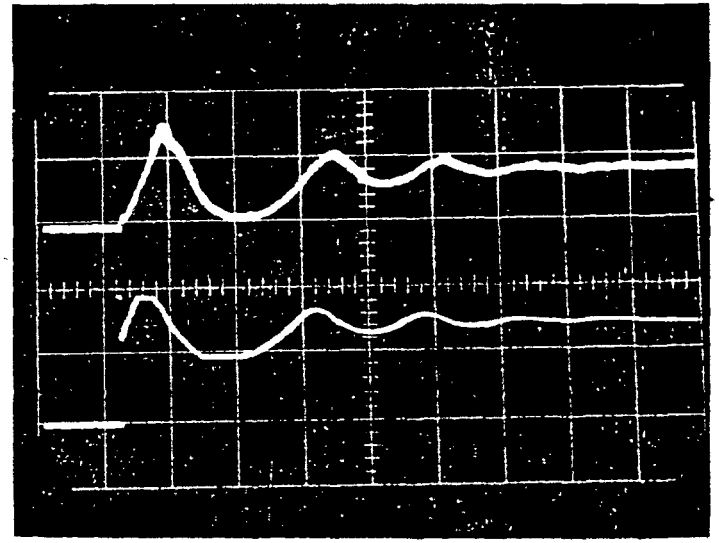

NO. 3b

K_{int}: 0.006

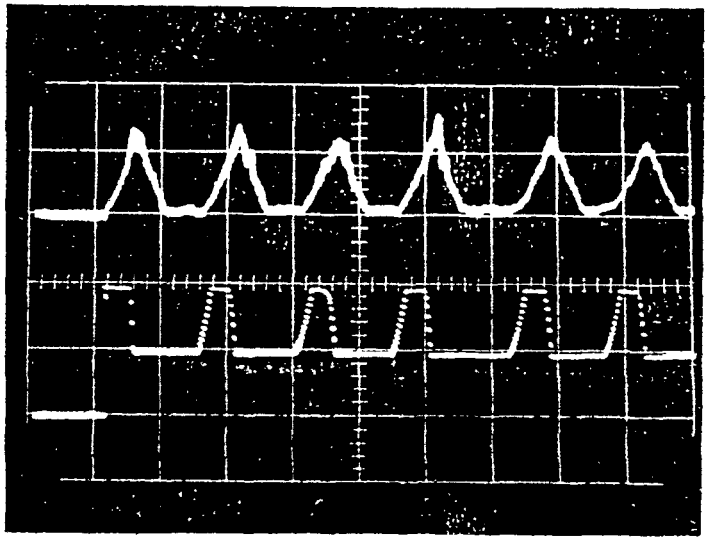

NO. 4b

K_{int}: 0.08

APPENDIX M.3 PROPORTIONAL-PLUS-INTEGRAL CONTROL

WITHOUT P.V.

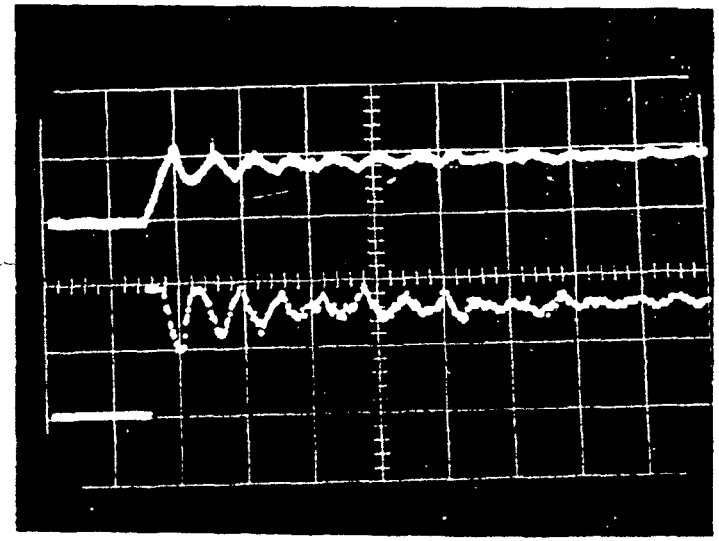

NO. 1a

K_{pro}: 0.20

K_{int}: 0.004

WITH P.V.

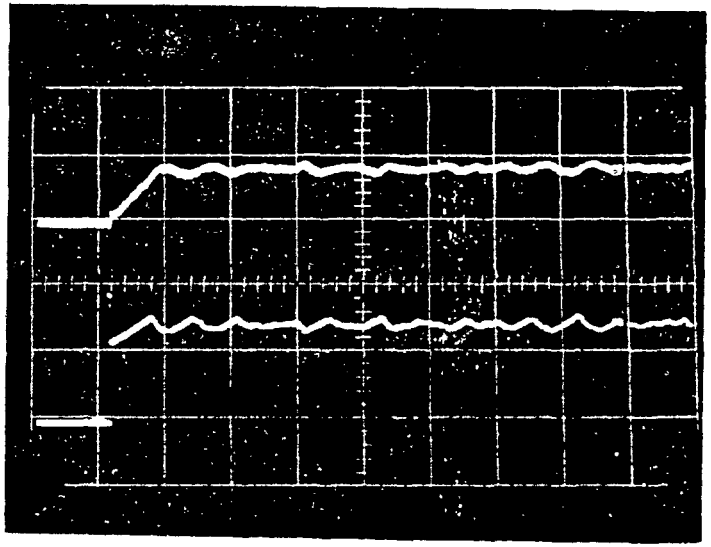

NO. 1b

K_{pro}: 0.15

K_{int}: 0.004

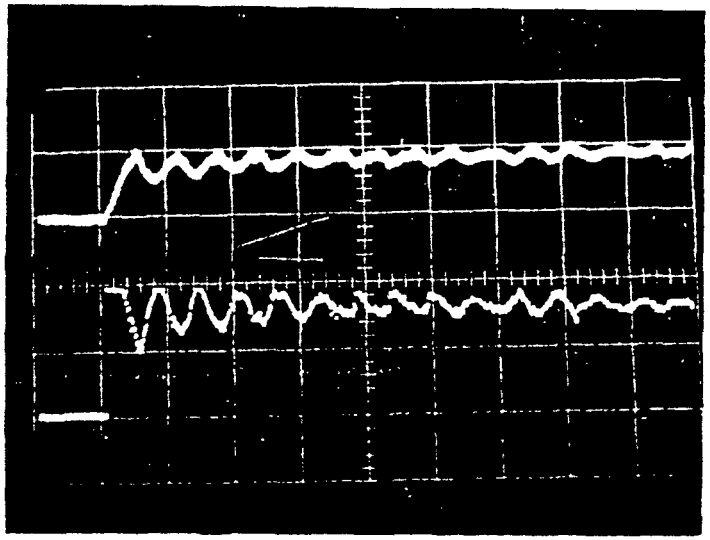

NO. 2a

K_{pro}: 0.24

K_{int}: 0.004

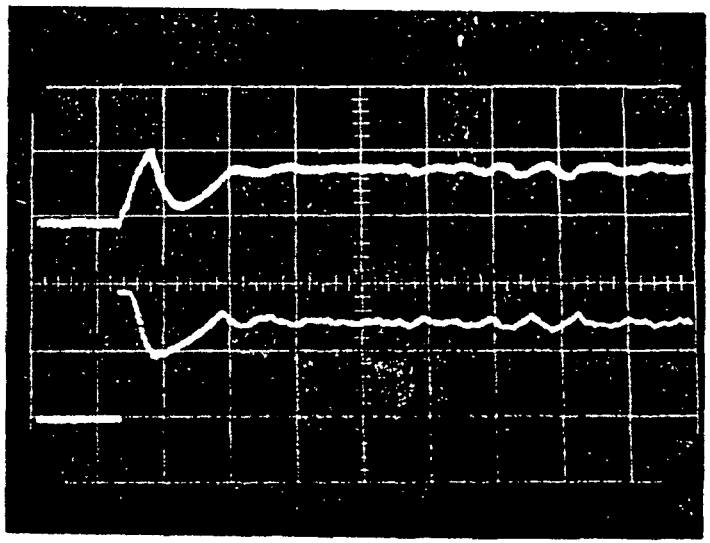

NO. 2b

K_{pro}: 0.15

K_{int}: 0.006

WITHOUT P.V.

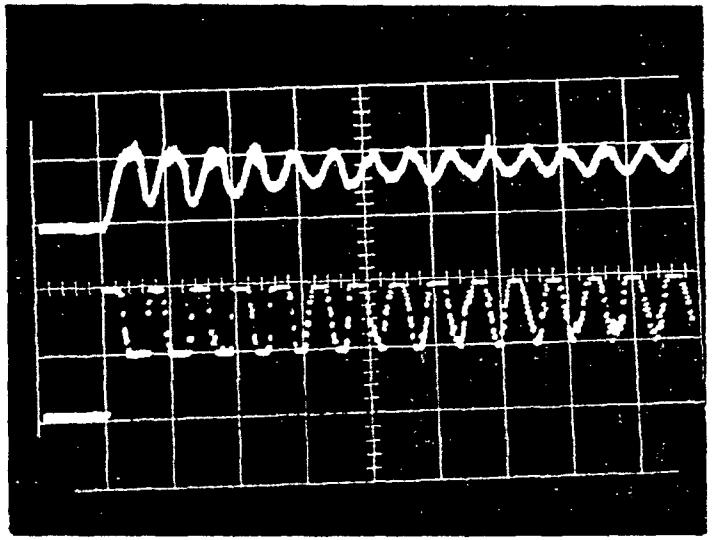

NO. 3a

K_{pro}: 0.35

K_{int}: 0.004

WITH P.V.

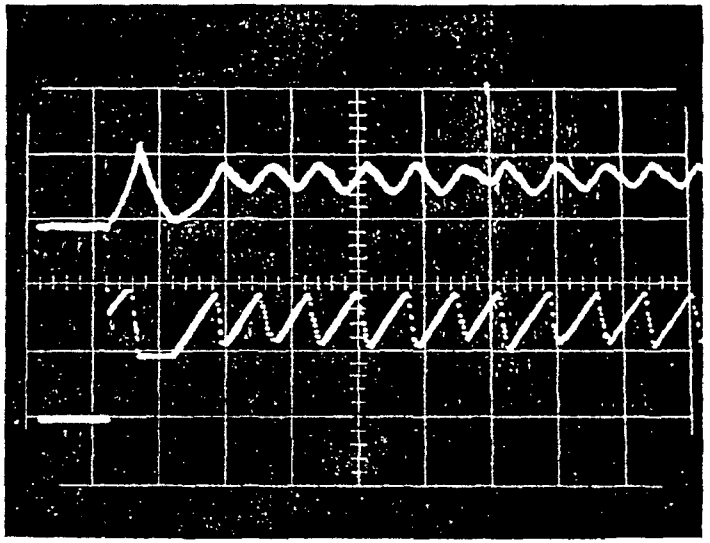

NO. 3b

K_{pro}: 0.35

K_{int}: 0.004

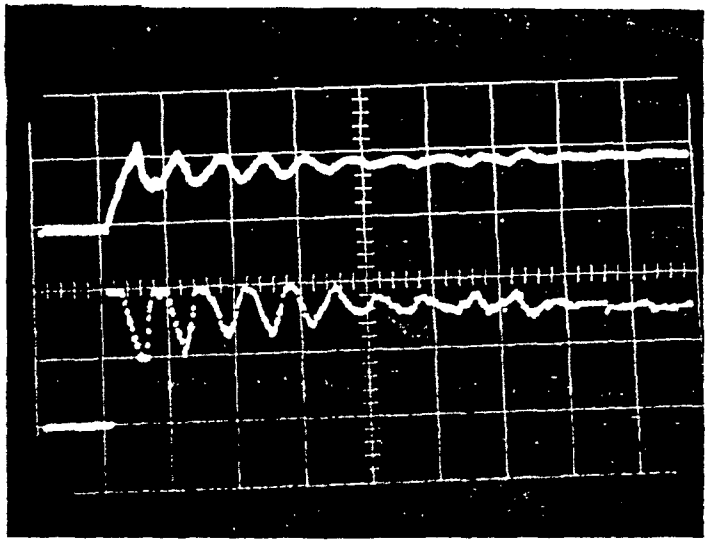

NO. 4a

K_{pro}: 0.20

K_{int}: 0.008

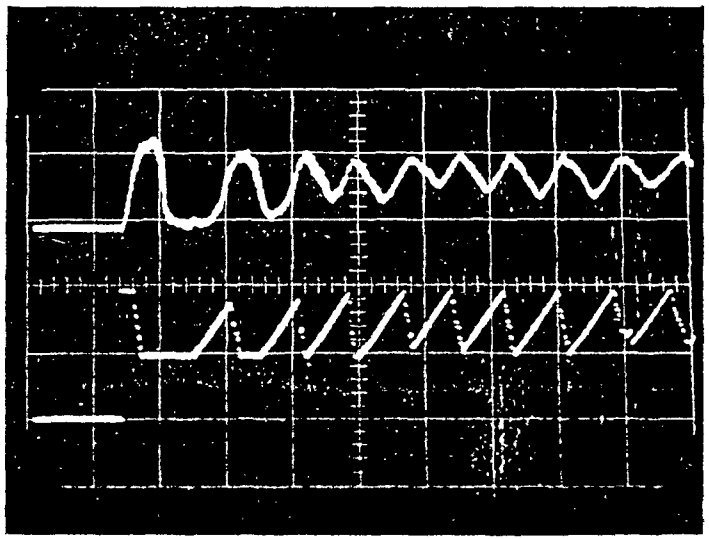

NO, 4b

K_{pro}: 0.35

K_{int}: 0.006

APPENDIX N

ECCENTRIC TURNING EXPERIMENTAL RESULTS FOR BOTH WITH AND WITHOUT PVM IN ALGORITHM

In this appendix the photos of eccentric turning results are collected. It has three sub-appendices as follows:

N.1 - the experimental results for a P controller

N.2 - the experimental results for a I controller

N.3 - the experimental results for a PI controller

APPENDIX N.1 PROPORTIONAL (P) CONTROL

WITHOUT P.V.

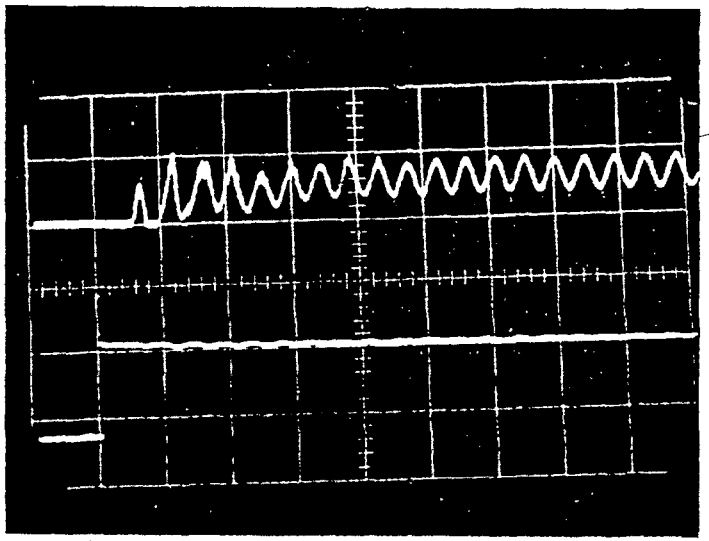

NO. 1a

K_{pro}: 0.005

WITH P.V.

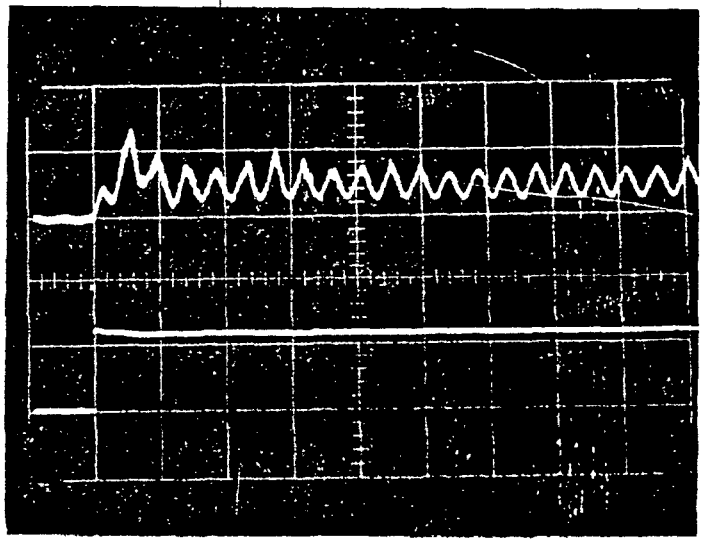

NO. 1b

K_{pro}: 0.005

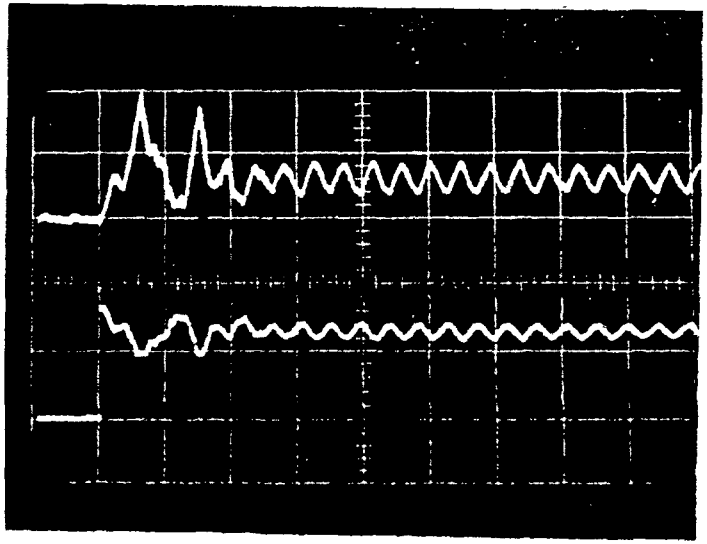

NO. 2a

K_{pro}: 0.05

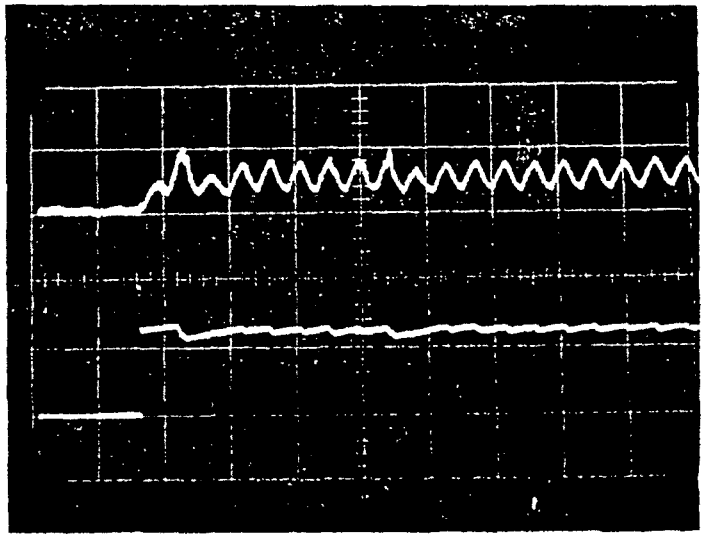

NO. 2b

K_{pro}: 0.05

WITHOUT P.V.

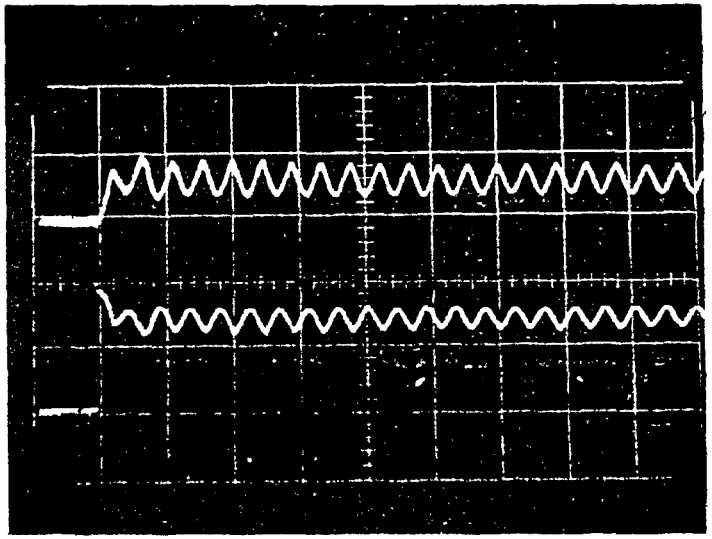

NO. 3a

K_{pro}: 0.07

WITH P.V.

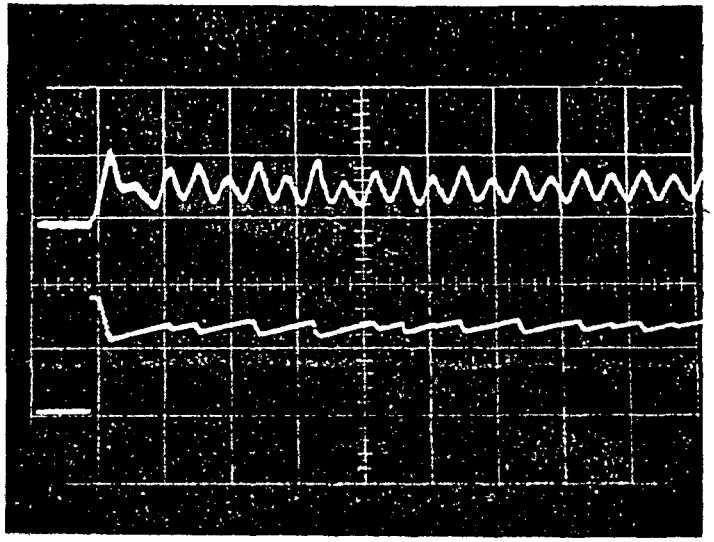

NO. 3b

K_{pro}: 0.07

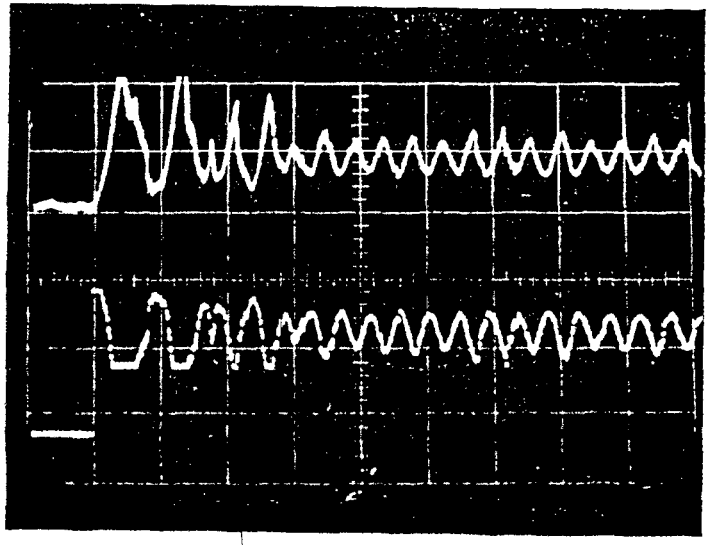

NO. 4a

K_{pro}: 0.10

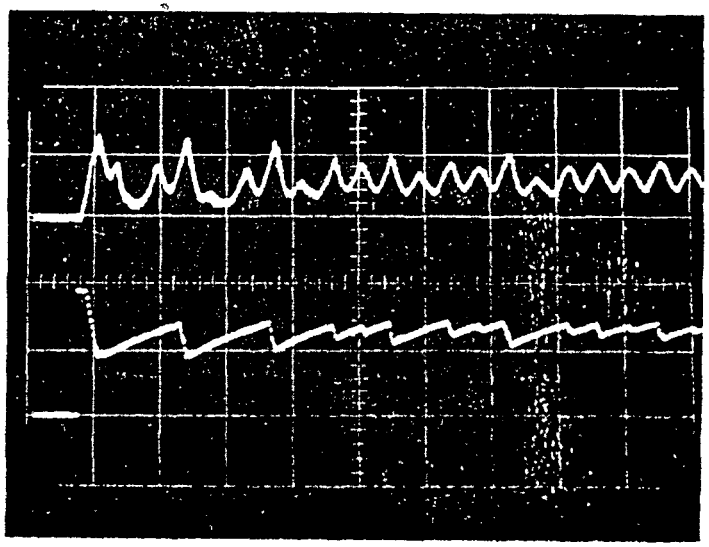

NO. 4b

K_{pro}: 0.10

WITHOUT P.V.

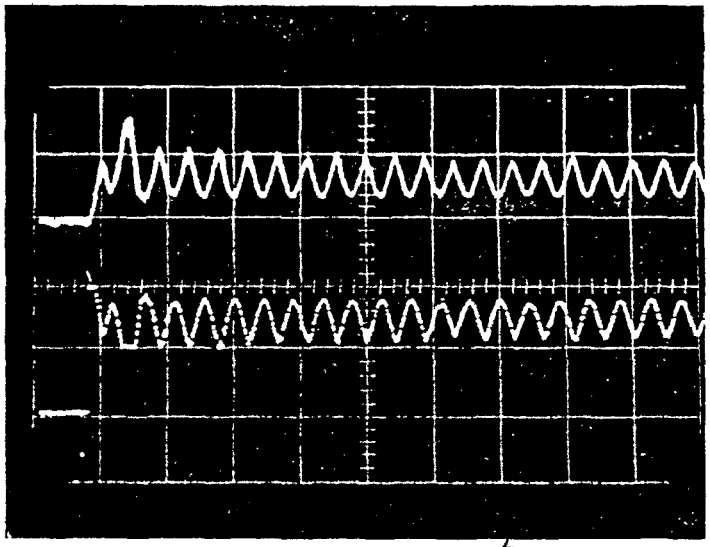

NO. 5a

K_{pro}: 0.12

WITH P.V.

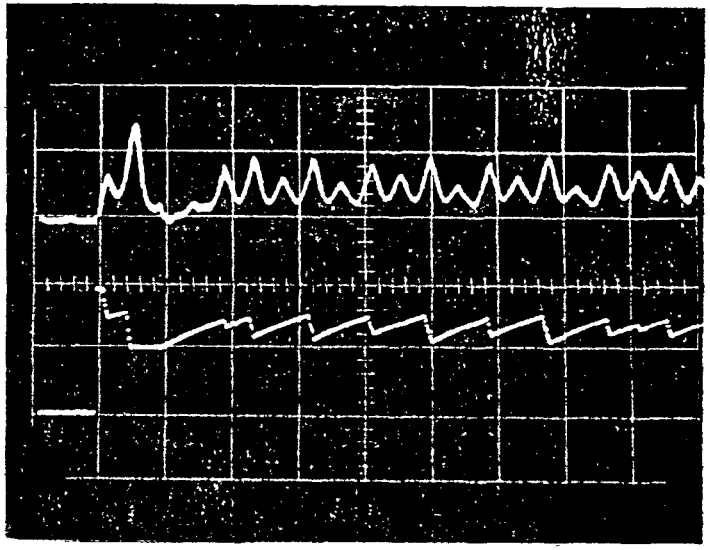

NO. 5b

K_{pro}: 0.12

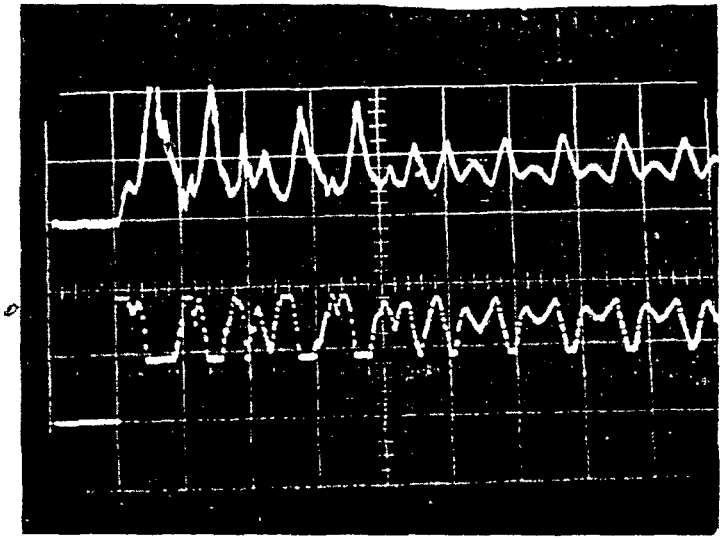

NO. 6a

K_{pro}: 0.15

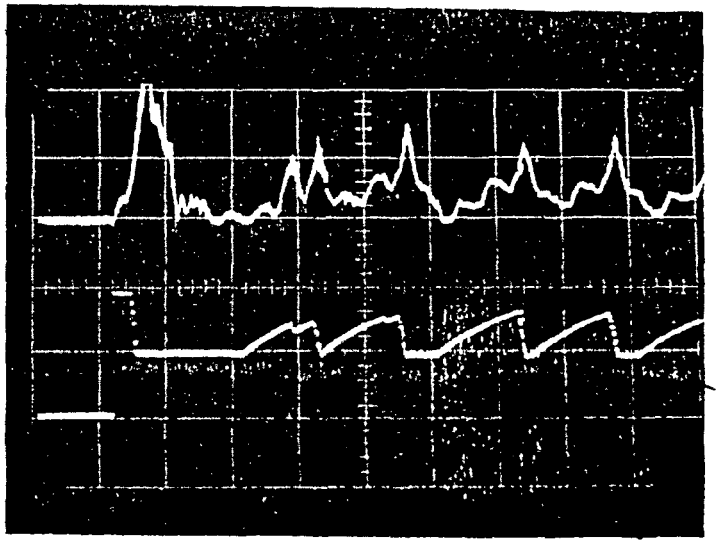

NO. 6b

K_{pro}: 0.15

WITHOUT P.V.

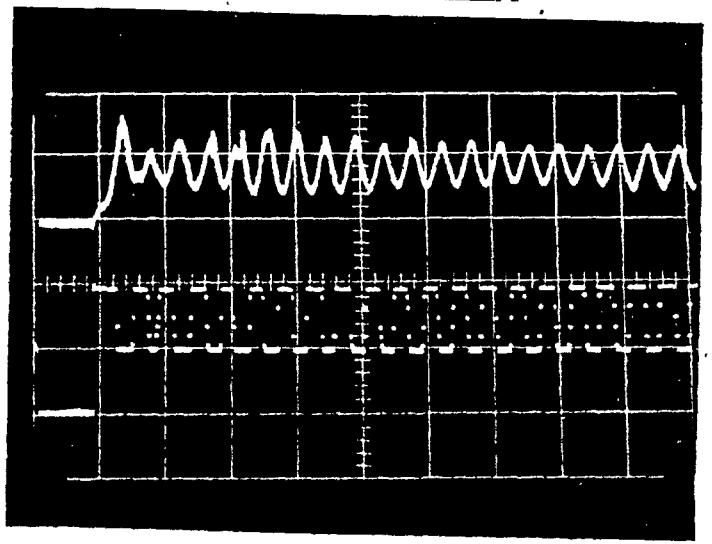

NO. 7a

K_{pro}: 0.70

WITH P.V.

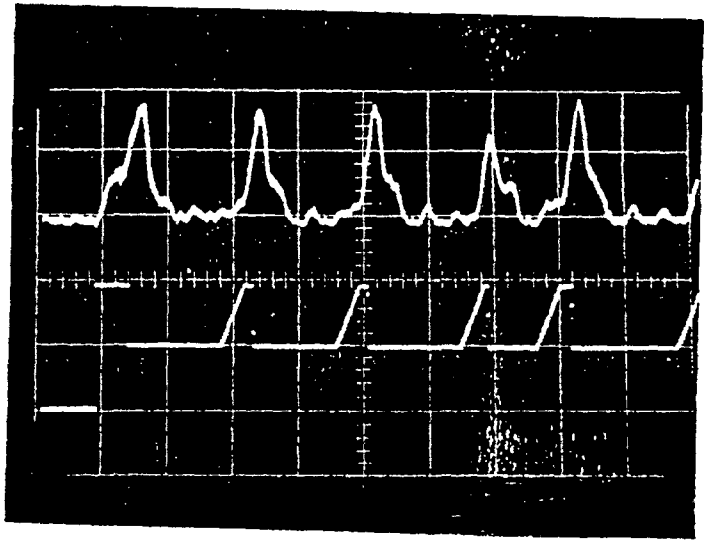

NO. 7b

K_{pro}: 0.70

APPENDIX N.2 INTEGRAL (I) CONTROL

WITHOUT P.V.

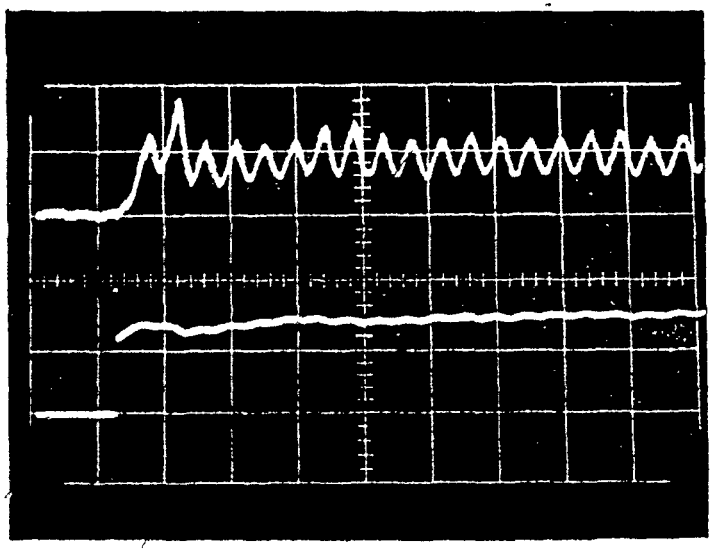

NO. 1a

K_{int}: 0.001

WITH P.V.

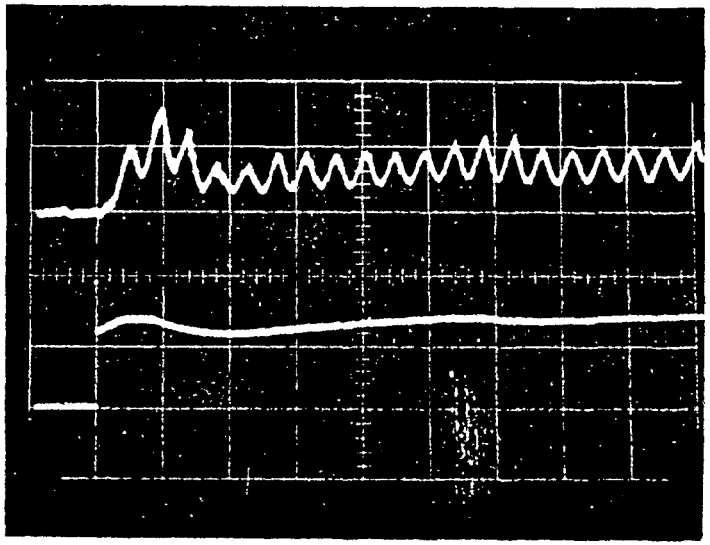

NO. 1b

K_{int}: 0.001

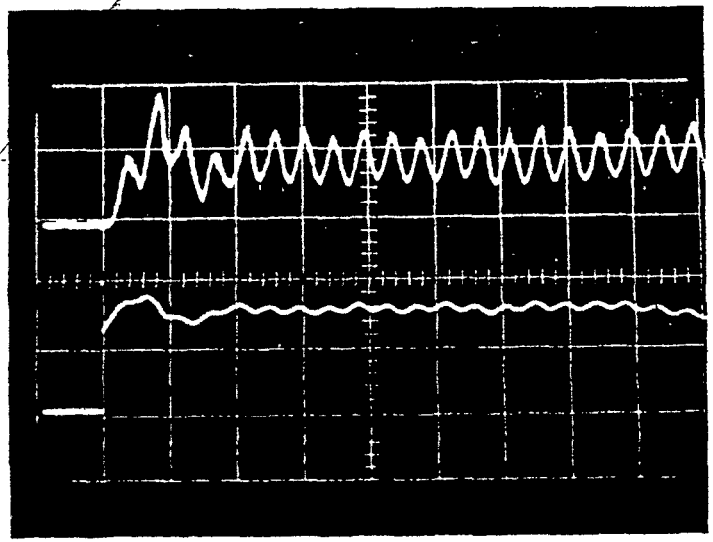

NO. 2a

K_{int}: 0.0022

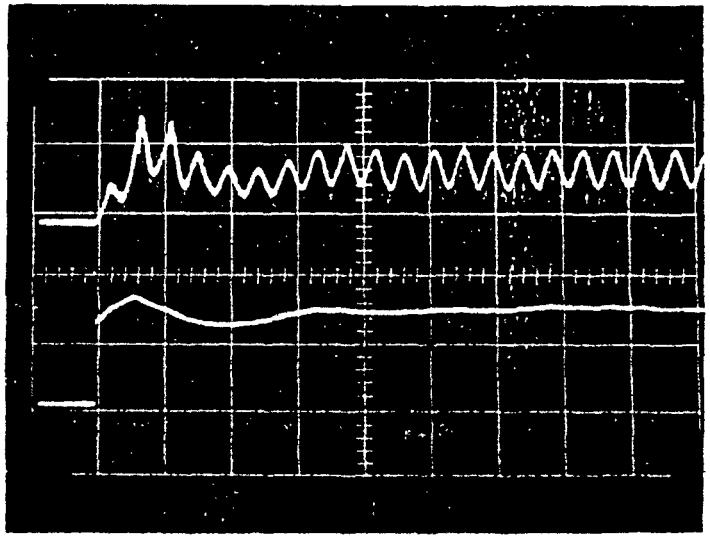

NO. 2b

K_{int}: 0.0022

WITHOUT P.V.

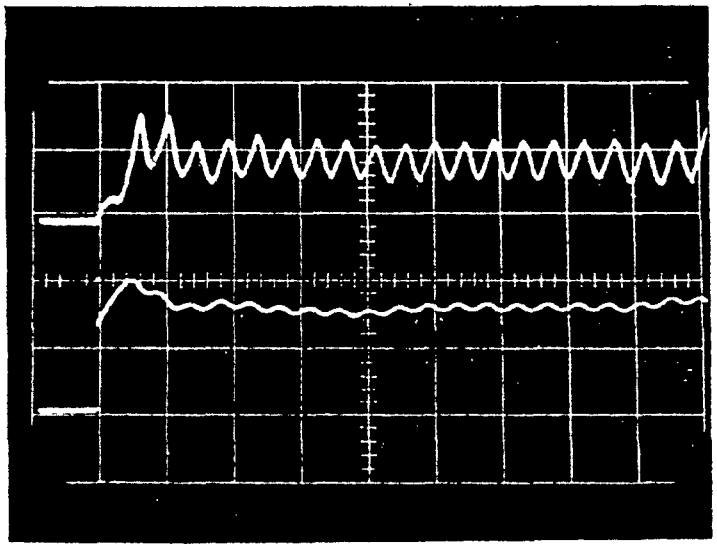

NO. 3a

K_{int}: 0.003

WITH P.V.

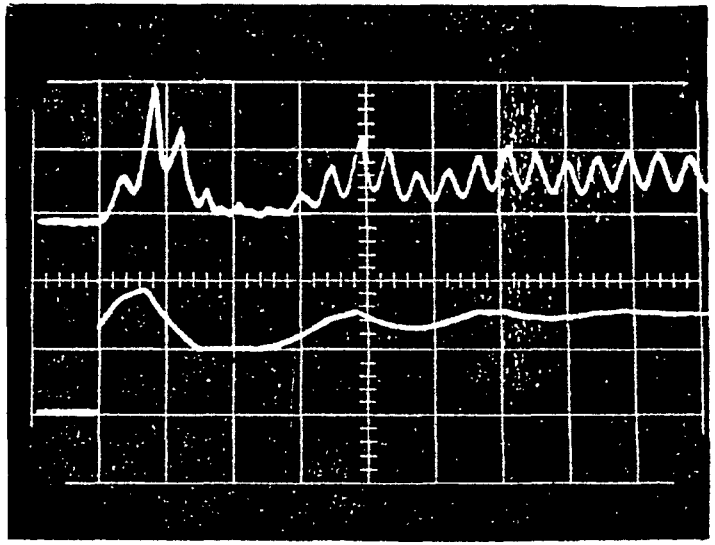

NO. 3b

K_{int}: 0.003

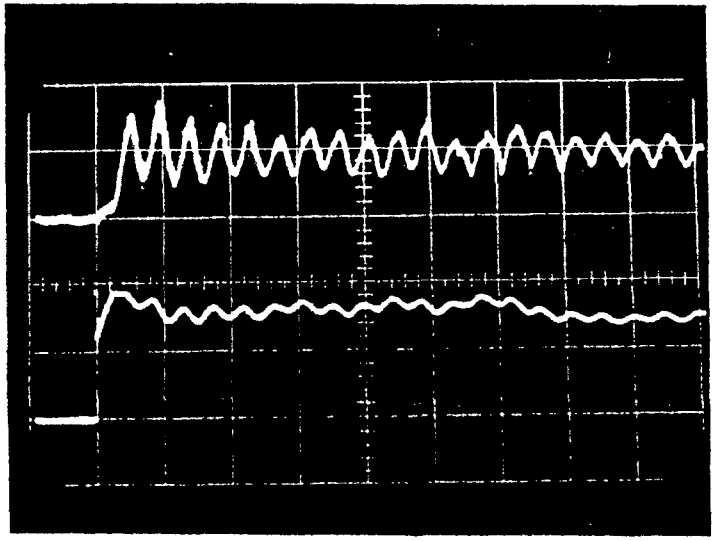

NO. 4a

K_{int}: 0.004

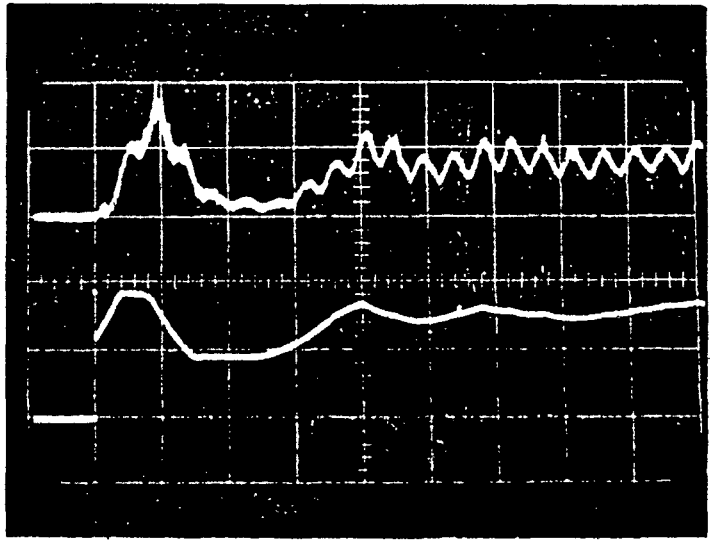

NO. 4b

K_{int}: 0.004

WITHOUT P.V.

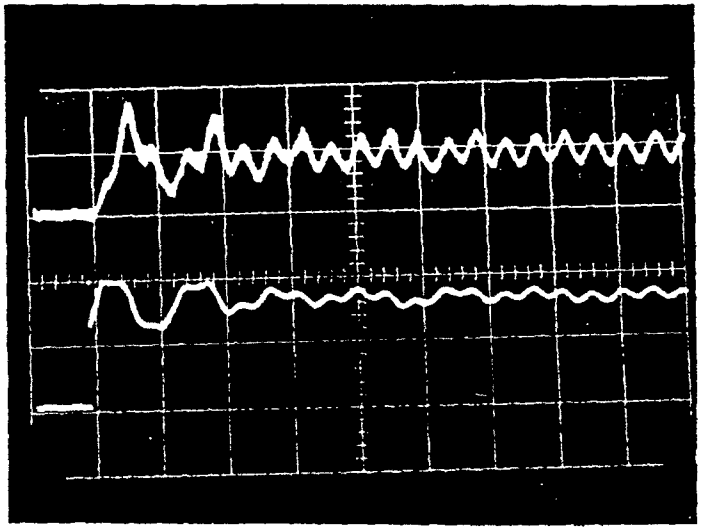

NO. 5a

K_{int}: 0.0055

WITH P.V.

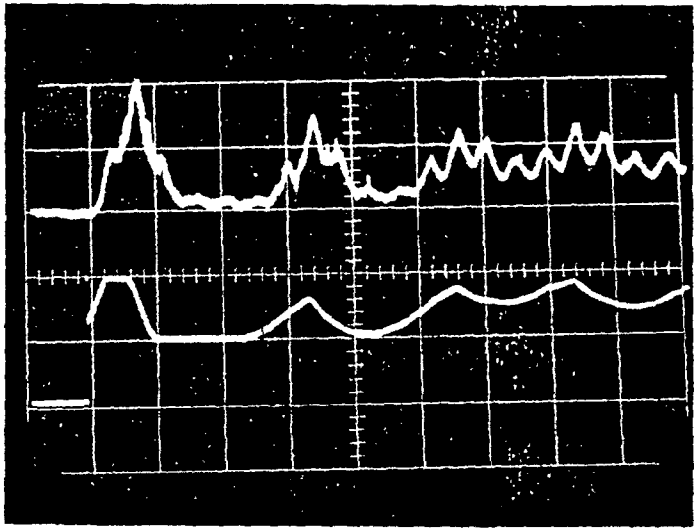

NO. 5b

K_{int}: 0.0055

APPENDIX N.3 PROPORTIONAL-PLUS-INTEGRAL CONTROL

WITHOUT P.V.

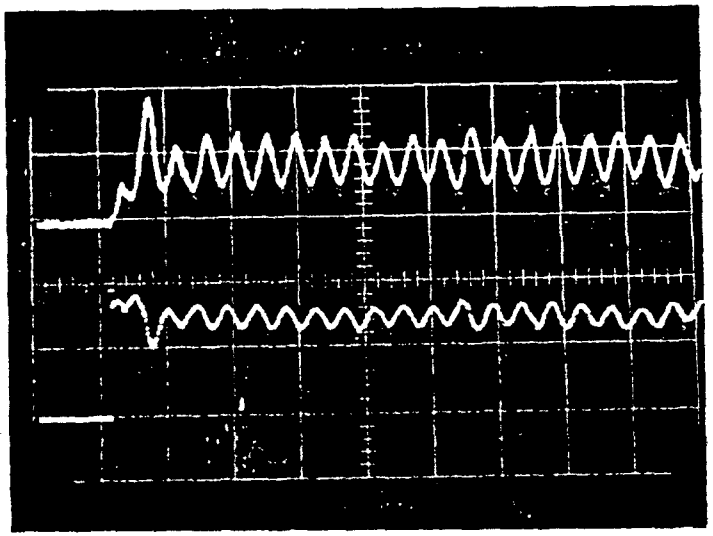

NO. 1a

K_{pro}: 0.05

K_{int}: 0.002

WITH P.V.

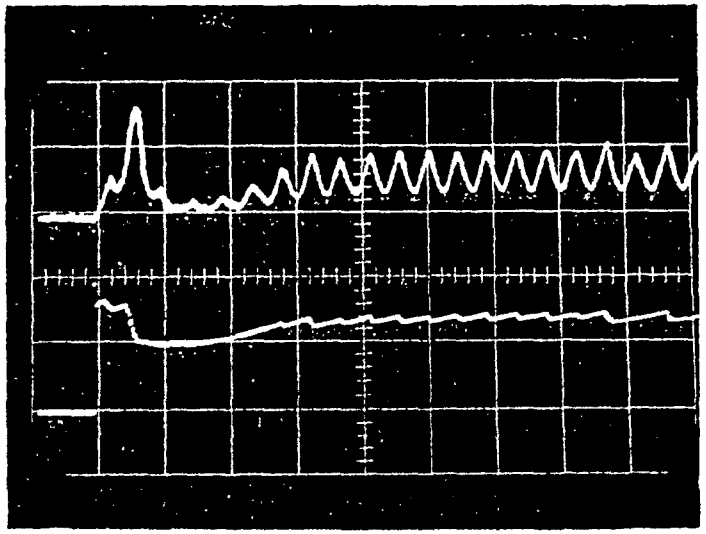

NO. 1b

K_{pro}: 0.05

K_{int}: 0.002

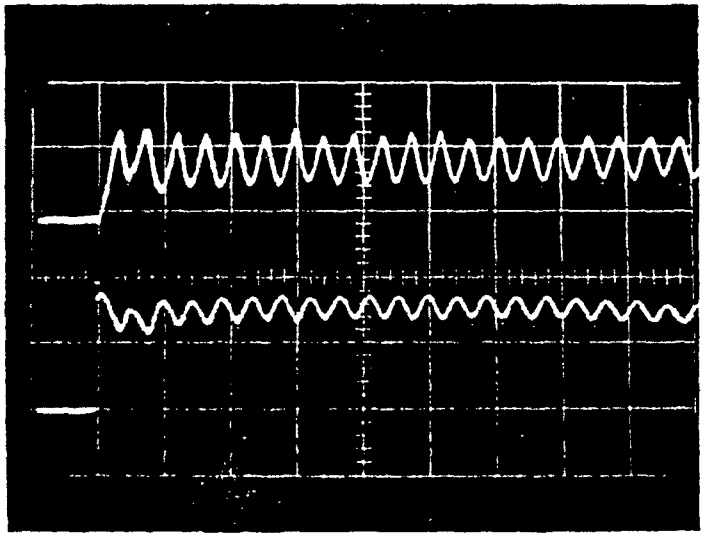

NO. 2a

K_{pro}: 0.05

K_{int}: 0.003

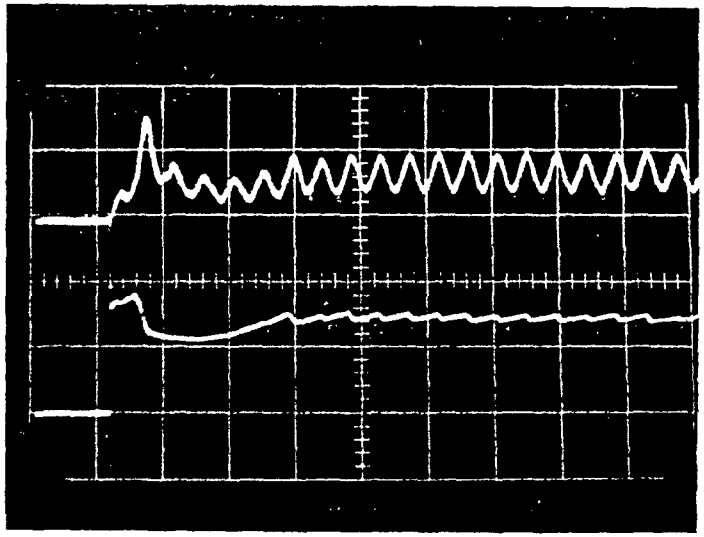

NO. 2b

K_{pro}: 0.05

K_{int}: 0.003

WITHOUT P.V.

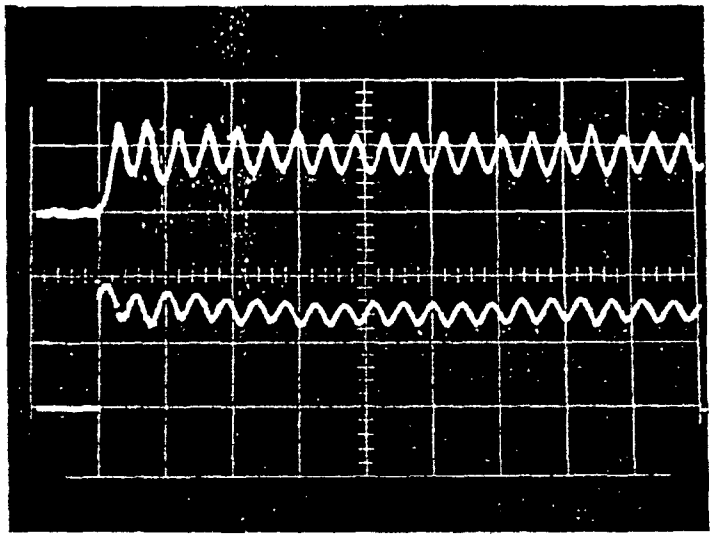

NO. 3a

K_{pro}: 0.05

K_{int}: 0.004

WITH P.V.

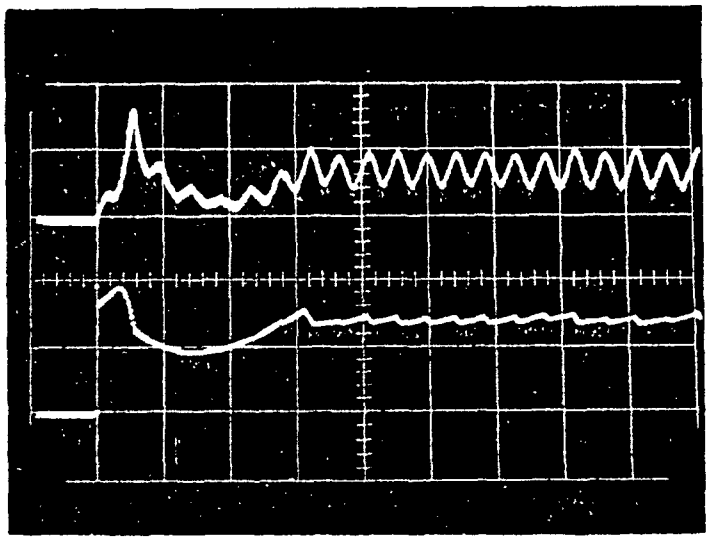

NO. 3b

K_{pro}: 0.05

K_{int}: 0.004

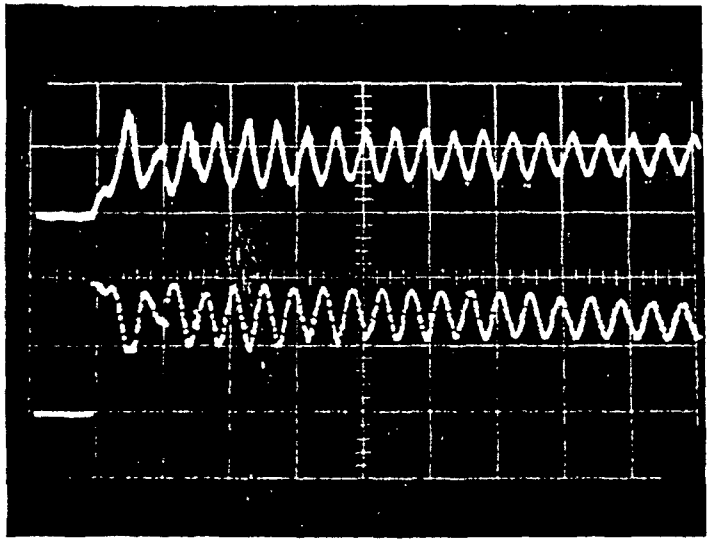

NO. 4a

K_{pro}: 0.10

K_{int}: 0.002

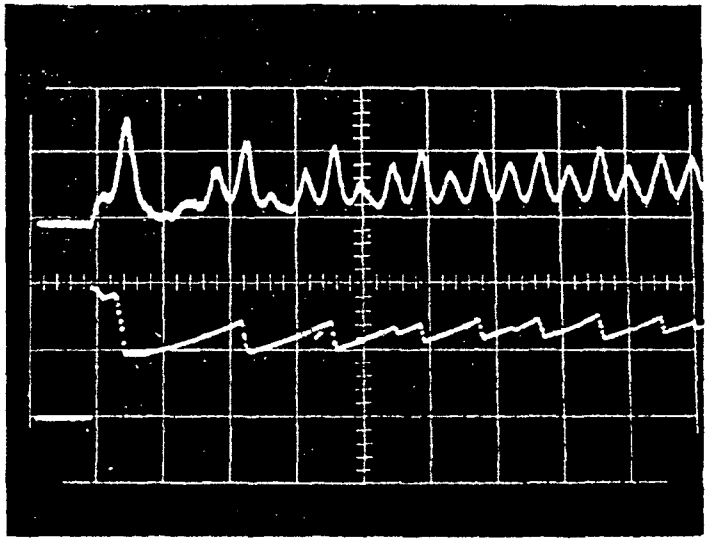

NO. 4b

K_{pro}: 0.10

K_{int}: 0.002

WITHOUT P.V.

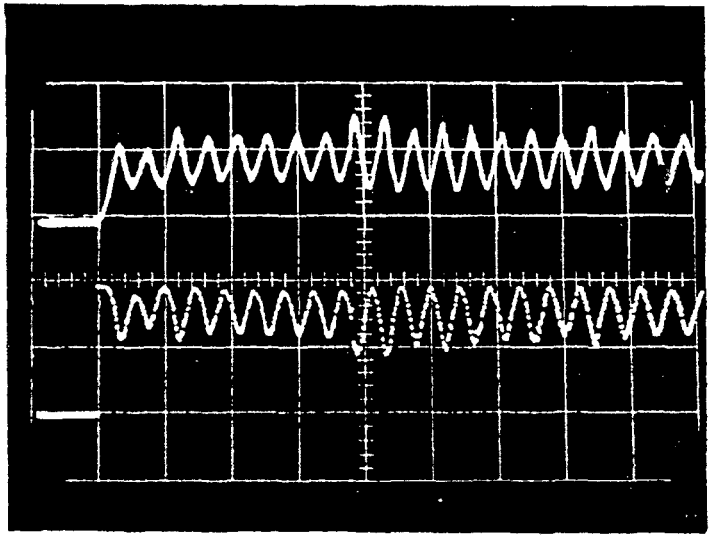

NO. 5a

K_{pro}: 0.10

K_{int}: 0.003

WITH P.V.

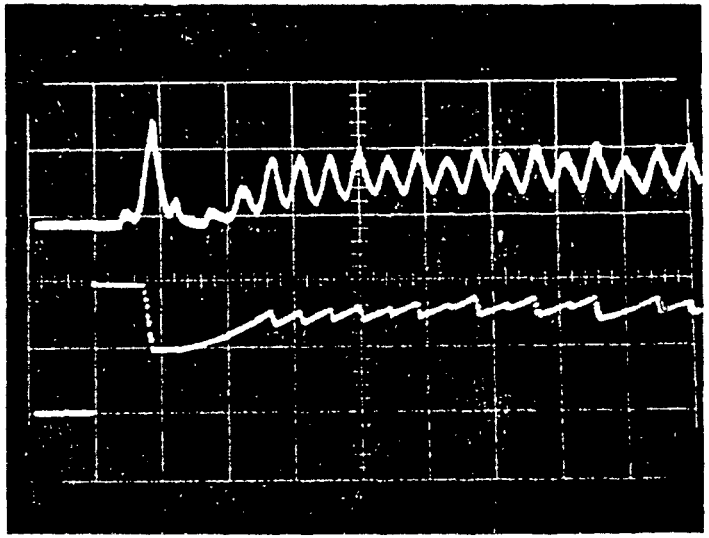

NO. 5b

K_{pro}: 0.10

K_{int}: 0.003

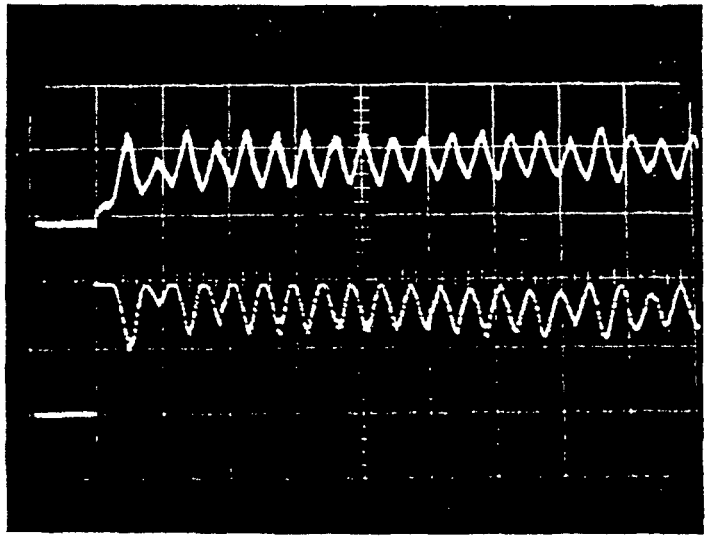

NO. 6a

K_{pro}: 0.10

K_{int}: 0.004

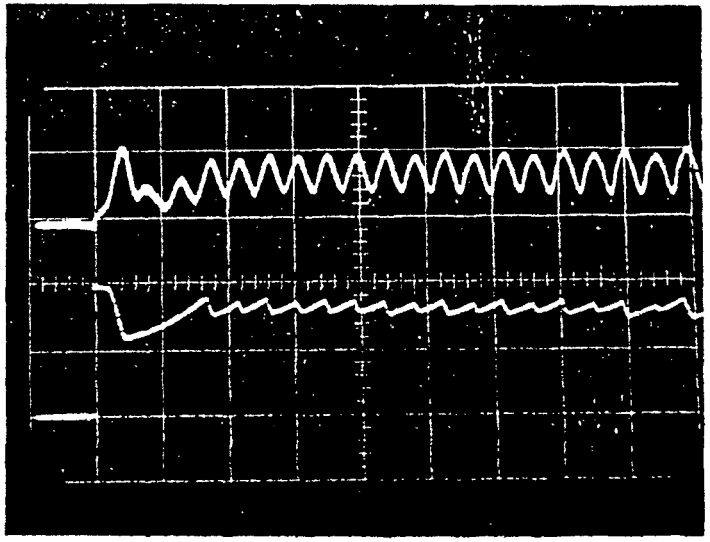

NO. 6b

K_{pro}: 0.10

K_{int}: 0.004

WITHOUT P.V.

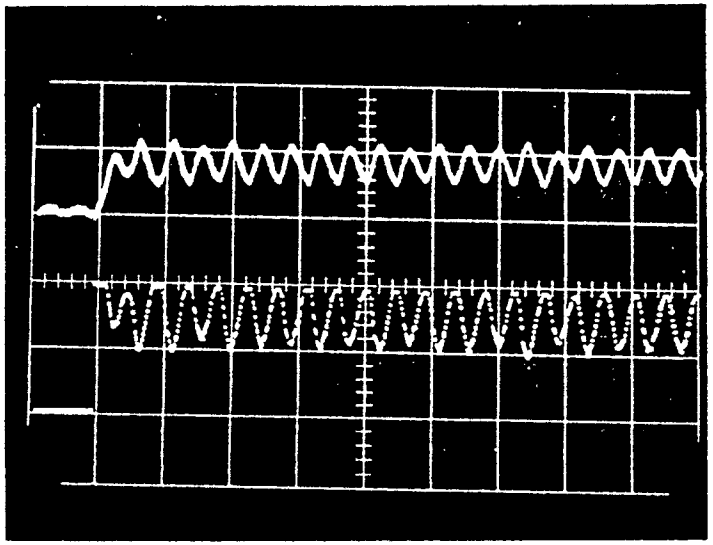

NO. 7a

K_{pro}: 0.20

K_{int}: 0.003

WITH P.V.

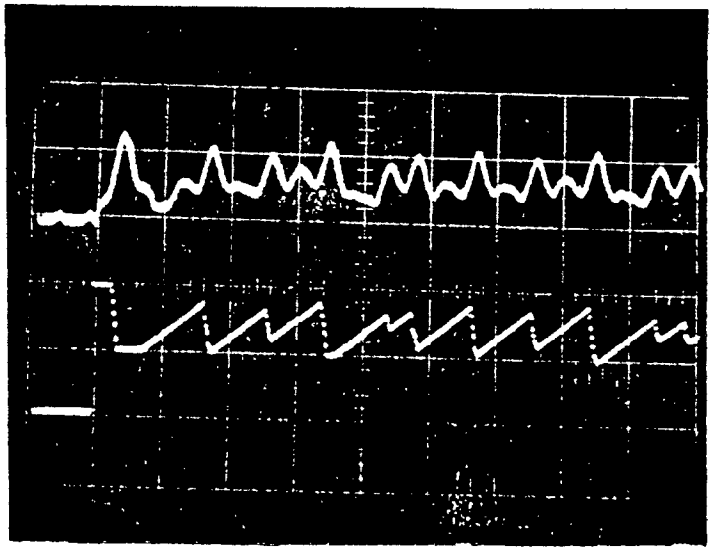

NO. 7b

K_{pro}: 0.20

K_{int}: 0.003

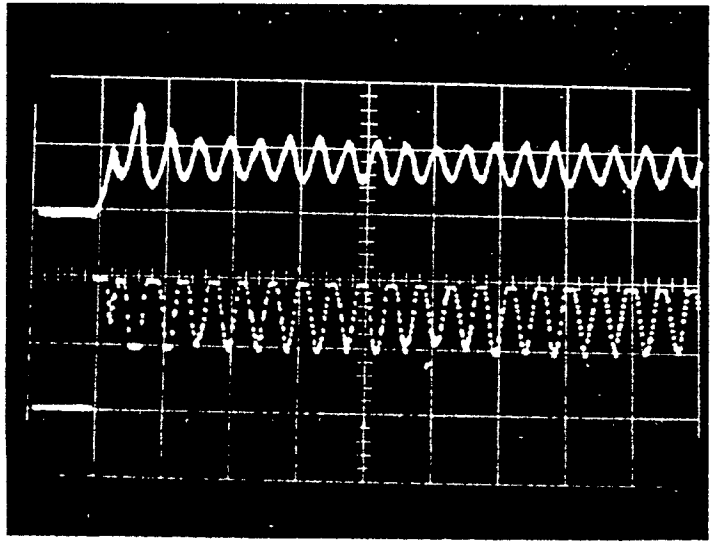

NO. 8a

K_{pro}: 0.20

K_{int}: 0.0055

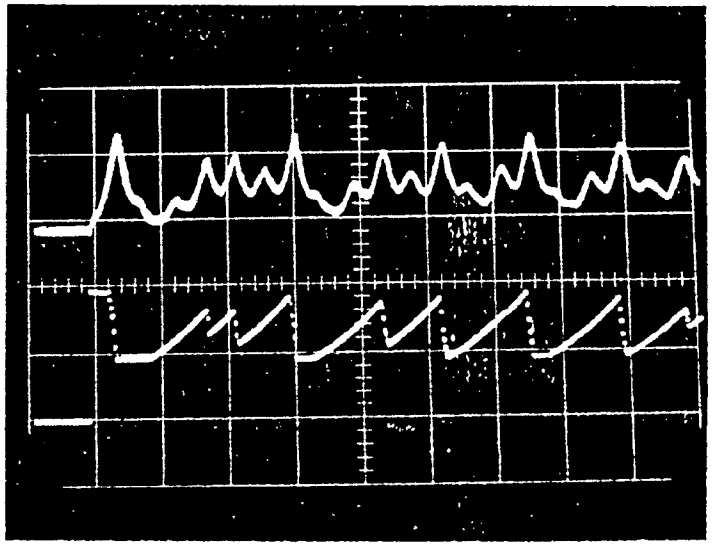

NO. 8b

K_{pro}: 0.20

K_{int}: 0.0055

WITHOUT P.V.

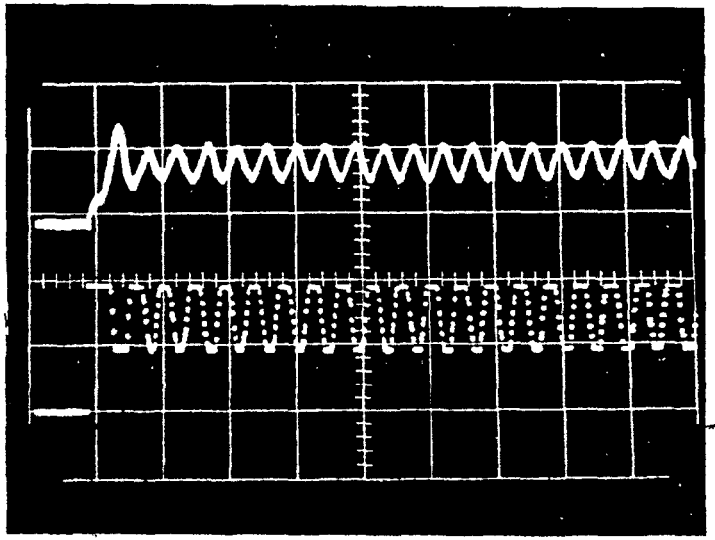

NO. 9a

K_{pro}: 0.35

K_{int}: 0.003

WITH P.V.

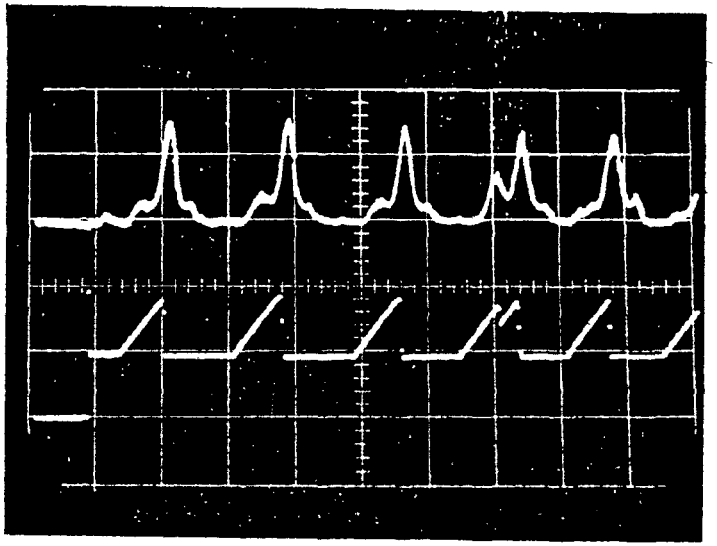

NO. 9b

K_{pro}: 0.35

K_{int}: 0.003